



Kent Academic Repository

Stymest, Krista Helen (2005) *Interaction of model peptides with the peptidyl-prolyl cis/trans isomerases SurA and PpiD*. Doctor of Philosophy (PhD) thesis, University of Kent.

Downloaded from

<https://kar.kent.ac.uk/94679/> The University of Kent's Academic Repository KAR

The version of record is available from

<https://doi.org/10.22024/UniKent/01.02.94679>

This document version

UNSPECIFIED

DOI for this version

Licence for this version

CC BY-NC-ND (Attribution-NonCommercial-NoDerivatives)

Additional information

This thesis has been digitised by EThOS, the British Library digitisation service, for purposes of preservation and dissemination. It was uploaded to KAR on 25 April 2022 in order to hold its content and record within University of Kent systems. It is available Open Access using a Creative Commons Attribution, Non-commercial, No Derivatives (<https://creativecommons.org/licenses/by-nc-nd/4.0/>) licence so that the thesis and its author, can benefit from opportunities for increased readership and citation. This was done in line with University of Kent policies (<https://www.kent.ac.uk/is/strategy/docs/Kent%20Open%20Access%20policy.pdf>). If you ...

Versions of research works

Versions of Record

If this version is the version of record, it is the same as the published version available on the publisher's web site. Cite as the published version.

Author Accepted Manuscripts

If this document is identified as the Author Accepted Manuscript it is the version after peer review but before type setting, copy editing or publisher branding. Cite as Surname, Initial. (Year) 'Title of article'. To be published in *Title of Journal*, Volume and issue numbers [peer-reviewed accepted version]. Available at: DOI or URL (Accessed: date).

Enquiries

If you have questions about this document contact ResearchSupport@kent.ac.uk. Please include the URL of the record in KAR. If you believe that your, or a third party's rights have been compromised through this document please see our [Take Down policy](https://www.kent.ac.uk/guides/kar-the-kent-academic-repository#policies) (available from <https://www.kent.ac.uk/guides/kar-the-kent-academic-repository#policies>).

**Interaction of model peptides with the peptidyl-prolyl
cis/trans isomerases SurA and PpiD**

by

Krista Helen Stymest

A thesis submitted to the University of Kent for the Degree of
PhD in the Faculty of Natural Science

December 2005

The Research School of Biosciences



F208379

DECLARATION

No part of this thesis has been submitted in support of an application for any degree or qualification of the University of Kent or any other university or institute of learning.



Krista Stymest

December 2005

ACKNOWLEDGEMENTS

Firstly I would like to say a huge thank you to my supervisor Dr Peter Klappa for his invaluable help and expertise and giving me this opportunity in the first place. Without your help I would never have got here.

I would also like to thank Dr Satish Raina for the mutants A99V and I75S.

Thank you to Judith Hardy for producing all the peptides and the various sequencing and analysis and also Sarah Reed for the primary antibodies. I would like to say a special thank you to Dr Mark Howard for his patience with the NMR and the molecular modeling.

Thank you to Panos, although we didn't always see eye to eye, you kept me smiling and I appreciate that.

I am really grateful to Lizanne Allcock, she will know why.

Finally, I would like to dedicate this to my Father and John, as without both of you I would never have achieved this x.

CONTENTS

FOLLOWING PAGE:

Title.....	i
Declaration.....	ii
Acknowledgements.....	iii
Contents.....	v-xi
Abbreviations.....	xii-xiii
Figures.....	xiv-xix
Abstract.....	xx-xxi

CHAPTER 1: INTRODUCTION

1.1	Introduction.....	2
1.2	Proteins and folding.....	3
1.3	Molecular chaperones and folding catalysts.....	4
1.4	Protein Folding Compartments.....	5
	1.4.1 The Cytoplasm.....	5
	1.4.2 The Endoplasmic Reticulum and periplasmic space.....	6
1.5	Oxidative Folding of Proteins in the ER and the Periplasmic Space.....	6
1.6	Peptidyl Prolyl <i>cis/trans</i> isomerisation	8
1.7	Discovery of PPIases.....	10
1.8	The Roles and Functions of the PPIases.....	11
1.9	Cyclophilins.....	12
1.10	FK506-Binding Proteins.....	12
1.11	Trigger Factor.....	13
1.12	Parvulins.....	14
1.13	PPIases in the Periplasmic Space of Prokaryotes.....	15
1.14	FKPA.....	19
1.15	PpiA.....	21
1.16	SurA.....	21

1.17	PpiD.....	24
1.18	Aims of this Study.....	26

CHAPTER 2: MATERIALS AND METHODS

2.1	Materials.....	31
2.2	Strains used in this study.....	31
	2.2.1 <i>Escherichia coli</i> strains.....	31
2.3	Growth media and solutions.....	32
	2.3.1 <i>Escherichia coli</i>	32
	2.3.2 Monitoring <i>E.coli</i> cell growth.....	33
2.4	Recombinant DNA techniques.....	33
	2.4.1 DNA markers.....	33
	2.4.2 Vectors.....	33
	2.4.3 Digestion of DNA with restriction endonucleases.....	34
	2.4.4 Ethanol precipitation.....	34
	2.4.5 Agarose gel electrophoresis of DNA (Sambrook <i>et al</i>).....	35
	2.4.6 Purification of DNA.....	35
	2.4.7 QIAGEN gel extraction.....	36
	2.4.8 pGEM-Teasy easy vector system.....	36
	2.4.9 Ligation of cohesive and non-cohesive termini.....	36
	2.4.10 Competent cells.....	36
	2.4.11 Transformation of <i>E.coli</i> with plasmid DNA using heat shock...	38
	2.4.12 Small scale QIAGEN mini-preps of plasmid DNA.....	38
	2.4.13 Maxiprep plasmid DNA purification.....	38
	2.4.14 Genomic DNA.....	39
2.5	Polymerase chain reaction (PCR).....	39
	2.5.1 PCR protocol.....	39
	2.5.2 QIAGEN QIAquick PCR purification.....	41
	2.5.3 Primers.....	41
	2.5.4 Diagnostic PCR.....	42

2.6	Protein analytical methods.....	43
2.6.1	Small scale expression of recombinant protein in <i>E.coli</i>	43
2.6.2	Large scale expression of recombinant protein in <i>E.coli</i>	43
2.6.3	Protein purification using HPLC.....	44
2.6.4	Protein Desalting.....	44
2.6.5	Slide-A-lyser.....	45
2.6.6	Concentrating proteins by speed vac.....	45
2.6.7	Centricon.....	45
2.6.8	Concentrating proteins by freeze drying.....	46
2.6.9	Resource Q Column.....	46
2.6.10	SDS polyacrylamide gel (PAGE) electrophoresis under denaturing conditions.....	47
2.6.11	Determining protein concentration.....	48
2.6.12	Chymotrypsin digest.....	49
2.6.13	Proteinase K digest.....	49
2.7	Immunological methods.....	49
2.7.1	Western blotting using the ECL detection system.....	49
2.7.2	Coomassie blue staining of PVDF membranes and SDS- polyacrylamide gels.....	50
2.7.3	Immunodecoration of PVDF membranes.....	50
2.7.4	ECL detection of antibodies.....	51
2.7.5	Antibody production.....	51
2.8	Peptide studies.....	52
2.8.1	Radioactivity storage.....	52
2.8.2	Measuring peptide concentration.....	52
2.8.3	Radiolabelling peptides.....	52
2.8.4	Cross-linking assay.....	53
2.8.5	Competition assay.....	53
2.8.6	Binding assay.....	54
2.8.7	scRNAase.....	54
2.8.8	Triton-X 100.....	54
2.8.9	Heat inactivation.....	54
2.9	Mutagenesis.....	55

2.9.1	Designing primers for mutagenesis.....	55
2.9.2	Mutagenesis.....	56
2.10	NMR.....	57
2.10.1	Preparation of NMR samples.....	57
2.10.2	NMR sample.....	57
2.10.3	STD-NMR.....	58
2.11	Molecular modeling.....	59
2.11.1	Outline of the system.....	59
2.11.2	Choosing the residues.....	59
2.11.3	The basic process.....	59
2.12	Bioinformatics.....	60

CHAPTER 3: EXPRESSION AND PURIFICATION OF THE N-TERMINAL FRAGMENT

3.1	Introduction.....	63
3.2	Initial experiments confirmed the presence of expression clones.....	64
3.3	Primary antibodies bind to full length SurA and fragments.....	67
3.4	Expression and purification.....	68
3.4.1	Expression and purification of the full length of SurA.....	69
3.4.2	Expression and purification of the N-terminal fragment of SurA.....	72
3.5	Concentrating full length SurA and the N-terminal fragment of SurA....	74
3.5.1	Resource Q concentration.....	74
3.5.2	Centricon concentration of the full length SurA.....	75
3.5.3	Freeze drying does not affect the SurA activity.....	75
3.5.4	Concentrating N-terminal fragment of SurA with Centricon.....	76
3.5.5	Concentrating N-terminal fragment of SurA with the Ultrafree-4 centrifugal unit.....	76
3.5.6	Buffer exchange with Ultrafree-4 centrifugal unit.....	77
3.5.7	Protein dialysis of the N-terminal fragment of SurA.....	77

3.6	Conclusions.....	78
-----	------------------	----

CHAPTER 4: BINDING OF PEPTIDES TO SURA AND THE N-TERMINAL FRAGMENT

4.1	Introduction.....	80
4.2	Crosslinking.....	81
4.3	Radiolabelling.....	83
4.4	The crosslinking approach.....	84
4.4.1	Direct crosslinking approach.....	84
4.4.2	Indirect crosslinking of radiolabelled peptides, the competition assay.....	86
4.5	Crosslinking of radiolabelled peptide to recombinant SurA in cell lysate.....	87
4.6	Initial direct crosslinking of radiolabelled peptides to SurA and competition assays.....	88
4.7	Competition assays of binding peptides to SurA.....	91
4.8	Direct binding of peptides to SurA.....	92
4.9	Binding to N-terminal fragment of SurA.....	93
4.10	STD-NMR of SurA shows amino acids directly involved in binding.....	94
4.11	Conclusions.....	97

CHAPTER 5: MOLECULAR MODELLING

5.1	Introduction.....	99
5.2	X-ray and CNS standard simulated annealing wild-type structures have insignificant differences.....	101
5.3	Selecting mutations for SurA.....	104
5.3.1	The mutants were selected by location.....	104
5.3.2	Residues were changed to different residues with similar	

	properties.....	105
5.3.3	Non-conservative changes had little effect.....	106
5.3.4	Mutations of residues outside the core structure do not significantly alter the overall structure.....	109
5.3.5	Mutations of the core structure have a pronounced effect to the structure of SurA.....	110
5.4	Measurements of residue distances from wild-type positioning highlight dramatic changes differences in the mutations.....	121
5.5	Mutagenesis of selected mutants.....	122
5.6	Conclusions.....	123

CHAPTER 6: THE PEPTIDYL PROLYL *CIS/TRANS* ISOMERASE PPiD

6.1	Introduction.....	126
6.2	Expression and purification of PpiD.....	127
6.3	Antibodies against PpiD.....	132
6.4	Proteinase K digest of PpiD.....	133
6.5	Generating the PpiD fragment.....	136
	6.5.1 Expressed protein shows binding.....	139
6.6	Determining the location of the binding region for PpiD.....	140
6.7	Binding assays for PpiD.....	145
	6.7.1 PpiD interacts with misfolded protein.....	145
	6.7.2 Crosslinking of radiolabelled peptide to recombinant PpiD in cell lysate.....	147
	6.7.3 Competition binding to PpiD with model peptides.....	149
6.8	STD-NMR for PpiD.....	152
6.9	Conclusions.....	155

CHAPTER 7: GENERAL DISCUSSION

7.1	Introduction.....	158
7.2	C-terminus of SurA is required for stability but not binding.....	158
7.3	Binding experiments show preferences of PPIases.....	161
7.3.1	PpiD interacts with model peptides and scRNAse A.....	161
7.3.2	Interaction of PPIases with model peptides.....	162
7.3.3	Biological significance.....	164
7.4	STD-NMR highlights another significant residue for SurA binding.....	165
7.5	Molecular modeling of full length SurA highlights important amino acids within the SurA structure.....	167
7.6	PpiD.....	168
7.7	The future.....	169

REFERENCES.....	170
------------------------	------------

APPENDICES.....	192
------------------------	------------

ABBREVIATIONS

A600	visible light absorbance at 600 nanometers
aa	amino acid
ATP	adenosine triphosphate
BSA	bovine serum albumin
C-terminus	carboxy-terminus
Da	Dalton
dH ₂ O	distilled water
DNA	deoxyribonucleic acid
EDTA	diaminoethanetetra-acetic acid
ECL	enhanced chemi-luminescence
<i>E.coli</i>	<i>Escherichia coli</i>
ER	endoplasmic reticulum
g	gram
hrs	hours
IPTG	isopropyl β -D-thiogalactopyranoside
kDa	kilodalton
kb	kilobase
LB	Luria-Bertani medium
M	molar
2-ME	2-mercaptoethanol
min	minute
ml	millilitre
NaCl	sodium chloride
NMWL	Nominal Molecular Weight Markings
N-terminus	amino-terminus
OD	optical density
PBS	phosphate-buffered saline solution
PCR	polynucleotide chain reaction
PDI	protein disulphide isomerase
PMSF	phenylmethylsulphonyl fluoride
PPase	peptidylprolyl <i>cis-trans</i> isomerase
rpm	revolutions per minute

SDS	sodium dodecyl sulphate
SDS-PAGE	sodium dodecyl sulphate-polyacrylamide gel electrophoresis
TAE	Tris-acetate-EDTA buffer
TBE	Tris-borate-EDTA buffer
TEMED	N,N,N',N-tetramethylethylenediamine
UV	ultra violet
XGAL	5-bromo-4-chloro-3-indolyl- β -D-galactoside

Other abbreviations are explained where appropriate in the text.

LIST OF FIGURES AND TABLES

CHAPTER 1: INTRODUCTION

Figure 1.3.1	Schematic overview of the function of molecular chaperones and folding catalysts.....	4
Figure 1.5.1	Oxidation of protein thiolates into a disulphide bond	7
Figure 1.5.2	Isomerisation of disulphide bonds	7
Figure 1.6.1	<i>cis/trans</i> isomerisation	9
Figure 1.13.1	The biogenesis of the inner membrane proteins.....	16
Figure 1.13.2	The biogenesis of bacterial outer membrane proteins	17
Figure 1.13.3	Overview of periplasmic & outer membrane folding factors...	18
Figure 1.13.4	Biogenesis of OMPs in Gram-negative bacteria	19
Figure 1.14.1	Three dimensional structure of FkpA.....	20
Figure 1.15.1	Three dimensional structure of PpiA.....	21
Figure 1.16.1	Domain structure of SurA.....	22
Figure 1.16.2	Three dimensional structure of SurA.....	23
Figure 1.17.1	Domain structure of PpiD.....	25
Figure 1.18.1	ClustalW alignment of the N-terminal binding site.....	28

CHAPTER 2: MATERIAL AND METHODS

Table 2.2.1	<i>E.coli</i> strains.....	31
Table 2.3.1.1	Antibiotics stock and working concentration.....	32
Table 2.3.1.2	Percentage of components in Luria broth.....	32
Table 2.4.8.1	Components required for the pGEM-T easy ligation.....	36
Table 2.5.1.1	Table showing the components of a general PCR	40
Table 2.6.10.1	Resolving gel composition.....	47
Table 2.6.10.2	Stacking gel composition.....	48
Figure 2.7.1.1	Semi-dry blotting.....	50

Table 2.9.3.1	Mutagenesis programme.....	56
---------------	----------------------------	----

CHAPTER 3: FULL LENGTH SURA AND THE N-TERMINAL FRAGMENT OF SURA

Figure 3.1.1	Diagram showing the different fragments of SurA cloned ...	64
Figure 3.2.1	SDS-PAGE showing the differences in the expression level of the different fragments of SurA.....	65
Figure 3.2.2	SDS-PAGE showing the proteins are soluble.....	66
Figure 3.2.3	Hex-His antibodies.....	67
Figure 3.3.1	Immunodecorated western blot indicating that SurA antibodies bind to the N-terminal fragment of SurA	68
Figure 3.4.1	Outline of the protein purification steps.....	69
Figure 3.4.1.1	Purification of SurA.....	71
Figure 3.4.1.2	Purification of SurA.....	71
Figure 3.4.2.1	Purification of the N-terminal fragment of SurA.....	73
Figure 3.4.2.2	Purification of the N-terminal fragment of SurA.....	73
Figure 3.5.1.1	Resource Q fractions.....	75

CHAPTER 4: BINDING OF PEPTIDES TO SURA AND THE N-TERMINAL FRAGMENT

Figure 4.2.1	NHS-ester reaction scheme	82
Figure 4.2.2	Cross-linker DSG.....	83
Figure 4.3.1	Direct coupling of the Bolton-Hunter reagent to Lysine residues.....	84
Figure 4.4.1.1	Direct crosslinking of radiolabelled peptides to protein.....	85
Figure 4.4.2.1	Competition Assay.....	86

Figure 4.5.1	Crosslinking of radiolabelled peptide to recombinant SurA in cell lysate.....	88
Figure 4.6.1	Interaction of SurA with model peptides by direct binding assay.....	89
Figure 4.6.2	Interaction of SurA with model peptides by competition assay.....	90
Table 4.7.1	Competition between peptides and radiolabelled Δ -somatostatin for the binding to SurA.....	91
Table 4.8.1	Direct binding of radiolabelled peptides to SurA.....	93
Figure 4.10.1	Δ -somatostatin STD-NMR contacts with SurA.....	95
Figure 4.10.2	NMR spectra for the interaction between Δ -somatostatin and SurA and PpiD.....	96

CHAPTER 5: MOLECULAR MODELING OF SURA

Figure 5.1.1	The crystallographic structure of SurA.....	99
Figure 5.2.1	X-Ray crystallographic structure of wild-type SurA without hydrogen atoms.....	102
Figure 5.2.2	X-Ray crystallographic structure of wild-type SurA.....	102
Figure 5.2.3	Original wild-type X-ray structure overlaid with the new wild-type structure of SurA.....	103
Figure 5.2.3.1	Orientation of the N-terminal domain of the wild-type SurA with the addition of hydrogen atoms.....	104
Figure 5.3.2.1	X-Ray crystallographic structure of native SurA with mutated residues highlighted.....	105
Table 5.3.2	Residues selected and their changes.....	106
Figure 5.3.3.1	Overlay of the wild-type SurA with hydrogen atoms and mutated SurA with A64P.....	107
Figure 5.3.3.2	Individual side views of the wild-type SurA and the mutated protein A64P.....	108
Figure 5.3.3.3	N-terminal fragments of the wild-type SurA and the	

	mutated protein A64P.....	108
Figure 5.3.4.1	Overlays of the wild-type SurA and mutants of SurA where residues outside the main core have been altered	109
Figure 5.3.5.1	Overlay of the wild-type SurA and the R73D mutant.....	111
Figure 5.3.5.2	Comparison between the wild-type SurA and the R73D mutant.....	112
Figure 5.3.5.3	N-terminal fragment of wild-type SurA and the R73D mutant.....	112
Figure 5.3.6.1	Overlay of the wild-type SurA and the A64V mutant.....	113
Figure 5.3.6.2	Comparison of the wild-type SurA and the A64V mutant....	114
Figure 5.3.6.3	Comparison of the N-terminal fragment of wild-type SurA and the A64V mutant.....	114
Figure 5.3.7.1	Overlay of the wild-type SurA and the I75S mutant.....	115
Figure 5.3.7.2	Comparison the wild-type SurA and the I75S mutant.....	116
Figure 5.3.7.3	Comparison the N-terminal fragment of wild-type SurA and I75S mutant.....	116
Figure 5.3.8.1	Overlay of the wild-type SurA and A99V mutant.....	117
Figure 5.3.8.2	Comparison of the wild-type SurA and the A99V mutant....	118
Figure 5.3.8.3	Comparison of the N-terminal fragment of wild-type SurA and the A99V mutant.....	118
Figure 5.3.9.1	Overlay of the wild-type SurA and the K90R mutant.....	119
Figure 5.3.9.2	Comparison between the wild-type SurA and the K90R mutant.....	120
Figure 5.3.9.3	Comparison between the N-terminal fragment of the wild-type SurA and the K90R mutant.....	121
Table 5.4.1	Table of differences in Å between wild-type residues and Mutants.....	122
Figure 5.5.1	SurA mutants and binding to the radiolabelled peptide.....	123

CHAPTER 6: PPIID

Figure 6.1.1	Diagram showing the domain architecture of PpiD	126
Figure 6.2.1	Flow diagram outlining protein purification steps.....	129
Figure 6.2.2	PpiD purification on a nickel-nitrilotriacetic acid column ...	130
Figure 6.2.3	Purification fractions from the Resource Q column.....	131
Figure 6.2.4	Expression of PpiD.....	132
Figure 6.3.1	Antibodies against PpiD.....	133
Figure 6.4.1	Proteinase K Digest of PpiD.....	134
Table 6.4.2	Sequencing of 45kDa fragment of PpiD from proteinase K digests.....	135
Figure 6.4.3	Sequence Alignment of PpiD and the Small Sequence by Proteinase K digest.....	136
Figure 6.5.1	PCR Products for Full Length PpiD and Fragment VAQQ....	137
Figure 6.5.2	Lysate and purified samples of PPIases.....	139
Figure 6.5.1.1	VAQQ PpiD binds radiolabelled peptide.....	140
Figure 6.6.1	Amino acid sequence of full length PpiD.....	141
Figure 6.6.2	PCR products for PpiD2 and PpiD3.....	142
Figure 6.6.3	PCR products for PpiD3.....	142
Figure 6.6.4	Fractions from PpiD3 purification.....	143
Figure 6.6.5	Fractions of PpiD2 purification.....	144
Figure 6.6.6	Binding assay for different PPIases including PpiD2 and PpiD3.....	144
Figure 6.7.1.1	Interaction of PpiD with 'scrambled' RNase.....	146
Figure 6.7.2.1	Interaction of PPIases with labelled Δ -somatostatin.....	147
Figure 6.7.2.2	Interaction of PpiD with model peptides.....	149
Figure 6.7.3.1	PpiD and SurA binding comparison.....	150
Figure 6.7.3.2	Competition between peptides and radiolabelled Δ - somatostatin for the binding to PpiD and SurA.....	151
Figure 6.8.1	STD contact with PpiD.....	153
Figure 6.8.2	Data for STD-NMR.....	154
Figure 6.8.3	Data for STD-NMR.....	154
Figure 6.9.1	Diagram showing PpiD.....	155

CHAPTER 7: GENERAL DISCUSSION

Figure 7.2.1	Crystal structure of SurA with colour coding of individual domains.....	159
Figure 7.2.2	Peptide binding to SurA.....	160
Table 7.3.2.1	Competition between peptides and radiolabelled Δ -somatostatin for the binding to SurA and PpiD.....	163
Table 7.4.1	Peptides without the Ar-X-Ar motif that bind to SurA.....	166
Figure 7.6.1	Domains of PpiD.....	168

ABSTRACT

Over the last 30 years there has been deep interest into the folding of proteins and the mechanisms in which they fold. One of the rate limiting steps of protein folding has been shown to be the *cis/trans* isomerisation of proline residues, which is catalysed by a range of peptidyl prolyl *cis/trans* isomerases (PPIases). In the periplasmic space of *E.coli* and other gram-negative bacteria two PPIases, SurA and PpiD, have been identified, which show high sequence similarity to the catalytic domain of the small PPIase parvulin. This observation raises the question about the biological significance of two apparently similar enzymes being present in the same cellular compartment: Do they interact with different substrates or do they catalyse different reactions? SurA has recently shown to be an important function in the formation of outer membrane porins and the pilus. Recent developments have revealed the crystallographic structure of SurA, indicating a possible region that could act as a binding cleft which corresponds to an area that has been shown to bind peptides. The substrate binding motif of PpiD has not been characterised so far and no biochemical data have been available on how this folding catalyst recognizes and interacts with substrates.

To characterise the interaction between model peptides and the periplasmic PPIases PpiD and SurA from *E.coli*, a chemical cross-linking strategy was employed that has been used previously to elucidate the interaction of substrates with PDI.

It was found that PpiD interacted with a range of model peptides independent of whether they contained proline residues or not. It was further demonstrate here that PpiD and SurA could interact with similar amino acids in a specific model peptide and therefore have overlapping substrate recognition motifs. However, the binding motif of PpiD is less specific than the one of SurA, indicating that the two PPIases might interact with different substrates, which was confirmed by *in vivo* crosslinking. We therefore propose that although PpiD and SurA have overlapping substrate recognition motifs they fulfil different functions in the cell. Molecular modeling coupled with mutagenesis has highlighted residues within SurA that are significant for the overall structure of the protein and subsequently the binding ability. This study has also shown that the N-terminal domain of SurA alone is sufficient for the binding

of peptides and does not require the C-terminal domain for binding but does require the C-terminal domain for stability.

Chapter 1

Introduction

1.1 INTRODUCTION

Over 60 years ago Anfinsen asked the questions how proteins fold into their distinctive three-dimensional shapes. Were they assisted by other enzymes and why do they adopt this particular structure? Using a model, in this case bovine pancreatic ribonuclease (RNase), Anfinsen and postdoctoral students Michael Sela and Fred White observed that the RNase can spontaneously, i.e. without the assistance of other enzymes, fold into its active form. Anfinsen called the resulting structure, although not known at this time, the enzyme's "native conformation". In a ground breaking article in the *Journal of Biological Chemistry* in 1954, Anfinsen showed that the folding pattern in a polypeptide chain is determined by sequence of the amino acids. Thus the mysterious and complex process of protein folding could be explained entirely by the physical and chemical interactions among the amino acid side groups (Anfinsen et al., 1954).

Later, in 1962, Anfinsen had developed what he called his "thermodynamic hypothesis" of protein folding to explain the native conformation of proteins. He hypothesized that the native or natural conformation occurs because this particular structure is thermodynamically the most stable in the intracellular environment. To test this hypothesis, Anfinsen chemically unfolded RNase with the chaotropic agent urea under reducing conditions. He observed that the enzyme refolded spontaneously back into its original form when he returned the chemical environment to natural cellular conditions (Anfinsen et al., 1961; Haber and Anfinsen, 1962). As he stated ten years later, in his 1972 Nobel Prize acceptance speech, "The native conformation is determined by the totality of interatomic interactions and hence by the amino acid sequence, in a given environment."

However, this hypothesis did not explain why some proteins do not fold spontaneously into their native conformations and why some proteins show aggregation upon folding. That proteins fold at all within a biologically reasonable time span is surprising after all. Assuming a relatively small polypeptide chain comprising 100 amino acids and also assuming that each amino acid can position itself in three different spatial orientations (which is probably a gross underestimate) the folding polypeptide chain can adopt $3^{100} = 10^{47}$ different conformations, only one of which is the native one. If all of these conformations were to be queried randomly,

allowing only 10^{-12} seconds for each conformation to be probed, then finding the thermodynamically most stable conformation would take 10^{35} seconds, or 3×10^{27} years. According to this calculation, termed Levinthal's paradox, proteins do not fold by a random process in which every single conformation is probed (Levinthal, 1968). Since protein folding operates on a very different timescale (milliseconds to minutes in most cases) a different mechanism of protein folding has to be postulated. Levinthal therefore postulated that a folding polypeptide chain follows a specific path to the final configuration, and therefore folding must be under kinetic control (i.e., under the control of a specific sequence of reactions). If the final, native state was one of lowest configurational energy, it would be a consequence of the biological evolution of specific chemical reaction sequences ("kinetic control"), and not of physical chemistry and the laws of thermodynamics ("thermodynamic control") (Levinthal, 1968).

1.2 PROTEINS AND FOLDING

A central dogma of biochemistry is that only proteins in their native conformation can perform their specific biological function. In other words, a misfolded protein will be biologically inactive. Examples of incorrect protein folding have been shown in many diseases including diabetes (Aridor and Balch, 1999) and Alzheimer's disease (Lomas and Carrell, 2002). Over the last few decades there has been increasing interest in the processes that lead to misfolding, which can be triggered by several factors such as heat or cold shock, osmotic shock, toxins, and heavy metal; and how the cell prevents misfolding and subsequent aggregation of proteins.

Early concepts of protein folding postulated the existence of 'templates' that somehow caused a folding polypeptide chain to adopt its native conformation. However, there still was the need to explain as to why or how the template obtained its native conformation. *In vitro* proteins often fold slowly into their native conformation whereas *in vivo* polypeptides fold quickly into their native conformations as they are being synthesized. The reason for this is that cells contain accessory proteins called molecular chaperones or folding catalysts that assist the folding of the protein (Gething and Sambrook, 1992) (figure 1.3.1).

1.3 MOLECULAR CHAPERONES AND FOLDING CATALYSTS

In general there are two types of proteins that assist in the protein folding process, specifically molecular chaperones and folding catalysts.

In 1978 Laskey coined the phrase ‘molecular chaperone’ for proteins involved in the folding of some polypeptide chains that were unable to correctly fold spontaneously *in vitro* (figure 1.3.1) (Laskey et al., 1978). These molecular chaperones are a ubiquitous family of proteins whose proposed role is to mediate the folding of polypeptides and the assembly into oligomeric complexes.

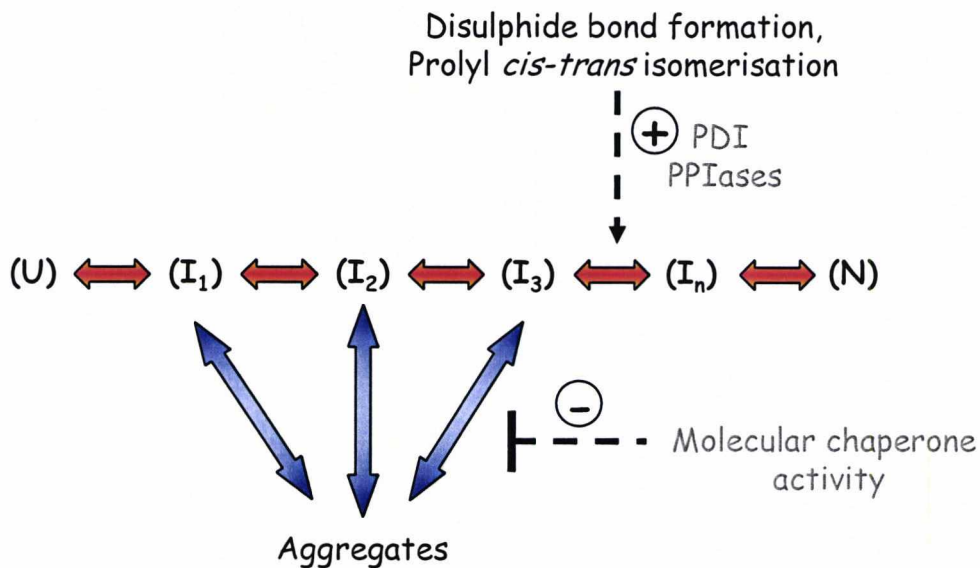


Figure 1.3.1 Schematic overview of the function of molecular chaperones and folding catalysts. Folding catalysts enhance the rate of slow folding steps, i.e. disulphide bond formation or peptidyl prolyl *cis/trans* isomerisation, whereas molecular chaperones prevent the aggregation of folding intermediates. U, unfolded polypeptide chain; I_x, folding intermediates; N, native conformation.

This essential function is achieved by preventing the formation of incorrectly folded structures, which may result from the transient exposure of usually hydrophobic surfaces on the folding polypeptide chains. This may occur during the synthesis of polypeptides, the unfolding and refolding while being transported across membranes, changes in protein-protein interactions during the physiological functioning of a complex, and recovery from stresses such as heat or cold shock.

Two types of folding catalysts have been characterized so far: those that catalyse disulphide exchange, thus ensuring native disulphide bond configuration, and those that catalyse the otherwise slow *cis/trans* isomerisation of peptidyl prolyl bonds (Schiene and Fischer, 2000).

1.4 PROTEIN FOLDING COMPARTMENTS

Eukaryotic cells comprise a number of compartments that perform different, but essential functions, thus contributing to the viability of the whole cell. In mammalian cells the endoplasmic reticulum (ER) and the cytoplasm are key compartments in which the folding of polypeptide chains occurs. For gram-negative bacteria the cytoplasm and an extracytoplasmic compartment between the outer cell wall and the inner membrane, called the periplasmic space, are involved in protein folding.

1.4.1 The Cytoplasm

Molecular chaperones like trigger factor, Hsp70, and prefoldin prevent nascent polypeptide chains on the ribosome from adopting non-native conformations, which may lead to aggregation. Subsequent folding of these chains in the cytosol is then achieved either by controlled chain release from these factors or after transfer of newly synthesized proteins to downstream chaperones, such as the chaperonins. These are large, cylindrical complexes that provide a central cavity large enough to accommodate a single polypeptide chain thus preventing aggregation and allowing the folding polypeptide to adopt its native conformation.

1.4.2 The Endoplasmic Reticulum and periplasmic space

The ER contains proteins that are essential for the folding and post-translational modification of secreted and membrane proteins (Feldman and Frydman, 2000; Gething and Sambrook, 1992; Gilbert, 1997). As proteins are transported through the

Sec61 translocon into the ER the polypeptide chain immediately begins the folding process (Brodsky, 1998). The chaperones in the ER, like their counterparts in the cytoplasm, prevent the aggregation of the folding polypeptides. They also serve as a quality control mechanism that recognises and selectively retains misfolded proteins before exit from the ER. This interaction then allows more time for the correct folding to occur. Failure of adopting its native conformation will ultimately result in the degradation of the misfolded protein (Cox et al., 1997). This can occur by ER-associated protein degradation (ERAD), which eliminates misfolded or unassembled proteins from the ER. ERAD targets are selected by a quality control system within the ER lumen and are ultimately destroyed by the cytoplasmic ubiquitin–proteasome system (Meusser et al., 2005).

Functionally similar to the ER is the periplasmic space of prokaryotic cells. Like the ER it contains a number of folding catalysts and molecular chaperones involved in the folding of newly translocated proteins.

1.5 OXIDATIVE FOLDING OF PROTEINS IN THE ER AND PERIPLASMIC SPACE

An important factor in the folding of various proteins is the formation of disulphide bonds, which stabilise the native conformation of the folding polypeptide chain. This oxidative folding process is assisted by the redox conditions in the ER lumen and the periplasmic space, respectively, as both compartments are more oxidizing than the respective cytosol (Fink, 1999). In addition to the redox conditions, both compartments also host folding catalysts that catalyse disulphide bond formation and rearrangement (Gilbert, 1997).

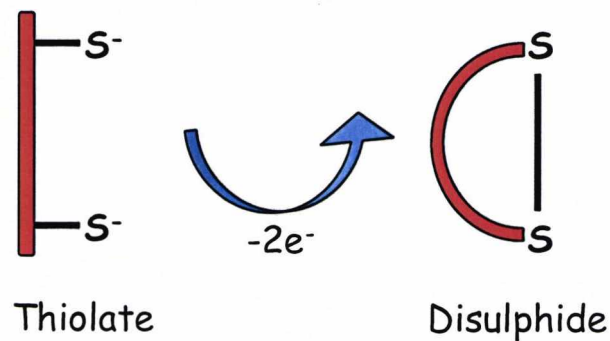


Figure 1.5.1. Oxidation of protein thiolates into a disulphide bond. Thiolates of cysteine residues are oxidized into a disulphide bond. This process leads to the loss of two electrons.

In eukaryotes the main oxidative folding catalyst is protein disulphide isomerase (PDI), which has been shown to function as a molecular chaperone and folding catalyst. PDI inserts disulphide bonds into folding proteins and also facilitates disulphide bond isomerisation (Gething and Sambrook, 1992; Gilbert, 1997). See figures 1.5.1 and 1.5.2.

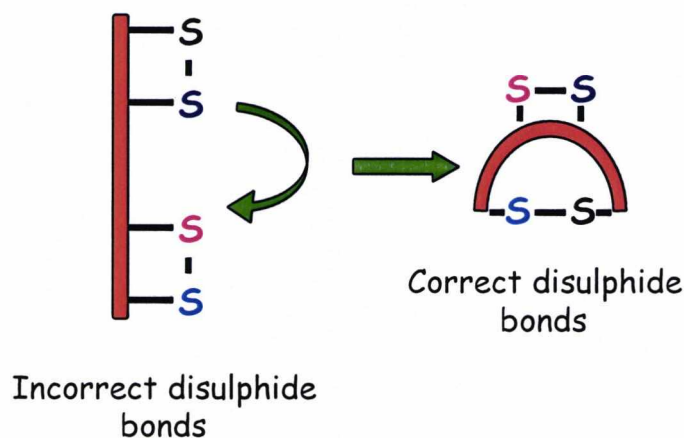


Figure 1.5.2 Isomerisation of disulphide bonds. An incorrectly formed pair of disulphide bonds is rearranged into the correct ensemble. This process is electro-neutral.

Along with PDI another important protein in the oxidation process is the ER-resident protein Ero1p. Ero1p plays an analogous role to the bacterial periplasmic protein DsbB. Both Ero1p and DsbB specifically oxidize a thioredoxin-like protein (PDI in

eukaryotes, DsbA in bacteria) that serves as an intermediary in the transfer of oxidizing equivalents to folding proteins (Bardwell et al., 1993; Frand and Kaiser, 1999; Tu et al., 2000). Molecular oxygen can serve as the terminal electron acceptor for disulphide formation in both prokaryotes and eukaryotes (Bader et al., 1999; Tu and Weissman, 2002). Under anaerobic conditions, the DsbB–DsbA system can support disulphide formation via alternate electron acceptors, such as fumarate (Bader et al., 1999). However, while in bacteria oxidative folding is coupled to molecular oxygen through the respiratory chain, Ero1p uses a flavin-dependent reaction to pass electrons directly to molecular oxygen (Tu and Weissman, 2002).

Past studies showed that peptides can bind PDI via hydrophobic interactions, which has also been observed with other molecular chaperones e.g. heavy chain binding protein BiP. However since PDI displays enzymatic activity, it is not clear whether this interaction is indicative of a distinct role as a molecular chaperone or whether it is an intrinsic property of the mechanism by which PDI acts as a catalyst of disulphide bond formation (Feldman and Frydman, 2000).

The periplasmic space of prokaryotes also contains proteins with similarity to the enzymatically active domains of PDI, specifically the Dsb proteins (Chen et al., 1999). These perform the various thiol-disulphide exchanges, oxidation, reduction or isomerisation of disulphide bonds. The *E.coli* cytoplasm is comparatively more reducing than the periplasm therefore the cytoplasm contains very few proteins with disulphide bonds (Missiakas and Raina, 1997).

1.6 PEPTIDYL PROLYL CIS/TRANS ISOMERISATION

Another slow step in the folding of a protein may be the *cis/trans* isomerisation of the proline residues. Unlike disulphide bond formation, however, this process is not restricted to specific redox conditions and hence occurs in every intracellular compartment, in which protein folding commences, e.g. in the ER, cytoplasm, mitochondria in eukaryotes and periplasmic space and cytoplasm in prokaryotic cells. Of all the twenty amino acids, proline is the most likely to adopt the *cis* conformation in peptide bonds, because of its unique side chain. In general, the peptide bond has partial double bond character and can exist in two conformations, either in the *cis* or

in the *trans* form. In every amino acid, except proline, steric hindrance between the adjacent side chains strongly disfavour the *cis* isomer but not the *trans* configuration (figure 1.6.1). However, in proline the side chain is linked to the back bone nitrogen, thereby reducing the energy difference between the two conformations. As a consequence non-prolyl peptide bonds are always in the *trans* conformation and only where there is a proline residue present the *cis* conformation of the peptidyl prolyl bond has been observed.

It is thought that all proteins are synthesised at the ribosome with bonds in the *trans* configuration, however, the native state of many proteins require specific prolyl peptidyl bonds to be present in the *cis* conformation. For example the slowest step in the folding of denatured RNase A is the isomerisation of the peptide bond around Pro 93. By the use of a *trans* proline-specific peptidase it has been established that 80% of unfolded RNase A exists in a slow folding form with Pro 93 in the *trans* form. The remaining 20% of the unfolded form has Pro 93 in the *cis* form, which can rapidly fold into the native state. Therefore it appears that the energy barrier of forming the *cis* proline isomer limits the rate of folding (Kiefhaber et al., 1990; Texter et al., 1992). Mutagenesis studies have shown that specific proline residues can be assigned to slow recovery phases from misfolded states (Evans et al., 1987; Hering et al., 1991; Kelley and Richards, 1987; Kiefhaber et al., 1990; Texter et al., 1992; Wood et al., 1988). However, in some cases complete refolding is required for a protein to escape from its misfolded state caused by proline isomerisation (Brandts et al., 1975).

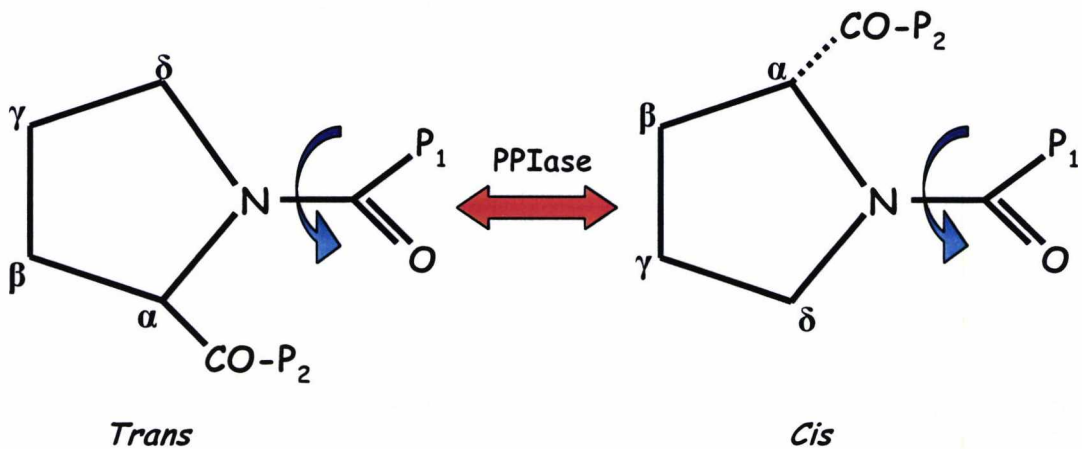


Figure 1.6.1 *cis/trans* isomerisation. Schematic presentation of *cis/trans* isomerisation about the peptidyl-prolyl bond catalysed by a PPIase. Blue arrows indicate the rotation.

The isomerisation reaction can occur spontaneously, however several specific enzymes have been isolated that can catalyse *cis/trans* isomerisation. These are called peptidyl-prolyl *cis/trans* isomerase or PPIases.

1.7 DISCOVERY OF PPIASES

In the 1980's an 18 kDa enzyme was extracted from pig kidney cortex that was claimed to be able to accelerate *cis/trans* isomerisation of the peptidyl-prolyl bond (Fischer et al., 1984). Handschumacher *et al.* and others reported the isolation of an 18 kDa protein from calf thymus cytosol (Handschumacher et al., 1984), which had a strong binding affinity to Cyclosporin-A (CsA), a cyclic immunosuppressive undecapeptide, and hence this protein was called cyclophilin (Handschumacher et al., 1984; Harding et al., 1986). In 1989 it was shown that the porcine 18 kDa cyclophilin and the PPIase had identical sequences. This result established a correlation between the catalytic activity of cyclophilin, its binding to the CsA and the basis of immunosuppression that had been induced by CsA (which was not well understood at the time)(Fischer et al., 1989; Takahashi et al., 1989). In the same year another family of PPIases was discovered, but the sequences of these enzymes were unrelated to the cyclophilins. Since these proteins had strong affinities to different immunosuppressive drugs, i.e. macrolide antibiotics FK506, ascomycin and rapamycin, this group was named FK506 binding proteins (FKBPs) (Harding et al., 1989). It was later shown that blocking the PPIase activity of cyclophilin-A or FKBP-12 by these immunosuppressive drugs was essential for immunosuppression (Siekierka et al., 1989a; Siekierka et al., 1989b) and hence these PPIases were named immunophilins (Fischer et al., 1998; Galat and Riviere, 1998; Schonbrunner and Schmid, 1992).

Four distinct families of PPIases have been identified so far, specifically the FKBPs, for example FkpA, the cyclophilins, for example RotA and RotB, and members of the parvulin family, for example SurA and PpiD, and trigger factor. Although there is sequence and structural similarity within the individual families, no sequence similarities between the FKBPs, the cyclophilins and the parvulins exist.

Since the various PPIases are highly conserved between pro- and eukaryotes it was inferred that they play an essential role in protein folding and loss of one of them would cause lethality, however this is not the case for most of the proteins (Gething, 1997).

PPIases are generally considered as folding catalysts, enhancing the otherwise slow *cis/trans* isomerisation around a peptidyl prolyl bond, however, some of the PPIases, such as SurA and trigger factor may also have activity as molecular chaperones.

1.8 THE ROLES AND FUNCTIONS OF THE PPIASES

The variety of functions performed by the PPIases is vast and highlights their significance and importance for the cell. Cyclophilins, FKBP's and parvulins have all been shown to catalyse the protein folding of RNase T1 *in vitro* (Dolinski et al., 1997; Scholz et al., 1997a). Cyclophilins and FKBP's, but not parvulins, have been reported to catalyse reactions in the vesicular pathway. One such example is the ER cyclophilin B, which is believed to be involved in the chaperoning of plasma membrane proteins such as apolipoprotein (Zhang and Herscovitz, 2003) through the secretory pathway (Price et al., 1994; Price et al., 1991). The human parvulin Pin1 has been reported to activate Bcl-2 by catalysing *cis/trans* isomerisation in the proline rich loop region (Pathan et al., 2001). Furthermore PPIases are involved in cell signalling processes (Abbott et al., 1998; Walsh et al., 1992), acting on transcription factors, steroid receptors, receptor protein kinases, the CD147 receptor, calcium release channels, mitochondrial-permeability transition pores, and components involved in apoptosis.

Cyclophilin A has been shown to help protect cells from oxidative stress brought on by the treatment with peroxide, possibly through its binding to the antioxidant protein Apo1 (Doyle et al., 1999) or through the activation of the peroxidase activity of peroxidins (Lee et al., 2001). Heat stress has been shown to up regulate the expression of some PPIases in rat myogenic cells (Andreeva et al., 1997), *S.pombe* (Weisman et al., 1996), *S.cerevisiae* (Gasch et al., 2000), *N.crassa* (Faou and Tropschug, 2003) and wheat cells (Dwivedi et al., 2003), with these observations mainly related to the heat

shock protein 90 (Hsp90) associated with cyclophilin 40 (Yokoi et al., 1996a; Yokoi et al., 1996b).

Other known functions of the PPIases include cell cycle regulation through Pin1 (Lu et al., 1996); (Yaffe et al., 1997), transcription (Yang et al., 1995), splicing (Horowitz et al., 2002), translation, nuclear pore export factors (Singh et al., 1999) and sugar enzyme trafficking (Hoffman and Chiang, 1996).

1.9 CYCLOPHILINS

The first cyclophilin identified was cyclophilin-A (Cyp-A), an 18 kDa cytoplasmic protein with peptidyl prolyl *cis/trans* isomerase activity that could be inhibited by cyclosporine A (Fischer et al., 1989). Various types of transcripts of cyclophilin genes have been discovered in eukaryotes, whereas in prokaryotes there is less diversity. *E.coli* has only two isoforms of cyclophilin, one cytosolic and one periplasmic. The size of the archetype cyclophilin may vary from 15 kDa in prokaryotes to 18 kDa in mammalian cells. Several members of the Cyp-A subgroup have been found in prokaryotes. *Bacillus subtilis* and *Synechococcus* sp. contain a 15 kDa acidic Cyp-A homologue. The cytoplasmic isoform has an acidic pI (CSCEB), whereas the highly basic counterpart (CSCEA) is translocated into the periplasm (Galat and Riviere, 1998). *E.coli* cyclophilins exhibit significantly reduced affinity for CsA, compared to eukaryotic cyclophilins, due to the presence of a polar residue that protrudes over the active site thus preventing the access of the CsA to the substrate binding pocket of the cyclophilin molecule (Konno et al., 1996).

1.10 FK506-BINDING PROTEINS

The FKBP's are ubiquitous proteins as various numbers of transcripts have been found in both eukaryotes and prokaryotes. Particular FKBP's have well defined cellular functions; for example the mammalian proteins, FKBP-12 is involved in the co-regulation of various molecular complexes while FKBP-13 and FKBP-52 are overproduced in response to heat shock (Galat and Riviere, 1998).

In prokaryotes, the cellular function of the FKBP is not as clearly defined. FKBP-12, FKBP-13, FKBP-25 and FKBP-38 have only one FK506 binding domain but the FKBP-52, FKBP-54 and FKBP-61 contain three or four sequence repeats specific for the FK506 binding domain (Galat and Riviere, 1998). Their functions remain to be established, although acidic FKBP-12 from *E.coli* has sequence homology with the mammalian FKBP-12. An FKBP-12 like sequence was also located in the operon encoding leader peptidase complex in *E. coli* and *Enterobacter aerogenes* (Wulfing et al., 1994). FKBP-20 has two different domains, a FKBP-like N-terminal domain and a C-terminal metal binding domain.

1.11 TRIGGER FACTOR

Trigger factor is a 48 kDa PPIase that has been found associated with the ribosome and hence an involvement in *de novo* protein folding has been postulated (Stoller et al., 1996). It was discovered during biochemical screening of the cytosolic components of the secretion machinery in *E.coli* (Crooke and Wickner, 1987). When the translocation of outer membrane protein A (OmpA) across the inner membrane was analyzed an activity was identified that stabilized the precursor of the OmpA in a loosely folded conformation thereby stimulating its membrane translocation (Crooke and Wickner, 1987; Hesterkamp and Bukau, 1996). Trigger factor is co-regulated with the genes that encode ribosomal components and can be isolated from ribosomal fractions of *E.coli* (Galat and Riviere, 1998). Studies of protein folding *in vivo* showed that trigger factor possess PPIase activity (Hesterkamp and Bukau, 1996). Trigger factor does not bind FK506 (Stoller et al., 1996) or CsA although it does have low sequence similarity with the FKBP family of proteins (Zarnt et al., 1997). Trigger factor has a catalytically active PPIase domain that catalyses the rate of folding of RNase T1 more efficiently than the cyclophilins or FKBP (Schmid, 1993; Zarnt et al., 1997). Trigger factor binds with high affinity to the unfolded RNase T1, and this function is the prerequisite for the excellent catalysis of protein folding (Scholz et al., 1997b). In cells where the deletion of the *tig* gene is accompanied by the absence of DnaK and DnaJ cells die above 30 °C and newly synthesized proteins aggregate. It has been shown that in wild type *E. coli* cells, about 9% to 18% of

newly synthesized proteins interact transiently with DnaK, but in the absence of Trigger Factor, this level is increased 2- to 3-fold, indicating that, upon loss of Trigger factor, DnaK can associate with the nascent polypeptide (Deuerling et al., 1999; Schaffitzel et al., 2001; Teter et al., 1999). In addition, it was shown that deletion of the *tig* gene induces the heat shock response in *E.coli* thereby leading to a compensatory increase in the steady state levels of chaperones, including DnaK (Deuerling et al., 2003). Therefore DnaK may serve as a back-up system in the absence of Trigger factor (Deuerling and Bukau, 2004). It has been shown that cells can be rescued from the effects due to the absence of Trigger factor and DnaK, either by the cell growth below 30 °C or by overproduction of the GroEL/GroES (Vorderwulbecke et al., 2005).

Like FkpA Trigger factor exhibits both PPIase activity and chaperone activity. It was shown that both activities take place in the same binding pocket of the central binding domain (Ramm and Pluckthun, 2001). It has also been shown in recent studies that trigger factor recognizes protein substrates independently of proline residues (Fischer et al., 1989; Galat and Riviere, 1998). Interestingly the PPIase activity of trigger factor is not essential for the folding of newly synthesized proteins (Kramer et al., 2004). In addition to its chaperone activity trigger can also act as an ‘anti-chaperone’ as it has been shown to directly promote the formation of protein aggregates under certain conditions (Callebaut and Mornon, 1995; Huang et al., 2002).

1.12 PARVULINS

Parvulin, from the Latin word ‘*parvus*’ meaning ‘small’, is the smallest protein that contains PPIase activity. Parvulin from *E.coli* was isolated and sequenced in 1994 (Rahfeld et al., 1994). The corresponding gene was identified (Rahfeld et al., 1994; Rudd et al., 1995) and shown to be between 84.5 and 86.5 minute on the *E.coli* genome. *E.coli* parvulin has a molecular weight of 10 kDa and a pI of 9.64. It was predicted that parvulin would be made up of mainly helices, which was confirmed by UV-CD spectra. Parvulin has no sequence homology with any of the cyclophilins from prokaryotes or eukaryotes although there is some similarity with FKBP-12 (Rahfeld et al., 1994). Parvulin from *E.coli* is not inhibited by the

immunosuppressant cyclosporin A or FK506. Homologies were found with domains of PrsA from *Bacillus subtilis* (Jacobs et al., 1993; Kontinen and Sarvas, 1993), SurA and PpiD from *E.coli* (Eisenstark et al., 1992), PrtM from *Lactococcus lactis* (Haandrikman et al., 1989), Ptf1/Ess1 from yeast (Hani et al., 1995), and human Pin1 (Lu et al., 1996). All of these proteins seem to be involved in protein folding or activation (Scholz et al., 1997a). Parvulin has catalytic activity that is comparable to the mammalian FKBP's as it has a binding preference for large hydrophobic residue before a proline residue (Hennig et al., 1998; Scholz et al., 1997a).

1.13 PPIASES IN THE PERIPLASMIC SPACE OF PROKARYOTES

The periplasmic space of prokaryotic cells can be regarded as a compartment that, despite of its extracellular location, fulfils important functions essential for the cell. In general this compartment can be compared to the ER in eukaryotic cells with respect to protein folding of secreted proteins and those that are integral proteins of the outer membrane (Outer Membrane Proteins, OMPs). In line with the function of the periplasmic space in protein folding is its specific repertoire of folding catalysts and molecular chaperones, which show some similarity to the ones found in the ER. In addition, even some elements of the translocation machinery, required for the transport of proteins across the inner membrane of prokaryotes and the membrane of ER in eukaryotes, show some structural and functional similarities. In both systems there is efficient targeting of newly synthesized proteins to a 'translocation machinery', which enables the protein to cross the membranous barrier (for extensive comparison translocation components between periplasmic space and ER see (Wiech et al., 1991).

Inner membrane proteins (IMPs) are targeted to in the inner membrane by the signal recognition particle (SRP) (Ulbrandt et al., 1997) which is an evolutionary conserved ribonucleoprotein complex that was first described in mammalian cells. The SRP in *E.coli* has been shown to bind to nascent polypeptides co-translationally (Bernstein, 2000). However, disruption of the SRP pathway has been observed to partially block the insertion of IMPs, suggesting that the insertion can also occur in an SRP

independent manner. Subsequently nascent IMPs are released from the SRP and transferred to the translocon (Scotti et al., 1999; Valent et al., 1998). The translocon has a signal sequence recognition function at the SecY – SecE interface (Bernstein, 2000). The transmembrane segments of the IMPs possibly displace the SecE subunit so that the hydrophobic segments are not exposed to the hydrophilic environment (Newitt and Bernstein, 1998). SecA is required for the translocation of IMPs that contain large periplasmic domains; SecA is not required for proteins that contain only small periplasmic loops or small nascent IMPs (Koch et al., 1999; Scotti et al., 1999). For inner membrane proteins to fold into their native conformation they follow the ‘positive inside rule’, i.e. positively charged loops are orientated towards the cytoplasmic face of the inner membrane. This orientation has not only been observed in prokaryotes but also in eukaryotic cells (von Heijne, 1989). The final formation of the native structure can occur after the translocation is complete, figure 1.13.1 (Bernstein, 2000).

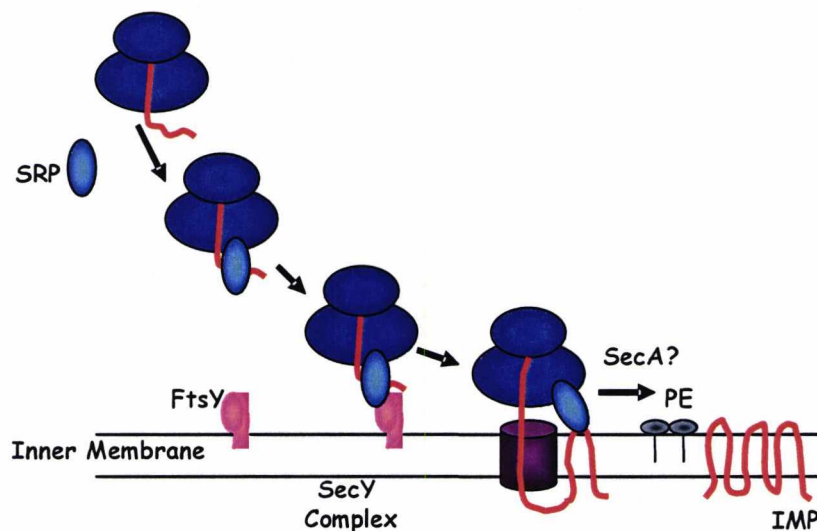


Figure 1.13.1 The biogenesis of the inner membrane proteins. IMPs are targeted to the IM co-translationally by the SRP. Interaction between the SRP and the FtsY catalyses the release of the nascent IMPs and their insertion into the SecY complex. SecA could be required to assist with the insertion of the protein in some cases. Post synthesis PE appears to facilitate the folding in the lipid bilayer to the final conformation.

OMPs follow a slightly different path compared to IMPs. Firstly, SecB appears to play a much more prominent role in the transport of OMPs by binding to mature

regions in the preprotein. This interaction prevents folding, thus facilitating the transit across the inner membrane (Collier et al., 1988; Gannon et al., 1989). In addition, SecB also interacts with the signal sequence and keeps it exposed for interactions with the SecY complex (Bernstein, 2000). The OMPs are then transported across the lipid bilayer by the SecY complex, (figure 1.13.2).

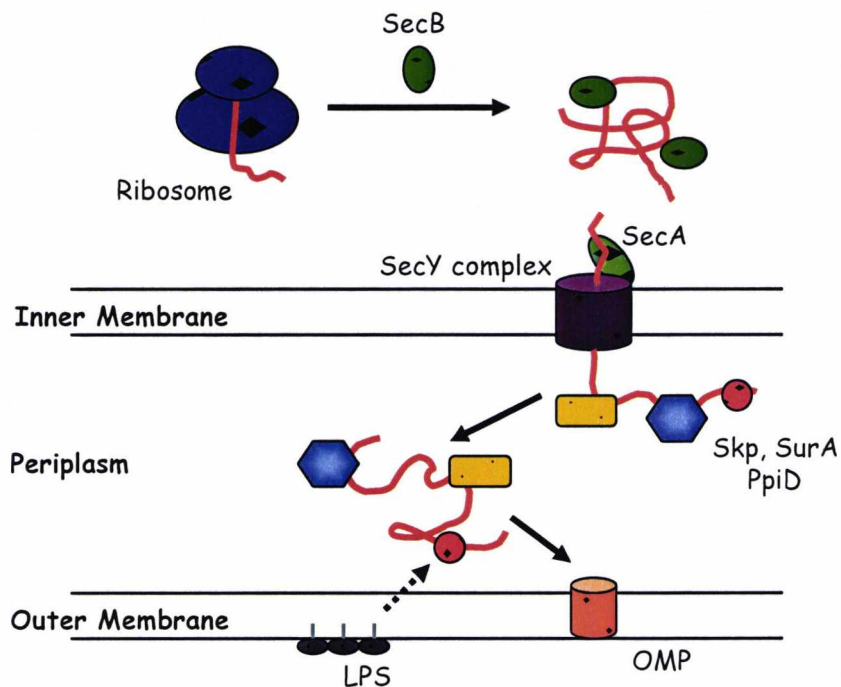


Figure 1.13.2 The biogenesis of bacterial outer membrane proteins. OMPs are targeted to the IM either by the late stage of translation or post-translationally by the molecular chaperone SecB. They are then transported across the membrane through a translocon called the SecY complex. SecA uses the energy of ATP hydrolysis to drive the translocon reaction. Proteins such as SurA may act as molecular chaperones that assist with folding or prevent aggregation of the OMPs during their transit through the periplasm. Interaction with LPS promotes folding into compact β -barrel structure and stabilise the insertion into the outer membrane. Diagram modified from *Bernstein 2000*.

SecA is essential for the translocation of most OMPs and periplasmic proteins and utilizes ATP hydrolysis to provide the energy required to push the protein cross the membrane (Wickner and Leonard, 1996). A number of studies have shown that when the OMPs are over expressed and folded incorrectly they build up in the periplasm. After translocation over the inner membrane by the Sec machinery the leader sequence is removed by a leader peptidase. It is the following stages of OMP biogenesis that are unclear, since OMPs, once in the periplasmic space, must be prevented from folding prematurely and from being inserted into the inner membrane.

The OMPs intermediates must somehow transverse the periplasmic space to arrive at the outer membrane in a conformation that is capable of being inserted into the lipid bilayer. A range of proteins have been identified as being significant for OMP formation, folding and transport, see figure 1.13.3.

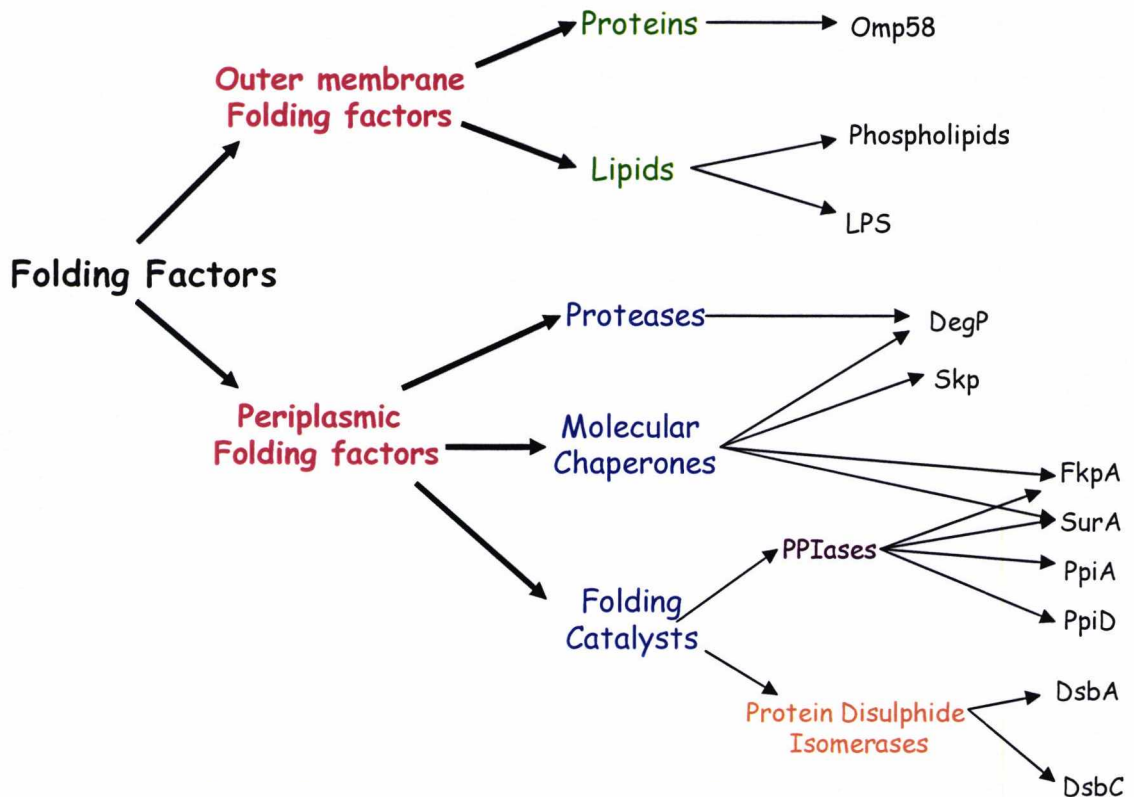


Figure 1.13.3 Overview of periplasmic and outer membrane folding factors. The folding factors that are relevant for understanding of the intermediate and late steps of OMP folding. Note that categorisation of the folding factors is not strict, as some of the proteins display more than one function. Diagram from *Morgensen et al, 2005*.

The most prominent folding catalysts in the periplasmic space involved in the biogenesis of OMPs are PPIases.

Four periplasmic PPIases, SurA, PpiA, PpiD and FkpA have been identified so far, their involvement in biogenesis of OMPs is outlined in figure 1.13.4. Some of these show secondary, non-catalytic chaperone activities and therefore must be considered as molecular chaperones as well as folding catalysts. The proteases DegS and DegP

are linked to OMP biogenesis by maintaining the homeostasis in the periplasm but do not promote the folding of the OMPs (Mogensen and Otzen, 2005).

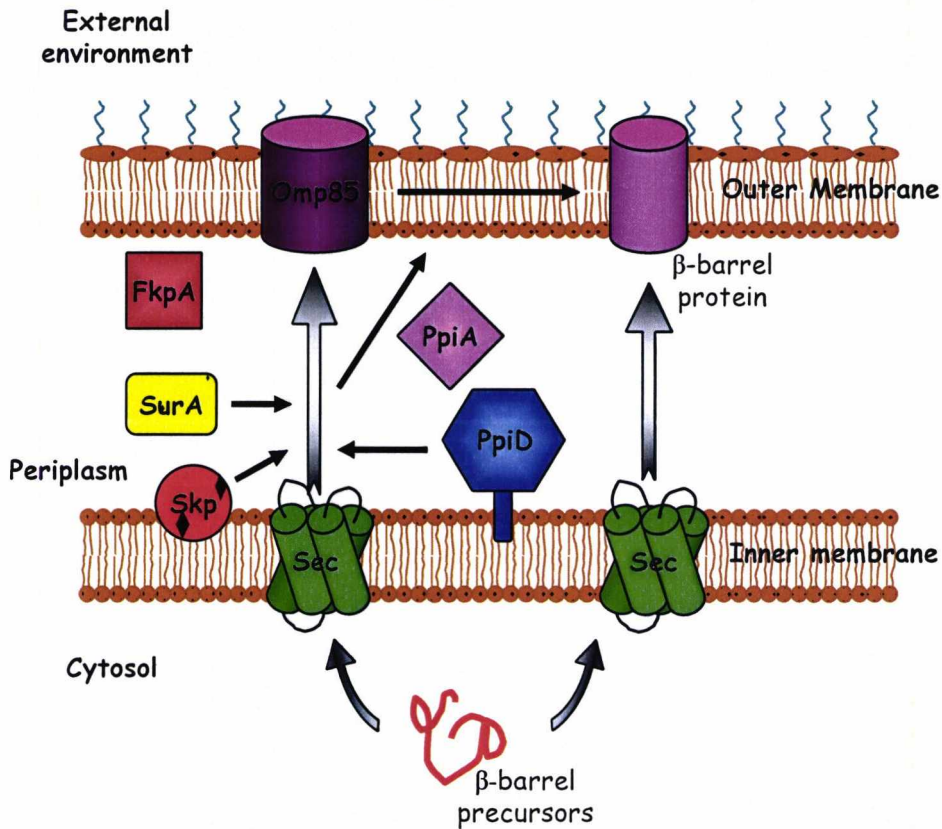


Figure 1.13.4 Biogenesis of OMPs in Gram-negative bacteria. The arrows from SurA, Skp and PpiD show that there is evidence that they are involved in OMP formation, lack of arrows from PpiA and FkpA indicate lack of evidence. There maybe several different pathways of chaperone activity, it is not known whether the periplasmic chaperones deliver OMPs to the outer membrane-integrated Omp85 or whether they are also responsible for the terminal step. Modified from *Morgensen et al, 2005*.

1.14 FKPA

FkpA is a periplasmic PPIase (Bothmann and Pluckthun, 2000; Lazar et al., 1998; Ramm and Pluckthun, 2000) under the control of the σ^E regulon (Missiakas et al., 1996). FkpA exists as a homodimer (Arie et al., 2001) with two subunits comprising of 245 amino acid residues. Each subunit contains an N-domain of ~ 100 amino acids that is important for the chaperone activity (Saul et al., 2004) and the catalytically active C-domain of ~ 110 amino acids. The dimer structure is V-shaped with the N-domains forming the dimer interface and the two 'legs'. Each 'leg' is capped by the

C-domain. It has been suggested that the cleft between the subunits may form the binding site. This would allow the binding of the substrate in a non-native conformation at the dimer interface while at the same time access to the C-domains is provided (Saul et al., 2004).

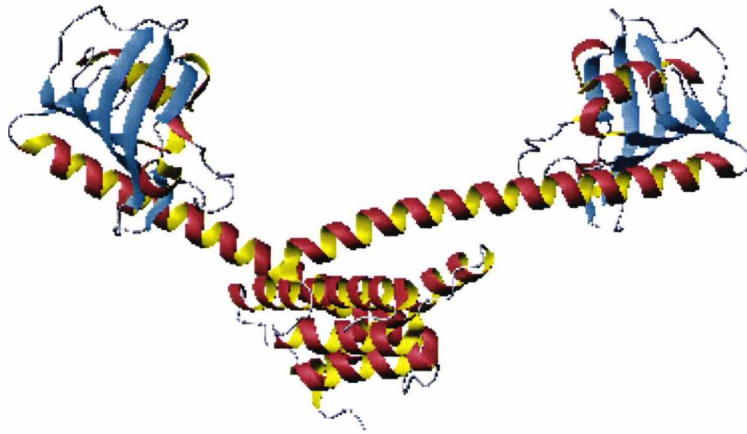


Figure 1.14.1 Three-dimensional structure of FkpA. The PDB file used to create this image was from the Protein Data Bank 1Q6H. FkpA is a dimer, the two structures are linked by the ‘legs’ that form the V-shape that has been suggested as the binding cleft.

Like other members of the FKBP family FkpA can be inhibited by the immunosuppressant FK506 (Arie et al., 2001; Ramm and Pluckthun, 2000; Ramm and Pluckthun, 2001). It has been proposed that FK506 inhibits the PPIase activity in this protein family by mimicking the transition state in the *cis/trans* isomerisation (Rosen et al., 1990). FkpA displays chaperone properties that are independent of its PPIase activity (Arie et al., 2001). For example FkpA has been shown to assist the folding of the scFv antibody fragment independently of its PPIase activity and of proline residues in the scFv fragment (Bothmann and Pluckthun, 2000; Ramm and Pluckthun, 2000). Furthermore FkpA was shown to interact with partially aggregated and unfolded proteins, which is a particular characteristic of chaperones (Arie et al., 2001).

The *fkpA* null mutant displays increased sensitivity to antibiotics and detergents, and hence it has been suggested that FkpA is involved in the folding of OMPs.

1.15 PPIA

PpiA, also known as RotA, is one of the periplasmic PPIases belonging to the cyclophilin family (Hayano et al., 1991; Liu and Walsh, 1990). PpiA has no known function but is a potent PPIase *in vitro* (Hayano et al., 1991; Liu and Walsh, 1990). The protein is expressed under the Cpx stress response system (Pogliano et al., 1997) but has been shown to not be essential for viability (Kleerebezem et al., 1995). The *ppiA* null mutant showed no effect to the steady state levels of OMPs or on the kinetics of their formation (Kleerebezem et al., 1995).

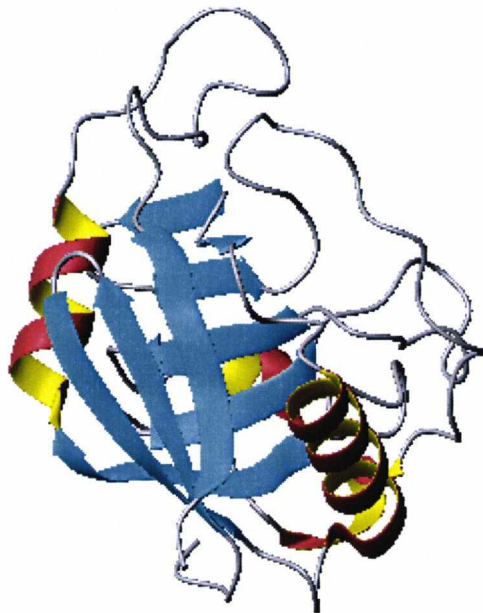


Figure 1.15.1 Three dimensional structure of PpiA. The PDB file used to create this image was from the Protein Data Bank 1J2A. PpiA is a periplasmic PPIase but has not been shown to have an important function *in vivo*.

1.16 SURA

SurA is a periplasmic PPIase required for the correct and efficient folding of extracytoplasmic proteins. Sequence analysis of SurA reveals that there is sequence homology to parvulin. SurA was originally isolated as a protein product of stationary phase survival genes of *E.coli* (Lazar et al., 1998; Lazar and Kolter, 1996; Tormo et al., 1990). Null mutants of *surA* resulted in the loss of cell viability after 3-5 days

incubation, which lead to the conclusion that SurA is essential during late stages of growth (Lazar et al., 1998). Although loss of viability in stationary phase also depends on the allelic state of the *rpoS* gene, coding for sigma S (sigma 38) factor of RNA polymerase, SurA is essential for the growth of cells under alkaline conditions, irrespective of the allelic state of *rpoS* (Lazar et al., 1998). *surA* null cells exhibit the pleiotropic phenotypes characteristic of a defective cell envelope, such as cell lysis and increased sensitivity to hydrophobic agents. Cells without SurA expression are constitutively induced for the σ^E -dependant extracytoplasmic stress response, one of two signal transduction pathways known to communicate the folding state in the periplasm to the cytoplasm (Lazar et al., 1998).

Functional studies showed that SurA is involved in the maturation of OMPs. Lack of SurA interferes with an early step in the folding of LamB maturation, the conversion of the unfolded to folded monomer, and negatively effects the expression of the major trimeric porins OmpC, OmpF and LamB (Lazar et al., 1998; Lazar and Kolter, 1996). SurA is comprised of 428 amino acids and has a molecular weight of 47283 Da. The first 20 amino acids are the N-terminal leader sequence and the two separate. The PPIase activity of SurA is present only in the C-terminal parvulin-like domain.

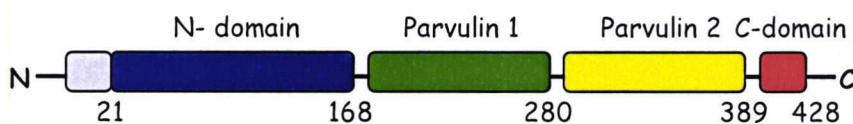


Figure 1.16.1 Domain structure of SurA. The blue region represents the binding domain, the green and yellow indicate the parvulin domains 1 and 2 respectively and the red indicates the C-terminal region.

The N-terminal domain is required for peptide binding, which has been shown by cross-linking experiments. Furthermore, this domain exhibits PPIase-independent chaperone-like activity and is required for the selective recognition of the OMPs (Rouviere and Gross, 1996).

Behrens *et al* have shown that a domain construct comprising the first 150 amino acids of the N-terminus of SurA fused to 43 amino acids at the very C-terminus has a PPIase-independent activity, which can mimic the *in vivo* activity of intact SurA

(Behrens et al., 2001). It has therefore been speculated that the 43 amino acids from the C-terminus of SurA stabilize the fragment containing the 150 N-terminal amino acids but were not involved in the overall chaperone activity of the fragment. The N-terminal domain has properties of a molecular chaperone, as it prevents heat-denatured citrate synthase from aggregation, and is essential for the interaction with model peptides (Webb et al., 2001).

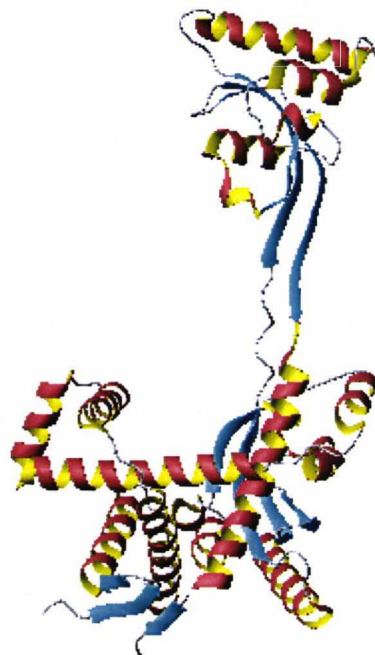


Figure 1.16.2 Three-dimensional structure of SurA. The PDB file used to create the image was from the Protein Data Bank 1M5Y. The core domain consists of the N-terminal domain, the PPIase domain and the C-terminal domain with the satellite domain tethered to the core via domain 1.

Recently the three-dimensional structure of SurA has been solved. The overall structure has been described to resemble an asymmetric dumbbell (Bitto and McKay, 2002). The C-terminal domain is sandwiched between the N-terminus and the first PPIase domain. Because of the location of the C-terminal domain it has been suggested to be essential for the stability of the protein (Behrens et al., 2001), however, the N-terminal binding domain without the C-terminal domain could be expressed in soluble form, indicating that the C-terminal domain is not essential for the stabilization of the N-terminal domain (Webb et al., 2001). The core domain has an elongated crevice with dimensions that are well suited for the binding of an extended polypeptide chain. Attached to the central core, comprising the N-terminal

substrate binding domain and the first PPIase domain, is the satellite domain containing the second PPIase domain (Bitto and McKay, 2002).

The substrate binding motif of SurA was recently identified and the enzyme was shown to bind to proteins with the motif Ar-X-Ar, where Ar is an aromatic residue (Bitto and McKay, 2003; Bitto and McKay, 2004). A peptide with the sequence WEYIPN bound to SurA with the highest affinity in the range of 1-14 μ M (Bitto and McKay, 2003; Bitto and McKay, 2004). It was also suggested that the minimum number of amino acids that were required for the binding was five, and that a proline residue at position five increased the binding affinity (Bitto and McKay, 2003; Bitto and McKay, 2004) although it has been shown that proline is not needed to be present in a peptide for it to bind to SurA (Webb et al., 2001). Further investigation into the Ar-X-Ar motif showed that it has a high occurrence in OMP's (Bitto and McKay, 2004; Hennecke et al., 2005), which makes it tempting to speculate that SurA is predominantly involved in the correct folding of this particular class of proteins.

However the view that SurA is involved with OMPs has recently been questioned by Justice *et al.* They showed that levels of the OMPs LamB and OmpA in mutants lacking SurA were indistinguishable from the wild-type (Justice et al., 2005). They also demonstrated that the importance of SurA was with the formation of P-pili and type I fimbriae, and mutants lacking SurA affected the pilus assembly and the usher pathway (Justice et al., 2005). They also showed that only a mutant with no FkpA, PpiA, PpiD and SurA resulted in a decreased growth rate and not a loss of cell viability (Justice et al., 2005), which is in contradiction to earlier experiments (Dartigalongue and Raina, 1998).

1.17 PPID

PpiD is a member of the parvulin family, like SurA. The gene encoding the PpiD protein was identified for its transcription by the two component system CpxR-CpxA (Dartigalongue and Raina, 1998). When the protein was purified it was shown to have PPIase activity *in vitro*. PpiD is 623 amino acids long and has a molecular weight of 68150 Da. It is anchored to the inner membrane of *E.coli* by a single

transmembrane segment of around 21 amino acids, with the catalytic domain facing the periplasmic space (Dartigalongue and Raina, 1998).

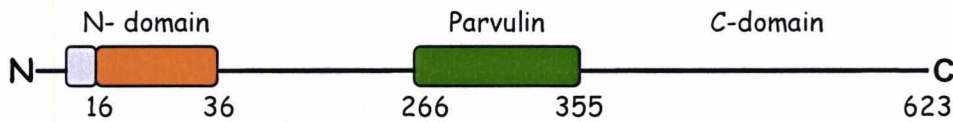


Figure 1.26.1 Diagram showing PpiD. The grey area indicates the signal sequence, followed by the orange region which represents the transmembrane domain. The green area is the parvulin like domain.

Figure 1.26.1 shows the proposed structure of PpiD. PpiD contains one parvulin like domain (Dartigalongue and Raina, 1998; Missiakas et al., 1996; Rouviere and Gross, 1996). PpiD was shown to be the first of the heat-shock induced protein that is involved in the folding of non-cytoplasmic proteins. What makes PpiD interesting is that the combination of the null mutants of *surA* and *ppiD* has been reported to lead to a lethal phenotype under all growth conditions. This has been reinforced by the observation that over expression of PpiD can complement the effect of the null *surA* mutant by restoring the normal membrane profile. Furthermore over expression of SurA can complement the effects of the null *ppiD* mutant, as well as the over expression of PpiD restoring elevated σ^E activity (observed in mutant *surA* strains) (Dartigalongue and Raina, 1998). These observations however were recently put into question as mutants created by Justice *et al* have shown that there was no loss in cell viability in a combined *ppiD/surA* null mutant and only a decrease in the growth rate of the cells was observed with a quadruple mutant lacking SurA, PpiD, PpiA and FkpA (Justice et al., 2005).

1.18 AIMS OF THE STUDY

The threat of antimicrobial resistance has become increasingly real and its dimensions have now been globally recognized. The cost of antimicrobial-resistant infections acquired in hospitals was estimated by the National Foundation for Infectious Disease to be as high as four billion dollars annually (USDA, 2006). In the UK the costs have been estimated to be in the order of \$100 million p.a. and likely to increase in the near future.

Since the beginning of the 1990s a strong increase of drug-resistant pathogenic Enterobacteria like *Shigella* ssp, *Salmonella* ssp and *Escherichia coli* (*E.coli*) have been reported (WHO, 2005). In humans, *Shigella* ssp, *Salmonella* ssp and *E.coli*, especially strain O157:H7, are important causes of food-borne illness, causing severe diarrhoea and in some cases renal failure and death. In addition *Salmonella* ssp and *E.coli* cause significant morbidity and mortality in livestock. Disease caused by enterotoxigenic *E.coli* (ETEC) follows ingestion of contaminated food or water and is characterized by profuse watery diarrhoea lasting for several days. It may lead to dehydration and malnutrition in young children in developing countries. ETEC is the most frequently isolated enteropathogen in community-based studies of children aged less than 5 years in the developing world, and probably accounts for approximately 200 million diarrhoea episodes and 380 000 deaths annually (WHO, 2006). The Centers for Disease Control and Prevention estimates that 73000 cases of *E.coli* O157:H7 infections occur annually in the United States with 2100 people being hospitalised and 61 casualties as a direct or indirect result of the infection (Rangel et al., 2005). Most importantly, however, *E.coli* is a leading cause of extraintestinal infections, mainly of the urinary tract, costing billions of dollars in health care costs, and an estimated 40,000 deaths from sepsis annually in the United States alone (Russo and Johnson, 2003). Since 2003, new highly resistant strains of *E.coli* have become widespread in England and parts of Northern Ireland. These strains of *E.coli* are able to destroy a large number of common antibiotics, making the infections they cause very difficult to treat. The bacteria produce enzymes called extended-spectrum β -lactamases (ESBLs) that destroy, and thus confer resistance to, beta-lactam antibiotics such as penicillins and cephalosporins. A study of 54 deaths linked to a recent outbreak in Shropshire showed that ESBL-producing *E. coli* directly contributed to a

quarter of the deaths. The same strain has been linked to 29 deaths in the Southampton area in 2004, in an outbreak of more than 1,000 cases that left 357 people needing treatment in hospital (Livermore and Hawkey, 2005). Shigellosis is endemic throughout the world with approximately 164.7 million cases, of which 163.2 million in developing countries and 1.5 million in industrialized countries. Each year 1.1 million people are estimated to die from *Shigella* infection and 580 000 cases of shigellosis are reported among travellers from industrialized countries. A total of 69% of all episodes and 61% of all deaths attributable to shigellosis involve children less than 5 years of age (WHO, 2003). Salmonellosis is one of the most common and widely distributed foodborne diseases. It constitutes a major public health burden and represents a significant cost in many countries. Millions of human cases are reported worldwide every year and the disease results in thousands of deaths (WHO, 2005).

A novel and promising target for new antimicrobial drugs is the periplasmic PPIase SurA, which is required for the correct folding of several outer membrane proteins in *E.coli*, *Salmonella ssp*, *Shigella ssp*, *Yersinia pestis* and other coliform bacteria.

In general, bacteria that do not contain SurA are less virulent than the wildtype strains. Expression of P-pili and type 1 fimbriae, produced by uropathogenic strains of *E. coli* and assembled by the chaperone/usher pathway, were severely diminished in the absence of SurA (Justice et al., 2005). A *Salmonella enterica serovar Typhimurium C5* strain with inactive SurA was found to be defective in the ability to adhere to and invade eukaryotic cells (Sydenham et al., 2000). Furthermore deletion of SurA in *E.coli* results in hypersensitivity to a variety of antibiotics (Justice et al., 2005). These results make SurA an attractive target for the development of inhibitors that interfere with the substrate binding site of SurA.

Administration of SurA inhibitors might improve the control and management of infections caused by a variety of pathogens since SurA from *E.coli* is very similar to paralogous proteins from other pathogenic gram-negative bacteria and therefore it can be assumed that antimicrobial compounds against *E.coli* SurA are also effective against these organisms.

```

E_coli      1  APQVVDKVAAVVNGVLESVDVGLMQSVKLNAAQARQQLPDDATLRHQIERLIMDQII
S_dysenteriae 1  APQVVDKVAAVVNGVLESVDVGLMQSVKLNAAQARQQLPDDATLRHQIERLIMDQII
S_typhi     1  APQVVDKVAAVVNGVLESVDVGLMQSVKLNAAQAGQQLPDDATLRHQIERLIMDQII
S_typhimurium 1  APQVVDKVAAVVNGVLESVDVGLMQSVKLNAAQAGQQLPDDATLRHQIERLIMDQII
Y_pestis   1  APQEVVDKVAAVVNGVLESVDVGLMQSVKLNAAQAGQQLPDDATLRHQIERLIMDQII

E_coli      61  LQMGQKMGVKISDEQLDQAIANIAKQNNMTLDQMRSLAYDGLNYNTYRNQIRKEMIISE
S_dysenteriae 61  LQMGQKMGVKISDEQLDQAIANIAKQNNMTLDQMRSLAYDGLNYNTYRNQIRKEMIISE
S_typhi     61  LQMGQKMGVKISDEQLDQAIANIAKQNNMTLDQMRSLAYDGLNYSTYRNQIRKEMIISE
S_typhimurium 61  LQMGQKMGVKISDEQLDQAIANIAKQNNMTLDQMRSLAYDGLNYSTYRNQIRKEMIISE
Y_pestis   61  LQMAKKMGITITDQALDKAIAITAAQNRMTLAQMRSLAADGLSYDITYREQIRKEMITISE

E_coli      121 VRNNEVRRRITLTPQEVESLACQVGNQNDASTELNLSHIL
S_dysenteriae 121 VRNNEVRRRITLTPQEVESLACQVGNQNDASTELNLSHIL
S_typhi     121 VRNNEVRRRITLTPQEVDALAKQITGTONDASTELNLSHIL
S_typhimurium 121 VRNNEVRRRITLTPQEVDALAKQITGTONDASTELNLSHIL
Y_pestis   121 VRNNEVRRRITLTPQEVESLACQVGNQVSCDTELNLSHIL

```

Figure 1.18.1 ClustalW alignment of the N-terminal binding site, excluding the leader sequence, of SurA. Sequences were taken from SwissProt.

These inhibitors of the substrate binding site of SurA are expected to exhibit a dual effect:

- they will increase the pathogen's sensitivity to antibiotics, thus facilitating the treatment of drug-resistant pathogens. Many drug-resistant pathogens have developed mechanisms to inactivate antimicrobials administered in standard concentrations although the pathogens are still sensitive to very high concentrations of the drugs. Combination of specific antibiotics with a SurA inhibitor acting as a sensitizer therefore is expected to bring back conventional antibiotics into the therapy of drug-resistant pathogens.
- they will prevent the pathogen from producing virulence factors, especially P-pili and type 1 fimbriae, thus reducing the severity of the infection.

To facilitate the development of potential inhibitors of SurA activity a detailed study of the interaction between SurA and its substrates is required. In particular one has to address the following questions:

- What is the binding motif that SurA recognises in a substrate?
- What is the specific mechanism by which SurA interacts with its substrates?

At the beginning of the study it was assumed that PpiD could complement a *surA* deletion, and hence it was speculated that PpiD and SurA have overlapping substrate specificities (Dartigalongue and Raina, 1998). To develop efficient inhibitors it was therefore deemed necessary to include PpiD in this study and investigate how this PPIase recognises its substrates.

Chapter 2

Materials and Methods

Chapter 2: Materials and Methods

2.1 MATERIALS

Biochemicals were purchased from Sigma or Roche (formally Boehringer Mannheim Ltd. (BCL)) unless otherwise stated. Bulk liquids (Organic solvents, acids, bases and glycerol) were purchased from BDL Ltd. Media components were purchased from Difco or Oxoid. Radiochemicals were purchased from Amersham International, UK. Pre-mixed Acrylamide/Bis acrylamide solutions were obtained from Bio-rad.

2.2 STRAINS USED IN THIS STUDY

2.2.1 *Escherichia coli* STRAINS

The *E.coli* strains used in this study are detailed in Table 2.1.1

STRAIN	GENOTYPE	SOURCE OR REFERENCE
BL21 (DE3)	hsdS gal (λ cIts857, ind1, Sam7, nin5, LacUV5-T7 gene 1	Studier and Moffatt, (1986)
DH5α	supE44, Δ lacIU169 (ϕ 80 lacZ Δ M15) hsdR17, recA1, endA1, gyrA96, thi-1, relA1	Hanahan (1983); Bethesda Research Laboratories, (1986)
XL1-BLUE	supE44, hsdR17, recA1, endA1, gyrA46, thi, relA1, lac ⁻ F'[proAB ⁺ lacI ^q , lacZ Δ M15 Tn10(tet ^r)]	Bullock et al.(1987)

Table 2.2.1 *E.coli* strains used in this study.

2.3 GROWTH MEDIA AND SOLUTIONS

2.3.1 *Escherichia coli*

All media were sterilised by autoclaving for 15 min at 126 °C (15lb/sq.in) using a Prestige autoclave. Solid medium was prepared by the addition of 1.5% (w/v) bactoagar (Difco). Antibiotic stock supplements (Table 2.3.1.1), were usually prepared at 100-1000 X concentration and filter sterilised with a 0.2 µm sterile filter before their addition to previously autoclaved and cooled (less than 40 °C) media.

ANTIBIOTIC	STOCK SOLUTION	WORKING CONCENTRATION
Ampicillin	50 mg/ml in H ₂ O	100 µg/ml
Choramphenicol	25 mg/ml in ethanol	25 µg/ml
Kanamycin	10 mg/ml in H ₂ O	30 µg/ml
Tetracycline	5 mg/ml in H ₂ O	10 µg/ml

Table 2.3.1.1 Antibiotics stock and working concentration.

MEDIA COMPONENT	AMOUNT
NaCl	1% w/v
Bacto tryptone	1% w/v
Yeast Extract	0.5% w/v
Agar	1.5% w/v

Table 2.3.1.2 Percentage of components in Luria broth. Agar is only added to components to make agar plates.

E.coli strains were grown for 16 hrs at 37 °C in Luria broth with shaking at 200 rpm for all recombinant DNA methods. *E.coli* strains were also grown on LB solid media

at 37 °C for 18-24 hrs and stored at 4 °C for up to one month. Longer term storage was achieved by storing the *E.coli* strains in 25% (v/v) glycerol at -70 °C.

2.3.2 MONITORING *E.coli* CELL GROWTH

E.coli cell growth was monitored by inoculating a known amount of stationary phase cells into fresh LB medium or LB medium containing selective antibiotics and, after 2 - 4 hrs, measuring the cell density by reading the absorbance at 600nm. An OD₆₀₀ = 0.2-0.5 was taken to be early to mid-exponential (log) phase, 0.6–1.0 as mid to late log phase and over 1.0 as stationary phase. Cells were grown to 0.3-0.4 for protein expression and 0.3-0.5 for making competent cells.

2.4 RECOMBINANT DNA TECHNIQUES

2.4.1 DNA MARKERS

DNA markers were obtained from Promega. These were the Lambda/Hind III marker supplied in 10mM Tris-HCL (pH 7.5), 10mM NaCl and 1mM EDTA. Bands of 23130, 9416, 6557, 4361, 2322, 2027, 564 and 125 base pairs (bp) were visible.

2.4.2 VECTORS

Vectors used in this study are listed below. The sequences and detail of each vector can be found in the appendix.

pLitmus 28i vector: blue / white selection, high copy number. The pLitmus 28i vector was supplied by the New England Biolabs.

pET28a(+) vector: His tag. The pET28a(+) vector was supplied by Novagen.

pET23a(+) vector: His tag. This vector has no *T7lac* promoter, just the T7 promoter. The pET23a(+) vector was supplied by Novagen.

pGEM[®]-T Easy vector: T7 and SP6 RNA polymerase promoters flank a multiple cloning region within the α -peptide coding region for β -galactosidase. The pGEM[®]-T Easy vector was supplied by Promega.

2.4.3 DIGESTION OF DNA WITH RESTRICTION ENDONUCLEASES

Restriction enzymes were purchased either from Roche or Promega. They were used according to the manufacturer's specifications, with typical DNA restriction digest conditions as follows:

- 1 μ g DNA (either plasmid or PCR product)
- 2 μ l 10x Enzyme Buffer
- 1.0 unit of restriction enzyme
- Sterile water up to 20 μ l

If a larger reaction was required then all the components were scaled accordingly. The DNA was usually digested for 3-4 hrs at 37 °C and the reaction stopped by heat-inactivation at 65 °C for 15 min. If more than one enzyme digest was carried out in the same reaction then the buffer that would produce the optimal activity for both enzymes was used. However if the same buffer could not be used then the two enzymes would be used separately with ethanol precipitation or purification (with Qiagen PCR purification kit) between the steps.

2.4.4 ETHANOL PRECIPITATION

Ethanol precipitation of DNA was carried out by the addition of 0.1 volume of 3 M sodium acetate (pH 5.2), and 2 volumes of 95% ethanol (2 times the volume after the

sodium acetate addition) at room temperature for 1-2 hrs. The sample was then centrifuged for 15 min in a microcentrifuge at 13000 rpm at room temperature. The supernatant was immediately decanted. Recentrifugation of the sample allowed removal of the residual supernatant. The pellet was washed by the addition of 200-500 μ l of cold (<10 °C) 70% ethanol, recentrifuged for 5 min and decanted as above. The pellet was then air dried and then resuspended in the appropriate volume of water or buffer (TE buffer 10mM Tris-HCl, 1mM EDTA), allowing at least 15 min for the nucleic acid to re-dissolve.

2.4.5 AGAROSE GEL ELECTROPHORESIS OF DNA (after Sambrook *et al* 1989)

Typically 1% (w/v) agarose gels were prepared using molecular biology grade agarose and 1 x TAE buffer (40mM Tris-acetic acid, 10mM EDTA, pH 8.0). The agarose was dissolved in the buffer by heating in a microwave for 1-2 min on full power and was left to cool to 50 °C. 0.5 μ l of 10 mM ethidium bromide was then added to the molten agarose. This was poured into the gel former and comb inserted before being left to set. Once completely set, the gel was placed into a gel holder and the sample to be electrophoresed were prepared by mixing with 10 x sample loading buffer (50 mM EDTA, 0.2% (w/v) bromophenol blue, 50% (w/v) Tris) and loaded into the wells with a micropipette. The gel was then electrophoresed at 5-10 volts / cm for approximately 45 min to 1 hour until the bromophenol blue dye had migrated to the bottom of the gel. The DNA was then visualised and photographed using a short wave UV transilluminator (312nm).

2.4.6 PURIFICATION OF DNA

The DNA to be excised from an agarose gel was loaded into an agarose gel made with high purity agarose and using TAE buffer. The gel was visualised using a short wave transilluminator and the DNA fragment of interest was removed with a clean razor blade. The DNA was then purified using a 'Qiagen Gel Extraction Kit'.

2.4.7 QIAGEN GEL EXTRACTION

Gel extraction of DNA fragments was carried out with Qiagen Gel Extraction Kit according to the manufacturer's instruction.

2.4.8 pGEM-T EASY VECTOR SYSTEM

The pGEM[®]-T Easy Vector System is a convenient system for the cloning of PCR products. The vectors were prepared by cutting Promega's pGEM[®]-T Easy Vectors with *EcoR* V and adding a 3' terminal thymidine to both ends. These single 3'-T overhangs at the insertion site greatly improve the efficiency of ligation of a PCR product into the plasmids by preventing recircularization of the vector and providing a compatible overhang for PCR products generated by certain thermo stable polymerases. These polymerases often add a single deoxyadenosine, in a template-independent fashion, to the 3'-ends of the amplified fragments. The high copy number pGEM[®]-T Easy Vector contain T7 and SP6 RNA polymerase promoters flanking a multiple cloning region within the alpha-peptide coding region of the enzyme beta-galactosidase. A typical pGEM-T Easy reaction contained the following components:

	STANDARD REACTION	POSITIVE CONTROL	BACKGROUND CONTROL
2X Rapid Ligation Buffer	5 µl	5 µl	5 µl
pGEM-T easy Vector	1 µl	1 µl	1 µl
PCR Product	2 µl	-	-
Control Insert DNA	-	2 µl	-
T4 DNA Ligase	1 µl	1 µl	1 µl
Deionised Water to a final volume of	10 µl	10 µl	10 µl

Table 2.4.8.1 Components required for the pGEM-T easy ligation.

The samples were incubated at room temperature for 1 hour or at 4 °C overnight. The ligations were transformed into competent DH5 α cells and plated on to agar plates containing Ampicillin, IPTG (1 mM) and XGAL (40 mg/ml). The plates were incubated at 37 °C overnight. White colonies should contain the insert.

2.4.9 LIGATION: COHESIVE AND NON-COHESIVE TERMINI

Ligation reactions of digested DNA were performed using T4 DNA ligase obtained from Promega. Ligations were typically carried out in 0.2ml PCR tubes and contained the following:

- 7:1 Molar ratio of insert DNA to vector DNA
- 2 μ l 10 x ligation buffer
- 1 μ l T4 ligase
- Sterile deionised water up to 20 μ l

The sample was mixed by pipetting and incubated overnight at 4 °C (12-16 hrs).

2.4.10 COMPETENT CELLS

A 2 ml culture of the *E.coli* strain to be made competent was prepared with LB medium and the appropriate antibiotics and incubated at 37 °C overnight with vigorous shaking (200 rpm). 0.5 ml of the overnight culture were then used to inoculate 40 ml of fresh liquid LB medium, the cells were then kept at 37 °C with vigorous shaking for 2-3 hrs until the OD_{600nm} ~ 0.3-0.5. The cells were then centrifuged in sterile 50 ml centrifuge tubes at 2500g for 5 min and the supernatant was discarded. The pellet was resuspended in 20 ml of sterile 50 mM calcium chloride solution and stored on ice for at least 30 min. The cells were centrifuged at 2500g for 5 min and the supernatant discarded and the pellet was resuspended in 4 ml of ice cold sterile calcium chloride solution and stored on ice for at least 30 min. Cells were stored with 25% glycerol at -70 °C.

2.4.11 TRANSFORMATION INTO *E.coli* WITH PLASMID DNA

100 µl of competent cells were mixed with the appropriate amount of DNA, 1-2 µl of uncut vector or up to 20 µl of ligation reaction in a microcentrifuge tube. These were incubated for 30 min on ice. The cells were then 'heat shocked' at 42 °C for 45 seconds, and then left to recover on ice for five min. 1 ml of fresh LB medium without antibiotics was added to each of the transformations, which were then incubated at 37 °C for an hour with shaking. The cells were then spun down at 5000g for 2 min and all but 100 µl of the supernatant was removed. The remaining 100 µl medium was used to resuspend the pelleted cells. These were then streaked on LB plates containing the appropriate antibiotics and were incubated overnight (12-16 hrs) at 37 °C.

2.4.12 SMALL SCALE QIAGEN MINIPREPS OF PLASMID DNA

Qiagen mini-prep kit was routinely used according to the manufactures instructions.

2.4.13 MAXIPREP PLASMID DNA PURIFICATION

The Wizard plus maxipreps (Promega) was routinely used according to the manufactures instructions.

500 ml liquid LB medium was inoculated with 50 µl of overnight culture and the appropriate antibiotics. This was left to grow overnight at 37 °C with shaking at 200 rpm. The cells were then pelleted by centrifugation at 5000g for 10 min. The pellet was resuspended using 15 ml of the cell resuspension solution, to this 15 ml of cell lysis solution was mixed in gently until the solution became clear and viscous. Neutralisation solution was added and mixed gently inverting the centrifuge bottle several times. This was centrifuged at 14000g for 15 min at 22 °C. The supernatant was transferred into a graded cylinder through autoclaved coffee filter and 0.5 volume of isopropanol was added, this was then mixed by inversion. The mixture was then centrifuged at 14000g for 15 min at 22 °C. The supernatant was discarded and the

pellet was resuspended in 2 ml of TE buffer. The walls of the tube were washed with the TE buffer to recover all the DNA. The DNA was purified by mixing 10 ml of purification resin to the DNA solution, the resin/DNA mix was transferred to the maxicolumn and attached to a vacuum to pull the resin/DNA mix through the column. The column was washed using the column wash solution and was pulled through the column using the vacuum. The resin was rinsed using 80% ethanol; the column was then placed in a screw top tube and spun in a swing bucket rotor at 2500 rpm for 5 min. The tube and the liquid were discarded. The column was left to dry. To elute the DNA, 1.5 ml of pre-heated (65 - 70 °C) nuclease free water was added to the column and left for 1 min, this was the centrifuged at 2500 rpm for 5 min. The resin fines were removed by filtration through a 0.2 µm syringe filter. The filtrate was centrifuged at 14000g for 1 min to remove the last resin fines. The supernatant was immediately removed and stored in microcentrifuge tubes at -20 °C.

2.4.14 GENOMIC DNA

E.coli colonies were picked and resuspended in 100 µl of water. The suspensions were heated to 100 °C for 10 min and centrifuged at 12000 rpm for 2 min.

2.5 POLYMERASE CHAIN REACTION (PCR)

2.5.1 PCR PROTOCOL

The primers used in the PCR are listed below in section 2.5.3.

The samples were mixed thoroughly and centrifuged briefly, the cycles and temperatures are described below in table 2.5.1.1. The dNTPs came from Promega as 100 mM stock solutions.

A typical PCR 100 μ l reaction contained the following components:

- 3 μ l DNA template
- 10 μ l 10x PCR reaction buffer
- 8 μ l 25 mM MgCl₂ (supplied with the polymerase, sometimes in the buffer)
- 16 μ l 5 mM dNTP mix (1.25 mM each of dATP, dTTP, dCTP and dGTP)
- 2 μ l 10 μ M Forward Primer
- 2 μ l 10 μ M Reverse Primer
- 58 μ l Distilled water
- 1 μ l *Pfu* or *Taq* polymerase

PROGRAMME	TEMPERATURE	DURATION	NUMBER OF CYCLES	LINK TO...
1	94 °C	30 sec	1	2
2	94 °C	3 min	} 25	3
	X °C **	30 sec		
	68 °C or 72 °C *	2 min		
3	68 °C or 72 °C *	7 min	1	4
4	4 °C	∞	1	End

Table 2.5.1.1 Table showing the components of a general PCR. *68 °C if using *Pfu* or 72 °C if using *Taq*. ** Annealing temperature dependent on the primer melting temperature, usually 4 °C lower than the lowest primer melting temperature.

The products were run on 1% agarose gel with standard gel loading buffer to confirm the presence of products.

2.5.2 QIAGEN QIAQUICK PURIFICATION

The QIAquick kit is designed to purify single- or double-stranded DNA fragments from PCR. The purification was carried out according to the manufacturer's instructions.

2.5.3 PRIMERS

The primers were designed to have a minimum GC content of 50%.

SurA Primers:

SurAF

5'-TTT TTT TTC ATA TGG CCC CCC AGG TAG TCG ATA AAG TCG-3'

SurAR

5'-TTT TTT TTC TCG AGC TAT TAG TTC CTC AGG ATT TTA ACG TAG GC-3'

PpiD Primers:

PpiDR

5'-TTT TTT TTC TCG AGC TAT TAT TGC TGT TGT TCC AGC GCA-3'

Initial reverse primer for the full length and fragments of peptidyl-prolyl isomeraseD to exclude the signal sequence. Used with PpiDF, 1, 2 and 3.

PpiDF

5'-AAA AAA AAC ATA TGG GAG GCA ATA ACT ACG CCG CCA-3'

Forward primer for the full length PpiD minus the signal sequence.

PpiD1

5'-AAA AAA AAC ATA TGC CGC AGC GTA CCC GCT ACA GCA-3'

Largest PpiD fragment.

PpiD2

5'-AAA AAA AAC ATA TGC CAG CGA AAG TGA AAT CGT TAG-3'

Medium PpiD fragment.

PpiD3

5'-AAA AAA AAC ATA TGC CGT TGG CAG ATG TTC AGG AAC-3'

Shortest PpiD fragment.

PpiD REV

5'-GGG GGG GGA TCC GTC GCG CAA CAA CGC GTG GTG CG-3'

Final reverse primer for PpiD.

PpiD VAQQ

5'-GGG GGG AAG CTT TTA TTG CTG TTC CAG CGC ATC GC-3'

Forward primer for PpiD without the first 187 residues.

2.5.4 DIAGNOSTIC PCR

For diagnostic PCR, such as the screening of potential positive clones, Taq polymerase from Promega was used. To confirm the presence of an insert for a SurA or PpiD mutant or fragment single colonies could not be used because of the endogenous PPIase. Mini cultures were grown overnight from single colonies. These were mini-preped and 3 µl of the mini-prep DNA was used in the PCR reaction. For the cloning of PpiD fragments, a plasmid containing the PpiD gene was used. The presence of the ligated vector was confirmed by transforming the vector into DH5α cells. A single colony was picked and resuspended in 100 µl of distilled water. The solution of cells was spun down at 13000 rpm for 2-3 min and resuspended in 50 µl distilled water. 10 µl of the vortexed sample was used as the template for the PCR reaction.

2.6 PROTEIN ANALYTICAL METHODS

2.6.1 SMALL SCALE EXPRESSION OF RECOMBINANT PROTEIN

An overnight culture of *E.coli*, transformed with the respective expression vector, was set up from a single colony in 2 ml of LB medium with the appropriate antibiotics and incubated at 37 °C with shaking at 200 rpm. 10 µl of the overnight culture was used to inoculate 2ml of fresh LB medium with the appropriate antibiotics. This was then incubated at 37 °C with vigorous shaking for 2-3 hrs until the OD reached 0.2 - 0.4.

The expression was induced using 1mM IPTG final concentration and incubated for another 3 hrs at 37 °C with vigorous shaking. The cells were then spun down at 13000 rpm for 5 min and the supernatant was removed. The pellet was resuspended in 100 µl of distilled water with 3 µl of DNase (0.5 mg/ml stock solution). The cells were then freeze-thawed by freezing at -70 °C and defrosting at room temperature three times.

2.6.2 LARGE SCALE EXPRESSION OF RECOMBINANT PROTEIN

An over night culture was set up in 50ml of LB medium with the appropriate antibiotics and incubated at 37 °C with shaking at 200 rpm. 1 ml of the overnight culture was used to inoculate 1 l of LB medium with the appropriate antibiotics. This was then incubated at 37 °C with vigorous shaking for 2-3 hrs until the OD reached 0.2-0.4. The expression was induced using 1 mM IPTG final concentration and the culture was incubated for another 3 hrs at 37 °C with vigorous shaking. The cells were then spun down at 8000 rpm for 20 min and the supernatant was removed. The pellet was resuspended in 5 ml of distilled water with 100µl of DNase (0.5 mg/ml stock solution). The cells were then frozen at -70 °C for 15 min, thawed at room temperature and then refrozen; this process was repeated 3 times.

2.6.3 PROTEIN PURIFICATION USING FPLC

After repeated freeze-thawing the samples were centrifuged at 8000g for 10 min to remove cell debris. The cleared supernatant was then passed through a 0.2 μm single use sterile filter unit and stored on ice until use.

For the purification an ÄKTA *design* system was used. The column was a 5ml HisTrap HP optimised for the purification of His-tagged proteins. All solutions were filter sterilised and degassed before use. The column and the pumps were washed with distilled water at 4 ml/min for 8 min. 50 ml of filter sterilised 100 mM nickel sulphate solution was run down the column at a flow rate of 2 ml/min. To prevent phosphate binding to the nickel sulphate, distilled water was passed down the column. 20 mM phosphate buffer was used to equilibrate the column before the sample was loaded. The sample was loaded at a flow rate of 2 ml/min and the column was then washed with 20 mM phosphate buffer pH 7.2 to remove unbound protein. To remove weakly bound protein from the column a wash buffer containing 20mM Phosphate buffer, 0.5 M NaCl and 50 mM imidazole pH 7.2 was used. The column was then washed using 20 mM phosphate buffer pH 7.2. To elute the protein, elution buffer was used, containing 20 mM phosphate buffer and 10 mM EDTA. Finally the column was washed with distilled water and stored in 20% ethanol.

2.6.4 PROTEIN DESALTING

Desalting of the sample was achieved using the NAPTM-10 Column (Pharmacia Biotech). The columns are made of Sephadex G-25 in distilled water. The column was equilibrated with 15 ml of 10 mM Phosphate buffer pH 7.2 - 7.3. The flow through was discarded and 1ml sample was added to the column. The desalted protein sample was eluted from the column with 1.5 ml of 10 mM Phosphate buffer pH 7.2-7.3.

2.6.5 SLIDE-A-LYZER[®]

The Slide-A-Lyzer[®] (Pierce), is used for low molecular weight contaminant removal, buffer exchange and desalting. The Slide-A-Lyzer[®] was hydrated for 30 seconds in the dialysis buffer (10 mM Phosphate buffer pH 7.2-7.3) before use. The sample was introduced to the cassette using a hypodermic needle. The used Slide-A-Lyzer[®] had a capacity of 0.5–3 ml and MW cut off of 10,000. Samples were typically dialysed in 500 times the volume of the sample. Initially the sample was dialysed for 2 hrs and the buffer was changed and the sample was dialysed again for 2 hrs, again the buffer was changed and the sample left at 4 °C overnight. The sample was removed from the cassette with a hypodermic needle.

2.6.6 CONCENTRATING PROTEIN BY DIALYSIS AND SPEED VAC

Dialysis tubing came from Medical International Ltd and had pore size of 12-14000 Da. A length of roughly 60 cm of dialysis tubing was cut and boiled in distilled water for 10 min; this was allowed to cool and stored in the fridge. To dialyse the protein sample 20 cm of tubing was cut using sterile scissors. One end was tied in a knot and a dialysis clip put next to the knot. 7ml of protein was pipetted into the dialysis tube and the second dialysis clip was put on the open end to seal the tube. This was then submerged in 10mM phosphate buffer pH 7.2 with a gentle stirring for 45 min. The dialysis buffer was changed and left for a further 45 min. The contents of the dialysis tube was aliquoted into 6 sterile microfuge tubes and put into the 'speed vac' on medium so the sample would stay cold but not frozen. This was usually left for 2-3 hrs or depending on what the final volume was required.

2.6.7 CENTRICON

Centricon is a centrifugal filter unit made by Millipore. The centricon was prerinse using distilled water or buffer. 2 ml of the distilled water or buffer was pipetted into

the sample reservoir. When at least half the original volume had passed through, the filter unit was inverted and spun at 300-1000g to remove the remaining rinse. This was repeated 3-5 times. The sample was spun at 5000g and the filtrate was removed and more sample added to the sample reservoir. This process was continued until the desired amount was left in the sample reservoir. To remove the sample the filter unit was inverted and spun at 1000g for 5 min.

2.6.8 CONCENTRATING PROTEIN BY FREEZE DRYING

Purified desalted protein was concentrated by freeze drying. 1 ml aliquots of the protein sample were transferred to 1.5 ml eppendorf tubes and covered with thermoplastic, self-sealing film (Parafilm M). Approximately a half dozen small holes were made in the sealing film.

The samples were frozen in liquid nitrogen. The frozen samples were left overnight in a Freeze-dryer. The samples were then stored at -20 °C.

2.6.9 RESOURCE Q COLUMN

Elution fractions from the IMAC purification (section 2.6.3) were loaded onto a 6 ml Resource Q column from Amersham Pharmacia Biotech that had been equilibrated with 20 mM phosphate buffer pH 7.2. The protein was eluted from the column with a linear gradient from 0 to 0.5 M NaCl in 20mM phosphate buffer pH 7.2. The fractions that contained SurA were dialysed in a Slide-A-Lyzer cassette against 10 mM phosphate buffer pH 7.2.

2.6.10 SDS POLYACRYLAMIDE GEL (PAGE) ELECTROPHORESIS UNDER DENATURING CONDITIONS

SDS-polyacrylamide gels were prepared using 10, 12.5, 15, and 17.5% (w/v) polyacrylamide resolving gels and 5% (w/v) stacking gels, (see tables 2.6.10.1 and 2.6.10.2 for the resolving and stacking gel compositions).

SOLUTION	COMPOSITION	AMOUNT
A	30% Acrylamide/Bis solution 37.5:1	
	10% gel	3.3 ml
	12.5% gel	4.2 ml
	15% gel	5.0 ml
B	Distilled Water	
	10% gel	4.5 ml
	12.5% gel	3.7 ml
	15% gel	2.8 ml
C	1.875M Tris, pH 8.85	2.0 ml
	10% SDS Solution	100 µl
	TEMED	10 µl
	AMPS (10 mg/ml)	50 µl

Table 2.6.10.1 Table outlining the Resolving Gel composition.

SOLUTION	COMPOSITION	AMOUNT
A	30% Acrylamide/Bis solution 37.5:1	0.88 ml
B	Distilled Water	3.6 ml
C	1M Tris, pH 6.8	0.3 ml
D	10% SDS Solution	50 μ l
E	TEMED	7 μ l
F	AMPS (10 mg/ml)	40 μ l

Table 2.6.10.2 Table showing the composition of the Stacking Gel

Protein samples were prepared by boiling for 5 min in 5x loading sample buffer (1.83 g Tris, 5g SDS, 25 ml glycerol and 12.5 ml Distilled water then 750 μ l of this was mixed with 250 μ l of β -mercaptoethanol and few bromophenol blue crystals pH 6.2. The running buffer composition was 0.05M Tris, 0.4M glycine, 0.1% (w/v) SDS at pH 8.85. Samples were loaded on to the gel using a Hamilton syringe and were electrophoresed in a Mini Protean II gel system from BioRad.

2.6.11 DETERMINING PROTEIN CONCENTRATION

The determination of the protein concentration was required for binding assays and NMR analysis. A standard curve was produced using known concentrations of BSA (1-10 mg). These were run on a 12.5% SDS-PAGE gel with three different amounts of the unknown protein. From a comparison between the different concentrations of the BSA and the unknown sample it was possible to make an estimation of the concentration of the protein of interest.

2.6.12 CHYMOTRYPSIN DIGEST

Purified SurA was incubated with chymotrypsin (30 µg/ml) for 30 min at 0 °C. The reaction was stopped by the addition of 10mM PMSF and subsequent incubation for 5 min at 0 °C.

2.6.13 PROTEINASE K DIGEST

Purified SurA was incubated with proteinase K (3 µg/ml) for 30 min at 0 °C. The reaction was stopped by the addition of 10mM PMSF and subsequent incubation for 5 min at 0 °C.

2.7 IMMUNOLOGICAL METHODS

2.7.1 WESTERN BLOTTING USING THE ECL DETECTION SYSTEM

Proteins were transferred after SDS-PAGE on to Millipore polyvinylidene (PVDF) membranes (Millipore) via the semi-dry western blot method. SDS-PA gels were submersed in transfer buffer (20% (v/v) methanol, 2.42 g Tris, 11.3 g glycine all made up to 1l with distilled water). The PVDF membrane was prepared by rinsing in 100% methanol and then left in transfer buffer until used. Six (10 x 7cm) pieces of 3 mm Whatman paper were also soaked in transfer buffer until used. The western blot was set up as shown in figure 2.7.1.1 and run at 15 volts for 35 min. The blot was disassembled and the proteins were visualised on the PVDF membrane using coomassie brilliant blue staining.

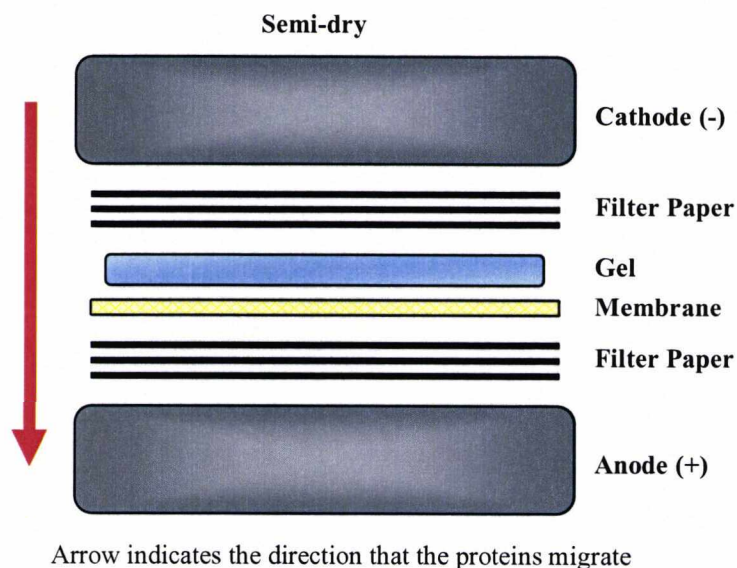


Figure 2.7.1.1 Diagram outlining the semi-dry blotting procedure for the PVDF membrane.

2.7.2 COOMASSIE BLUE STAINING OF PVDF MEMBRANES AND SDS-POLYACRYLAMIDE GELS

Coomassie stain was made using 40% v/v methanol, 10% v/v acetic acid and 50% distilled water with the coomassie brilliant blue crystals dissolved in the solution. The stain was then filtered through Whatman No.1 filter paper.

The PVDF membrane was submersed in the coomassie stain for 1-2 min. The coomassie stain was removed and the membrane was washed in destain (40% v/v methanol, 10% v/v acetic acid and 50% distilled water) for 5 min.

For the SDS-PA gels the coomassie stain was left on the gel for 30 min after which the gel was destained on a rotating platform for 1 hour.

2.7.3 IMMUNODECORATION OF PVDF MEMBRANE

The PVDF membrane was photocopied so that comparisons could be made with the ECL film and the original band pattern. The PVDF membrane was washed with

100% methanol until no bands were visible and rinsed with distilled water. The membrane was placed into a sterile 50 ml polypropylene test tube with the protein side facing the lumen of the tube. 20 ml of fat-free milk (~10 ml 'Marvel' milk powder dissolved in 50 ml of distilled water) was added to the tube and incubated at room temperature on a roller for 1 hour. The milk was then discarded and replaced with primary antibody in milk, and incubated on the roller at room temperature of 1 hour. The PVDF membrane was washed with 20 ml TBS (18.5 mM Tris and 0.14 M NaCl at pH 7.6) for 5 min on the roller and then with water for 5 min, this was then repeated. The secondary antibody was then added to the tube and incubated on the roller at room temperature for 1 h. The PVDF membrane was washed as before.

2.7.4 ECL DETECTION OF ANTIBODIES

The ECL western blotting detection agents were purchased from Amersham pharmacia biotech and used according to the manufacturer's instructions.

2.7.5 ANTIBODY PRODUCTION

The primary antibodies against SurA and PpiD were produced at the University of Kent. Full length SurA and PpiD proteins were purified by FPLC. Residual imidazole was removed by dialysis against phosphate buffer. For full length SurA, 100 µg of protein was emulsified with Freund's complete adjuvant and injected into a rabbit into the subcutaneous layer on four areas of the rabbit. This was followed with a booster of Freund's incomplete adjuvant which contained 100 µg of protein. The first test bleed showed high levels of antibody, terminal bleed was performed 1 week later. For the PpiD antibodies 100 µg of protein was introduced to the rabbit with Titermax, the usual 5 boosters followed and the terminal bleed one week after the final booster.

Secondary antibodies were obtained from DAKO (Denmark). These were polyclonal swine anti-rabbit immunoglobulins, which had been peroxidase-conjugated. The antibodies were used as a 1:1000 dilution in 10% (v/v) milk solution.

2.8 PEPTIDE STUDIES

2.8.1 RADIOACTIVITY STORAGE

For radioactive labelling of peptides ^{125}I Bolton and Hunter reagent (*N*-succinimidyl 3-(4-hydroxy,5-[^{125}I] *iodophenyl*) propionate) was used (Amersham Pharmacia Biotech). The radioactivity was supplied in dry benzene containing 0.2% dimethyl formamide. Aliquots were transferred into microcentrifuge tubes and sealed with parafilm and stored at 4 °C in lead lined containers.

2.8.2 PEPTIDE SYNTHESIS

All peptides were synthesised at the University of Kent. Peptides were received as freeze dried powder and were stored at -20 °C.

The peptides used in this study were made up in PBS solution. The pH was adjusted by the addition of 2 M NaOH, a small sample was dripped on to pH paper to check that the pH was roughly between pH 7 and 8. The peptides in solution were stored at -20 °C.

2.8.3 MEASURING PEPTIDE CONCENTRATION

The peptide concentration was measured at A_{260} . 1 μl of the peptide solution described in 2.8.2 was added to 100 μl of distilled water in an appropriately sized cuvette. Using the extinction coefficients of the aromatic residues the concentrations were calculated.

2.8.4 RADIOLABELLING OF PEPTIDES

Solvent from an aliquot of ^{125}I Bolton and Hunter reagent was removed by passing compressed air through a pasture pipette over the top of the microcentrifuge tube. To

the dry tube, 3 μ l of 1X PBS and 4 μ l of high concentration peptide was added. Incubation was carried out on ice for at least 90 min. 13 μ l PBS and 15 μ l 50% TCA (w/v) was added and the sample was incubated on ice for 1 hour. The samples were then spun at 13000 rpm for 30 min at 4 °C. The supernatant was removed and the pellet resuspended in 75 μ l of ice cold acetone. This was then immediately centrifuged at 13000 rpm for 20 min at 4 °C. The supernatant was removed and the pellet was left to air dry for 5 min. The pellet was resuspended in 95 μ l of PBS and 5 μ l of DMSO (dimethyl sulfoxide). The radiolabelled sample was stored at 4 °C in a lead line container until use.

2.8.5 CROSS-LINKING ASSAY

Cross-linking was performed using the homobifunctional cross-linking reagent DSG (discuccinimidyl glutarate). The samples were incubated with one-fifth volume of cross-linking solution (30 mg/ml in DMSO) at 0°C for 60 min and the reaction was stopped by the addition of SDS-polyacryamide gel electrophoresis loading buffer.

2.8.6 COMPETITION ASSAY

The peptide Δ -somatostatin has been shown to have a high affinity to SurA and PpiD, and was used as the reporter peptide in the competition assay. In each competition assay, the final concentration of the competing peptide used was 0.5 mM. Pure SurA was used as well as cell lysate containing the expressed protein. 1 μ l SurA was mixed with the appropriate amount of peptide made up to 5 μ l with 1x PBS and 3 μ l of radiolabelled Δ -somatostatin, this was left on ice for 10 min. Then 2 μ l of DSG mix (2 μ l of DSG 30 mg/ml in 40 μ l 1X PBS) was added and left for 1 hr on ice. The samples were run on an SDS-PA gel and subsequently electrotransferred onto PVDF membrane. The blot was covered with a layer of cling film and placed in a cassette with MP film; this was stored at -70°C.

2.8.7 BINDING ASSAY

The reporter peptide was radiolabelled as described in 2.8.2. 2 μ l of protein was mixed with 3 μ l of radiolabelled peptide and 2 μ l of 1X PBS and left for 10 min on ice. Then 2 μ l of DSG mix was added and the sample was incubated on ice for 1 hour. The sample was run on an SDS-PAGE gel, western blotted onto a PVDF membrane and exposed to MP film as described before.

2.8.8 scRNase

Freeze dried scRNase as described by Hawkins and Freedmann (Klappa et al., 1997), was dissolved in 50 μ l of 1X PBS giving a final concentration of 5 mg/ml. In each binding assay 1.5 μ l of scRNase and 3 μ l of protein were cross linked using 2 μ l of DSG (made up as before). Samples without crosslinker or scRNase served as controls. Samples were incubated on ice for 1 hour. They were then run on SDS-PAGE gels and blotted onto PVDF membranes and immunodecorated with the appropriate antibodies.

2.8.9 TRITON-X-100

Protein samples were incubated for 10 min with 0.1% solution of Triton X-100 and radiolabelled Δ -somatostatin with subsequent cross-linking for 1 hour on ice. The samples were analysed on 10% polyacrylamide gels, Western blotted and exposed to MP film to detect the radioactivity.

2.8.10 HEAT INACTIVATION

Radiolabelled Δ -somatostatin was incubated with proteins that were either untreated or treated with heat inactivation for 5 min at 95°C prior to cross-linking. After cross-

linking the samples were analysed on 10% polyacrylamide gels, Western blotted and exposed to MP film to detect the radioactivity.

2.9 MUTAGENESIS

2.9.1 DESIGNING PRIMERS FOR MUTAGENESIS

Primers were designed following the instructions from QuikChange™ Site-Directed Mutagenesis Kit by Stratagene. Both mutagenic primers contained the desired mutation and anneal to the same sequence on opposite sides of the plasmid. In all cases the primer length was between 25 and 45 bases and the T_m was greater than 78°C. The mutations had at least 10-15 bases of correct sequence each side of the mutation, each terminated with one or more GC and had roughly a 40% GC content.

A64VF

5'-GCA AGG CAG CAA CTT CCG GAT GAC GTG ACG CTG CGC CAC CAA
ATC-3'

A64VR

5'-GAT TTG GTG GCG CAG CGT CAC GTC ATC CGG AAG TTG CTG CCT
TGC-3'

R73DF

5'-CTG CGC CAC CAA ATC ATG GAA GAT TTG ATC ATG GAT CAA ATC-3'

R73DR

5'-GAT TTG ATC CAT GAT CAA ATC TTC CAT GAT TTG GTG GCG CAG-3'

2.9.2 MUTAGENESIS

A typical mutagenesis reaction contained the following components:

- 37 μl ddH₂O
- 1 μl dNTP's
- 5 μl 10X Reaction buffer
- 2 μl of dsDNA template (5-50 ng)
- 2 μl Forward Primer (125 ng)
- 2 μl Reverse Primer (125 ng)

1 μl of *PFU* polymerase turbo (2.5 U/ μl) was added to the above components. The cycles and temperatures are described below in figure 2.9.3.1.

PROGRAMME	TEMPERATURE	DURATION	NUMBER OF CYCLES	LINK TO...
1	94 °C	3 min	1	2
2	94 °C	30 seconds	12-18*	3
	55 °C	1 min		
	68 °C	8 min		
3	68 °C	7 min	1	4
4	4 °C	∞	1	End

Table 2.9.3.1 Cycles of a general mutagenesis reaction. * 12-18 cycles depending on the type of mutation required, where 12 is for a point mutation, 16 for single amino acid changes and 18 for multiple amino acid deletions or insertions.

The products were run on 1% agarose gel with standard gel loading buffer to confirm the presence of products.

The restriction enzyme DpnI was used to digest the parental DNA. 1 μl (10 U/ μl) was added directly to the amplification. The reactions were incubated at 37 °C for 1 hour.

The circular, nicked dsDNA is then transformed into super competent XL1-Blue cells. 100 μ l of super competent cells were mixed with varying concentrations of reaction that had been digested with *DpnI* (1 μ l-10 μ l). The transformations were carried out as described as above.

Individual colonies were then picked and incubated in LB media with the appropriate antibiotics overnight. The DNA was mini-preped and then sent off for sequencing to confirm the presence of the mutation.

2.10 NMR

2.10.1 PREPARATION OF NMR SAMPLES

The protein samples used in NMR had to be at a minimum concentration of 3 mM. The proteins were produced as in section 2.6.2 and purified as in section 2.6.3.

2.10.2 NMR SAMPLE

The microtubes used in the NMR were made by Shigemi. These were cleaned with concentrated Nitric acid (65%). The nitric acid was left inside the Shigemi tube for more than an hour to remove all traces of protein. The tubes were then thoroughly rinsed with Milli-Q water and dried with compressed air.

The samples were added to the Shigemi tube using either a 22 gauge needle or a NMR pipette.

Standard NMR tubes had a total volume of 330 μ l, 300 μ l of protein at 3 mM and 10% D₂O. Samples were prepared in an eppendorf tube and spun at 13000 rpm for 1 min before being carefully pipetted into the Shigemi tube.

Saturation Transfer Difference (STD) NMR samples were also analysed in the Shigemi tubes and had 330 μ l final volume, 80 μ M protein, 2 mM peptide and 10% D₂O.

Analysis of the 2 mM peptide had a total volume of 660 μl including 10% D_2O .

2.10.3 SATURATION TRANSFER DIFFERENCE NMR

The STD-NMR experiment was composed of two stages and a number of analytical steps.

The first stage involves a sample containing both the protein and peptide. The final peptide concentration was 2 mM and the final concentration of the protein was 80 μM . The sample was in a total volume of 300 μl in PBS, to this 10% D_2O was added. The sample was then spun at 13000 rpm for 1 min to remove any insoluble matter. The supernatant was pipetted into a Shigemi tube.

The second sample contained only peptide. The final concentration of the peptide was 2 mM in a total volume of 600 μl with 10% of D_2O added. Again the sample was spun at 13000 rpm of 1 min and the sample was pipetted into an NMR tube.

All NMR experiments were recorded using a Varian UnityINOVA 600 MHz NMR spectrometer at 25°C using samples dissolved and/or suspended in 600 μl PBS (25 mM phosphate, 100mM NaCl, pH 6.5) in standard Norell 509 or Wilmad 535-PP7 NMR tubes. Saturation transfer difference NMR (STD NMR) experiments were recorded using a modified version of the basic sequence (Mayer and Meyer, 2001) using a comb of Gaussian shaped pulses applied for 2.0 s with each pulse having 100 Hz bandwidth. Saturation transfer difference was measured by addition and subtraction of data on the spectrometer with the on-resonance excitation at -3.0 ppm and off-resonance excitation at -80.0 ppm. Suppression of saturation signals from the target was achieved using a $T_{1\rho}$ -filter of Hahn Echo pulses set for 30 ms duration with a $\gamma\text{-B}_1$ of 9,500 Hz. STD NMR difference experiments were run with 16,384 transients (8,192 additions and subtractions) with a run time of 15 hrs and STD NMR control experiments were run with 32 transients with a run time of 2 min.

All STD-NMR experiments were executed with the kind help of Dr Mark Howard at the University of Kent at Canterbury.

2.11 MOLECULAR MODELLING

Molecular dynamic simulation of mutants was an alternative way of visualising the changes to a protein with altered/changed residues. This is only possible with proteins that have been assigned structures by X-ray crystallography, or NMR e.t.c. In the case of SurA the X-ray crystallography structure has already been published.

2.11.1 OUTLINE OF THE SYSTEM

In silico molecular modelling and simulated annealing of mutants of SurA were carried out using Crystallography and NMR system (CNS) [Brunger *et al*, 1998] running on Silicon Graphics O2+ and Octane2 workstations. The process of simulated annealing requires that hydrogen atoms be added to the X-ray structure so that all force fields are quantitative for energy minimisation.

2.11.2 CHOOSING THE RESIDUES

The residues were chosen because of their location in the full length SurA molecule. The binding site of SurA was shown to be within the first 110 amino acids, so the changes were made to only this region of the protein.

2.11.3 THE BASIC PROCESS

The residue to be mutated was changed in MolMol. The hydrogen atoms were also added in MolMol. The PDB was then edited for the HIS+, LYS+ and ARG+ and these were replaced with HIS, LYS and ARG.

The CNS standard simulated annealing (SA): model-anneal.inp. This involved using Cartesian molecular dynamics that includes simulated annealing for 0.5 ps (1000 steps of 0.0005 ps) at a constant temperature of 298 K in accordance with the standard SA protocol.

The rmsd was found to be 1.1Å for C^α between the X-ray and SA wild-type structures. This validated the SA method and proved that SA did not adversely perturb the structural model.

2.12 BIOINFORMATICS

Structure of SurA and other PPIases were taken from the Protein Data Bank:

<http://www.rcsb.org/pdb/>

H.M. Berman, J. Westbrook, Z. Feng, G. Gilliland, T.N. Bhat, H. Weissig, I.N. Shindyalov, P.E. Bourne: The Protein Data Bank. *Nucleic Acids Research*, **28** pp. 235-242 (2000)

MolMol, Molecule analysis and Molecule display:

<http://hugin.ethz.ch/wuthrich/software/molmol/>

Koradi, R., Billeter, M., and Wüthrich, K. (1996) *J Mol Graphics* **14**, 51-55.

MOLMOL: a program for display and analysis of macromolecular structures.

AGADIR:

<http://www.embl-heidelberg.de/Services/serrano/agadir/agadir-start.html>

Muñoz, V. & Serrano, L. (1994).

Elucidating the folding problem of α -helical peptides using empirical parameters, II. Helix macrodipole effects and rational modification of the helical content of natural peptides. *J. Mol. Biol* **245**, 275-296.

Muñoz, V. & Serrano, L. (1994).

Elucidating the folding problem of α -helical peptides using empirical parameters III: Temperature and pH dependence *J. Mol. Biol* **245**, 297-308.

Muñoz, V. & Serrano, L. (1997).

Development of the Multiple Sequence Approximation within the **Agadir** Model of α -Helix Formation. Comparison with Zimm-Bragg and Lifson-Roig Formalisms. *Biopolymers* **41**, 495-509.

Lacroix, E., Viguera AR & Serrano, L. (1998).

Elucidating the folding problem of α -helices: Local motifs, long-range electrostatics, ionic strength dependence and prediction of NMR parameters. *J. Mol. Biol.* 284, 173-191

Sequence alignments used BCM:

<http://www.hgsc.bcm.tmc.edu/>

(Clustalw does multiple alignments of nucleic acid and amino acid sequences).

Protein searches used Swiss Prot:

<http://www.expasy.org/>

Gasteiger E., Gattiker A., Hoogland C., Ivanyi I., Appel R.D., Bairoch A. *ExPASy: the proteomics server for in-depth protein knowledge and analysis* *Nucleic Acids Res.* 31:3784-3788(2003).

Digest of DNA used NEBcutter:

<http://tools.neb.com/NEBcutter2/index.php>

Vincze, T., Posfai, J. and Roberts, R.J. NEBcutter: a program to cleave DNA with restriction enzymes. *Nucleic Acids Res.* 31: 3688-3691 (2003).

Accelrys Discovery Studio Visualiser Version 1.6:

www.accelrys.com

Chapter 3

Full Length SurA and the N-Terminal Fragment of SurA

Chapter 3: N-Terminal Fragment of SurA

3.1 INTRODUCTION

surA was originally identified during a search for *Escherichia coli* genes that were essential for stationary phase survival, hence the name SurA. An insertion of a mini-Tn10 element located near 1 minute on the *E. coli* chromosome lead to marked loss of cell viability in stationary phase (Tormo et al., 1990).

surA encodes a protein of 428 amino acids, 47284 Da unprocessed. The first 20 amino acids at the N-terminus belong to the signal sequence (Yura et al., 1992), which is followed by the cleavage sequence Ala – Pro – Glu – Val – Val (Rouvière and Gross, 1996). The presence of a signal sequence indicates that the protein would be likely to be found in the periplasmic space. This has been shown by purifications of C-terminally tagged proteins and native proteins being purified from the periplasm of *E. coli* cells (Lazar and Kolter, 1996; Rouvière and Gross, 1996). The first 150 amino acids at the N-terminal end have been shown to contain the region essential for binding to peptides (Webb et al., 2001). The two parvulin domains are positioned from 150-252 and 265-364. Sequence alignments of the two domains show that domain 1 (150-252 of mature SurA) shows 36% identity and 55% similarity to parvulin and domain 2 (265-364 of mature SurA) shows 36% identity and 51% similarity to parvulin. The PPIase activity of SurA has been deduced from the similarity of the two domains to parvulin (Lazar et al., 1996; Missiakas et al., 1996; Scholz et al., 1997) and the activity of SurA has been assigned to these two parvulin like domains. Further investigation showed that the PPIase activity was only found in the second domain and exhibited the same activity as the intact protein (Missiakas et al., 1996; Rouvière and Gross, 1996).

The importance of SurA was shown by subjecting null mutants to the osmotic stresses of a stationary phase environment, during which cells lost viability after 3 – 5 days (Lazar et al., 1998). Further investigation showed that the outer membrane integrity was reduced in the absence of SurA, indicating that SurA was probably binding to peptidoglycans (Lazar et al., 1996; Lazar et al., 1998). It was also shown that null mutants, or mutants with decreased levels of SurA, resulted in a decrease in the maltose-inducible porin LamB (Lazar et al., 1998). This leant towards the reasoning

that SurA was not only important for maintaining the outer cell wall but was also binding to outer membrane proteins (Missiakas et al., 1996).

A clone of the full length SurA, without the signal sequence was generated by Webb et al, as well as the N-terminal region (first 150 amino acids without the signal sequence) and the C-terminal region with the two parvulin domains but without the N-terminal region. These clones were used to demonstrate that the binding domain was in the first 150 amino acids.

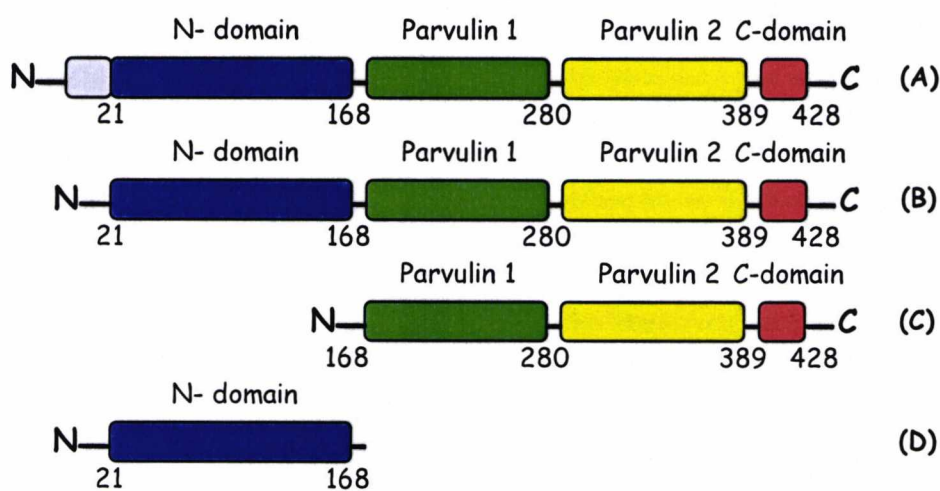


Figure 3.1.1 Diagram showing the different fragments of SurA cloned. The blue region represents the binding domain, the green and yellow indicate the parvulin domains 1 and 2 respectively and the red indicates the C-terminal region. A is the full length SurA, B with the signal sequence removed, C with the binding domain removed and D is just the N-terminal region without the parvulin domains.

This chapter describes the series of experiments that were used to produce purified full length SurA and the N-terminal fragment of SurA. This was important as the concentrated and purified proteins would be later used in the binding assays and NMR analysis.

3.2 INITIAL EXPERIMENTS CONFIRMED PRESENCE OF EXPRESSION CLONES

Clones that had been previously made (Webb et al., 2001) were used to confirm that the protein was in the soluble fraction, which is essential if it is to be purified and

used in further experiments. Secondly they were used to confirm that the protein was being expressed at reasonably high levels and it had the appropriate tag to be purified by metal affinity chromatography using a nickel-nitrilotriacetic acid column.

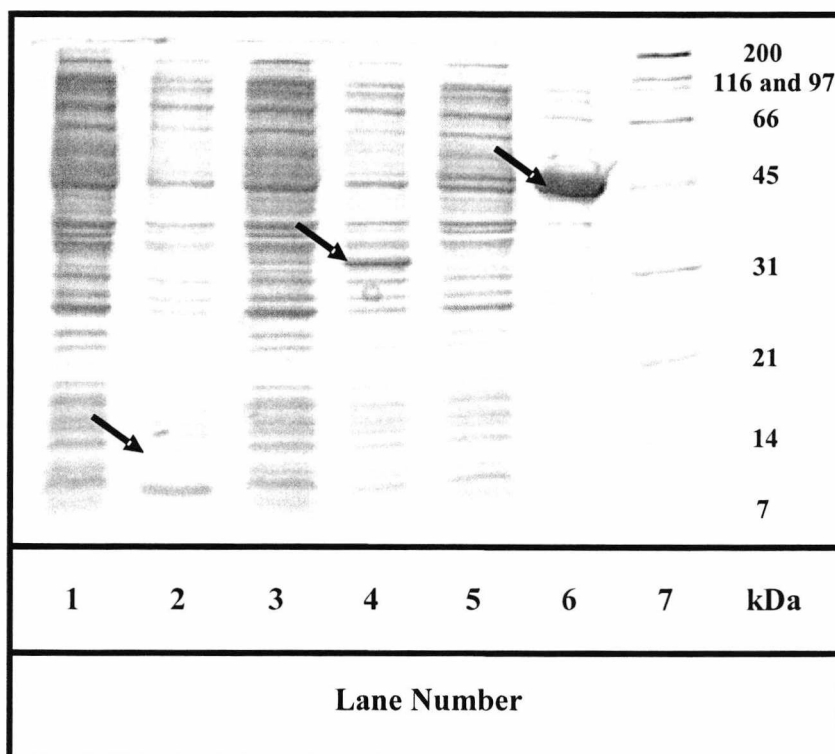


Figure 3.2.1 12.5 % SDS-PAGE showing the differences in the expression levels of the different fragments of SurA. Lanes 1-2 are the N-terminal fragment, 3-4 are the parvulin domains only, 5-6 are the full length SurA without the signal sequence. The even numbers are the samples that were induced to express the various proteins. Lane 7 is the SDS-PAGE molecular weight standards, broad range marker.

Figure 3.2.1 indicates that expression of all the fragments can be detected. Protein expression was induced by adding IPTG. The expression was confirmed by the positions of the bands indicated by arrows at the expected molecular weight levels on the 12.5 % SDS – polyacrylamide gel. The N-terminal fragment is between markers 8 and 9 (14400 – 6500 daltons), the parvulin domains is near marker 6 (31000 daltons) and the full length SurA is near the 5th marker (45000 daltons). For the N-terminal fragment and the parvulin domains there is a slightly raised level of expressed protein. For the full length SurA the increased expression is clearly visible in lane 6 in figure 3.2.1.

Samples of lysates from the expressed N-terminal fragment, full length SurA and parvulin domains of SurA were subjected to electrophoresis in 12.5 % SDS – polyacrylamide gels. Samples for the previously mentioned proteins were from uncentrifuged culture, the pellet and supernatant from a centrifuged culture. This was to show that the protein was present in the soluble fraction, see figure 3.2.2.

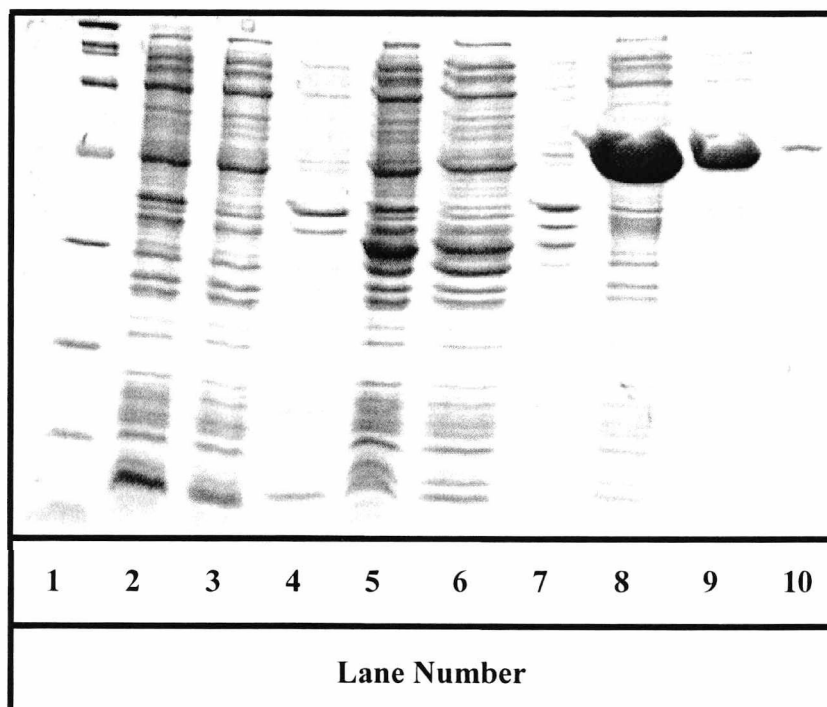


Figure 3.2.2 12.5 % SDS-PAGE showing that the SurA proteins are soluble. Lane 1 is the SDS-PAGE molecular weight standard, broad range marker. Lanes 2-4 are the N-terminal fragment, lane 2 is the uncentrifuged culture, lane 3 is supernatant and lane 4 is the pellet. Lanes 5-7 show the parvulin domains of SurA, lane 5 is the uncentrifuged culture, lane 6 is supernatant and lane 7 is the pellet. Lanes 8-10 show full length SurA, lane 8 is the uncentrifuged culture, lane 9 is supernatant and lane 10 is the pellet. Arrows indicate respective proteins.

A hexa-histidine tag was engineered onto the N-terminus of the mature full length protein and fragments, respectively, to facilitate rapid purification. To verify the presence of the hexa-histidine tag proteins from SDS-PAGE gels were transferred to PVDF membranes and subsequently decorated with hexa-histidine tag antibodies, see figure 3.2.3.

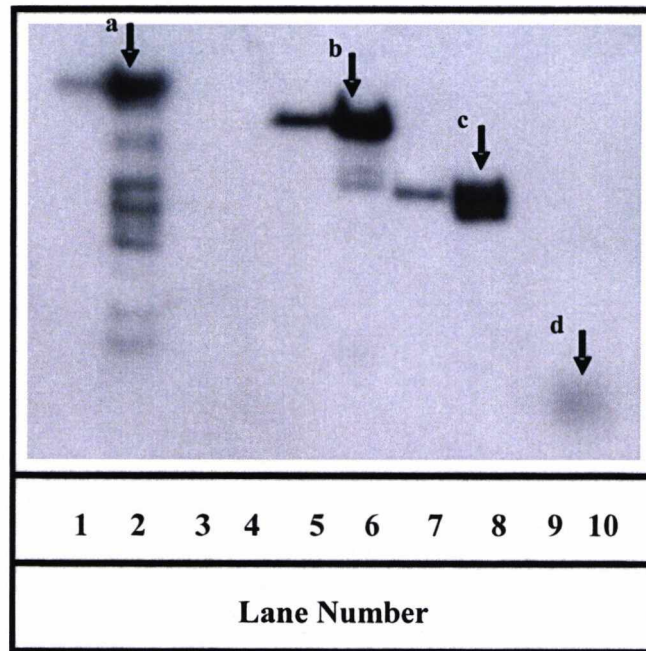


Figure 3.2.3 Hex-His Antibody decoration of SurA and fragments of SurA. Protein samples were separated on 12.5 % SDS-PAGE gels, the proteins were transferred to PVDF membrane and decorated with primary antibodies to detect the His-tag. Lanes 1-2 show PpiD, indicated by the arrow labelled (a). Lanes 3-4 are protein without the His-tag. Lanes 5-6 are the full length SurA, indicated by the arrow labelled (b). Lanes 7-8 are the SurA fragment of just the parvulin domains, indicated by the arrow labelled (c). Lanes 9-10 are the N-terminal fragment of SurA, indicated by the arrow labelled (d). Bands that are labelled by the arrows are the induced proteins.

3.3 PRIMARY ANTIBODIES BIND TO FULL LENGTH SURA AND FRAGMENTS

Polyclonal antibodies were produced using Freund's Complete Adjuvant with SurA. PVDF membranes that had the appropriate protein transferred by western blot were probed with the primary antibody and visualised by using secondary antibodies conjugated with horse radish peroxidase.

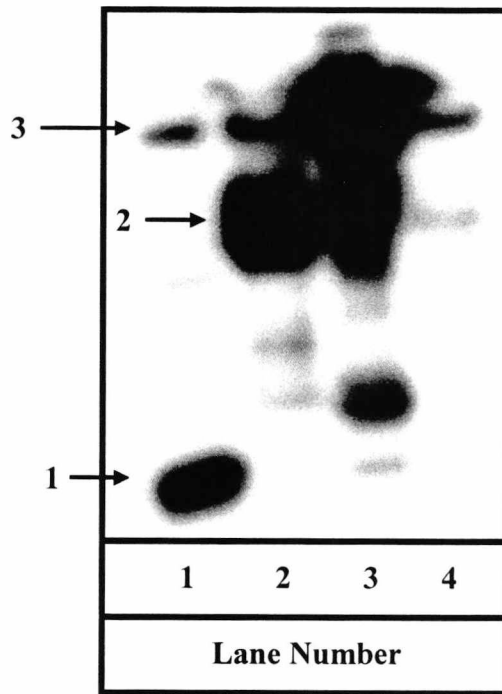


Figure 3.3.1 Immunodecorated Western blot of SurA and SurA fragments from cell lysates indicating that the SurA antibodies bind to the N-terminal fragment of SurA. Lane 1 shows the N-terminal fragment of SurA, lane 2 shows the fragment of SurA with the parvulin domains, lane 3 shows the full length SurA. The specific protein bands are indicated by arrows and numbers that relate to the lane number.

The SurA antibody was able to discriminate between the different cellular proteins and SurA in an untreated *E.coli* culture. The antibody was also suitable to use with the fragments of SurA and the point mutations produced. The specificity is shown in figure 3.3.1. The bands that are smaller than those indicated by the arrows are believed to be degraded protein in the cell sample. Endogenous full-length SurA is visible in lanes 1, 2 and 4, respectively.

3.4 EXPRESSION AND PURIFICATION

As it has been shown that only the N-terminal fragment of SurA is necessary and sufficient for binding, the SurA fragment containing the parvulin domains only was not further studied and purified. Figure 3.4.1 is an outline of the basic process.

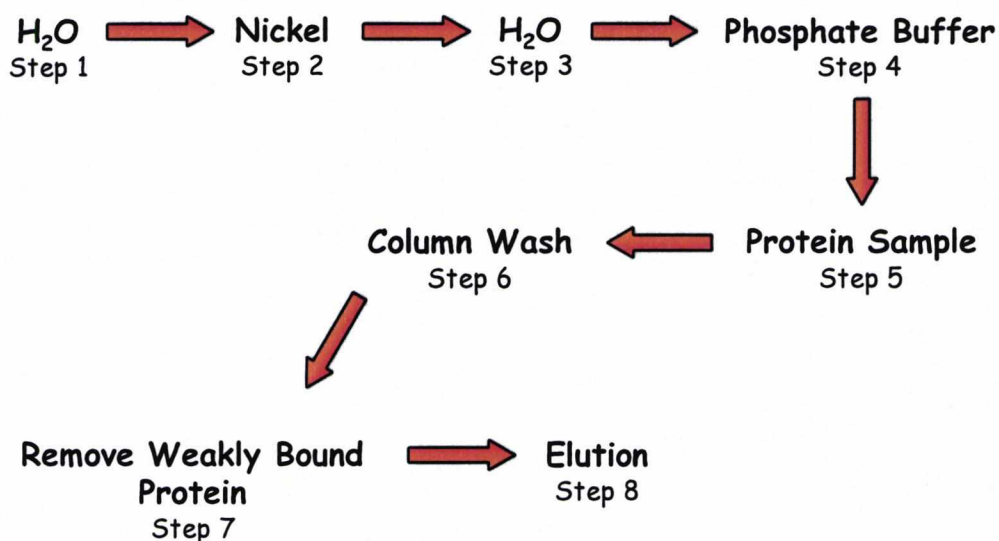


Figure 3.4.1 Flow diagram outlining simplified protein purification steps. The purification process is discussed in detail in the materials and methods section 2.6.3. Both SurA and the N-terminal fragment of SurA were purified using the HPLC method with the steps outlined above.

3.4.1 EXPRESSION AND PURIFICATION OF FULL LENGTH SURA

A large 2L batch culture was inoculated with cells that were grown in an overnight culture. Induction of the protein expression was achieved by the addition of IPTG when the culture reached the appropriate OD_{600} and then left for 3 hours. The culture was then centrifuged. The pellet was re-suspended in buffer and DNase and freeze-thawed twice. The lysed cells were centrifuged at 8000 rpm to remove the cell debris and filtered through a 0.2 μm filter before being passed down a nickel-nitrilotriacetic column. At each step of the purification process samples were collected, see figures 3.4.1.1 and 3.4.1.2.

The column was stored and run at ambient temperature. All buffers that were pumped through the column were filtered and de-gassed before use. The process was monitored using an ÄKTA system connected to the programme Unicorn.

Water was pumped down the column at a flow rate of 4 ml/min for 10 min and then 6 ml/min for another 10 min to remove the 20 % ethanol storage buffer. The 50 ml of 100 mM nickel sulphate solution was pumped onto the column at a flow rate of 2 ml/min. The column then was washed with water for 4 ml/min for 10 min and then 6 ml/min for 5 min. The column was equilibrated using phosphate buffer which was

pumped over the column at 6ml/min until the conductivity increased by 3. The lysed cell sample was pumped on to the equilibrated column at 2 ml/min. The column was washed at a flow rate of 4 ml/min using phosphate buffer to remove the unbound protein. The weakly bound proteins were washed from the column with phosphate buffer containing 50 mM imidazole and 0.5 M sodium chloride pH 7.2 until the UV_{280nm} was a steady flat line. The column was then rinsed with phosphate buffer until the conductivity was a steady flat line for 10 min.

Two elution buffers were used in this study, the first was phosphate buffer containing 10 mM EDTA, pH 7.2, which removed all bound protein from the column as well as the nickel, the second was phosphate buffer with 500 mM imidazole, which removed all the protein but not the nickel. In both situations the elution buffer was pumped down the column at a flow rate of 4 ml/min until there was a UV_{280nm} flat line. When the imidazole was used as the elution buffer the phosphate buffer with 10 mM EDTA was used to clean the column after the elution.

Samples were only collected after the protein sample was loaded onto the column. The protein sample was loaded on the column at step 5 and the first fraction was collected when the OD reading began to rise, indicating the presence of molecules other than the buffer. Following the addition of the protein sample to the column there was a wash step using just buffer to remove any unbound protein, this is shown in figure 3.4.1.1, lanes 3-5. This wash step was monitored by the change in the UV reading, and was stopped when it remained constant. Step 7 is shown in lanes 6-7, wash buffer containing imidazole was used to remove the loosely bound proteins. Step 7, shown in figure 3.4.1.2 in lanes 2-3 is a further wash with phosphate buffer. The protein was eluted from the column during step 8 with elution buffer containing EDTA, this is shown in lanes 4-7 (figure 3.4.1.2), the full length SurA protein is clearly visible and is indicated by the arrows. Although using the EDTA elution buffer to remove the bound protein from the column was effective, the concentration of EDTA in the final sample was too high for any detailed protein analysis. This is because high levels of EDTA in NMR analysis interfere with the signal. The EDTA also 'strips' the column, which results in nickel in high concentration in the eluted protein, however these samples were usable in binding assays. An alternative method used to elute the full length SurA from the purification column was using a higher concentration of imidazole.

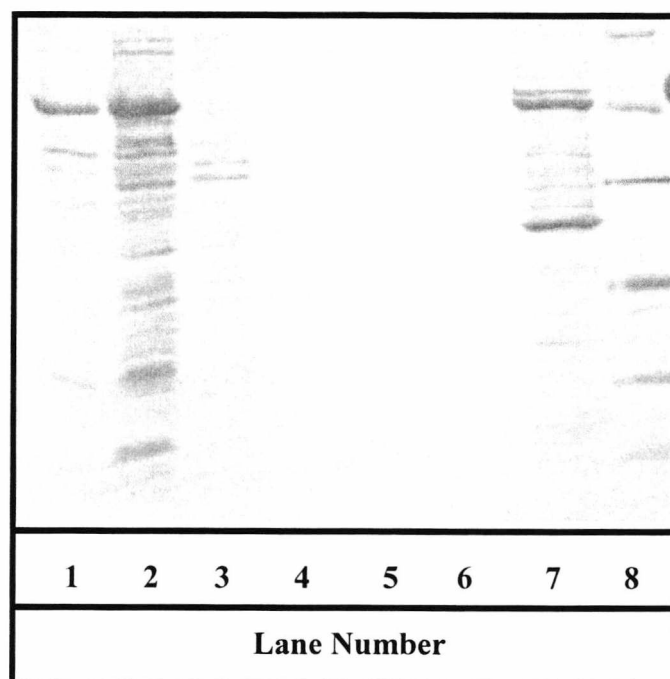


Figure 3.4.1.1 Purification of SurA. Each of the fractions collected from the protein purification were run on a 12.5 % SDS-PAGE gel. Lanes 1-2 indicate fractions taken when the protein sample was loaded on to the column. Lanes 3-5 indicate where the column was washed after the loading of the protein sample to the column using phosphate buffer. Lanes 6-7 is where the weakly bound protein is eluted from the column. Lane 8 is the molecular weight standard.

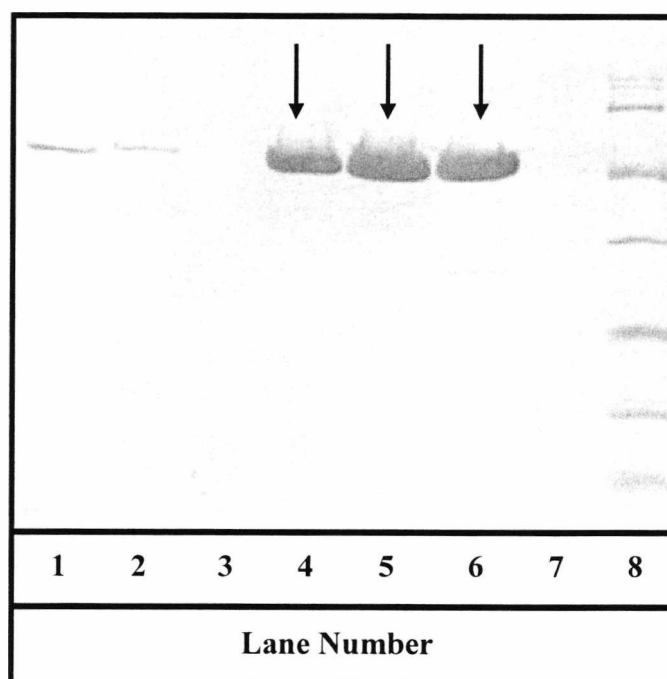


Figure 3.4.1.2 Purification of SurA continued. Each of the fractions collected from the protein purification were run on a 12.5 % SDS-PAGE gel. Lane 1-3 is where the weakly bound protein is eluted from the column. Lanes 4-7 shows the purified sample that was eluted using EDTA. Lane 8 is the molecular weight standard. The arrows indicate the fractions containing the purified full length SurA.

Different concentrations of imidazole were tried, 150 mM, 200 mM, 300 mM, 400 mM and 500 mM. The protein was eluted at 400 mM, therefore 400 mM was used to remove the protein from the column.

3.4.2 EXPRESSION AND PURIFICATION OF THE N-TERMINAL FRAGMENT OF SURA

A large 2L batch culture was inoculated with cells that were grown in an overnight culture. Induction of the protein expression was achieved by the addition of IPTG when the culture reached the appropriate OD_{600nm} , the culture was left for 4 hours. The culture was then centrifuged. The pellet was re-suspended in buffer containing DNase and was subsequently freeze-thawed to lyse the cells. The lysed cells were centrifuged to remove the cell debris and filtered before being passed over a nickel-nitrilotriacetic column. At each step of the purification process samples were collected, see figures 3.4.2.1 and 3.4.2.2. The protein was initially eluted from the column using 100 mM EDTA elution buffer as with the full length SurA. Due to the reasons mentioned for the full length SurA an alternative method to the EDTA elution was preferred, using a higher concentration of imidazole. For the N-terminal fragment different concentrations of imidazole were used to elute the protein, unlike the full length SurA, which was eluted at 400 mM imidazole, the N-terminal fragment was eluted at 500 mM imidazole. Figures 3.4.2.1 and 3.4.2.2 show the two 12.5 % SDS-PAGE gels showing the different fractions taken from the protein purification.

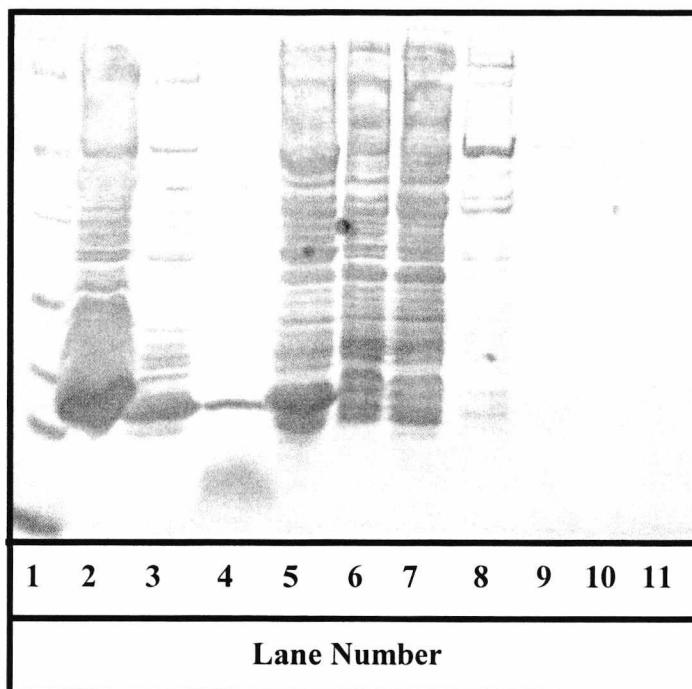


Figure 3.4.2.1 Purification of the N-terminal fragment of SurA. Lane I is the molecular weight standard. Lanes 2-3 show the protein content in the pellet. Lane 4 shows the expressed N-terminal fragment of SurA. Lane 5 is the sample that was loaded on to the column. Lane 6 is the fraction taken when the protein sample was loaded on to the column. Lanes 7-9 indicate where the column was washed after the loading of the protein sample to the column using phosphate buffer. Lane 10 and 11 are the last two wash steps prior to the elution, see figure 3.4.2.2.

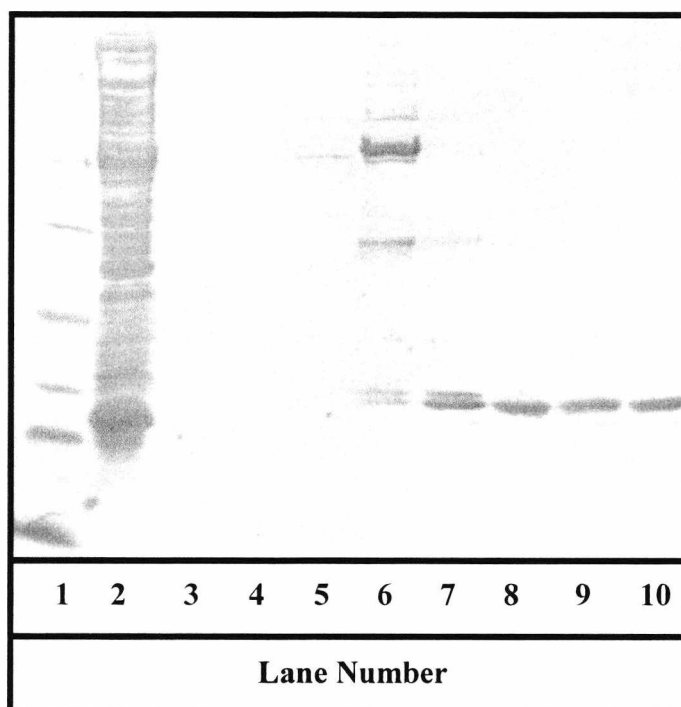


Figure 3.4.2.2 Purification of the N-terminal fragment of SurA continued. Lane 1 is the molecular weight standard, lane 2 sample that was loaded on to the column and lanes 3-10 are the subsequent elution steps.

The N-terminal fragment expression levels were found to be much lower than the full length SurA. Although this did not cause a problem with the purification procedure it meant that the cell lysate could not be easily used in binding assays and purified protein could not be used in any NMR studies. To be able to use the protein effectively in later binding assays and NMR the concentration of the protein needed to be much higher. The NMR experiments need the final concentration of the protein to be at least 3 mM. The concentration of the protein from the column was at only 0.5 mg/ml (37 μ M).

For the N-terminal fragment to be used it needed to be concentrated and purified, as simply concentrating the sample would concentrate the salts and any other chemicals within the sample.

3.5 CONCENTRATING FULL LENGTH SURA AND THE N-TERMINAL FRAGMENT OF SURA

For the proteins to be used in NMR experiments, the protein needed to be in buffers with minimal salt and as few impurities as possible, this meant removing all EDTA, nickel, and reducing the levels of imidazole and salt.

3.5.1 RESOURCE Q CONCENTRATION

The fractions from the nickel-nitrilotriacetic column containing full length SurA were loaded on to a Resource Q column. The main bulk of the protein eluted immediately after loading. There were some subsequent small peaks but these contained very little of the desired protein. The largest peaks were seen in the post load fractions, followed by further peaks in fractions 12, 14, 20 and 24. Samples were loaded onto a 12.5 % SDS gel, figure 3.5.1.1. The protein concentration in the samples after the load was low. This indicates that the full length SurA did not bind to the column. Subsequently the Resource Q was not used for the purification and concentration of the N-terminal fragment.

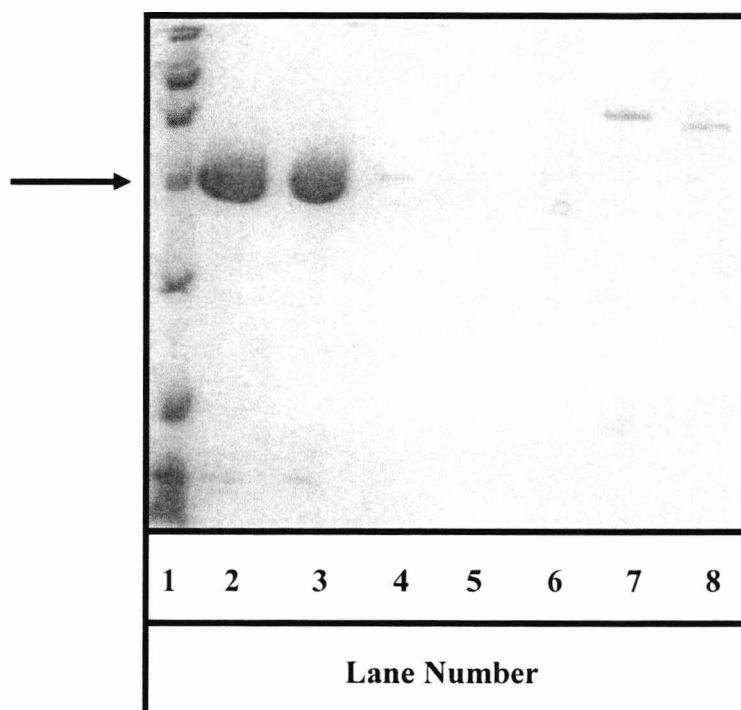


Figure 3.5.1.1 Resource Q Fractions for full length SurA. Fractions that had peaks were analysed on 12.5 % SDS-PAGE gels. Lane 1 shows the molecular weight marker standard, lane 2 the pre-loaded sample. Lanes 3 and 4 are the flow through from the loaded sample and lanes 5-8 are the eluted fractions.

3.5.2 CENTRICON CONCENTRATION OF FULL LENGTH SURA

The full length SurA was concentrated using a Centricon 30. Samples were spun at the maximum speed for 15 min. At 15 min intervals the filtrate was poured off and more samples were added. The final volume of retentate collected was 11 ml with 30 ml of filtrate. The retentate was then washed with three times the retentates volume with phosphate buffer to remove some of the EDTA. The final concentration of the full length SurA sample was measured at OD_{280nm} and the final concentration was calculated at 6.7 mg/ml (150 μ M).

3.5.3 FREEZE DRYING DOES NOT AFFECT SURA ACTIVITY

The least labour intensive method of concentrating the protein was to freeze dry the eluted protein. Protein was desalted by using NAPTM-10 Column (Pharmacia

Biotech), however although there was less than 3% salt contamination to the eluted sample, this would still be concentrated when the sample was freeze dried unless the sample was resuspended in the original volume. The N-terminal fragment and the full length SurA retained their binding ability even after they had been freeze dried.

3.5.4 CONCENTRATING N-TERMINAL FRAGMENT OF SURA WITH CENTRICON

Concentrating was achieved by filtering the sample through an anisotropic membrane. Centrifugal force drives solvents and low molecular weight solutes through the membrane into the filtrate vial. The Centricon was pre-rinsed using distilled water or buffer. This pre-rinsing removes the glycerol that contaminates the samples and can interfere with NMR scans. The centricon concentrated the full length SurA, however it was time consuming and only a small volume was concentrated. For the N-terminal fragment there was a loss in the protein concentration. The retentate and the filtrate both had less protein than the initial protein sample. Therefore it was assumed that the N-terminal fragment was becoming immobilised on the membrane. It was also noted that although the centricon had been pre-rinsed, there were still levels of glycerol in the retentate.

3.5.5 CONCENTRATING N-TERMINAL FRAGMENT OF SURA WITH THE ULTRAFREE®-4 CENTRIFUGAL FILTER UNIT

The filter unit was pre-rinsed using 10mM phosphate buffer to remove trace amounts of glycerol, 12ml of buffer was then washed through the unit at 1500rpm. Each 4ml wash took approximately 10 min to pass through the unit. The flow rate was affected by several parameters, including the MW, solute concentration, viscosity, centrifugal force and temperature. The protein samples were spun at 4°C, the same temperature as for the pre-rinsing. The full length SurA and the N-terminal fragment were spun in different filter units at the same time. The solution started decreasing in volume at the same rate after the first 4ml had passed through the filters. The filtrate passing

through the filter containing the N-terminal fragment began to slow down. As with the Centricon the N-terminal fragment was believed to be immobilised on the membrane.

3.5.6 BUFFER EXCHANGE WITH THE ULTRAFREE®-4 CENTRIFUGAL UNIT

The full length SurA was concentrated from 4 ml down to 0.5 ml and the filtrate was discarded. The concentrate was reconstituted back to 4ml with buffer; the sample was concentrated and again made up to 4 ml. This was also tried with the N-terminal fragment of SurA but again the filter unit became blocked.

3.5.7 PROTEIN DIALYSIS OF THE N-TERMINAL FRAGMENT OF SURA

Two methods were employed to dialyse the protein: dialysis tubing with a pore size of 12-14000 Da and Slide-A-Lyzer® with a capacity of 0.5 – 3 ml and MW of 10,000. Both methods were equally effective for changing the buffer conditions of the proteins. Initially the N-terminal fragment was dialysed for 2 hours, the buffer was changed and the protein was dialysed again for 2 hours, again the buffer was changed and the protein left at 4 °C overnight.

Typically 25 mM phosphate buffer, 100 mM sodium chloride pH 6.5 was used as these are the conditions that are used in the NMR.

Dialysis was effective for full length SurA and the protein could be dialysed against a buffer containing no salt. The protein remained stable and lost no activity. The N-terminal fragment was stable with the imidazole removed from the buffer, but when there was no sodium chloride present the protein precipitated quickly. Sequential reduction of the sodium chloride revealed that the protein precipitated at salt concentrations below 150 mM.

3.6 CONCLUSIONS

The full length SurA was purified using a nickel-nitrilotriacetic column. Although the full length protein did not bind to the Resource Q column, the other methods employed were successful. The fractions containing the desired full length SurA were subsequently concentrated and washed of EDTA impurities using a Centricon 30 filter unit. The final concentration of the protein was 6.7 mg/ml. The results suggest that the protein is soluble and therefore usable in further experiments related to this study. The N-terminal fragment of SurA was not as stable as the full length protein. Attempts to concentrate the N-terminal fragment were made difficult by its instability in solutions with low salt concentrations. Subsequently, washes using the Centricon filter unit and the Ultrafree centrifuge unit were unsuccessful probably due to a build-up of precipitated N-terminal fragment protein on the membranes. The lack of stability of the protein was shown using dialysis. With increasingly lowered salt concentrations the N-terminal fragment of SurA precipitated out of the solution.

Chapter 4

Binding of Peptides to SurA and N-terminal Fragment

Chapter 4: Binding of Peptides to SurA and the N-Terminal Fragment

4.1 INTRODUCTION

Over the last decade there has been increased interest in the problem of antibiotic resistance. Antibiotic resistance can manifest itself in a number of different ways. Firstly the antibiotic target may be inaccessible. One example of this is the peptidoglycan in Gram-negative bacteria being inaccessible to penicillins as they cannot penetrate the Gram-negative cell's outer membrane (Finch, 2003). If the antibiotic does enter the cell the presence of efflux pumps can actively pump out antibiotic from cell. For example Gram-negative bacteria are resistant against the activity of tetracyclines by this mechanism (Poole, 2005). In some types of resistance the antibiotic target may be modified to prevent the action of the drug; Trimethoprim resistance occurs by alterations in the dihydrofolate reductase (Burchall and Hitchings, 1965); quinolone resistance is facilitated by point mutations in the DNA gyrase, which prevent binding of the drug to its target (Willmott and Maxwell, 1993). Antibiotic resistance may occur because the antibiotic is chemically modified or destroyed; such examples include the β -lactamases and the various aminoglycoside-modifying enzymes (Woodford, 2005). The cause of chloramphenicol resistance is often by acetylation by the chloramphenicol acetyl transferase enzyme (Shaw, 1983). Bacteria may employ alternative pathways, avoiding the drug target; Methicillin resistance in methicillin-resistant *Staphylococcus aureus* results from the production of an additional penicillin binding protein: PBP2', which is not susceptible to inhibition by penicillins (Velasco et al., 2005).

One of the problems associated with antibiotic resistance is that large compounds have to pass through a selective membrane into the cytoplasm to be effective. Therefore a potential alternative would be to find a drug target within the periplasmic space. One such target could be SurA as it has been shown in previous studies that knockouts of SurA lose viability in the stationary phase due to incorrectly formed outer membrane proteins. An inhibitor that could pass freely into the periplasmic space and bind to SurA and inhibit its activity, possibly by mimicking a potential

substrate would be desirable. For such an inhibitor to be successful *in vivo* it would have to be < 600 Da so that it could freely diffuse into the periplasmic space.

To find a potential inhibitor of SurA it is first necessary to identify the binding motif of SurA.

One such way of achieving this would be to use a Phage display library. The phage display would be used for high-throughput screening of potential peptides, however this method is potentially very expensive (Sidhu et al., 2000) and labour intensive.

To identify the binding motif of SurA, a novel approach has been taken. Instead of a large peptide library being constructed, specific changes have been made to a model peptide that has been shown to bind to native SurA (Webb et al., 2001). By using chemical cross-linkers, which can be applied to even crude cell extracts, it is possible to study the interactions between protein and peptide. This specific technique to crosslink model peptides to a specific protein has shown that the **b'** domain of human PDI, which does not contain active sites, is essential and sufficient for the binding of small peptides (Klappa et al., 1998a). Furthermore it was shown that the tyrosine and tryptophan residues within a peptide are the recognition motifs for PDI_p, a pancreas-specific form of PDI (Ruddock et al., 2000) and that the interactions could be inhibited by a ligand containing a hydroxyaryl-group (Klappa et al., 2001). The key components of the binding experiments are described in the following sections.

4.2 CROSSLINKING

Crosslinking is the process of chemically joining two or more molecules by a covalent bond. Crosslinking reagents contain reactive ends to specific functional groups (primary amines, sulfhydryls, etc.) on proteins or other molecules. Crosslinking reagents have been used to assist in determination of near-neighbour relationships, three-dimensional structures of proteins, and molecular associations in cell membranes. They also are useful for solid-phase immobilization, hapten-carrier protein conjugation, preparing antibody-enzyme conjugates, immunotoxins and other labelled protein reagents. Other uses include modification of nucleic acids, drugs and solid surfaces.

Crosslinkers can be either homobifunctional or heterobifunctional. Homobifunctional crosslinkers have two identical reactive groups and often are used in one-step reaction procedures to crosslink proteins to each other or to stabilize quaternary structure. Even when conjugation of two different proteins is the goal, one-step crosslinking with homobifunctional reagents often results in self-conjugation, intramolecular crosslinking and/or polymerization.

One type of the homobifunctional crosslinkers are the amine reactive *N*-hydroxysuccinimide esters. The esters react with amine functionality on the protein to form stable amide bonds and release two molecules of *N*-hydroxysuccinimide (NHS). The esters tend to react with the α -amines at the N-terminus and the ϵ -amines of lysine residues. It is also possible for these reagents to react with sulfhydryl and hydroxyl groups, but this does not lead to stable adduct formation (Green et al., 2001) see figure 4.2.1.

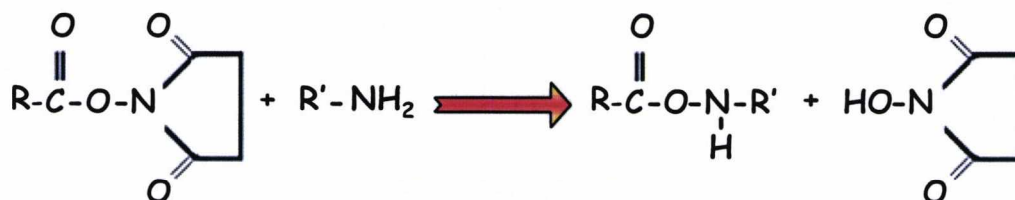


Figure 4.2.1 NHS-ester reaction scheme. Accessible α -amine groups present on the N-termini of proteins and ϵ -amines on lysine residues react with NHS-esters and form amide bonds, releasing *N*-hydroxysuccinimide. Scheme adapted from the Pierce website.

In this study the water soluble homobifunctional *N*-hydroxysuccinimide ester (NHS-ester) Disuccinimidyl glutarate DSG (figure 4.2.2), was used (Ruddock et al., 2000). The cross-linker is noncleavable and often used for conjugating radiolabelled ligands to cell surface receptors (Carlsson et al., 1978).

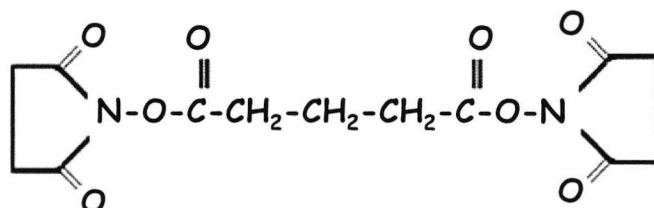


Figure 4.2.2 Cross-linker DSG. Disuccinimidyl glutarate MW 326.26, spacer arm length 7.72Å.

4.3 RADIOLABELLING

Radiolabelling peptides in this study was carried out using Bolton-Hunter reagent. The Bolton-Hunter reagent can be iodinated before or after coupling to a molecule of interest, but in this case it was used iodinated with radioactive iodine [^{125}I]. Bolton-Hunter reagent can be used for the iodination of sensitive proteins and proteins not containing tyrosine residues. It conjugates to amino groups via an active ester reaction, takes place under mild conditions and avoids exposure of the protein to the reactive reagent commonly used in radioiodinations (Bolton and Hunter, 1973). The coupling reaction is shown in figure 4.3.1.

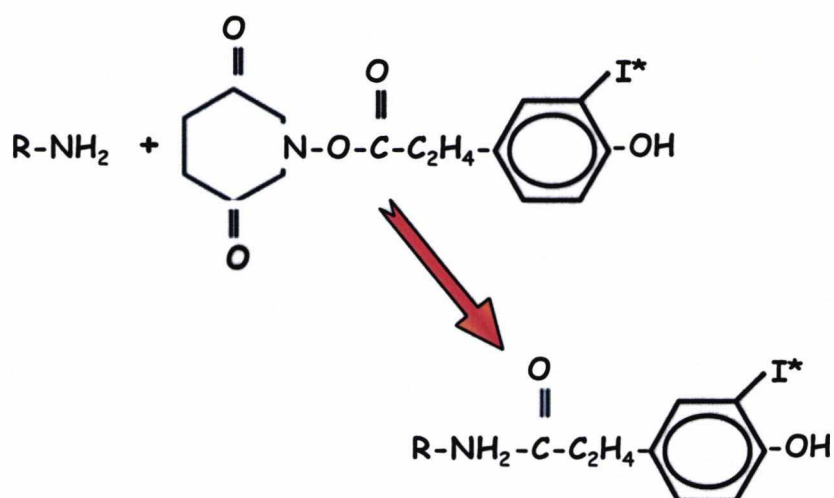


Figure 4.3.1 Direct coupling of the Bolton-Hunter reagent to Lysine residues. The Bolton-Hunter reagent is used for the labelling of peptides in this study. The radio labelled peptides are subsequently cross-linked to the protein of interest.

4.4 THE CROSSLINKING APPROACH

4.4.1 DIRECT CROSSLINKING OF RADIOLABELLED PEPTIDES

To investigate whether a protein interacts with a specific substrate we used the chemical crosslinking of a [^{125}I] Bolton-Hunter radiolabelled peptide. The figure 4.4.1.1 shows a schematic of the principle of the crosslinking process.

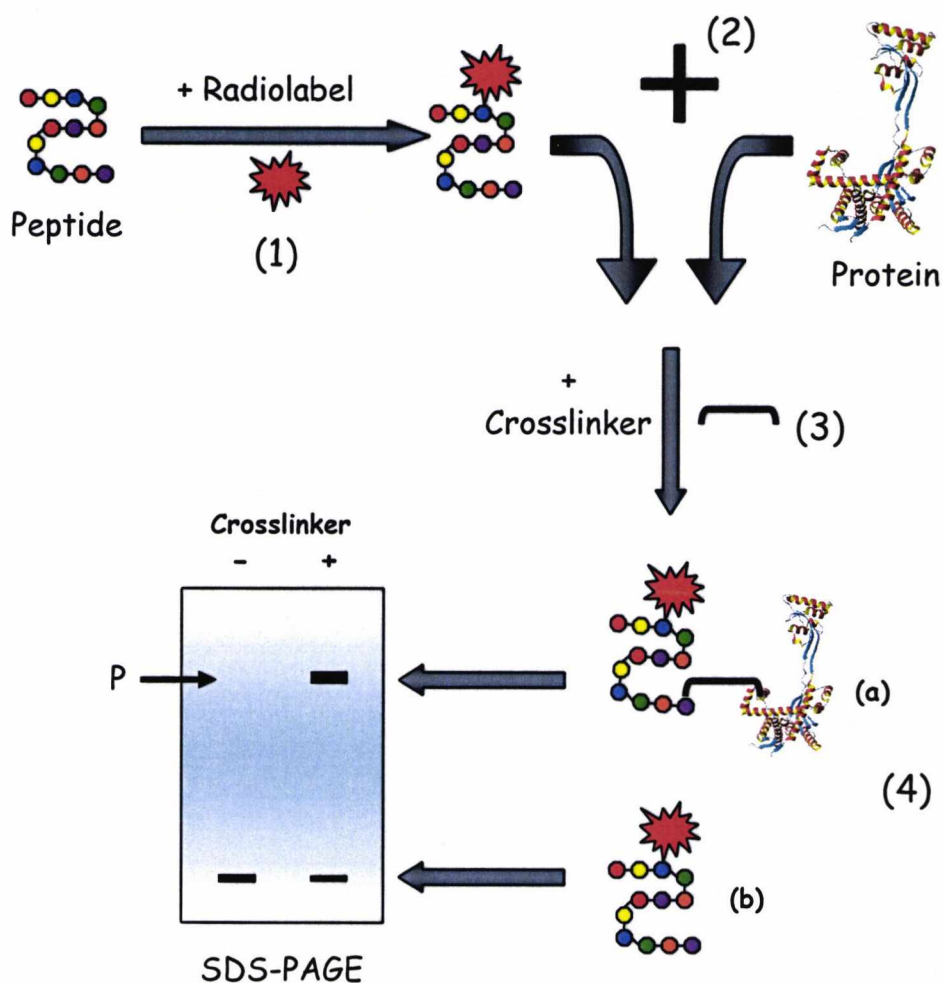


Figure 4.4.1.1 Direct crosslinking of radiolabelled peptides to protein. The radiolabel is indicated by the red star. At position (1) the radiolabel is coupled to the peptide, this is described in detail in section 4.3. The radiolabelled peptide is incubated with a protein (2), or cell lysate. After the incubation period the crosslinker is added to the radiolabelled peptide and protein (3). The sample is run on SDS-PAGE. If the crosslinking has been successful the product (4a) will be visible on the film after autoradiography, band is indicated by the P. Uncrosslinked radiolabelled peptide is visible at the bottom of the gel (4b).

Direct crosslinking of peptides that have been radiolabelled *in vitro* can help to establish which peptides bind to a protein. If there is no binding of a radiolabelled peptide to the protein then there will subsequently be no crosslinking product and therefore no band visible on the exposed autoradiograph. However if there was an interaction between the protein and the radiolabelled peptide there would be crosslinking product and therefore a visible band.

4.4.2 INDIRECT CROSSLINKING OF RADIOLABELLED PEPTIDES, THE COMPETITION ASSAY

The direct radiolabelling of peptides is time consuming and expensive. The alternative method to test binding of a peptide to a protein is by the indirect crosslinking of radiolabelled peptides or competition assay.

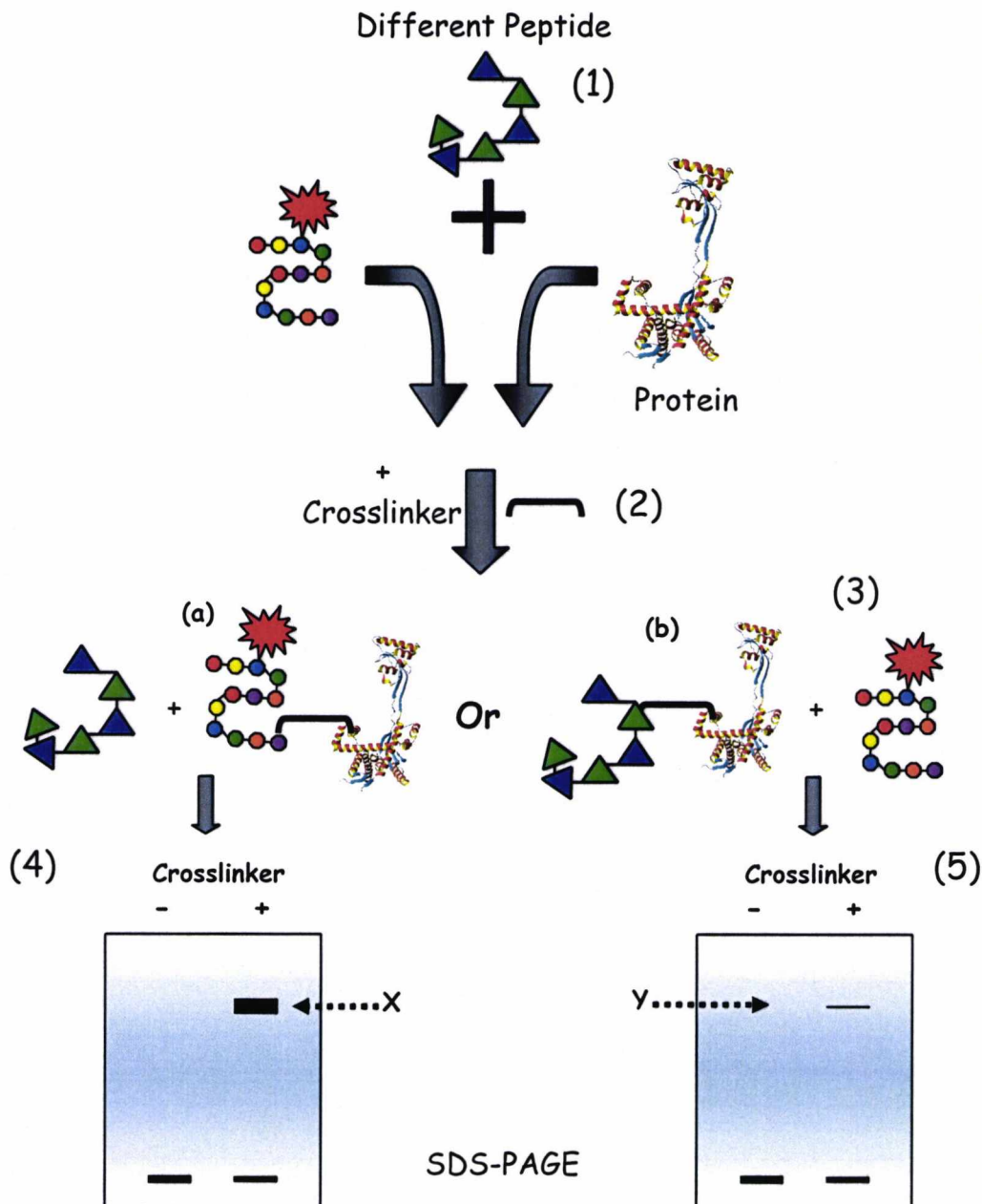


Figure 4.4.2.1 Competition Assay. The schematic shows the principle of the competition assay. At stage (1) the radiolabelled peptide (shown in figure 4.4.1.1) is incubated with protein and another unlabelled peptide. (2) The crosslinker is added. (3) If the unlabelled peptide has a lower affinity for the protein (a) then more of the radiolabelled peptide will be crosslinked to the protein, (4). However if the un-radiolabelled peptide has a higher affinity for the protein than the radiolabelled peptide (b) then more of the un-radiolabelled peptide will be crosslinked to the protein, (5).

The competition assay is an efficient means of testing the ability of un-radiolabelled peptides to bind to a protein.

4.5 **CROSSLINKING OF A RADIOLABELLED PEPTIDE TO RECOMBINANT SURA IN CELL LYSATE**

It has been previously shown that SurA interacts with misfolded proteins, for example scRNase was successfully chemically crosslinked to purified SurA (Webb et al., 2001).

To confirm that SurA specifically binds to Δ -somatostatin, [125 I] Bolton-Hunter radiolabelled Δ -somatostatin was chemically crosslinked to overexpressed SurA in an *E.coli* cell lysate, (figure 4.5.1). A cell lysate that did not express recombinant SurA was used as a negative control (lanes 1 and 2). Cell lysates that contained recombinant SurA, showed cross-linking products, indicated by arrow marked S (lanes 4). The lysate expressing SurA showed only one specific crosslinking product with an approximate molecular weight of 47 kDa. In the absence of DSG, no cross-linking products could be detected (lane 3). Heat-inactivation of the lysate (5 min at 95°C) prior to addition of the peptide and chemical cross-linking inhibited the interaction between radiolabelled peptide and SurA (lane 5), indicating that the interaction was specific for native proteins. All the cell lysates, irrespective of whether they expressed recombinant SurA or not, showed an unidentified cross-linking product, denoted x, which has been observed previously (Klappa et al., 1998b).

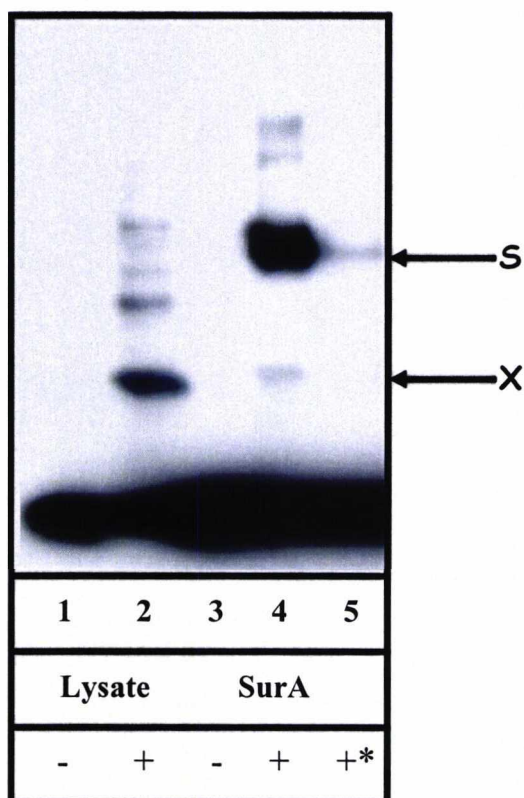


Figure 4.5.1 Crosslinking of radiolabelled peptide to recombinant SurA in cell lysate. [^{123}I] Bolton-Hunter labelled Δ -somatostatin (33 μM) was incubated with *E.coli* lysate expressing recombinant SurA or no SurA in buffer B for 10 min at 0°C in a total volume of 10 μl . As controls *E.coli* lysates expressing recombinant SurA, were heat-inactivated at 95°C for 5 min (*) prior to the addition of the radiolabelled peptide. Samples were subsequently incubated with DSG (final concentration 0.5 mM) for 60 min at 0°C or were kept untreated. After cross-linking the samples were analyzed on 10 % polyacrylamide gels with subsequent autoradiography. The symbol (+) indicates presence of cross-linker and (-) no cross-linker.

4.6 INITIAL DIRECT CROSSLINKING OF RADIOLABELLED PEPTIDES TO SURA AND COMPETITION ASSAYS

To investigate binding of the radiolabelled peptide Δ -somatostatin to SurA in the *E.coli* lysate, different radiolabelled peptides were crosslinked to SurA. A lysate expressing human archetypal PDI served as a positive control. From the experiments it was observed that SurA only showed strong interaction with Δ -somatostatin (AGSKNFFWKTFTSS) and SRIF (AGCKNFFWKTFTSC), while the other peptides only gave weak crosslinking signals. To confirm the observations with the

radiolabelled peptides competition experiments were carried out using cell lysates expressing SurA. Cell lysate containing SurA were incubated with radiolabelled Δ -somatostatin in the presence of an excess of unlabelled peptide. The competition between radiolabelled and unlabelled Δ -somatostatin served as a positive control. Figure 4.6.1 shows an example typical of the direct binding experiment, and figure 4.6.2 the competition assay with the same peptides.

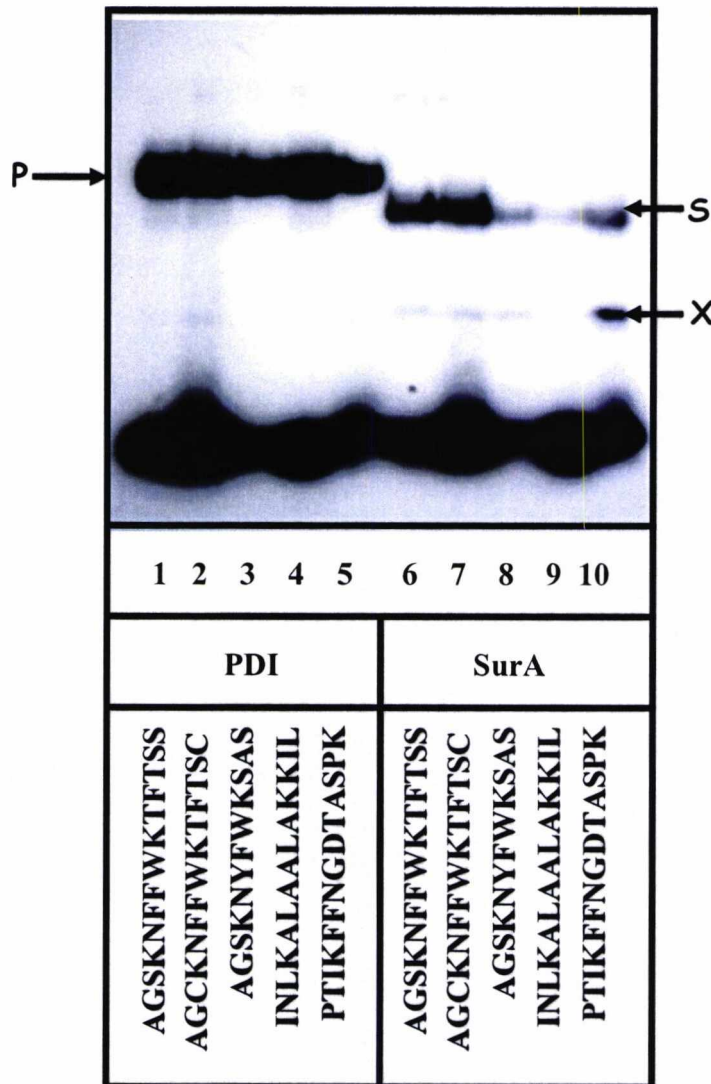


Figure 4.6.1 Interaction of SurA with model peptides by direct binding assay. The indicated [125 I] Bolton-Hunter labelled peptides (30 μ M) were incubated with *E.coli* lysates expressing recombinant SurA or human PDI, respectively, in buffer B for 10 min at 0°C in a total volume of 10 μ l. After crosslinking with DSG the samples were analyzed on 10 % polyacrylamide gels with subsequent autoradiography. The X indicates the unspecified crosslinking product. P indicates PDI and S SurA. Lane 1 is Δ -somatostatin.

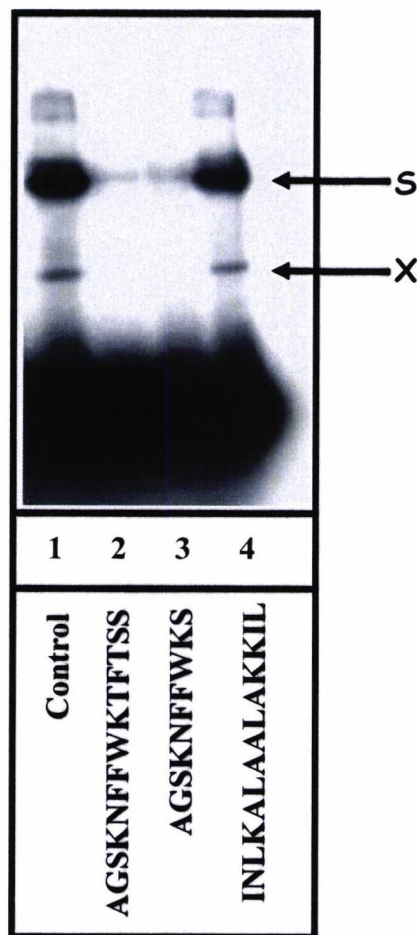


Figure 4.6.2 Interaction of SurA with model peptides by competition assay. [125 I] Bolton-Hunter labelled Δ -somatostatin (10 μ M) was incubated with *E.coli* lysate expressing recombinant SurA in the presence of 100 μ M of the indicated unlabelled peptides. Sample without unlabelled peptides served as controls. After crosslinking with DSG the samples were analyzed on 10 % polyacrylamide gels with subsequent autoradiography. X indicates the unspecified crosslinking product.

Unlabelled INLKALAALAKKIL (Peptide M) did not compete with radiolabelled Δ -somatostatin for the binding to SurA. This result is in excellent agreement with the results in figure 4.6.1, in which radiolabelled peptide M does not interact with SurA. Unlabelled peptide AGSKNFFWKS (Peptide A), however, inhibited the interaction between radiolabelled Δ -somatostatin and SurA. This result is in line with experiments using radiolabelled peptide A, where the peptide bound weakly (not shown).

4.7 COMPETITION ASSAYS OF BINDING PEPTIDES TO SURA

To continue the investigation in to which amino acids were significant for a peptide to bind to SurA more peptides were generated based around the peptide Δ -somatostatin as this has shown good binding in the previous experiments.

Peptide	SurA
AGSKNEFFWKTFTSS (Δ -som)	+++
AGCKNEFFWKTFTSC (SRIF)	+++
AASKNEFFWKTFTSS	+++
AGAKNEFFWKTFTSS	+++
AGSKAFFWKTFTSS	++
AGSKNAFWKTFTSS (F6A)	+
AGSKNEFAWKTFTSS (F7A)	+
AGSKNFFAKTFTSS (W8A)	-
AGSKNEFFWKAFTSS	+++
AGSKNYFWKTFTSS (F6Y)	+
AGSKNYFAKTFTSS (F7Y)	-
AGSKNWFWKTFTSS	+++
AGSKNFFWKTFT	+++
AGSKNEFFWKT	+++
AGSKNYFWKSAS (peptide S)	-
AGSKNFFWKS (peptide A)	+++
AASKAFFWKS	+++
AGSKNFFWAT	+++
TKWFFNKSGA	+++
--SKNEFFWKTFT	+++
--SKNEFFWKT	-
----NEFFWKT	-
INLKALAALAKKIL (peptide M)	-
WEYIPNV	+
WEYIP	-
PTIKFFNGDTASPK (peptide P)	-

Table 4.7.1 Competition between peptides and radiolabelled Δ -somatostatin for the binding to SurA. *E.coli* cell lysates expressing recombinant SurA, were incubated with 10 μ M radiolabelled Δ -somatostatin in the presence of a tenfold excess of the indicated unlabelled peptides prior to crosslinking. Samples were subsequently incubated with DSG (final concentration 0.5 mM) for 60 min at 0°C. After cross-linking the samples were analyzed on 10 % polyacrylamide gels with subsequent autoradiography. Quantification was performed with a BioRad PhosphoImager. A sample without competing peptides served as a control. Competition was expressed as reduction in the intensity of the respective crosslinking product relative to the control without unlabelled peptides. +++, strong competition (intensity of crosslinking product < 10 % of control); ++, moderate competition (intensity of crosslinking product between 10 % - 30 % of control); +, weak competition (intensity of crosslinking product between 50 % - 80 % of control); -, no competition (intensity of crosslinking product > 80 % of control).

Table 4.7.1 summarises the competition experiments. The competition between unlabelled and radiolabelled Δ -somatostatin was used as the reference point: strong competition between radiolabelled Δ -somatostatin and unlabelled peptide is indicated by +++, no competition by -.

The results demonstrate that changing the phenylalanine in position 6 to alanine (F6A) in the Δ -somatostatin sequence prevented this peptide to compete with the binding of radiolabelled Δ -somatostatin to SurA. Changing phenylalanine in position 7 to alanine (F7A) reduced the competitive effect of the peptide for the interaction with SurA. A similar result was observed for the tryptophane to alanine (W8A) modification. A change of the phenylalanine in position 6 to a tyrosine (F6Y) prevented the peptide to compete with the binding of radiolabelled Δ -somatostatin to SurA.

Taken together the results clearly show that the interaction between peptides and SurA is strongly dependant on the motif -FFW- in the peptide.

4.8 DIRECT BINDING OF PEPTIDES TO SURA

To verify the results of the competition assays, direct binding assays were carried out with some of the peptides. The binding is listed in table 4.8.1.

Peptide	SurA
AGSKNFFWKFTFTSS (Δ -som)	+++
AGCKNFFWKFTFTSC (SRIF)	+++
AGSKNFFAKTFTSS (W8A)	-
AGSKNFFWKAFTSS	+++
AGSKNYFWKTFTSS (F6Y)	+
AGSKNYFAKTFTSS (F7Y)	-
AGSKNWFWKFTFTSS	+++
AGSKNFFWKFTFT	+++
AGSKNFFWKFT	+++
AGSKNYFWKSAS (peptide S)	-
AGSKNFFWKS (peptide A)	+++
INLKALAAALAKKIL (peptide M)	-
PTIKFFNGDTASPK (peptide P)	-

Table 4.8.1 Direct binding of radiolabelled peptides to SurA. *E.coli* cell lysates expressing recombinant SurA, were incubated with 10 μ M radiolabelled peptides prior to crosslinking. Samples were subsequently incubated with DSG (final concentration 0.5 mM) for 60 min at 0°C. After cross-linking the samples were analyzed on 10 % polyacrylamide gels with subsequent autoradiography. Quantification was performed with a BioRad PhosphoImager. +++, strong binding; ++, moderate binding; +, weak binding; -, no binding.

There were no differences between what was observed between the competition assays and the direct binding assays.

4.9 BINDING TO N-TERMINAL FRAGMENT OF SURA

The same peptides were used for investigating the N-terminal fragment of SurA as well as the full length protein. In chapter 3 it was shown that the N-terminal fragment has the ability to bind to the model peptide Δ -somatostatin. It was important to show that binding properties of the SurA fragment was not impaired by the removal of the rest of the protein.

The N-terminal fragment of SurA was used in competition assays with the same peptides as the full length SurA (listed in table 4.7.1). Overall the binding assays that were performed using the N-terminal fragment gave the same result as the full length recombinant protein, there were only a few slight differences in which the peptides did and did not bind to SurA, and this could be attributed to the fact that the N-terminal fragment band runs closely to the dye front on the gel.

The main differences observed were that SKNFFWWKT and NFFWKT showed reduced binding instead of no binding that was seen in the full length SurA. WEYIPNV showed reduced binding to the N-terminal fragment as with full length SurA and WEYIP did not bind to the fragment.

4.10 STD-NMR OF SURA SHOWS AMINO ACIDS DIRECTLY INVOLVED IN BINDING

To investigate which specific amino acids of the peptide are in close contact with the binding site of SurA, Saturation Transfer Difference NMR (STD-NMR) was carried out. STD NMR experiments detect magnetisation that is transferred from a protein to a bound ligand. Any small molecule in solution reversibly interacting with the binding domain of a protein shows characteristic differences in its relaxation behaviour from those molecules having no affinity for the protein (Mayer and Meyer, 2001). Experiments were carried out with Δ -somatostatin and purified recombinant SurA. STD-NMR shows where there were contacts between the protein and the peptide. From the image in figure 4.10.1, there was noticeably more than one significant contact with the SurA protein. The image was created by Dr Mark Howard at the University of Kent at Canterbury. It was generated using the graphs shown in figure 4.10.2.

Quantitative analysis of the peaks, using the strongest peak as a reference for SurA showed strong interactions with the phenylalanine residues in position 6, 7 and 11.

The residues are shown in colours ranging from blue 0 - 14% contact, green 15 - 29% contact, yellow 30 - 40% contact, orange 41 - 65% contact and red 66 - 100%. Residues displaying red are therefore much more significant than blue residues. The contacts are shown in figure 4.10.1.

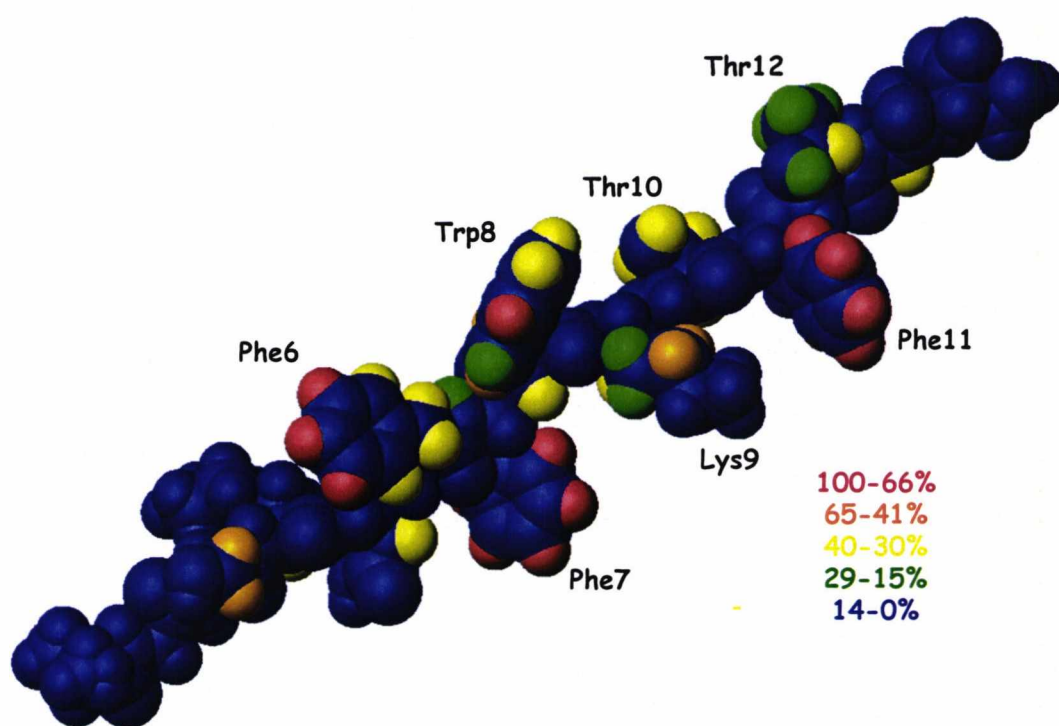


Figure 4.10.1 Δ -somatostatin STD-NMR contacts with SurA. The colours indicate the percentage of transfer from the largest peak. Significant amino acids are labelled next to the residue.

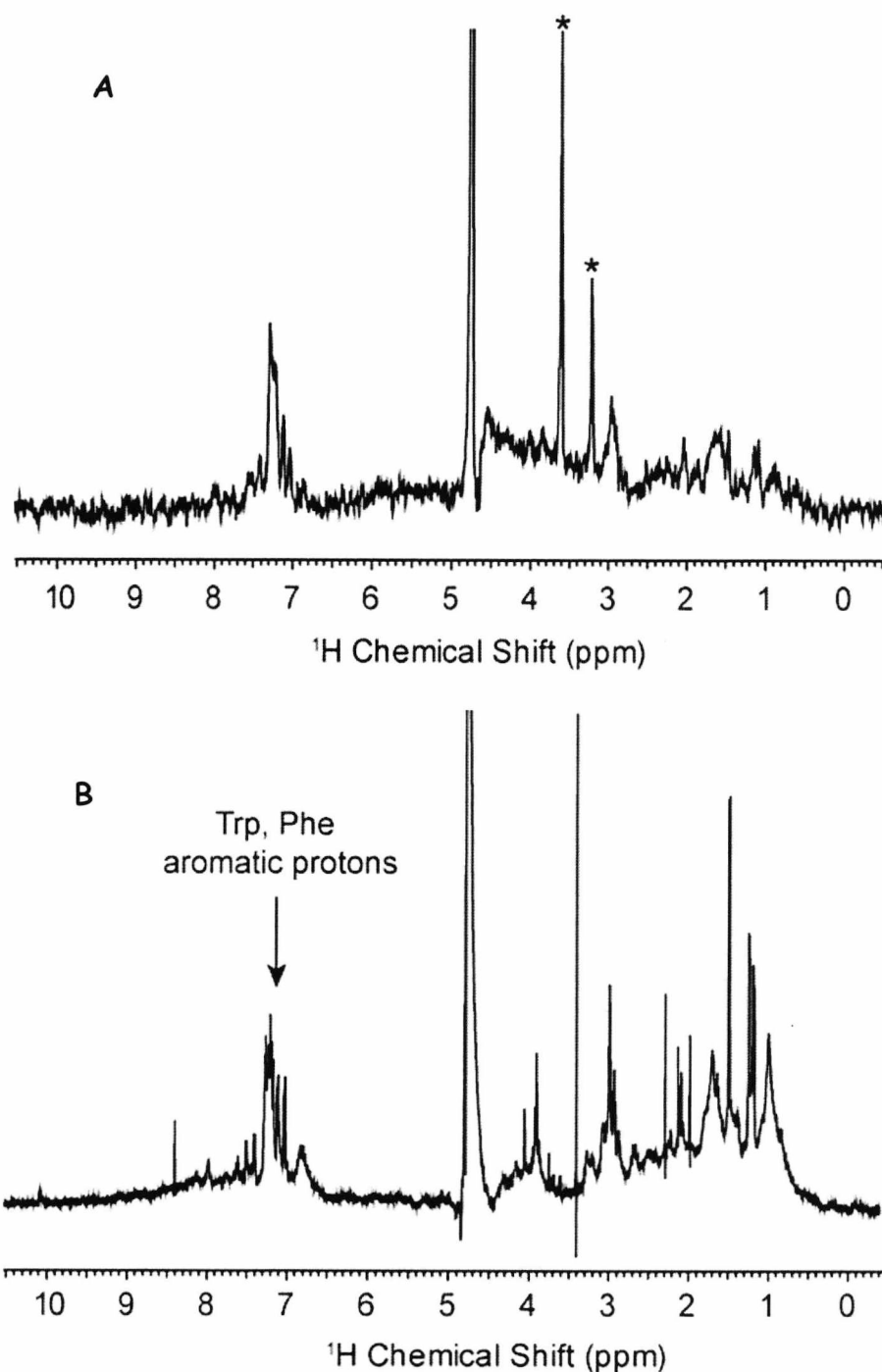


Figure 4.10.2 STD NMR spectra for the interaction between Δ -somatostatin and SurA and PpiD. *A* STD NMR spectrum for the interaction between SurA and Δ -somatostatin. A standard Δ -somatostatin 1D ^1H spectrum is shown in *B*. STD resonances attributed to breakthrough from the sample are identified with asterisks.

It appears as if the residues at positions 6, 7, 8 and 11 are most important for the interaction because these residues had over 66% contact with the protein. The first 5

amino acids showed very little interaction with the protein apart from the Serine at position 3 which showed 41 – 65% contact around the side chain. Amino acids 13 and 14 also appear not to have had contact with the protein. The phenylalanine at positions 7 and 11 both showed the highest contacts with the protein, with all the visible hydrogen atoms on both showing that they had 66 -100% contact. The phenylalanine at position 6 showed less contact over the whole amino acid but still had 3 atoms that had 66 -100% contact higher contact, 41 – 60%, than the atoms on the ring of the tryptophan. The threonines at positions 10 and 12 had some interaction with the binding site of SurA as did the lysine at position 9. The atoms that made the contacts were around the side chains and quite near to the back bone of the peptide.

4.11 CONCLUSIONS

Binding studies were used to find the binding motif for SurA. Different peptides were used that were loosely related to the initial binding peptide Δ -somatostatin.

Overall the binding is not dependent on one particular amino acid but a group of amino acids and that the removal of one or the alteration only reduced the binding instead of abolishing it completely.

To investigate in more detail the nature of the interactions between model peptides and SurA we used competition experiments with unlabelled peptides. Replacement of phenylalanine 6 (F6) with alanine in Δ -somatostatin strongly reduced the interaction with SurA. This result is in excellent agreement with our STD NMR data: F6 is an important residue for the interaction with SurA. From the STD NMR experiment we further concluded that the para-position in F6 is important for the interaction with SurA. Modifications of this position therefore should reduce binding. Indeed, replacing F6 with tyrosine strongly reduced the interaction with SurA. Our STD NMR results also showed that there are significant interactions between phenylalanine in position 7 and SurA, which was confirmed in the competition experiments. Another important residue for the interaction of Δ -somatostatin with SurA, is the tryptophan residue in position 8, as shown by competition and STD NMR analysis. From these experiments, the competition assays, direct binding assays and the STD-NMR

analysis it appears that the aromatic residues play a significant role in the binding to SurA.

Chapter 5

Molecular Modelling

Chapter 5: Molecular Modelling

5.1 INTRODUCTION

The crystallographic structure of SurA was solved using multiwavelength anomalous dispersion (MAD) phasing with data from crystals of selenomethionine (SeMet)-labelled protein. This was refined to 3.0Å resolution (Bitto and McKay, 2002).

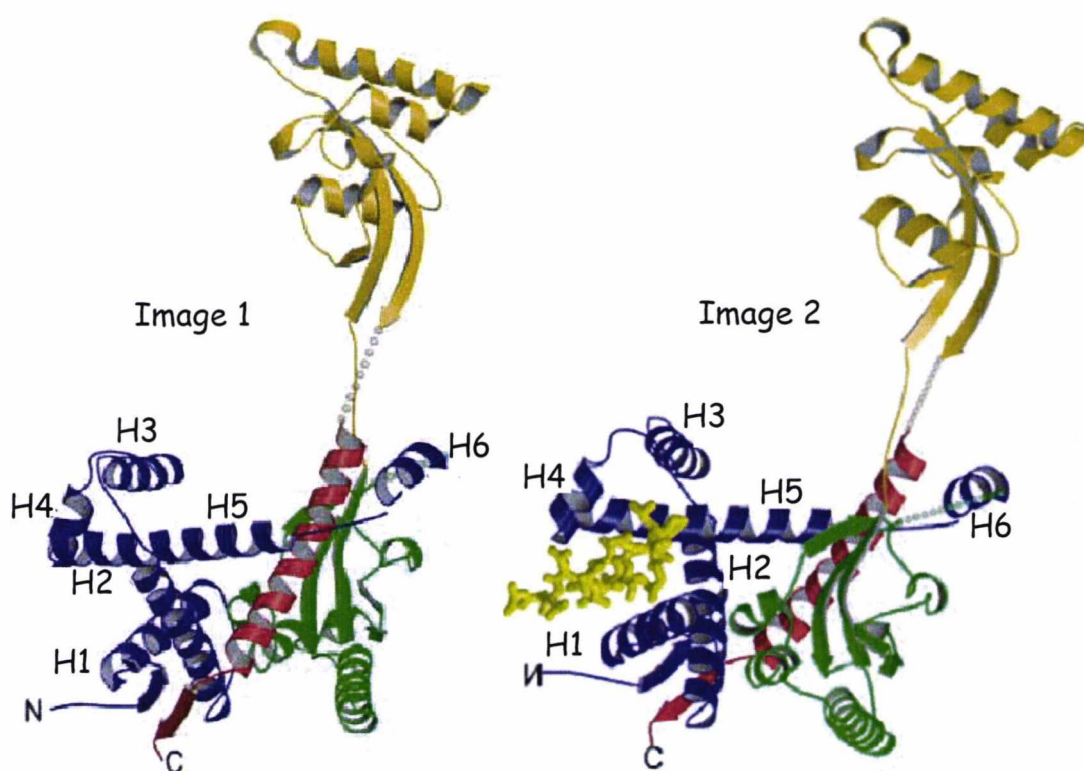


Figure 5.1.1 The Crystallographic Structure of SurA. Blue region: N-terminal domain. Green: first parvulin domain. Yellow: second parvulin domain. Red: C-terminal region.

The N-terminal and the C-terminal regions are labelled, and the helices are labelled with the letter H and the corresponding number.

Image 1 shows the native wild-type SurA structure, image 2 shows the wild-type structure with a peptide (yellow) from a neighbour molecule binding to the theoretical crevice in the core domain. Dotted lines indicate the connections between the core domains and P2 domains that could not be traced. Images were taken from Bitto et al. Structure **10**, 1489-1498 (2002).

The SurA protein consists of four domains, the N-terminal domain, the two parvulin domains and the C-terminal domain. Bitto and McKay have shown that in the tertiary

structure the domains form two distinct modules, the larger of the two containing the N-terminal domain, the first parvulin domain and the C-terminal domain. This has been referred to as the core module of SurA with the second parvulin domain being labelled the satellite module. The core domain and the satellite domain are connected by a polypeptide chain $\sim 25\text{-}30$ Å in length. The core domain begins with a pair of small antiparallel β strands which are followed by six α helices, these make up the N-terminal region. This is followed by a small linker to the first parvulin domain. The first parvulin domain shows some homology with the structures of human Pin1 (Ranganathan, 1997) and Par14 (Sekerina et al., 2000). Within the C-terminal domain residues 396-422 form a long α helix that is sandwiched between the N-terminal domain and the first parvulin domain. Nearly 60% is in contact with the N-terminal domain and 40% is in contact with the first parvulin domain. The majority of the C-terminal domain's surface is buried in the centre of the core domain. The C-terminal domain, N-terminal domain and the first parvulin domain form an extended crevice in the core domain. The crevice is walled by the helices of the three domains that make the core module. It has been suggested that the crevice is involved in the binding of peptides. Bitto and McKay show that crevice in the core module form a novel fold as searches though the protein data bank showed no positive hits of a similar fold. The end of the C-terminal domain forms a β -strand of residues 423-426 that run antiparallel to the initial β strand of the N-terminal domain.

The satellite domain consisting of the second parvulin domain also has a parvulin fold. There are differences between the two parvulin domains, for example residues 184-191 give rise to a larger loop than the corresponding residues, 295-299 in the second parvulin domain. There is also the deletion of a single residue in the first parvulin domain and the insertion of a single residue in the second parvulin domain, Gly333.

The structure has given a unique insight into the binding site of SurA (figure 5.1.1), and the importance of the surrounding residues. By generating mutations of SurA in a modelling programme that is designed to simulate the relaxing and reforming of bonds when residues are altered, substituted, deleted or inserted it could be possible to 'predict' residues that have an important role in the overall structure. For example radical changes in the predicted binding site would be likely to reduce the binding ability of the protein due to the altered structure as it has been shown with other

proteins that a very small change can completely alter the protein's binding characteristics.

Molecular dynamic simulation of mutants was an alternative way of visualising the changes to a protein with altered residues. This is only possible with proteins that have been assigned a structure. In the case of SurA the X-ray crystallography structure has already been solved, with the structure being publicly available in the Protein Data Bank (PDB).

The descriptions of the following changes seen in the different mutants are based on the orientation of the PDB structure of SurA in the figure 5.1.1; any changes are therefore described in relation to the original structure. To enable an easier understanding of the changes in the structures, cropped structures have been added, these have been given the same length as the N-terminal fragment that was described in Chapter 3. The difference in positioning of the atoms is given as an RMSD number, root-mean-square deviation, between specified sets of atoms and is a useful way of comparing the positioning of atoms in the structures in this chapter.

5.2 X-RAY AND CNS STANDARD SIMULATED ANNEALING WILD TYPE STRUCTURES HAVE INSIGNIFICANT DIFFERENCES

Before the process of simulated annealing to SurA can begin the X-ray crystallographic structure requires addition of the hydrogen atoms, see figures 5.2.1 and 5.2.2.

An accurate representation of the mutations of the protein is required so that all force fields are quantitative for energy minimisation. This is critical as a high deviation in the RMSD values for the two different structures would mean that the molecular simulation was not giving an accurate representation of the native protein. The hydrogen atoms were added in MolMol. The PDB was then edited for the HIS+, LYS+ and ARG+, these were replaced with HIS, LYS and ARG. The CNS standard simulated annealing (SA): model-anneal.inp. involved using Cartesian molecular dynamics. The SA includes simulated annealing for 0.5 ps (1000 steps of 0.0005 ps) at a constant temperature of 298 K in accordance with the standard SA protocol.



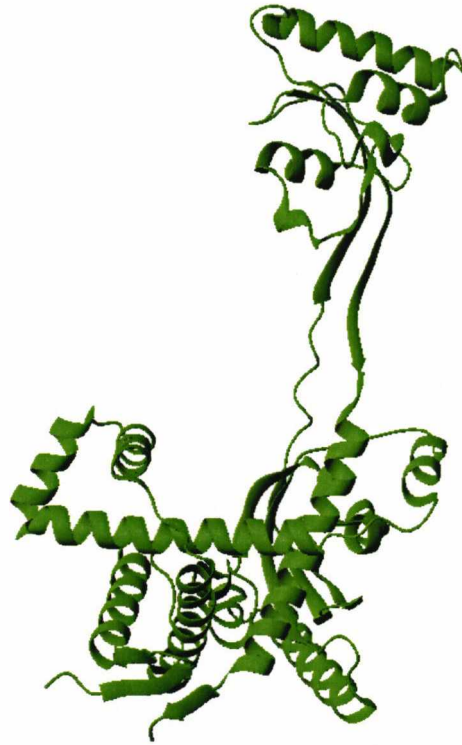


Figure 5.2.1 X-Ray crystallographic structure of wild-type SurA without hydrogen atoms. The image shows the crystallographic structure before the addition of the hydrogen atoms, which are necessary for the CNS standard simulated annealing process.

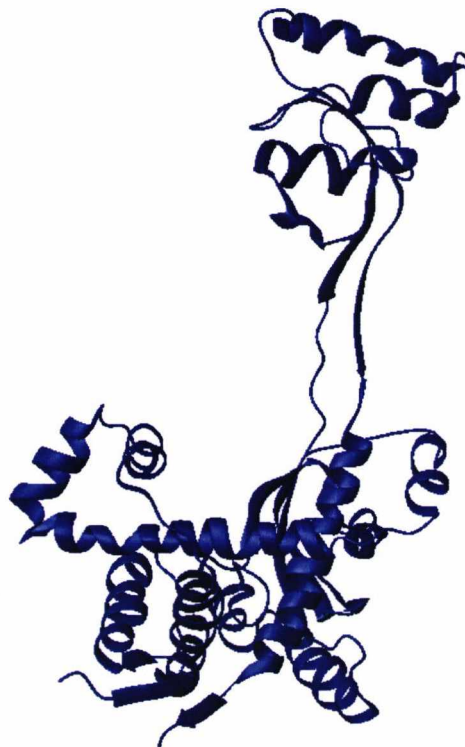


Figure 5.2.2 X-Ray crystallographic structure of wild-type SurA. The image shows the crystallographic structure after the addition of the hydrogen atoms.

The two structures were overlaid in the MolMol programme where the RMSD values are given as standard when two structures are overlaid at the same point. The RMSD was found to be 1.1Å for C^α between the X-ray and SA wild-type structures. This validated the SA method and proved that addition of hydrogens did not adversely perturb the structural model.

By following through the helices from the N-terminus to the C-terminus of the folded protein in figures 5.2.1 where the wild-type protein has no hydrogen atoms as it is in its crystallographic form, 5.2.2 where the hydrogen atoms have been added so that the CNS SA can be carried out on the structure and 5.2.3 where the two proteins are overlaid, there are only very slight changes in the overall structure. The wild-type with the addition of hydrogen atoms (blue ribbon) even appears to have ‘relaxed’, as it is still possible to see through the overlaying helices. In some areas the overlay is so perfect that it is not possible to tell the two structures apart.



Figure 5.2.3 Original wild-type X-ray structure overlaid with the new wild-type structure of SurA. Blue ribbon is the wild-type SurA without the hydrogen atoms and the green ribbon is the wild-type protein with the addition of the hydrogen atoms. The two structures were overlaid in Mol Mol and aligned at the same atom. The RMSD value given was 1.114.

To aid the process of observing the differences between the wild-type figure 5.2.3.1 shows the N-Terminal region of SurA missing the main portion of the structure. The orientation of the original structure is shown (image A) as well as the positioning (image B). This is so that all the N-terminal regions can be displayed. By utilising this method the differences can be clearly seen.

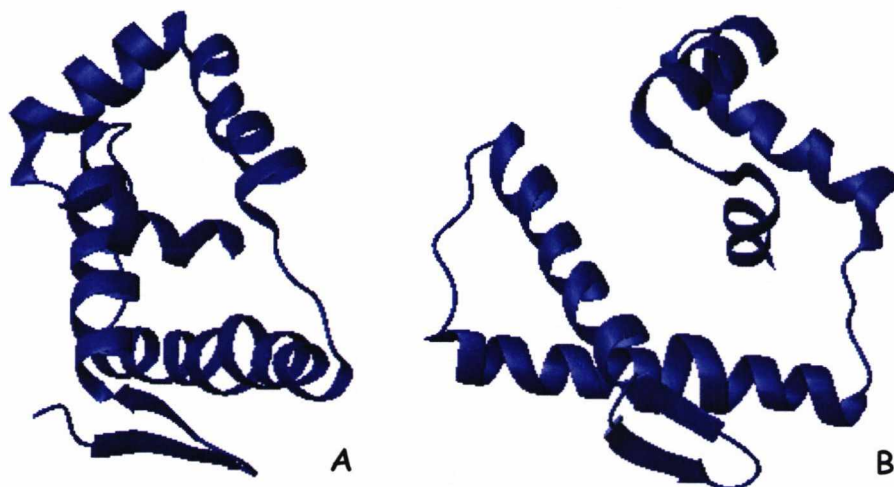


Figure 5.2.3.1 Orientation of the N-terminal domain of the wild-type SurA with the addition of hydrogen atoms. The image shows the different orientations of the N-terminal fragment of the wild-type SurA. Figure A is the position of the structure in the complete protein. Figure B is the chosen orientation to display the structure so the differences can be compared to later mutations.

5.3 SELECTING THE MUTATIONS OF SURA

5.3.1 THE MUTANTS WERE SELECTED BY LOCATION

The crystallographic structure shows a region that has been postulated to act as a binding cleft. The binding region was shown to be in the first 110 amino acids of the SurA sequence (Webb et al., 2001). By combining the knowledge of the location of the binding region on the protein sequence and the possible binding cleft observed in the crystal structure all the residues in the combined areas are potentially important. However the peptide in the binding cleft in figure 5.1.1 image 1 could be located in the position because of the crystal formation and therefore not be representative of its position in its native environment.

5.3.2 RESIDUES WERE CHANGED TO DIFFERENT RESIDUES WITH SIMILAR PROPERTIES

The residues that were selected to be altered were changed to residues that had similar properties to the original, (although R73D is a major change). Changes that involve size differences, polarity and charge could all have a detrimental effect to the surrounding residues and therefore will affect the over all structure of the protein. The different mutated residues are indicated by the CPX highlighted amino acids in figure 5.3.2.1.

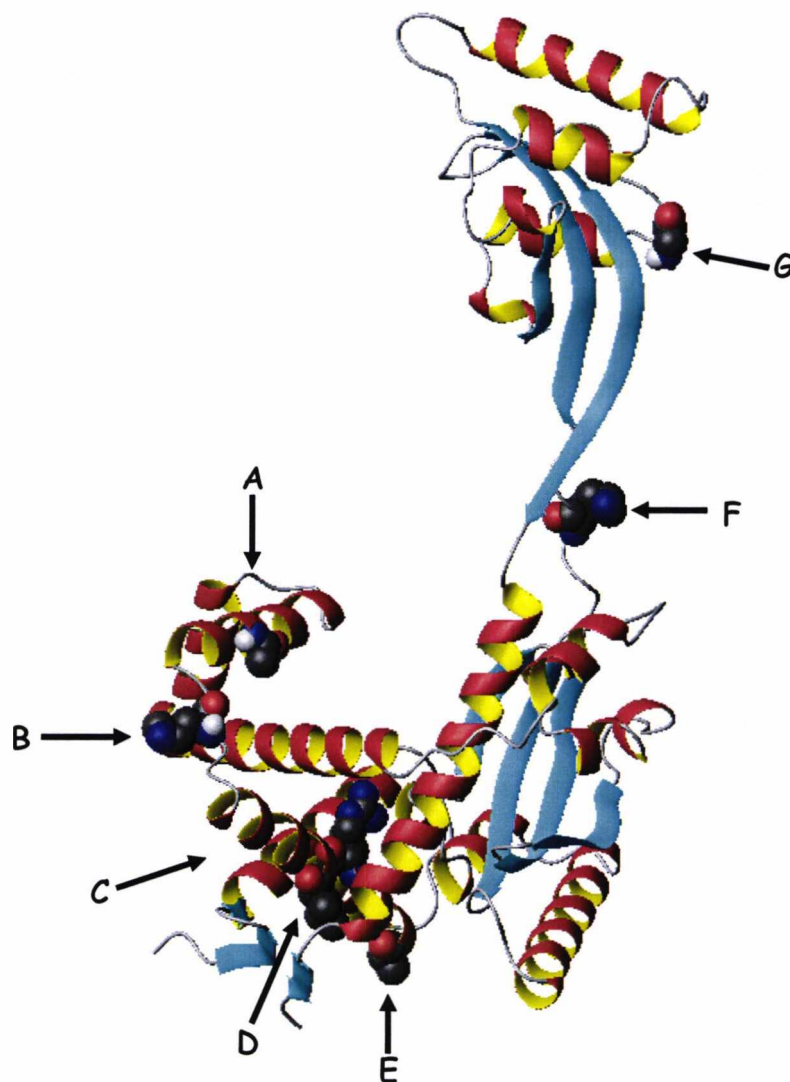


Figure 5.3.2.1 X-Ray crystallographic structure of native SurA with mutated residues highlighted. Locations of the residues that were selected for mutation are shown in the image above. Each altered residue is displayed as a CPX structure and by an arrow. (A) position 99, (B) position 90, (C) position 73, (D) position 75, (E) position 64, (F) 278 and (G) position 363.

Original Residue	Position	New Residue
Alanine	99	Valine
Alanine	64	Valine
Arginine	73	Aspartic Acid
Isoleucine	75	Serine
Lysine	90	Arginine
Alanine	64	Proline
Glycine	363	Alanine
Lysine	278	Arginine

Table 5.3.2 Residues selected and their changes. Residues were changed to residues with similar properties. Residues were selected on the basis of their position in the wild-type SurA and exposure to the possible binding region in the protein.

5.3.3 NON-CONSERVATIVE CHANGES HAD LITTLE EFFECT

As a control, one of the residues that had been altered was also changed to a very different residue. Alanine at position 64 in the SurA protein was altered to a proline residue. Changing from aliphatic residue to a cyclic imino acid was thought likely to have a pronounced effect on the overall structure of SurA. The RMSD value of the two overlaid structures was 8.267Å, in comparison with the other altered residues the value was not as high as expected.

The addition of the proline residue has completely disturbed the beta sheet structures at the N-terminal and C-terminal regions of the purple representation. This is shown more clearly in the figure 5.3.3.2 which shows the sections that have undergone the changes. The blue wild-type structure has three beta sheet strands in close proximity, these are two beta sheet strands of the N-terminus and one at the C-terminus. The purple mutated structure does not contain this grouping of the beta sheets, instead the presence of the proline has pushed up the beta sheet at the C-terminal end. The beta sheets at the N-terminal end have moved away from the main structure. The first helix has moved slightly but still links up with the second helix in the same position. As the beta sheet at the C-terminus has slightly moved away from the altered residue

the final C-terminal helix, which is shown in red in figure 5.1.1 has distorted and bulges towards the middle of the coil. Overall there are few changes to the structure of the protein and the satellite domain is almost unaffected by the change. The protein still has the region that has been labelled as a possible binding cleft.

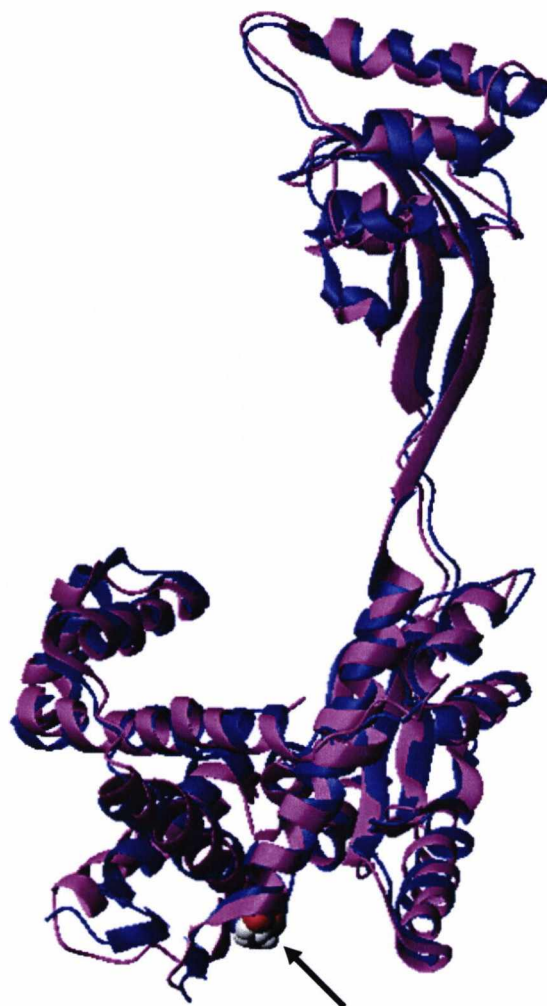


Figure 5.3.3.1 Overlay of the wild-type SurA with hydrogen atoms and mutated SurA with A64P. Wild-type SurA is the blue ribbon structure and the mutant is shown in purple. The CPX indicates where the mutation is located on the protein shown by the arrow.

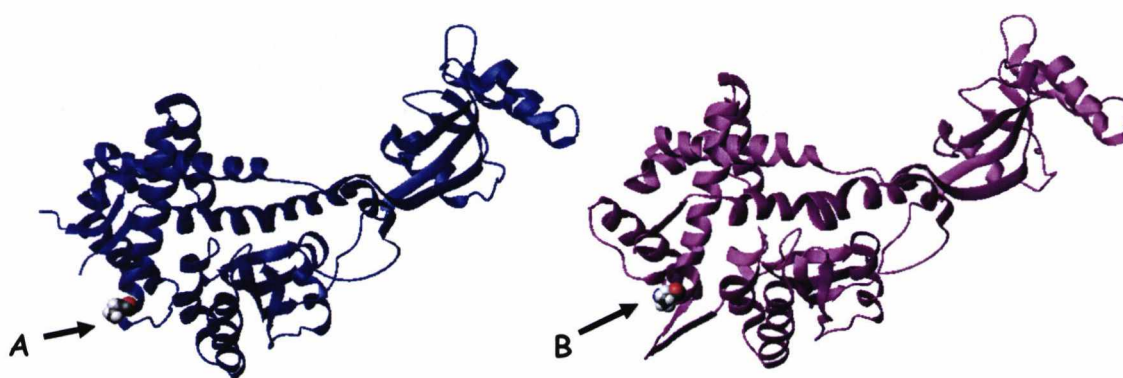


Figure 5.3.3.2 Individual side views of the wild-type SurA and the mutated protein A64P. The wild-type protein is shown in blue with the alanine is indicated (A). The mutated protein is shown in purple where the proline is indicated (B).

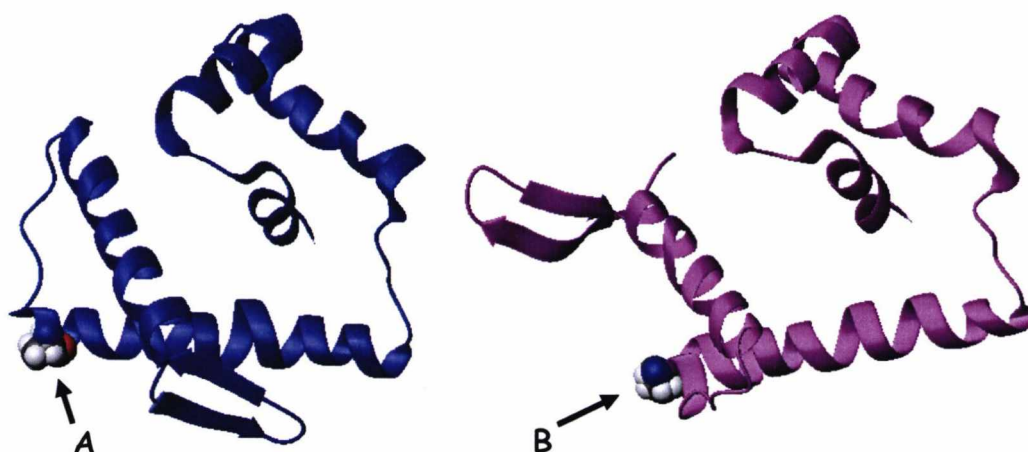


Figure 5.3.3.3 N-terminal fragments of the wild-type SurA and the mutated protein A64P. The wild-type protein is shown in blue with the alanine is indicated (A). The mutated protein is shown in purple where the proline is indicated (B).

Figure 5.3.3.3 shows only the N-Terminal region of SurA. In these images it is clear to see that the first two β -sheets and the first α -helix have moved to almost the opposite orientation as compared to their positioning in the wild-type protein.

5.3.4 MUTATIONS OF RESIDUES OUTSIDE THE CORE STRUCTURE DO NOT SIGNIFICANTLY ALTER THE OVER ALL STRUCTURE

Some of the changes made to the protein had very little effect to the satellite domain. As another control two residues were chosen at random in the structured region of the satellite domain. This was to show that no effect was passed significantly to the main structure. Two residues were chosen; glycine at position 363 was changed to an alanine and lysine at position 278 was changed to an arginine (figure 5.3.4.1).

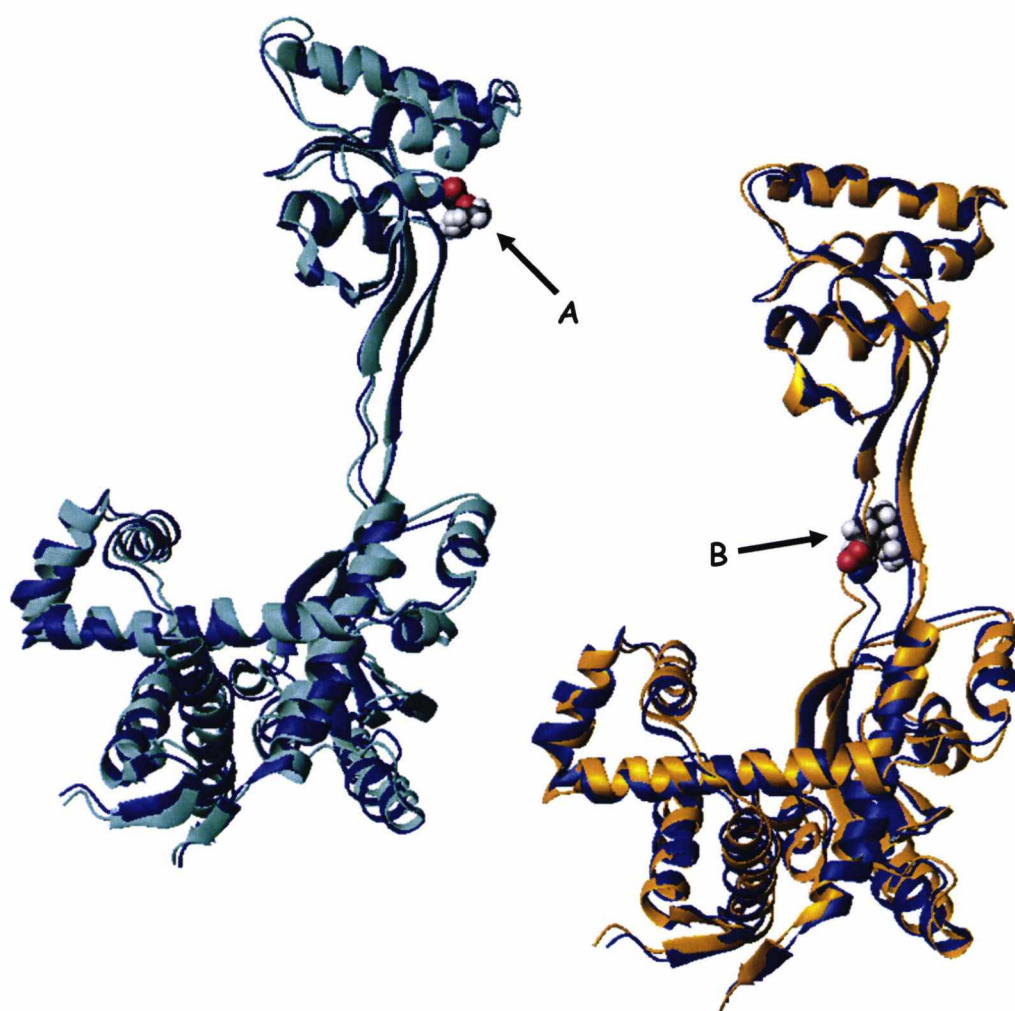


Figure 5.3.4.1 Overlays of the wild-type SurA and mutants of SurA where residues outside the main core have been altered. Image A is an overlay of the wild-type SurA shown in blue and the mutated protein shown in turquoise, where glycine at position 363 has been changed to alanine. B is an overlay of the wild-type SurA shown in blue and the mutated protein shown in orange, where lysine at position 278 has been changed to arginine. The mutations are indicated by the CPX and arrows.

The RMSD for the first of the two proteins was 1.627Å, which indicates that this change has little effect on the overall structure of SurA. To confirm this observation a second mutant was simulated, lysine at position 278 was changed to an arginine. This change gave an RMSD value of 1.514Å, which was lower still. This mutant was positioned in the polypeptide chain that joins the core domain and the satellite domain. In both of the two mutants the structures overlay the wild-type SurA, all the major helices and the beta sheets overlay. The structures appear as both the crystallographic structure and the wild-type, but less tightly coiled.

5.3.5 MUTATIONS TO THE CORE STRUCTURE HAVE A PRONOUNCED EFFECT TO THE STRUCTURE OF SURA

Mutations to the main core structure of SurA produced much more pronounced effects to the protein structure. Changes made were considered to be less extreme than the mutant where residue 64 was changed from an alanine to a proline. The following changes were made: Arginine at position 73 was changed to an aspartic acid residue. Alanine at position 64 was changed to a valine residue. Isoleucine at position 75 was changed to a serine. Alanine at position 99 was changed to a valine. Arginine at position 73 changed to an aspartic acid (R73D) gave an RMSD value of 7.346Å. The altered residue is in the second helix of the core domain (figure 5.3.5.1). The effect of the mutation is most marked on the first helix and beta sheets at the N-terminus. The N-terminus in the mutant has moved to the opposite side of the core domain of the protein. The repositioning of the second helix has not affected the side of the protein that it has moved to. The move has been indicated by highlighting the first residue of the N-terminal region by changing the ribbon representation of the structure to a CPX structure. In the mutant helix three has formed a tighter coil and helix four is distorted. Helix five looks almost more structured in the mutant and helix six has formed a tighter coil. The change of the residue has also had an effect on the satellite domain; the larger helix in the satellite domain has become looser than in the wild type and the following smaller helix has become tighter as has the helix that follows. The following beta sheet has also been affected by the change.



Figure 5.3.5.1 Overlay of the wild-type SurA and the R73D mutant. The wild-type protein is shown in blue and the mutant in pink. The altered residue location is indicated by an arrow and (A), it is obscured by the helix 5.

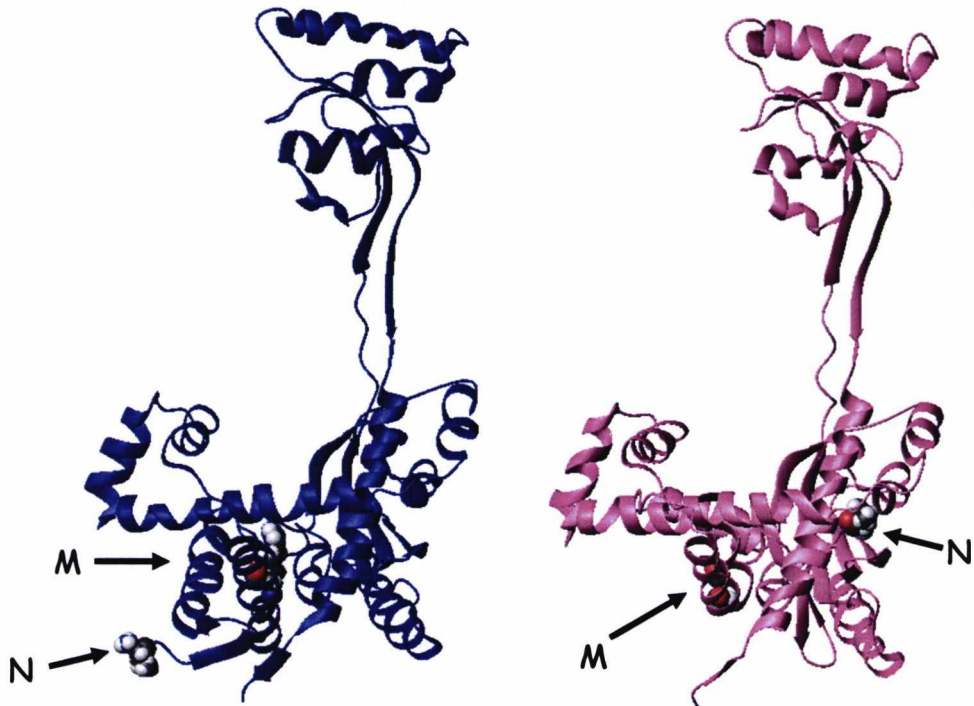


Figure 5.3.5.2 Comparison between the wild-type SurA and the R73D mutant. The start of the N-terminus is indicated by the CPX and the arrows labelled N. The mutant is indicated by the CPX and the arrows labelled M.

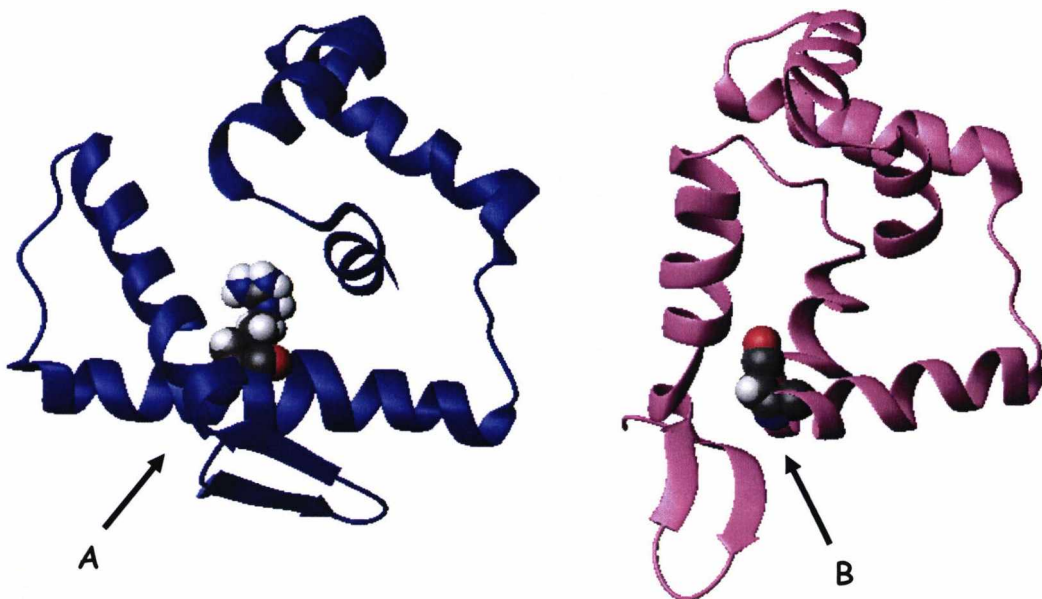


Figure 5.3.5.3 N-terminal fragment of wild-type SurA and the R73D mutant. The wild-type protein is shown in blue with arginine highlighted by the CPX (A). The mutant protein is shown in pink, and the altered residue is highlighted by the CPX (B).

The mutant resulting from the alanine at position 64 being changed to a valine (A64V) gave an RMSD value of 8.252Å when aligned with the wild-type protein (figure 5.3.6.1). The changed residue is in the second helix in the core domain. This change has caused the beta sheet structure in the N-terminal region to flip out by nearly 180 degrees. The first helix following the beta sheets at the N-terminus has moved away from the main domain as if it has been repelled by the changed residue, it is the first helix that is closest to the altered residue.

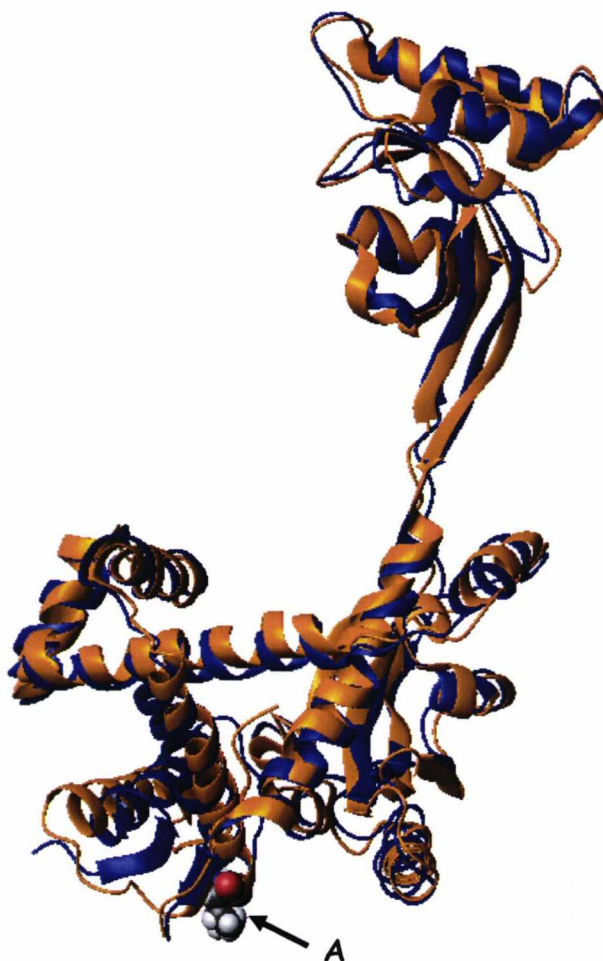


Figure 5.3.6.1 Overlay of the wild-type SurA and the A64V mutant. The wild-type protein is shown in blue and the mutant in dark orange. The altered residue location is indicated by an arrow (A), and the ball and the CPX.

The second helix, in which the mutation is located at position 64, has changed very little, it appears more stretched but its positioning is the same as in the wild-type protein. Helix four has been ‘squashed’ and the fifth helix, which runs through the core of the protein is generally unchanged, but has moved slightly. The main beta

sheet region of the core domain has been repositioned but this has not had a marked effect on the satellite domain. The C-terminal helix which passes through the centre of the protein is unaffected by the changes. The figures 5.3.6.1 and 5.3.6.2 show the overlay of the wild-type protein and the mutated protein, and the changes to its core domain.

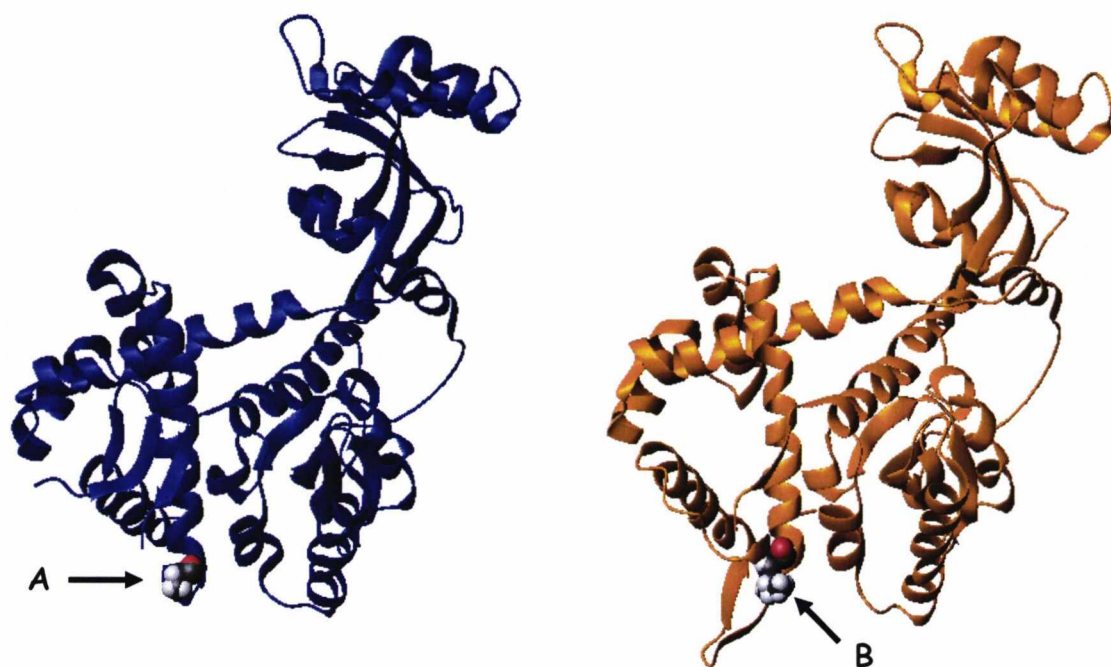


Figure 5.3.6.2 Comparison of the wild-type SurA and the A64V mutant. The wild-type protein is shown in blue the alanine is indicated by the arrow (A). The mutant protein is shown in dark orange and valine indicated by the CPX and (B).

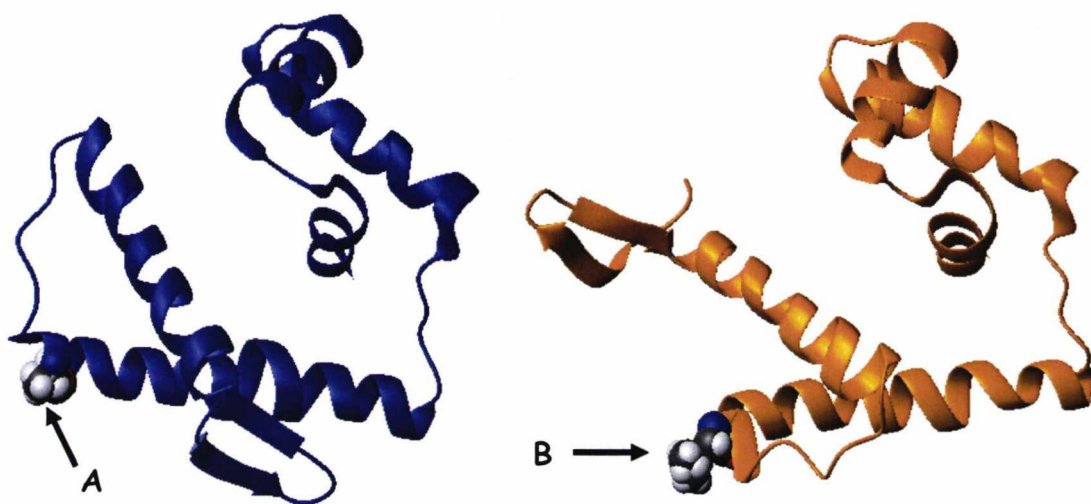


Figure 5.3.6.3 Comparison of the N-terminal fragment of wild-type SurA and the A64V mutant. The wild-type protein is shown in blue and the mutant in dark orange.

Figure 5.3.6.3 shows the N-terminal comparison of the mutant and the wild-type protein. There is a pronounced difference in the positioning of the first β -sheets and the first α -helix and to the third, fourth and fifth helices. The second α -helix has seemingly been unaffected by the change.

The mutant that simulated the change from an isoleucine at position 75 to a serine gave an RMSD value of 9.61Å when the wild-type was aligned with the mutant (figure 5.3.7.1).

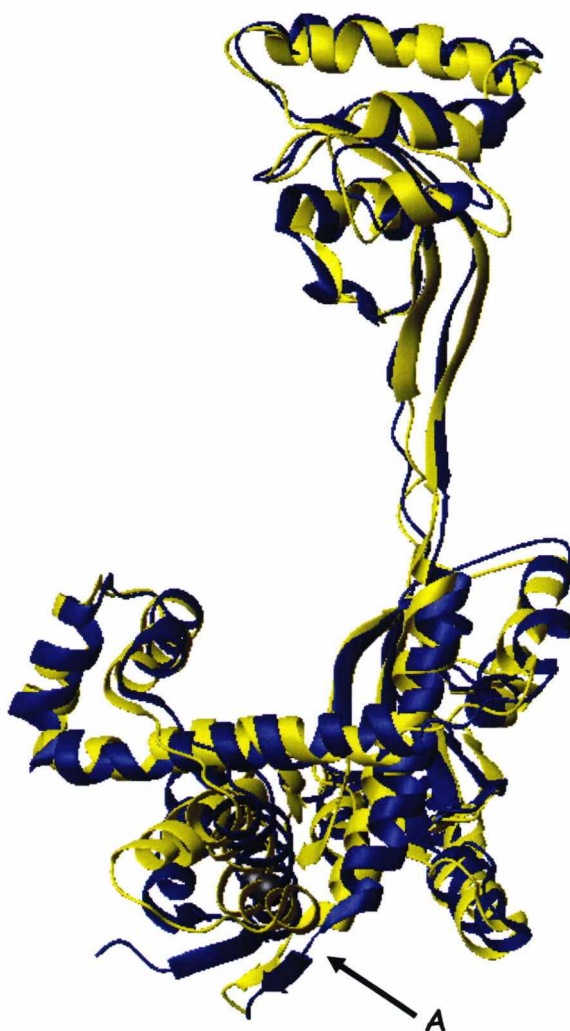


Figure 5.3.7.1 Overlay of the wild-type SurA and the I75S mutant. The wild-type protein is shown in blue and the mutant in yellow. The altered residue location is indicated by an arrow (A), and the CPX.

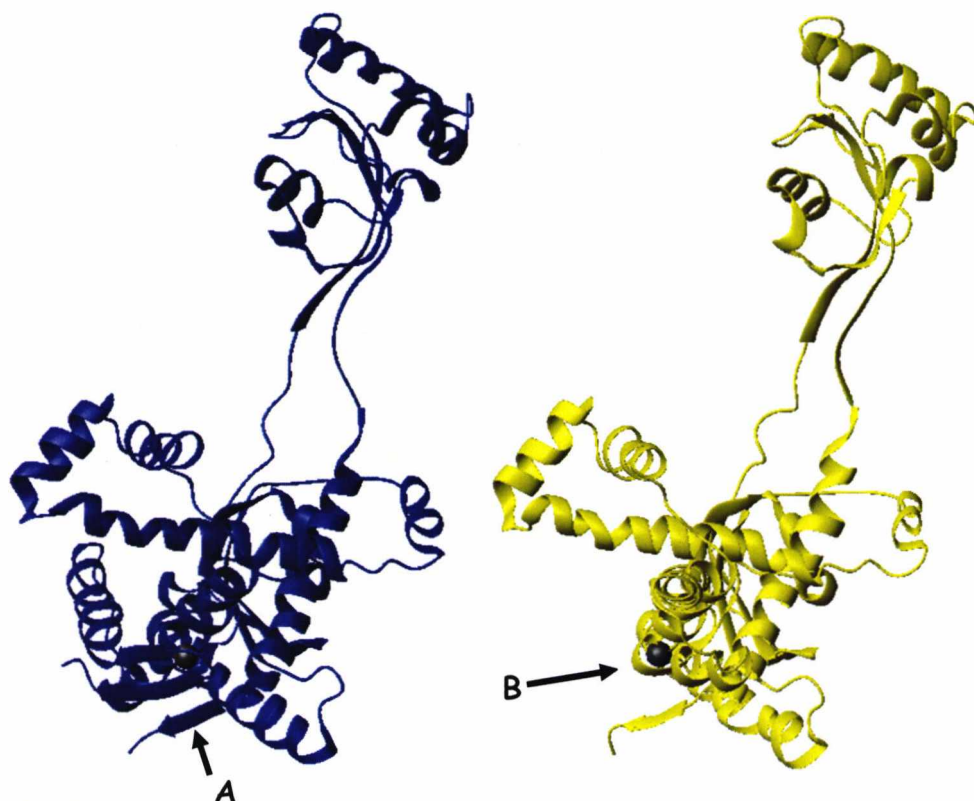


Figure 5.3.7.2 Comparison the wild-type SurA and the I75S mutant. The wild-type protein is shown in blue and the mutant in yellow. They have been rotated so that the satellite domain is to the right of the image.

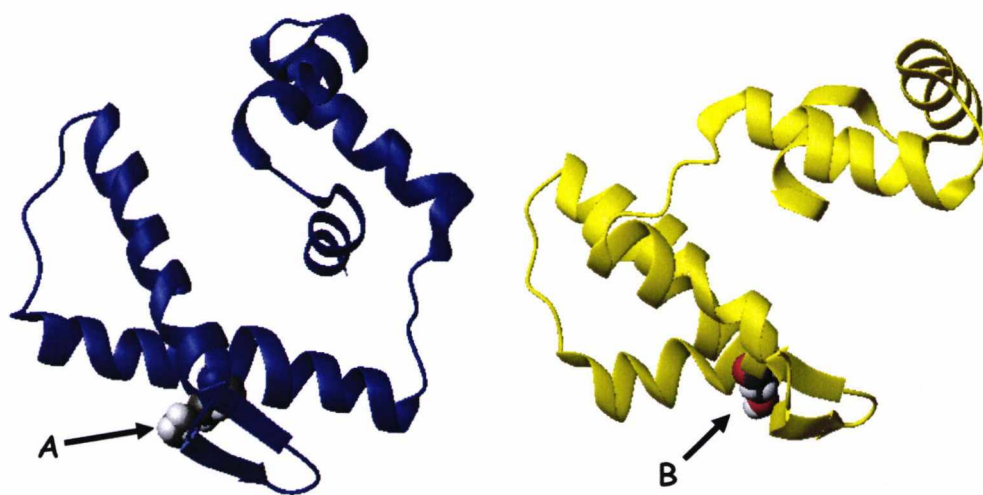


Figure 5.3.7.3 Comparison the N-terminal fragment of wild-type SurA and I75S mutant. The wild-type protein is shown in blue and the mutant in yellow.

One mutation where residue located at position 99, originally occupied by an alanine; this was replaced by a valine (A99V) was shown to be significant (figure 5.3.8.1).

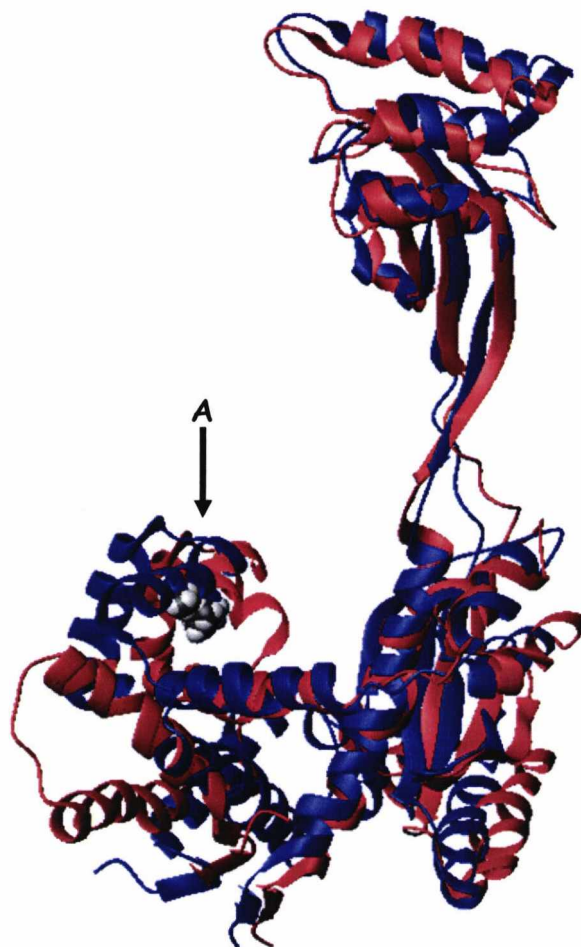


Figure 5.3.8.1 Overlay of the wild-type SurA and A99V mutant. The wild-type protein is shown in blue and the mutant in red. The altered residue location is indicated by an arrow (A), and the CPX.

The change from an alanine to a valine at the position 99 in the SurA gave an RMSD value of 12.479Å. From the initial overlay of the two proteins, there appears to be very little change to the structure, however when the structures are rotated the changes can be seen more clearly. The beta sheets at the N-terminus have moved up out and away from the main structure. The first helix has moved almost to the opposite side of the protein, it has moved up and to the left from the original position in the figure 5.3.8.1. Helix two has move to the left of the protein in the displayed orientation. Helix three is where the mutation is located; the helix is no longer complete with the

mutation present. Helix four has become thinner, tighter coiled, like a 3_{10} helix, helix five has lost its overall shape and helix 6 seems unaffected. The following helix and the main beta structure in the protein seem unaffected. The structure of the satellite domains is only very slightly affected by the change as the wild-type and mutated protein still overlay.

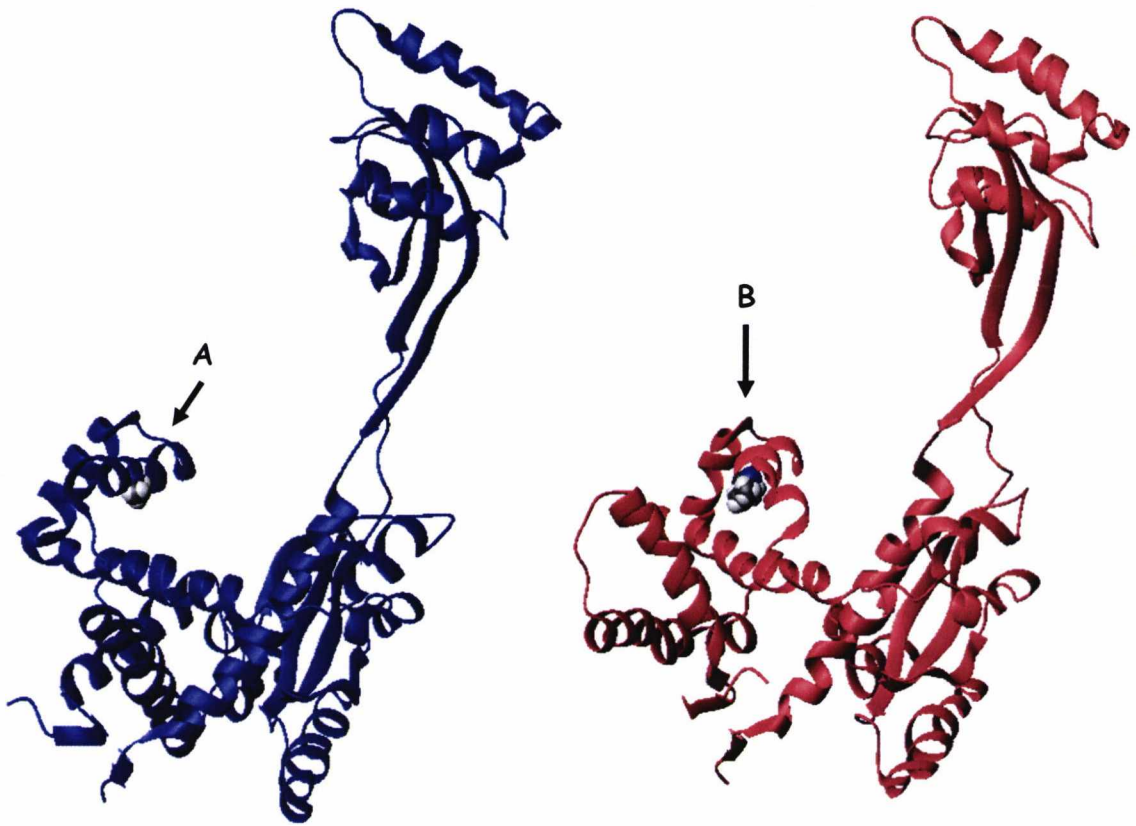


Figure 5.3.8.2 Comparison of the wild-type SurA and the A99V mutant. The wild-type protein is shown in blue and the mutant in red. The altered residue location is indicated by an arrow, and the CPX.

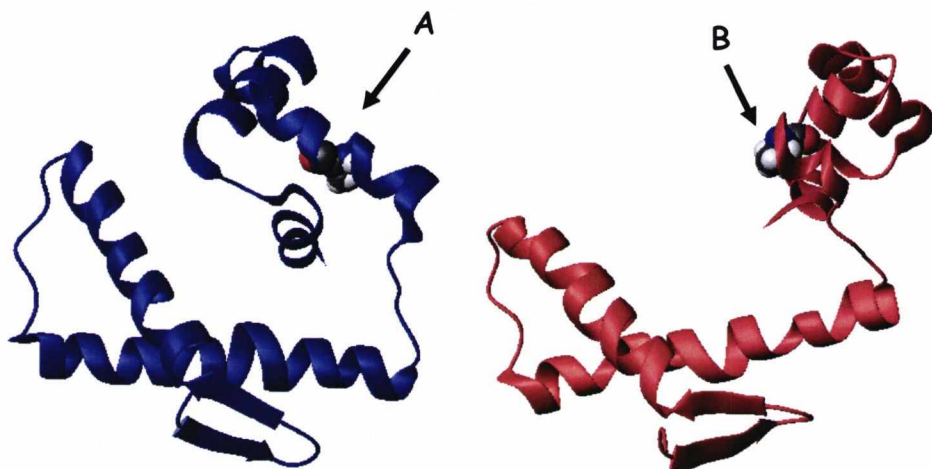


Figure 5.3.8.3 Comparison of the N-terminal fragment of wild-type SurA and the A99V mutant. The wild-type protein is shown in blue and the mutant in red.

Figure 5.3.8.2 shows the dramatic change to the core domain of SurA. The mutated residue has not moved far from its original position but has had a significant impact on the overall structure.

The overlay between wild-type and the mutant where residue at position 90 is altered from a lysine to an arginine (K90R) is shown in figure 5.3.9.1. When the two structures were overlaid the RMSD value was given as 14.015Å. Following the helices through the structure from the N-terminus to the C-terminus it is possible to see the differences in the structures. The initial β -sheets at the N-terminus have moved to the opposite orientation i.e. their starting point is in the opposite direction to the wild-type protein, this impacts the following α -helices 1 and 2, which have been forced out of the core domain. The following α -helices 3 and 4 have not really moved from their original positions, the angle of helix 5 has altered by 45° but the positioning has not changed, the same is true for helix 6.

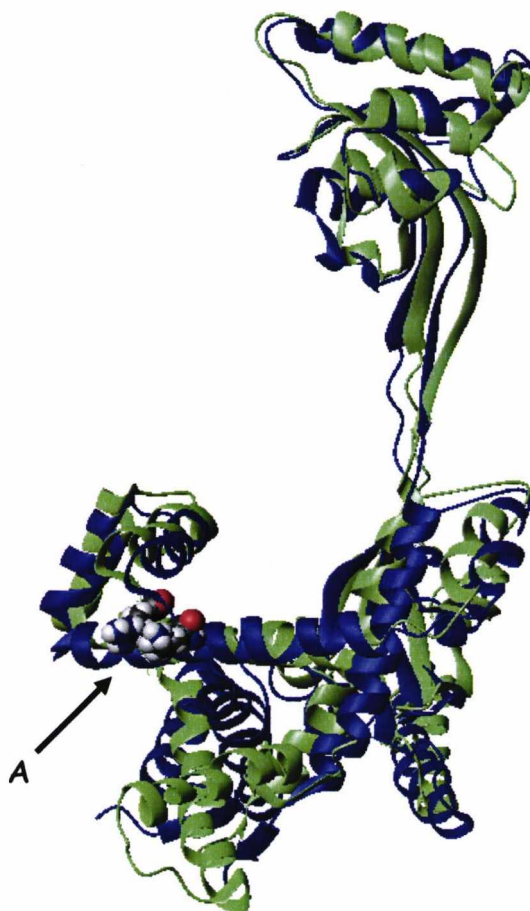


Figure 5.3.9.1 Overlay of the wild-type SurA and the K90R mutant. The wild-type protein is shown in blue and the mutant in light green. The altered residue location is indicated by an arrow (A), and CPX.

The main β -sheet structure in the protein has become fractionally less ordered than in the wild-type protein. There has been almost no effect on the satellite domain. The final helix that runs back down from the satellite domain into the core domain has suffered little change due to the mutation, apart from appearing more tightly coiled. The differences between the two structures can be seen more clearly in figure 5.3.9.2, which specifically highlights the differences between the first two α -helices in the structures making them easier to see. The positioning of the altered residue seems to be almost the same in both of the structures, shown by the CPX. The most noticeable differences are in the first two helices.

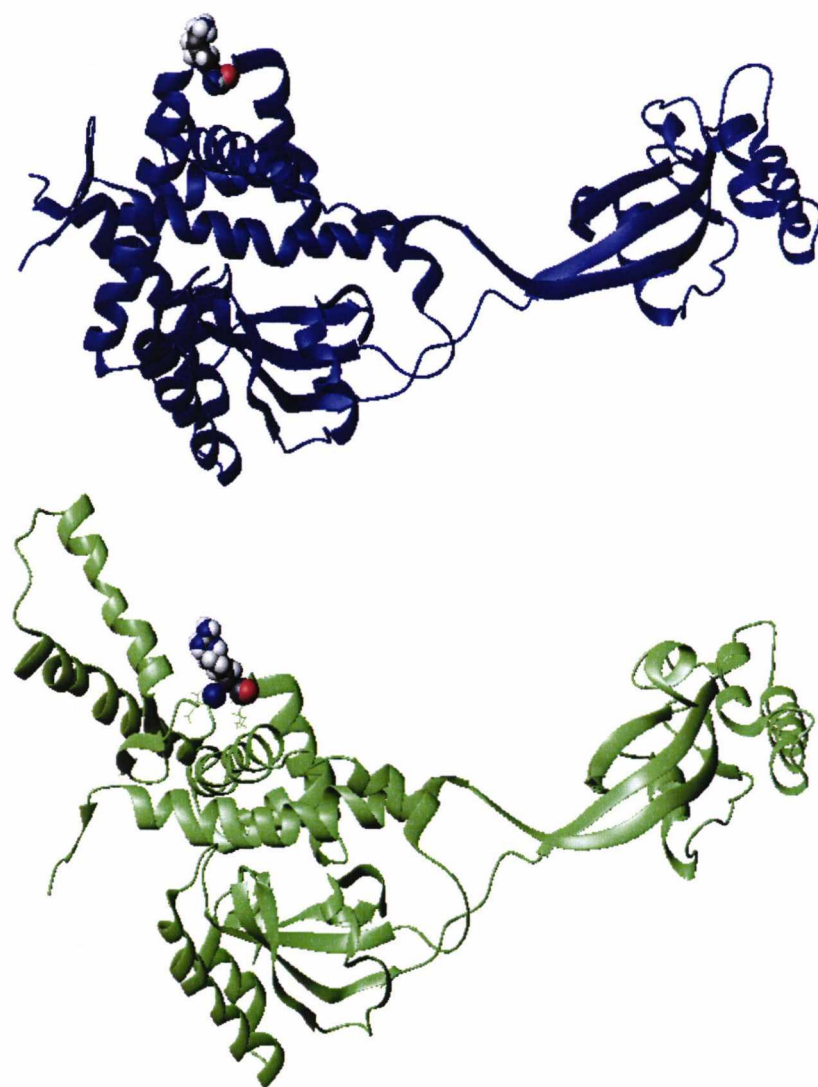


Figure 5.3.9.2 Comparison between the wild-type SurA and the K90R mutant. The wild-type protein is shown in blue and the mutant in light green. The altered residue location is indicated by an arrow and CPX.

In the two compared images in figure 5.3.9.2 the changes in the satellite domain is clearer to see, the satellite domain has rotated clockwise in the mutant protein.

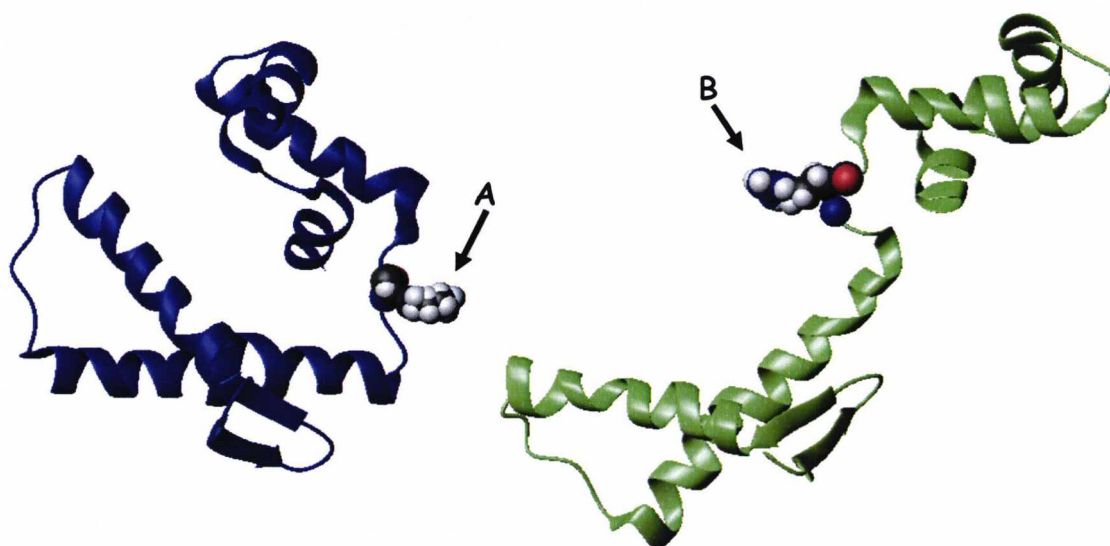


Figure 5.3.9.3 Comparison between the N-terminal fragment of the wild-type SurA and the K90R mutant. The wild-type protein is shown in blue, Lysine is shown by the CPX labelled (A). The mutant is shown in light green and the Arginine by the CPX labelled (B).

The effect of the change is clearly shown in figure 5.3.9.3. There is a marginal difference in the orientation of the first two β -sheets in comparison to the first two α -helices. There is a marked difference in the positioning of the third, fourth and fifth α -helices are that they have moved out of the core domain.

5.4 MEASUREMENTS OF RESIDUE DISTANCES FROM WILD-TYPE POSITIONING HIGHLIGHT DRAMATIC DIFFERENCES IN THE MUTATIONS

Using the CNS standard simulated annealing molecular modelling programme it is possible to measure the distances between the individual residues. For the purpose of this study comparisons were made between the wild-type protein SurA and the mutants of SurA.

The numbers generated by measuring the distances between specific residues were compared to the structural images in this chapter. There is a clear indication that the

structures with the greatest overall differences are the ones with the highest numbers in the Table 5.4.1. The table illustrates the differences in the positioning of residues in structures after the mutations that have been presented at the beginning of this chapter.

Residue	WT	A64V	A99V	I75S	R73D	A64P	K90R	K278R	G363A
64	0.33	2.08	37.93	24.64	24.85	1.59	34.46	1.38	0.64
99	0.26	1.84	8.31	4.11	2.09	1.80	10.05	0.39	0.54
75	0.02	2.31	8.63	5.52	1.82	2.24	7.72	1.07	2.22
278	0.39	1.47	2.33	2.00	2.76	1.71	2.75	1.22	0.42
73	0.53	2.79	17.04	8.46	3.43	1.85	19.93	1.02	2.28
363	0.64	2.53	3.56	2.84	1.97	0.85	6.12	1.68	0.76
90	1.14	2.19	23.53	4.98	2.59	3.13	10.76	0.85	2.80

Table 5.4.1 Table of differences in Å between simulated wild-type residues and Mutants. Measurements were performed between the overlays of the wild-type protein and the mutant, for example, for residue 64 the difference between the original PDB protein and simulated wild-type protein is only 0.33Å but when the wild-type is overlaid with A99V the distance is much greater, 37.93Å.

5.5 MUTAGENESIS OF SELECTED SIMULATED MUTANTS

Mutants were selected as they showed marked differences in structure. The mutants were created in two different ways. The first mutants were created by changing the alanine at position 99 to a valine and changing the isoleucine at position 75 to a serine. These were created by Dr Satish Raina (unpublished results), who observed that the mutants did not grow as well as the wild-type *E.coli* cells (I75S) or did not grow at all (A99V). To study the effect of these mutants over expression was attempted to produce high levels of the protein that could be purified and used in binding studies as a comparison to the wild-type SurA.

Competent cells that were transformed with the mutant plasmid coding for A99V did not give a viable clone for expression of the protein. The I75S mutant did not show any binding to radiolabelled Δ -somatostatin.

Further mutants were created using the method of site directed mutagenesis. The A64V mutant showed good binding, the same as would be expected for the wild-type SurA, see figure 5.5.1.

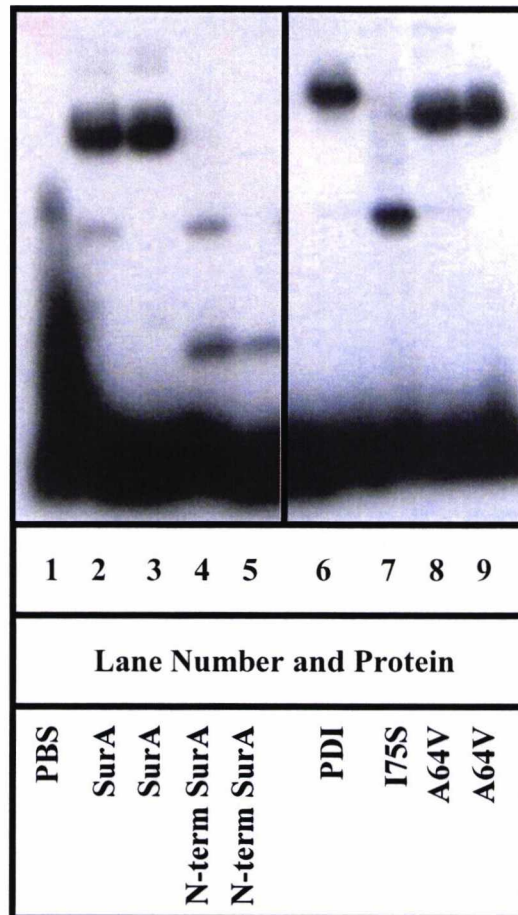


Figure 5.5.1 SurA mutants and binding to the radiolabelled peptide. Samples of protein were incubated with radiolabelled peptide Δ -somatostatin as in chapter 4 (standard binding assay). Lane 1 PBS, Lane 2 full length lysate, lane 3 full length purified SurA, Lane 4 N-terminal fragment of SurA lysate, lane 5 purified N-terminal fragment of SurA, Lane 6 purified PDI, lane 7 SurA mutant I75S lysate and lanes 8 and 9 mutant A64V lysate and purified protein respectively.

5.6 CONCLUSIONS

The CNS standard simulated annealing molecular modelling programme was tested as a method that could successfully be used in predicting which mutations would have a significant effect on the structure of a protein and affect the binding characteristics. By using this method it has been possible to visualise the changes to the protein and predict the protein's ability to still bind substrates. This has enabled informed predictions to be made about substrate binding.

Dr M Howard kindly assisted with the CNS standard simulated annealing of different mutations selected throughout the structure.

The original crystal structure solved by Bitto and McKay had little difference to the wild-type protein structure to which hydrogen atoms were added. Mutations outside

the core domain, in the satellite domain and in the region connecting the satellite domain to the core domain also had very little effect on the overall structure to SurA. Any significant effects on the structure were from changes to the core domain. Six mutations to the core domain in the area designated as the binding region gave six very different results. The biggest change was thought to be the alteration from an alanine at position 64 to a proline; however this did not give the expected dramatic change as the effect seemed to be localised around the altered residue. The same residue was altered again but to a valine, which gave a very similar RMSD value and again localised differences were noticed around the residue. This was further reinforced by successful site directed mutagenesis. The protein produced with the mutation had no decrease in binding in comparison to the wild-type protein. This therefore suggests that the residue is not of importance to the binding of substrates. Mutations to residue 73 gave a lower RMSD value than changes to residue 64 which could also suggest that it is of little importance to binding of substrates.

The mutation at position 75 where the wild-type residue was changed from isoleucine to a serine gave a higher RMSD value than the previously mentioned mutations. This had also had some growth defects as it took six hours longer to produce colonies. This protein was successfully expressed and purified and used in binding studies alongside the wild-type protein. It showed no binding ability to radiolabelled Δ -somatostatin in comparison to the wild-type protein. The following mutations gave even higher RMSD values. Residue at position 99 where alanine had been changed to valine gave a value of 12.479Å. All attempts to express this protein failed, which could suggest that it is not a stable protein. The mutation at position 90 where lysine was altered to arginine gave an even higher RMSD value. The models of the N-terminal regions of both proteins show a distorted binding region, which could suggest inability to bind to a substrate.

Chapter 6

The Peptidyl-Prolyl *Cis/Trans* Isomerase PpiD

Chapter 6: PpiD

6.1 INTRODUCTION

PpiD, Peptidyl-prolyl *cis/trans* isomerase D, is a member of the parvulin family. The gene encoding the PpiD protein was identified because of its ability to be transcribed by the two component system CpxR-CpxA (Dartigalongue and Raina, 1998). When the protein was purified it was shown to have PPIase activity *in vitro* (Dartigalongue and Raina, 1998). PpiD is 623 amino acids long and has a molecular weight of 68150 Da, it is anchored to the inner membrane of *E.coli* by a single transmembrane segment of around 21 amino acids, with the catalytic domain facing the periplasmic space (Dartigalongue and Raina, 1998).

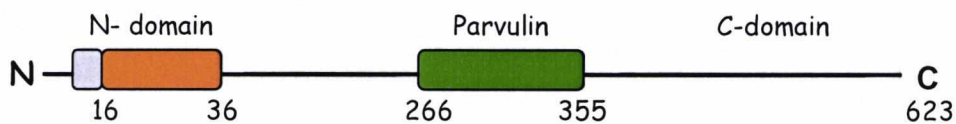


Figure 6.1.1 Diagram showing the domain architecture of PpiD. The grey area indicates the signal sequence, followed by the orange region, which represents the transmembrane domain. The green area is the parvulin like domain.

Figure 6.1.1 shows the proposed domain architecture of PpiD. PpiD has been shown to only contain one parvulin like domain unlike SurA which has two (Dartigalongue and Raina, 1998; Missiakas et al., 1996; Rouviere and Gross, 1996). PpiD was shown to be the first heat-shock induced protein that is involved in the folding of non-cytoplasmic proteins, believed to be in the outer membrane. The initial observation that the combination of the null mutants of *surA* and *ppiD* lead to a lethal phenotype under all growth conditions has recently been questioned (Justice et al., 2005). It has been shown that if *ppiD* is over-expressed it can cancel the effect of the null SurA mutant by restoring the normal membrane profile, and over expressing the *surA* gene can cancel the effects of the null *ppiD* mutant, as well as the over expression of the *ppiD* gene restoring elevated activity of σ^E activity (observed in mutant SurA strain) and can restore the defects caused by *htrM* mutants (Dartigalongue and Raina, 1998).

Moreover a recent study has shown that there was no effect to the growth rate of cells lacking PpiD (Justice et al., 2005).

This chapter describes the series of experiments that were used to produce purified full length PpiD and fragments. The purified proteins would be later used in the binding assays and NMR analysis. Also the binding properties of PpiD would be compared to SurA, as it is claimed that they have overlapping substrate specificity but as yet there has been no data to show interaction between the specificity for specific peptides between SurA and PpiD.

6.2 EXPRESSION AND PURIFICATION OF PPIID

Initially a truncated form of PpiD was constructed, lacking the membrane spanning segment. This construct has allowed for high levels of expression of the PpiD protein. A hexa-histidine tag was engineered on to the N-terminus of PpiD that has facilitated the purification of the protein, and has been shown that it does not influence the binding properties of the protein.

The gene encoding PpiD without the transmembrane portion (position 37 to 623) was amplified from *E.coli* genomic DNA using an extended PCR cycle using the forward and reverse primers:

Forward Primer:

5'-TTT TTT TTC ATA TGG GAG GCA ATA ACT ACG CCG CAA AAG-3'

Reverse Primer:

5'-TTT TTT TTC TCG AGC TAT TAT TGC TGT TCC AGC GCA TCG C-3'

These primers allowed the insertion of the *NdeI* site at the N-terminus and an *XhoI* site at the C-terminus. The primers complementary to the 3'-end included a stop codon. The inserts were cloned between the *NdeI* and *XhoI* site of pLWRP51, a modified pET23d vector, which contained an insert coding for an initiating

methionine residue followed by a hexa-histidine tag, as previously described (Webb et al., 2001).

The products were digested with the restriction enzymes NdeI and XhoI and purified using QIAGEN PCR purification kit. The vector pLWRP51 was also digested using the restriction enzymes NdeI and XhoI, and purified by QIAGEN PCR purification. The fragments and the vector were ligated at room temperature for 2 hrs. This was then transformed into competent XL1-blue and plated on to the appropriate agar plates.

Plates with the vector containing the PpiD insert grew twice as many colonies as the control. Colonies were picked and the subsequent cultures minipreped to extract the plasmid DNA. The plasmid DNA was subjected to PCR under the same conditions as the fragments were generated to confirm the presence of the insert. The clone was sequenced.

The minipreped DNA was transformed into BL21-pLysS cells before it was used in expression cultures.

500 ml of LB with ampicillin in a 2 L flask was inoculated with cells from an overnight culture and incubated at 37°C for approximately 3 hrs until the cell density reached 0.3 – 0.5 at OD_{600nm} indicating that the cells were at mid-log phase. To induce the expression of the PpiD protein IPTG was added to the culture and again left for another 3 hrs. The cell culture was centrifuged at 8000 rpm to pellet the cells. The supernatant was removed and the cells were resuspended in buffer with DNase. The cells were freeze thawed to release the protein from the cells.

The cell lysate was spun for a further 20 min at 9000 rpm to remove the cell debris and then filtered through a 0.2 µm filter before being loaded on to the column.

The PpiD protein was purified using a nickel-nitrilotriacetic acid column, for further detail see chapter 2. For the PpiD purification the method was altered slightly. The weakly bound protein was washed from the column with phosphate buffer containing 100 mM imidazole and 0.5 M sodium chloride until the UV_{280nm} was a steady flat line. To elute the protein 10 mM EDTA in phosphate buffer was used. The diagram below figure 6.2.1 outlines the basic steps in the purification process.

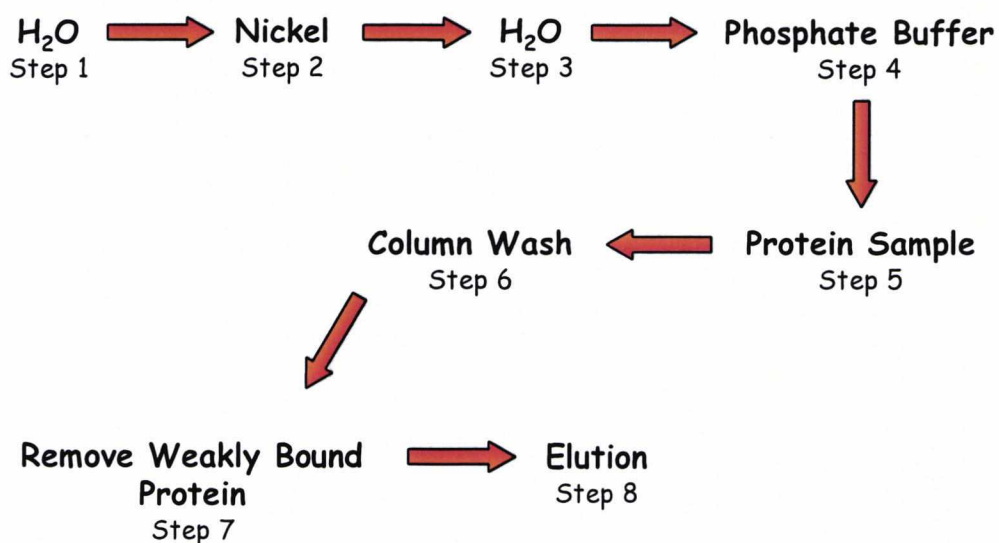


Figure 6.2.1 Flow diagram outlining protein purification steps. The purification process is discussed in detail in the materials and methods section 2.6.3. This diagram shows the key steps for full length PpiD and the fragments of PpiD.

Samples were only collected after the protein sample was loaded onto the column. The protein sample was loaded on the column at step 5; the first fraction was collected when the OD_{280nm} reading began to rise, indicating the presence of protein. Each purification step was analysed on 12.5 % SDS polyacrylamide gels, see Figure 6.2.2.

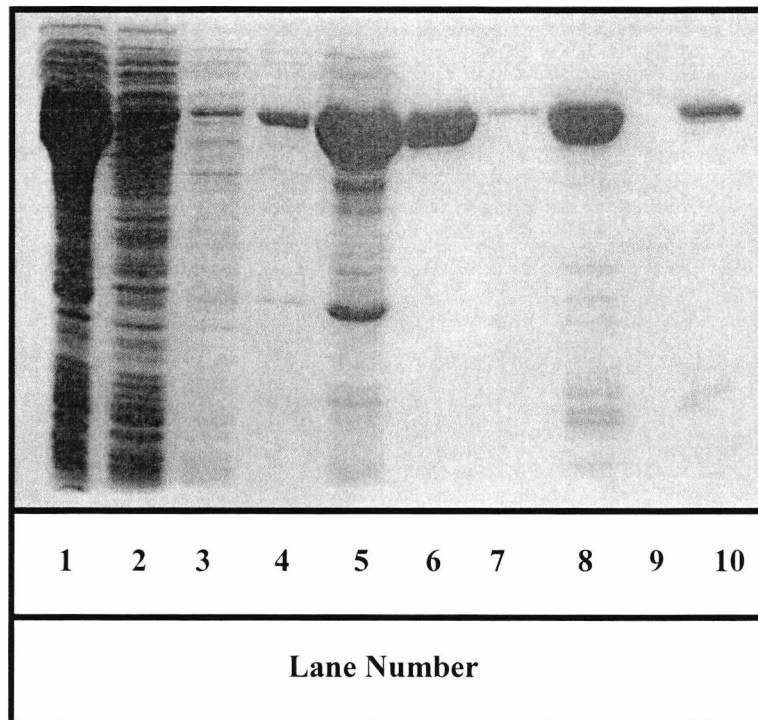


Figure 6.2.2 PpiD purification on a nickel-nitrilotriacetic acid column. Lane 1 is the pre loaded cell lysate, lane 2 is the flow through from the loaded sample, lanes 3 and 4 are the first wash, lane 5 is the loosely bound protein eluted with 100 mM imidazole, lanes 6 and 7 are the following washes, lane 8 is the main elution peak and lane 10 the peak after the main elution.

Fractions from the main elution peak (lane 8 in figure 6.2.2) were further concentrated using a Resource Q column, figure 6.2.3.

The trace from the Resource Q purification had a number of peaks. The main peak started at fraction 8 and ended at fraction 15. Fractions 16, 19 and 24 were progressively smaller peaks.

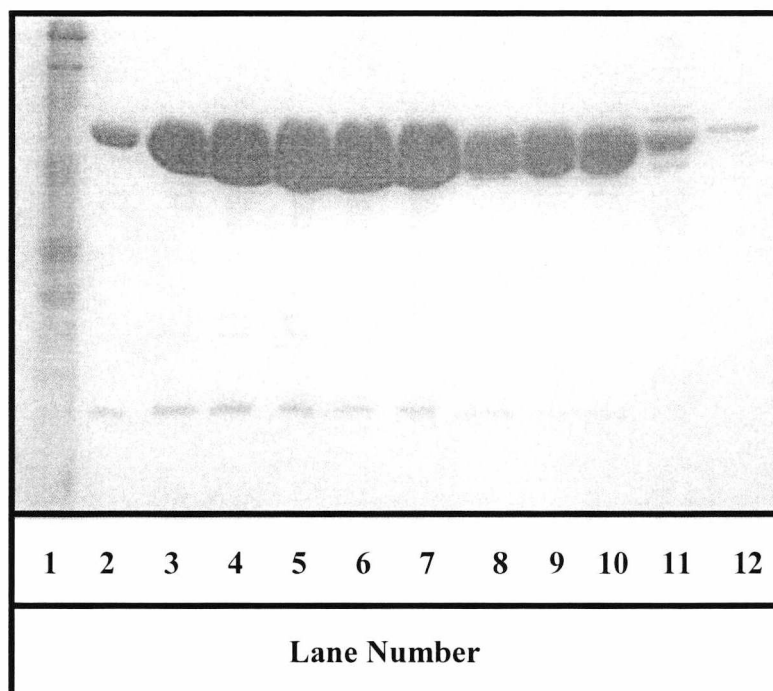


Figure 6.2.3 Purification fractions from the Resource Q column. Lane 1 is the markers, lanes 2-10 are fractions 8-16 respectively, lane 11 is fraction 19 and lane 12 is fraction 24.

Protein samples from fractions 13 and 16 were analysed using mass spectrometry to determine whether they were the same protein. Results indicated that the fractions had the same contents, as they had the same molecular weights of 65.41 kDa, so it was decided to pool the fractions from 8 to 16.

The presence of the small molecular weight contaminants was investigated. The PpiD samples were filtered through a Centricon 30 filter unit to try to remove the small molecular weight contaminants. One spin for 15 min gave 1.7 ml of retentate and 5 ml of filtrate but did not remove the small proteins. Samples were run on a 15% SDS-polyacrylamide gel and transferred to a PVDF membrane by Western Blotting. The band of interest was removed and sequenced by Edman-degradation at the protein facility at The University of Kent. Sequencing indicated that the proteins were degradation products of PpiD from the N-terminal end of the protein as the hexahistidine tag was at the beginning of the sequence.

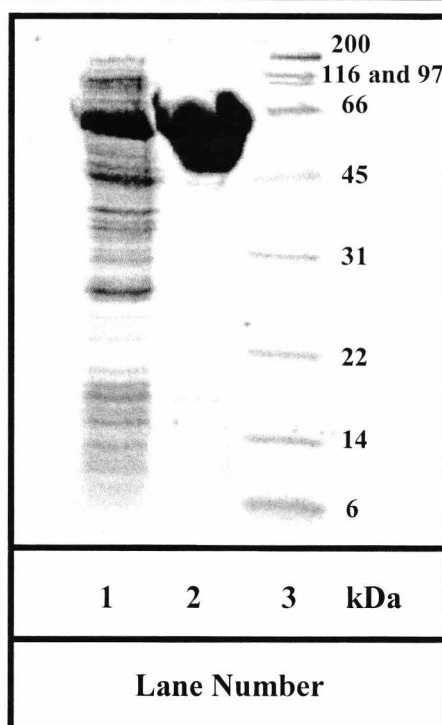


Figure 6.2.4 Expression of PpiD. Initial construct of PpiD, containing only the periplasmic region. Samples of protein were run on 12.5% SDS-PAGE gels and stained with coomassie blue stain. Lane 1 is the expressed protein in cell lysate sample and lane 2 is the protein purified and concentrated. Lane 3 is the molecular weight marker and the lane sizes are indicated in kDa.

Final concentration of the PpiD protein was measured at OD_{280nm} and calculated to be 14.3 mg/ml. The protein sample was diluted by the addition of phosphate buffer to give a final concentration of 7 mg/ml (110 μ M).

6.3 ANTIBODIES AGAINST PPIID

Polyclonal antibodies were produced using Trimax Gold with PpiD, for more details see Materials and Methods. PVDF membranes that had the appropriate protein transferred by western blot were decorated with the primary antibody and visualised by using secondary antibodies conjugated with horse radish peroxidase.

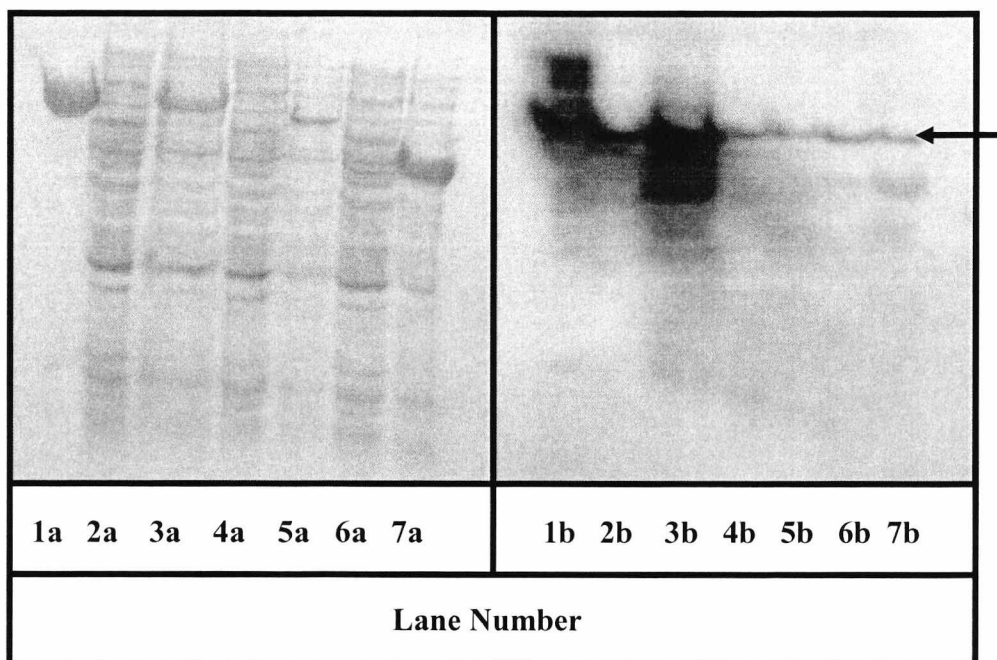


Figure 6.3.1 Antibodies against PpiD. Samples were run on 12.5 % SDS-polyacrylamide gel and then transferred to PVDF by western blotting. The blot was probed for PpiD proteins using a specific antibody for the PpiD protein. Lane 1 is pure PpiD, lane 2 is PpiD culture without induced expression, lane 3 is PpiD with induced expression, lanes 4 and 5 are PDI without and with induced expression and finally lanes 6 and 7 is SurA without and with induced expression. Lanes with **a** are the stained western blot membrane and lanes with **b** are the images from the ECL film. The arrow indicates the bands for PpiD.

6.4 PROTEINASE K DIGEST OF PPID

Proteinase K is a highly active non-specific serine protease isolated from *Tritirachium album*. While capable of cleaving all peptide bonds, Proteinase K exhibits a preference for aliphatic, aromatic and other hydrophobic amino acids in the P1 position. Proteinase K can digest both native and denatured proteins, the reaction is stopped by the addition of Phenylmethanesulfonyl fluoride (PMSF). By digesting the protein with Proteinase K for only 30 min the exposed regions of the protein were digested. Figure 6.4.1 shows the Proteinase K digest of PpiD, lane 2 shows the undigested PpiD protein which has a molecular weight of 65150 Da, this is the over expressed protein and has had the signal sequence and the membrane spanning domain removed and therefore is positioned nearer the 66200 Da marker. With the addition of the Proteinase K the band drops next to the 45000 Da markers indicating a

loss of 20 kDa. To determine which residues have been removed by the Proteinase K the band indicated by **D** in figure 6.4.1 was sequenced by Edman-degradation.

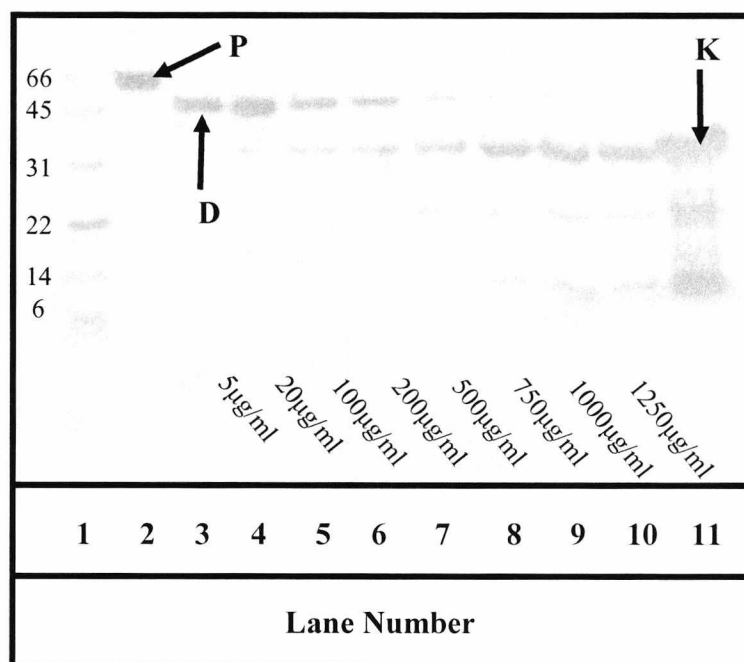


Figure 6.4.1 Proteinase K Digest of PpiD. PpiD was digested with increasing concentrations of Proteinase K for 30 min, the reactions were stopped using PMSF and the samples ran on 12.5 % SDS-polyacrylamide gels. Lane 1 is the marker, lane 2 is PpiD without any Proteinase K lanes 3-10 have the following concentrations of Proteinase K 5, 20, 100, 200, 500, 750, 1000, 1250 µg/ml. **P** indicates undigested protein; **D** indicates the band sequenced and **K** proteinase K band. The molecular weight markers are on the left of the gel.

The protein was transferred from the SDS-PAGE to PVDF membrane by Western blotting, and the band was cut out of the PVDF and sequenced. The sequencing was performed on site at The University of Kent by Judith Hardy. The results are shown in Table 6.4.2 below.

On the table in figure 6.4.2 two of the cycles had more than one amino acid with a high degree of certainty. Cycle 1 was predicted to be valine, glycine or phenylalanine. It was however unlikely to be glycine as there were high levels of glycine in the buffer. For cycle 4 the amino acids predicted with high level of certainty to be either Glutamine or Aspartic acid, but the peak indicating Glutamine was higher than Aspartic acid. Cycle 8 had only one residue, arginine, the recovered quantities suggested that there was a low degree of certainty that it was the predicted amino acid, but as there were no other predictions it was assumed that this residue

was probably arginine. The sequence was compared to the full length sequence of PpiD.

Cycle Number	Amino Acid
1	V,F,G *1
2	A
3	Q
4	Q,D *2
5	R
6	V
7	V
8	r
9	E
10	A

Table 6.4.2 Sequencing of 45kDa fragment of PpiD from proteinase K digests. Capital indicates residue with high degree of certainty and lower case indicates residue call with lower degree of certainty. *1 indicates that G is unlikely at this position and *2 likely to be Q as it had very high peak.

In figure 6.4.3 the small sequenced region at the beginning of the Proteinase K digested fragment is shown in red, it highlights amino acids 187 – 197. The Proteinase K therefore removed 151 amino acids from the beginning of the mature PpiD sequence. The next step was to investigate whether the 151 amino acids contained the binding region of PpiD, or a section that was important for the binding, such as structural properties for the binding characteristics of PpiD.

```

PpiD      1  MMDSLRTAANSILVLKIIIFGIIIVSFILTVGVSGLIGGGNNYAAKVNDQEISRGQFENAFN
Small     1  -----

PpiD     61  SERNRMQQQLGDQYSELAANEGYMKTLRQQVLNRLIDEALLDQYARELKLGISDEQVKQA
Small     1  -----

PpiD    121  IFATPAFQVDGKFDNSRYNGILNQMGMTADQYAQALRNQLTTQQLINGVAGTDFMLKGET
Small     1  -----

PpiD    181  DELAALVAQQRVVREATIDVNALAAKQPVTEQEIASYYEQNKNNFMTPEQFRVSYIKLDA
Small     1  -----VAQQRVVREA-----

PpiD    241  ATMQQPVSADADIQSYDQHQDQFTQPQRTRYSIIQTKTEDEAKAVLDELNKGDFAAALAK
Small     -----

PpiD    301  EKSADIISARNGGDMGWLEDATIPDELKNAGLKEKQQLSGVIKSSVGFIVRLDDIQPAK
Small     -----

PpiD    361  VKSLDEVRRDIAAKVKHEKALDAYYALQQKVSDAASNDTESLAGAEQAAGVKATQTGWFS
Small     -----

PpiD    421  KDNLPEELNFKPVADAI FNGGLVGENGAPGINSDIITVDGDRAFVLRRISEHKPEAVKPLA
Small     -----

PpiD    481  DVQEQVKALVQHNAEQQAKVDAEKLLVDLKAGKGAEMQAAGLKFGEPKTLRSRGRDPI
Small     -----

PpiD    541  SQAAFALPLPAKDKPSYGMATDMQGNVLLALDEVKQGSMPEDQKKAMVQGITQNNAQIV
Small     -----

PpiD    601  FEALMSNLRKEAKIKIGDALEQQ
Small     -----

```

Figure 6.4.3 Sequence Alignment of PpiD and the Small Sequence by Proteinase K digest. FASTA format of the PpiD sequence was aligned with the sequence in the BCM multiple alignment programme on the BCM web page www.hgsc.bcm.tmc.edu/HGSCHome.html. Red indicates the sequence alignment, grey the signal sequence, orange the transmembrane sequence and green the parvulin like domain.

6.5 GENERATING THE PPIID FRAGMENT

E.coli containing the truncated form of PpiD was streaked onto LB plates containing the appropriate antibiotics and incubated over night at 37°C. Resulting colonies were

picked and grown up in small 2 ml mini-cultures overnight at 37°C, these were then used in mini-preps to extract the DNA. The extracted DNA was then used as a template for the Polymerase Chain Reaction.

Primers were designed to produce a protein fragment that had the first 187 amino acids removed starting with the VAQQ sequence. As well as the VAQQ PpiD a full length protein without the transmembrane domain was also used.

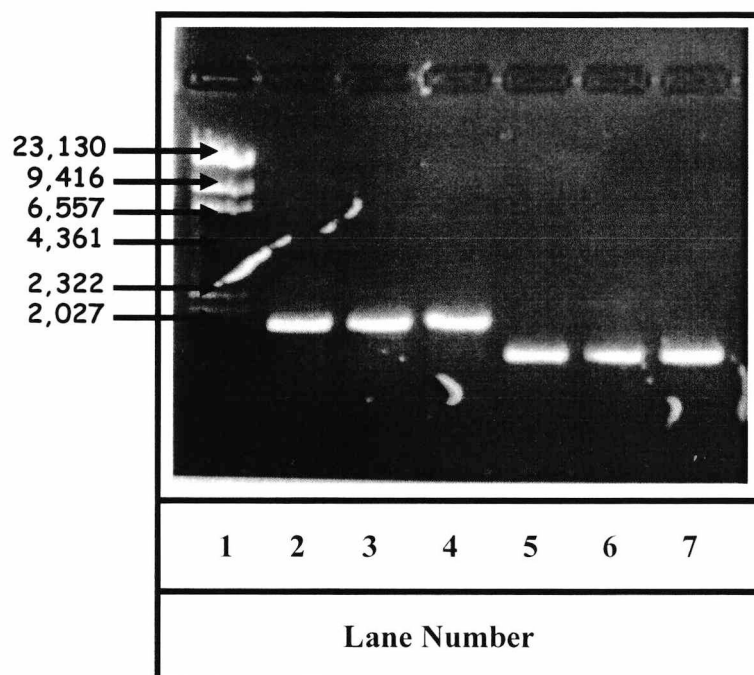


Figure 6.5.1 PCR Products for Full Length PpiD and Fragment VAQQ. 10 µl of PCR mix with 2.5 µl of loading buffer. Lane 1 is the lambda Hind III markers sizes are indicated in base pairs, lanes 2-4 full length PpiD and lanes 5-7 are the PpiD fragment.

Figure 6.5.1 shows the PCR products produced at 64°C with 25 cycles. The PCR products were PCR purified. To confirm that that PCR products were the correct size whole cells were used as templates for the PCR, these reactions also gave the same size bands but lower concentration. A number of different approaches were used to allow the insertion of the amplified products into the pET28a vector, including

PpiD F

5' - AAA AAA AAC ATA TGG GAG GCA ATA ACT ACG CCG CCA-3'

Forward primer for the full length PpiD minus the signal sequence.

Ppid VAQQ

5'-GGG GGG AAG CTT TTA TTG CTG TTC CAG CGC ATC GC-3'

Forward primer for PpiD without the first 187 residues.

PpiD REV

5'-GGG GGG GGA TCC GTC GCG CAA CAA CGC GTG GTG CG-3'

Final reverse primer for PpiD.

pGEM-Teasy, however a simple digest and ligation proved to be the most successful. Full length PpiD was digested with NdeI and HindIII and the fragment of PpiD was digested with BamHI and HindIII overnight at 37°C, the pET28a vector was digested for two 2 hour periods with the appropriate enzymes for each insert. All the digested vector and PCR products were purified to remove the impurities and enzyme and ligations were set up overnight at 16°C. These were transformed into competent DH5α cells and plated onto the appropriate LB plates. Colonies were picked and grown in small cultures and the DNA from the subsequent mini-preps was confirmed to be positive by PCR before finally being sequenced. The pET28a vector was chosen as it contained a hexa-histidine tag. The positive clones were transformed into BL21 (DE3) cells carrying the pLysS plasmid.

The subsequent expression indicated the presence of a smaller protein shown in figure 6.5.2.

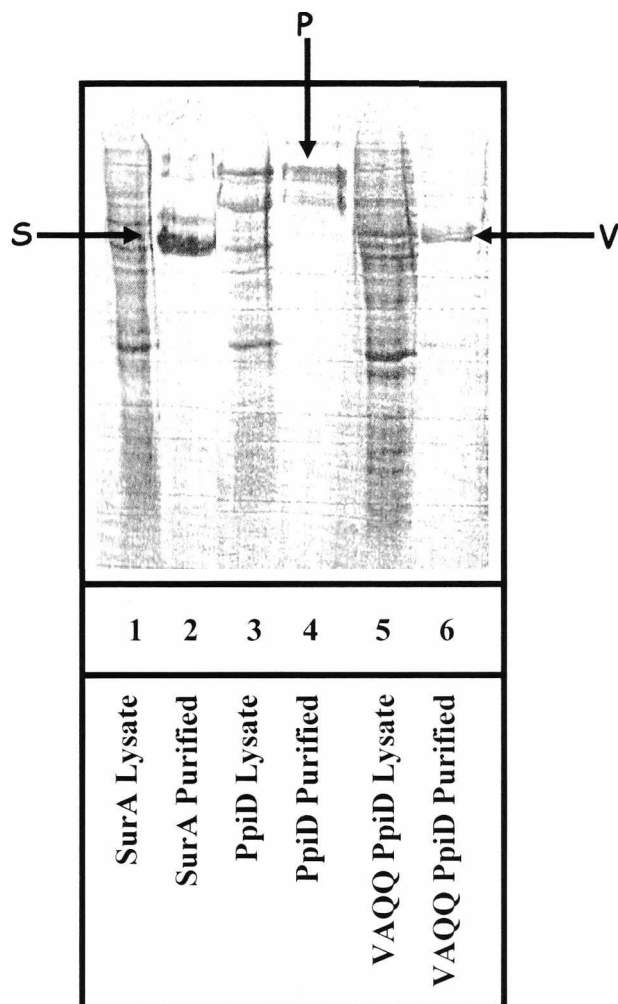


Figure 6.5.2 Lysate and purified samples of PPIases. The lysates and purified samples were analysed using 12.5% SDS-PAGE and were subsequently blotted on to a PVDF membrane. The purified SurA sample is indicated by the S, purified PpiD by P and the PpiD fragment by the V.

6.5.1 EXPRESSED PROTEIN SHOWS BINDING

The expressed VAQQ protein was tested for binding ability. The protein was used in binding assays using radiolabelled Δ -somatostatin. For both PpiD and the fragment binding ability was demonstrate, figure 6.5.1.1. The full length PpiD binding is shown in lane 2 and the fragment in lane 3. The band in lane 3 appears to be fainter than the PpiD full length; this is likely to be because the concentration of the fragment was much lower than that of the full length protein.

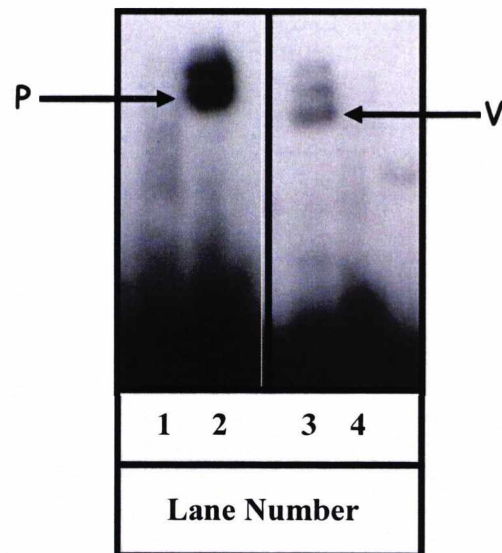


Figure 6.5.1.1 VAQQ PpiD binds radiolabelled peptide. Full length PpiD and VAQQ PpiD fragment were incubated with ^{125}I -Bolton-Hunter labelled Δ -somatostatin. Lane 1 and lane 4 are PBS with radiolabelled peptide, lane 2 is full length PpiD and lane 3 is the fragment VAQQ PpiD. The full length protein binding is indicated by P, and the fragment by V.

6.6 DETERMINING THE LOCATION OF THE BINDING REGION FOR PPIID

To determine the location of the binding region of PpiD more fragments were generated. These were labelled as PpiD2 and PpiD3. PpiD2 gave a fragment of the PpiD protein starting from the 360th amino acid to the 623rd amino acid, therefore excluding the parvulin domain. The PpiD3 fragment was smaller than the PpiD2 fragment; in this case the 478th amino acid was the start of the fragment ending with the 623rd amino acid. This is illustrated in figure 6.6.1 where the two protein fragments are highlighted in the main PpiD sequence. Primers were designed to complement the sequence and used to generate the fragments, figure 6.6.1.

```

MMDSLRTAAN SLVLKI IFGI IIVSFILTV SGYLIGGGNN YAAKVNDQEI
SRGQFENAFN SERNRMQQQL GDQYSELAAN EGYMKTLRQQ VLNRLIDEAL
LDQYARELKL GISDEQVKQA IFATPAFQVD GKFDNSRYNG ILNQMGMTAD
QYAQALRNQL TTQQLINGVA GTDFMLKGET DELAALVAQQ RVVREATIDV
NALAAKQPVT EQEIASYYEQ NKNNFMTPEQ FRVSYIKLDA ATMQQPVSDA
DIQSYDQHQ DQFTQP DRTR YSIIQTKTE EAKAVLDELN KGGDFAALAK
EKSADIISAR NGGDMGWLED ATIPDELKNA GLKEKGQLSG VIKSSVGFLI
VRLDEIQPAK VKSLDEVRDD IAAKVKEKA LDAYYALQQK VSDAASNDTE
SLAGAEQAAG VKATQGTGWF S KDNLPEELNF KPVADAI FNG GLVGENGAPG
INSDIITVDG DRAFVLRIS E HKPEAVKPLA DVQE QVKALV QHNKAEQQAK
VDAEKLLVDL KAGKGAEAMQ AAGLKFGEPK TLSRSGRDP I SQAAFALPLP
AKDKPSYGMA TDMQGNVLL ALDEVKQGS M PEDQKKAMVQ GITQNNAQIV
FEALMSNLRK EAKIKIGDAL EQQ

```

Figure 6.6.1 Amino acid sequence of full length PpiD. The highlighted regions indicate where the PpiD2 and the PpiD3 primers are designed to anneal. **Red** for the PpiD2 and **Blue** for the PpiD3, these are indicated in bold, the protein is shown in the same colour, PpiD2 also includes the blue highlighted area. The green corresponds to the area, which is the parvulin domain and the yellow to the N-domain, see figure 6.1.1.

The primer sequences used were:

PpiD2

5'-AAA AAA AAC ATA TGC CAG CGA AAG TGA AAT CGT TAG-3'

Forward primer for the PpiD2 fragment.

PpiD3

5'-AAA AAA AAC ATA TGC CGT TGG CAG ATG TTC AGG AAC-3'

Forward primer for the PpiD3 fragment.

PpiDR

5'-GGG GGG GGA TCC GTC GCG CAA CAA CGC GTG GTG CG-3'

Reverse primer for the two PpiD fragments PpiD2 and PpiD3.

Figure 6.6.2 shows the PCR products from a 25 cycle PCR at 60.5°C. There are products for the larger of the two fragments but not for the small PpiD3. To produce the PpiD3 fragment the PCR temperature was increased to 63°C. At the elevated temperature a very faint band was visible (see figure 6.6.3). A sample of the PCR product from the cycle at 63°C was then used in a further PCR for PpiD3 to amplify the product at the same temperature, 63°C. Figure 6.6.3 shows the resulting product.

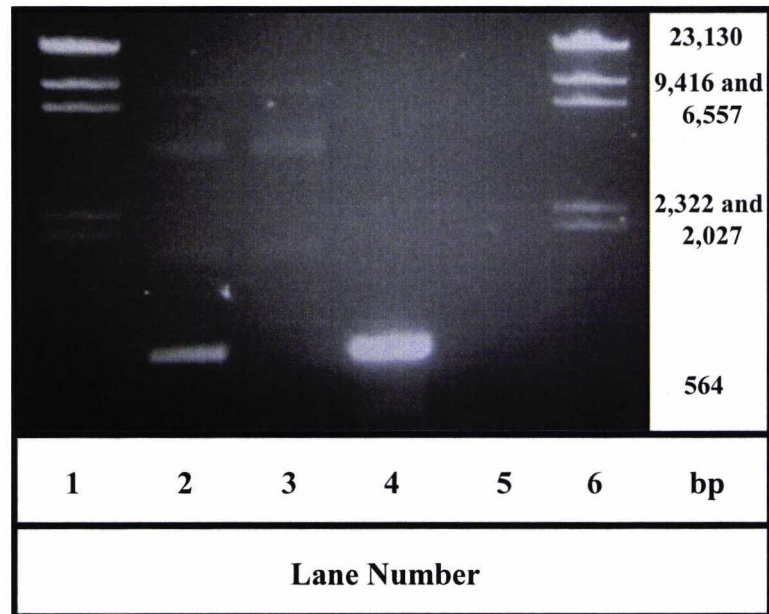


Figure 6.6.2 PCR products for PpiD2 and PpiD3. Standard PCR with melting temperature of 60.5°C and 25 cycles. Lanes 1 and 6 show the Lambda DNA/Hind III markers, lane 3 is the reaction with SurA DNA and lanes 4 and 5 with the PpiD DNA. The lanes 2 and 4 were the PpiD2 PCR products and lanes 3 and 5 were the PpiD3 PCR products.

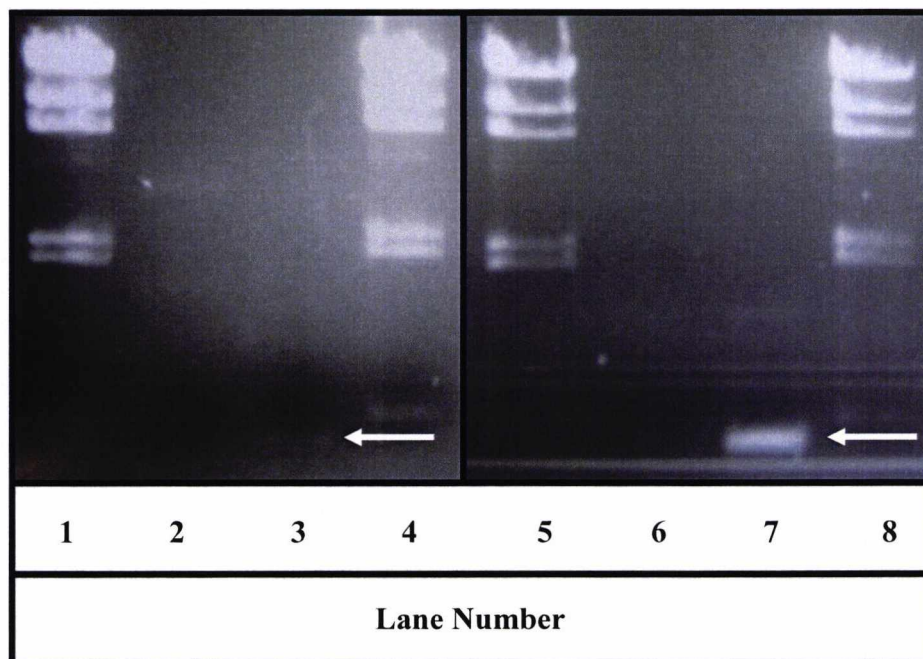


Figure 6.6.3 PCR products for PpiD3. PCR of PpiD3 and the re-amplification of the products in lane 3. Reactions were run at 63°C with 25 cycles. Lanes 1, 4, 5, and 8 are the Lambda Hind III markers. Lanes 2 and 3 show initial PCR products. Lanes 6 and 7 show the products from re-amplification of the products from lanes 2 and 3. Arrows indicate the location of the desired product.

These were subsequently purified and digested using the appropriate restriction enzymes and ligated into the pET28a vector. The resulting ligations were transformed into competent DH5 α cells. After sequencing the positive clones were grown and the DNA extracted and transformed into competent BL21plysS cells.

Colonies were selected and grown in 2 ml cultures. The positively expressing colonies were then used to inoculate a 1 L culture. The protein expression was induced by the addition of IPTG. The cells were subjected to lysis by freeze thaw, see section 6.2. The proteins were purified on a nickel-nitrilotriacetic acid column as before. The eluted fractions were subsequently analysed on 12.5% SDS polyacrylamide gels. The proteins were transferred on to PVDF membrane by Western blotting. The PVDF membrane was probed with antibodies raised against PpiD. The PVDF membrane was also probed for the hexa-histadine tag on the PpiD protein using anti-his antibodies.

Expression levels were very low for the two PpiD protein fragments (figures 6.6.4 and 6.6.5). The concentrations were estimated to be approximately 0.5 mg/ml. This however was enough to show the ability of the protein to bind to peptides.

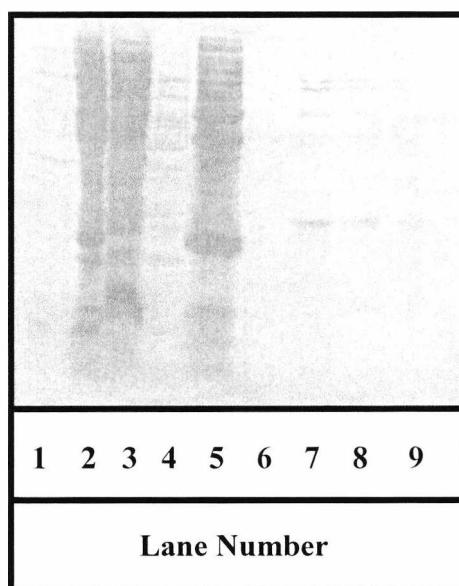


Figure 6.6.4 Fractions from PpiD3 purification. Lane 1 is the loaded sample, lane 2 is the pellet. Lanes 3-5 are the initial wash steps and lanes 6-9 are the elution steps with 500mM imidazole.



Figure 6.6.5 Fractions of PpiD2 purification. Lane 1 is the loaded sample, lane 2 is the pellet. Lanes 3-4 are the initial wash steps and lanes 5-9 are the elution steps with 500mM imidazole.

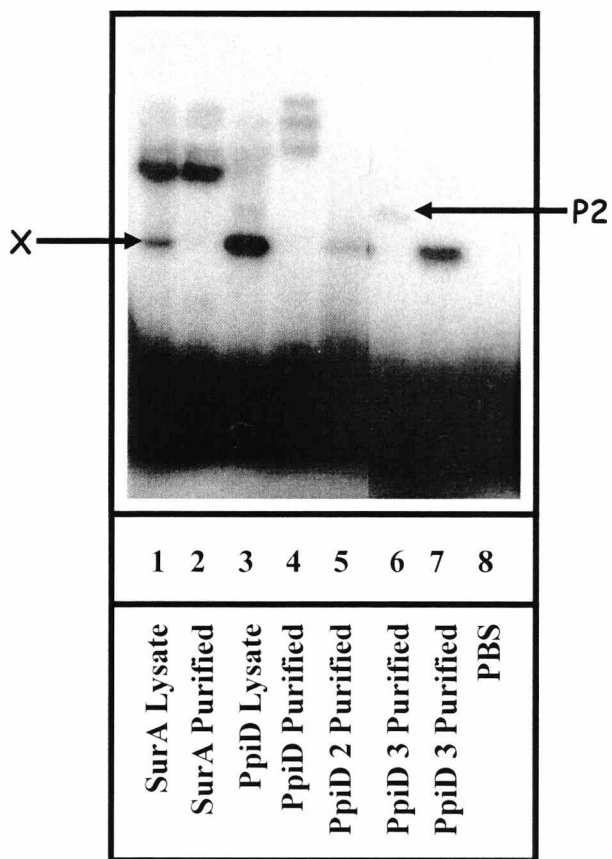


Figure 6.6.6 Binding assay for different PPIases including PpiD2 and PpiD3. Samples of listed PPIases were incubated with radiolabelled Δ -somatostatin. The PpiD2 is indicated by the P2. The unspecified crosslinking product is indicated by X.

A binding assay was performed to determine whether the proteins could perform the peptide binding function. Radio-labelled Δ -somatostatin was used to demonstrate binding in PpiD2 but not with PpiD3, shown in figure 6.6.6.

6.7 BINDING ASSAYS FOR PPIID

Following the experiments carried out in chapter 4 which investigated the binding properties of SurA it was decided to demonstrate the ability of full length PpiD protein to bind to peptides and to determine a possible binding motif for PpiD. To address whether PpiD has the same substrate specificity as SurA, PpiD was chemically crosslinked with radiolabelled peptides. Binding assays were performed using cell lysates and pure PpiD protein. In all cases there was no difference between the binding properties of the protein in the cell lysate and the pure protein sample. Peptides that were used were the same as those used for SurA binding studies so comparisons could be drawn between the two proteins. The binding was assessed by the comparison between the different peptides competing with the radiolabelled Δ -somatostatin and the intensity of the control binding which was between radiolabelled Δ -somatostatin and unlabelled Δ -somatostatin.

6.7.1 PPIID INTERACTS WITH MISFOLDED PROTEIN

To see if PpiD would potentially interact with the same model substrates, scrambled ribonuclease A (scRNase) was used as it has previously demonstrated that biotinylated scrambled ribonuclease A scRNase could be chemically cross-linked to purified SurA (Webb et al., 2001). To avoid potential artefacts through interaction with the biotin-moiety we used unmodified scRNase, which was incubated with crude *E.coli* lysates expressing recombinant PpiD. Samples without scRNase and DSG served as controls.

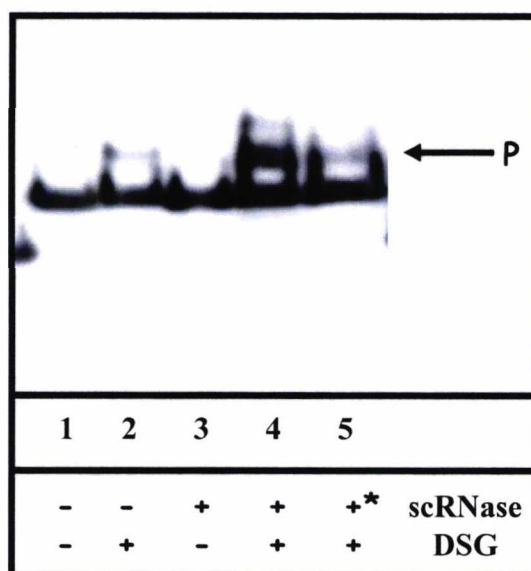


Figure 6.7.1.1 Interaction of PpiD with ‘scrambled’ RNase. *E.coli* lysate expressing recombinant PpiD, was heat-inactivated at 95°C for 5 min (*) or left untreated. The samples were then incubated with 100 μ M ‘scrambled’ RNase’ (scRNase) or buffer B prior to crosslinking with DSG. After crosslinking the samples were analyzed on 10 % polyacrylamide gels with subsequent electro-transfer onto PVDF-membranes. The samples were probed with an anti hexa-histidine primary antibody, raised in mouse, and a secondary anti mouse antibody, conjugated to horseradish peroxidase and visualized by ECL. Cross-linking products are indicated by an arrow and P.

Analysis was carried out by Western-blotting of the gels with subsequent detection using an anti hexa-histidine antibody (figure 6.7.1.1). In the absence of DSG or scRNase, no cross-linking products could be detected (lanes 1 – 3). In the presence of DSG and scRNase a single specific cross-linking product was observed for PpiD (lane 4), respectively, indicating an interaction between the PpiD and the misfolded protein. That this interaction was dependent on the native conformation of the PpiD was demonstrated by heat-inactivation of the lysate: After heat-treatment of the lysate (5 min at 95°C) prior to the addition of scRNase and chemical crosslinking, the interaction between scRNase and the PpiD was strongly reduced (lane 5). This result clearly demonstrates that PpiD can interact with misfolded protein.

6.7.2 CROSSLINKING OF RADIOLABELLED PEPTIDE TO RECOMBINANT PPI D IN CELL LYSATE

In previous experiments with SurA it has been shown that SurA can be chemically crosslinked to [125 I] Bolton-Hunter radiolabelled peptide (Webb et al., 2001), so to investigate whether PpiD requires the same recognition motif as SurA the same approach was taken. A cell lysate without any PPIases was used as the negative control in this experiment. Recombinant PpiD was chemically crosslinked to [125 I] Bolton-Hunter radiolabelled peptide. The cell lysate containing PpiD showed two crosslinking products, these are indicated by the A and B in figure 6.7.2.1. They had molecular weights of 64 kDa and 82 kDa respectively.



Figure 6.7.2.1 Interaction of PPIases with labelled Δ -somatostatin. [125 I] Bolton-Hunter labelled Δ -somatostatin (33 μ M) was incubated with *E.coli* lysates expressing recombinant PpiD or none of the PPIases (lysate) in buffer B for 10 min at 0°C in a total volume of 10 μ l. As controls *E.coli* lysates expressing recombinant PpiD, was heat-inactivated at 95°C for 5 min (*) prior to the addition of the radiolabelled peptide. Samples were subsequently incubated with DSG (final concentration 0.5 mM) for 60 min at 0°C or were kept untreated. After cross-linking the samples were analyzed on 10 % polyacrylamide gels with subsequent autoradiography. The X indicates the unspecified crosslinking product.

An identical crosslinking product was also detected with purified PpiD, indicating that this crosslinking product did not comprise proteins from the *E.coli* lysate interacting with PpiD. Electrospray mass spectroscopy demonstrated that this crosslinking product is not due to dimerization of PpiD, but is most likely a trapped conformation of native PpiD with a different mobility. Although both conformations (**a**) and (**b**) were recognized by the antibody directed against PpiD (data not shown), an anti hexa-histidine antibody did only recognize conformation (**a**), but did not react with conformation (**b**). It is therefore tempting to speculate that in conformation (**b**) the N-terminal hexa-histidine tag is no longer exposed and therefore not recognized by the hexa-histidine antibody.

Without DSG there were no crosslinking products (lane 3 figure 6.7.2.1). The heat inactivation of the lysates prior to the addition of the radiolabelled peptide and the crosslinker inhibited the reaction (lane 5); this indicates that the binding of the peptide is specific for native proteins. All lysates had the band marked X in figure 6.7.2.1 which has been observed previously (Klappa et al., 1998).

PpiD showed a strong interaction with most of the peptides that were tested; however the interaction with Δ -somatostatin was rather weak (figure 6.7.2.2). For all the peptides tested we observed crosslinking products related to the different PpiD conformations (**a**) and (**b**) respectively.

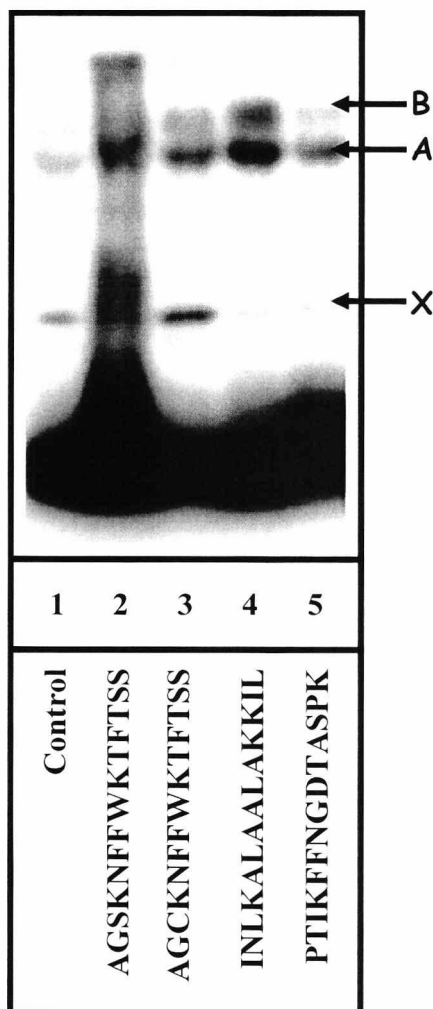


Figure 6.7.2.2 Interaction of PpiD with model peptides. The indicated [^{125}I] Bolton-Hunter labelled peptides (30 μM) were incubated with *E.coli* lysates expressing recombinant SurA, PpiD or human PDI, respectively, in buffer B for 10 min at 0°C in a total volume of 10 μl . After crosslinking with DSG the samples were analyzed on 10 % polyacrylamide gels with subsequent autoradiography. X indicates the unspecified crosslinking product.

6.7.3 COMPETITION BINDING TO PPID WITH MODEL PEPTIDES

To verify these results, competition assays were carried out using a cell lysate expressing recombinant PpiD and radiolabelled Δ -somatostatin in the presence of excess unlabelled peptides. Although PpiD did not show a strong affinity for Δ -somatostatin it was used so that direct comparison could be made with SurA. The

competition between the labelled and the un-labelled Δ -somatostatin served as a positive control. See figure 6.7.3.1.

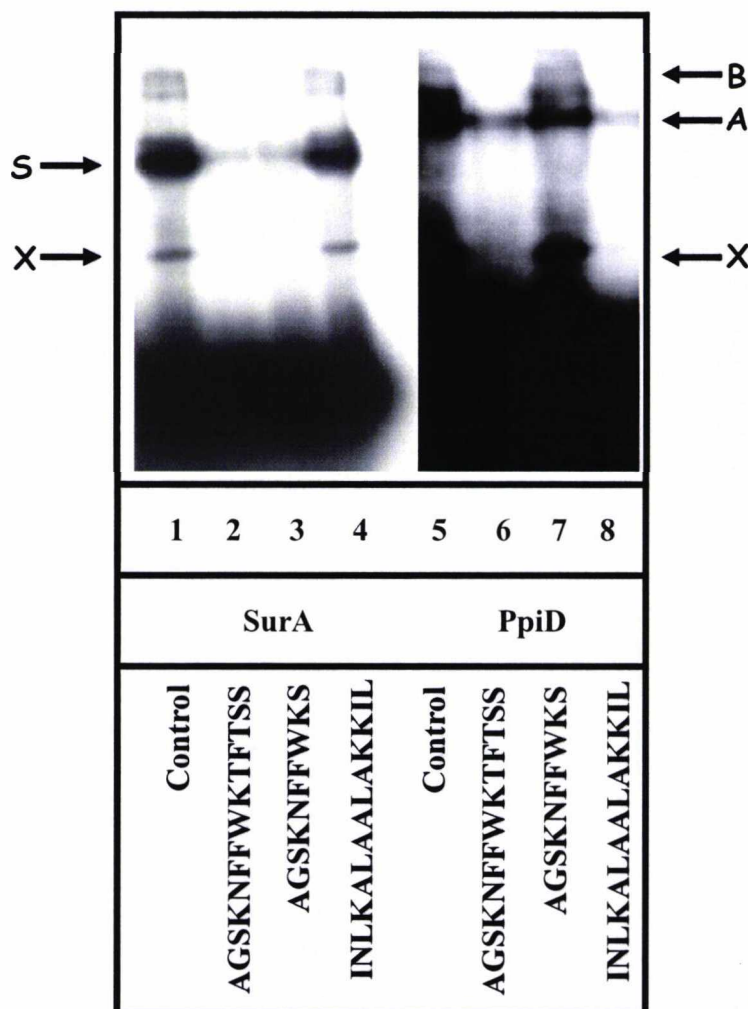


Figure 6.7.3.1 PpiD and SurA binding comparison. Bolton-Hunter labelled Δ -somatostatin (10 μ M) was incubated with *E.coli* lysates expressing SurA and PpiD, respectively, in the presence of 100 μ M of the indicated unlabelled peptides. Sample without unlabelled peptides served as controls, lanes 1 and 5. After crosslinking with DSG the samples were analyzed on 10 % polyacrylamide gels with subsequent autoradiography. Lanes 2 and 6 are proteins with radiolabelled Δ -somatostatin, lanes 3 and 7 are proteins with peptide A and lanes 4 and 8 are proteins with mastoparan. a, crosslinking to PpiD conformer (A); b, crosslinking to PpiD conformer (B); (X), unspecified crosslinking product.

Unlabelled peptide M (Pep M) did compete with radiolabelled Δ -somatostatin for the binding to PpiD. This result is in excellent agreement with the results in figure 6.7.3.1 (direct binding assay), in which radiolabelled peptide M (INLKALAALAKKIL) interacts with PpiD. Unlabelled peptide A (Pep A), however, did not inhibit the

interaction between radiolabelled Δ -somatostatin and PpiD. Table 6.7.3.2 summarises the competition experiments.

Peptide	PpiD
AGSKNFFWKTFTSS (Δ -som)	+++
AGCKNFFWKTFTSC (SRIF)	+++
AASKNFFWKTFTSS	+++
AGAKNFFWKTFTSS	++
AGSKAFFWKTFTSS	++
AGSKNAFWKTFTSS (F6A)	+++
AGSKNFAWKTFTSS (F7A)	+
AGSKNFFAKTFTSS (W8A)	+
AGSKNFFWKAFTSS	+++
AGSKNYFWKTFTSS (F6Y)	+++
AGSKNYFAKTFTSS (F7Y)	+
AGSKNWFWKTFTSS	+++
AGSKNFFWKTFT	-
AGSKNFFWKT	-
AGSKNYFWKSAS (peptide S)	-
AGSKNFFWKS (peptide A)	-
AASKAFFWKS	-
AGSKNFFWAT	-
TKWFFNKSGA	-
--SKNFFWKTFT	-
--SKNFFWKT	-
----NFFWKT	-
INLKALAALAKKIL (peptide M)	+++
WEYIPNV	-
WEYIP	-
PTIKFFNGDTASPK (peptide P)	+++

Table 6.7.3.2 Competition between peptides and radiolabelled Δ -somatostatin for the binding to PpiD. *E.coli* cell lysate expressing recombinant PpiD, were incubated with 10 μ M radiolabelled Δ -somatostatin in the presence of a tenfold excess of the indicated unlabelled peptides prior to crosslinking. Samples were subsequently incubated with DSG (final concentration 0.5 mM) for 60 min at 0°C. After cross-linking the samples were analyzed on 10 % polyacrylamide gels with subsequent autoradiography. Quantification was performed with a BioRad PhosphoImager. A sample without competing peptides served as a control. Competition was expressed as reduction in the intensity of the respective crosslinking product relative to the control without unlabelled peptides. +++, strong competition (intensity of crosslinking product < 10 % of control); ++, moderate competition (intensity of crosslinking product between 10 % - 30 % of control); +, weak competition (intensity of crosslinking product between 50 % - 80 % of control); -, no competition (intensity of crosslinking product > 80 % of control).

The competition between radiolabelled Δ -somatostatin and unlabelled Δ -somatostatin was used as the reference point.

The results demonstrate that changing the phenylalanine in position 6 to alanine (F6A) in the Δ -somatostatin sequence showed strong competition for the interaction with PpiD. Changing phenylalanine in position 7 to alanine (F7A) reduced the competitive effect of the peptide for the interaction with PpiD. A similar result was observed for the tryptophane to alanine (W8A) modification. A change of the phenylalanine in position 6 to a tyrosine (F6Y) did not prevent the peptide to compete with Δ -somatostatin for the binding to PpiD.

It was noticed that peptides shorter than 14 amino acids did not compete for the binding of radiolabelled Δ -somatostatin to PpiD. Interestingly, peptide S did not compete for the binding to PpiD, although radiolabelled peptide S interacted with PpiD (figure 6.7.3.1, lane 3). This result is most likely due to the increase in size of peptide S during direct radiolabelling: Treatment of peptides with [125 I] Bolton-Hunter labelling reagent results in an increase of the peptide chain by one residue. Therefore it is likely that the interaction of PpiD with model peptides is strongly dependent on their size.

6.8 STD-NMR FOR PPIID

STD-NMR shows the possible residues in small peptides that have contact with a much larger protein. This was the method used to show the residues in Δ -somatostatin that were in contact with PpiD.

The residues are shown in colours ranging from blue 0 – 14 % contact, green 15 – 29 % contact, yellow 30 – 40 % contact, orange 41 – 65 % contact and red 66 – 100 %. Residues displaying red are therefore much more significant than blue residues.

The amino acid sequence of Δ -somatostatin is as follows, AGSKNFFWKTFSTSS. The contacts are shown in figure 6.8.1.

The significant contacts are shown to be in serine at position 3, but only in the side chain. Phenylalanine at position six has significant contact around the β -carbon on the hydrogen atoms, 30 – 40 % around the δ^1 hydrogen and the δ^2 hydrogen and 15 – 29 % around the ε^1 hydrogen and ε^2 hydrogen atoms. The phenylalanine residue at position seven shows 41 – 65 % contact around the ε^1 hydrogen and ε^2 hydrogen atoms, and only 15 – 29 % around the δ^1 hydrogen and the δ^2 hydrogen atoms. For the

tryptophan at position eight, the ϵ^1 hydrogen shows to have significant contact as well as the ζ^2 hydrogen, the η^2 hydrogen shows 41 – 65 % contact and ζ^3 shows 15 – 29 % contact. Lysine at position nine shows very little contact except around the γ hydrogen atoms where there is 41 – 65 % contact. The threonine at position ten shows 41 – 65 % contact on one of the end hydrogen atoms. Residue eleven, the phenylalanine has the same contacts as on the phenylalanine seven so it shows 41 – 65 % contact around the ϵ^1 hydrogen and ϵ^2 hydrogen atoms, and only 15 – 29 % around the δ^1 hydrogen and the δ^2 hydrogen atoms. Finally, threonine at position twelve shows 41 – 65 % contact on all the hydrogen atoms on the γ carbon and 66 – 100 % contact with the hydrogen atom on the central β carbon.

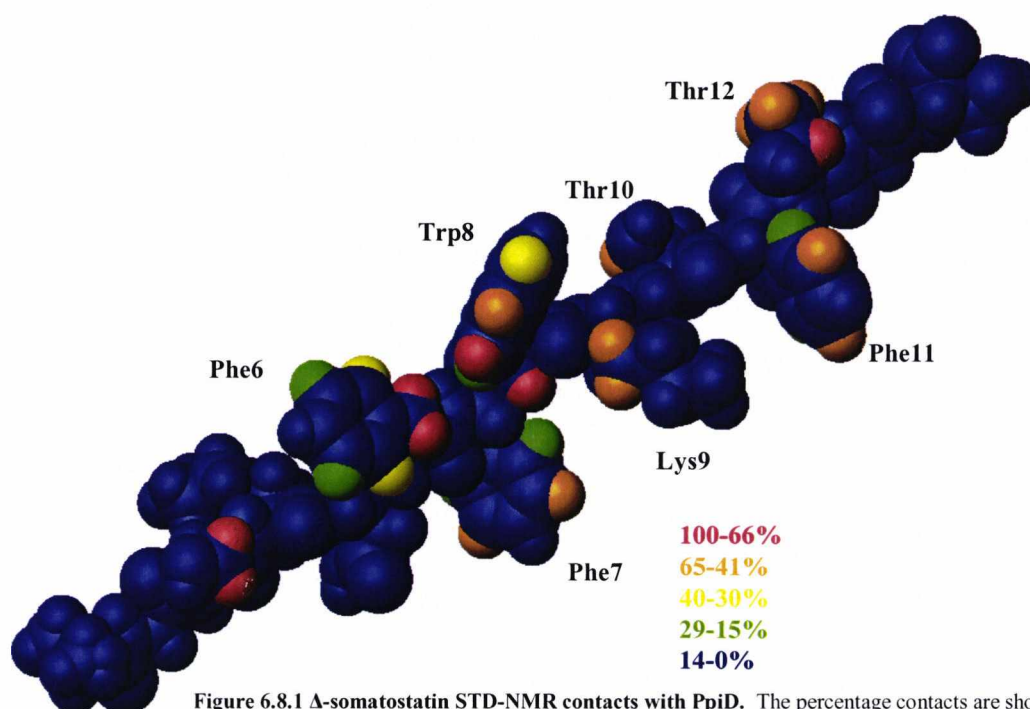


Figure 6.8.1 Δ -somatostatin STD-NMR contacts with PpiD. The percentage contacts are shown in the colours which correspond to the image above.

Figures 6.8.2 and 6.8.3 show the original data for the STD-NMR. The largest central peak is the heavy water that was added to the sample.

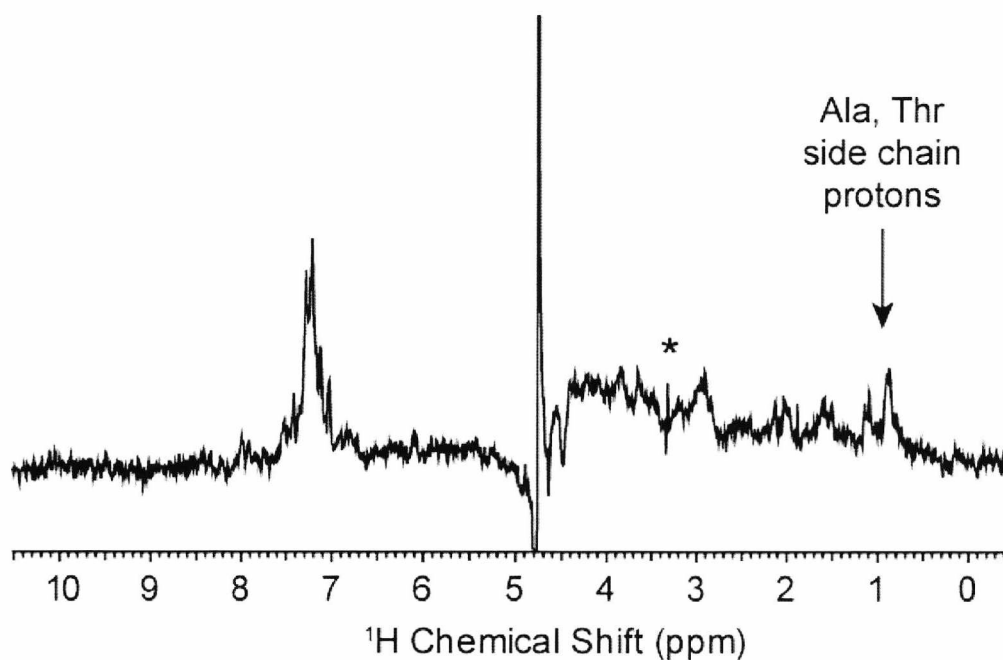


Figure 6.8.2 Data for STD-NMR. Graph (A) shows the original STD-NMR data. Peaks indicate contacts with the peptide Δ -somatostatin. The largest peak is produced by the additional heavy water.

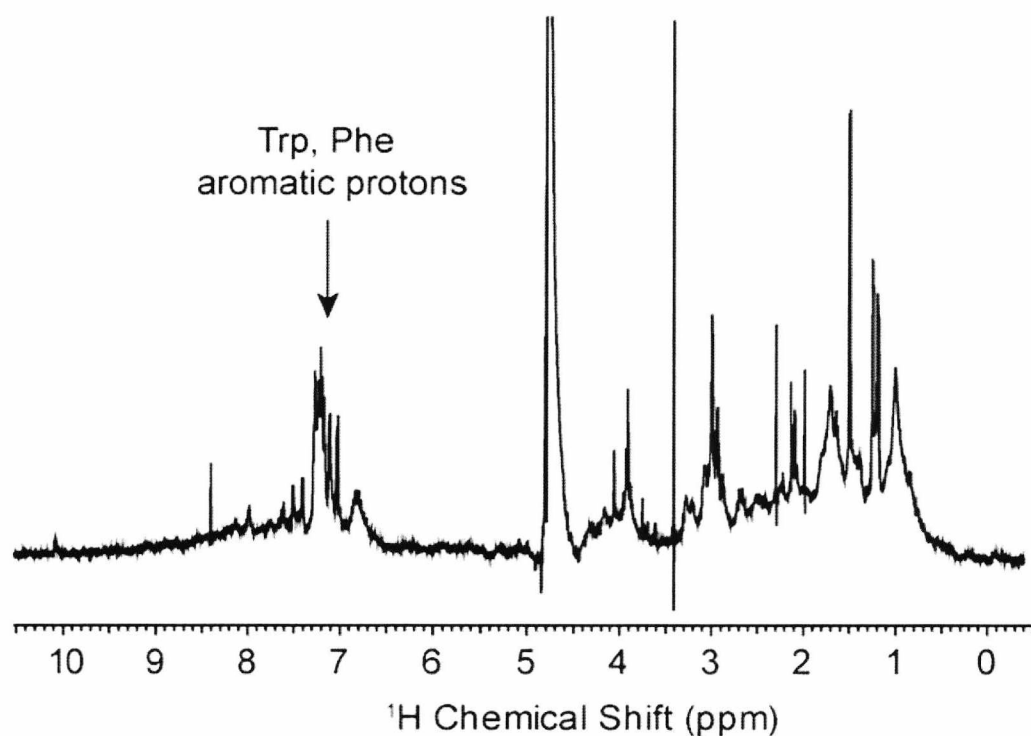


Figure 6.8.3 Data for STD-NMR. A standard Δ -somatostatin 1D ^1H spectrum.

The peaks on the left of the image in figure 6.8.3 represent the aromatics and the peaks on the right represent the aliphatic residues.

6.9 CONCLUSIONS

Although PpiD has recently been shown not to be as important in maintaining the cell integrity as previously thought (Justice et al., 2005), there is now some evidence to suggest that it does have a function in the periplasm with assisting with protein chaperoning (Dartigalongue and Raina, 1998).

The full length PpiD protein was successfully purified to 7 mg/ml using a Resource Q column. The small molecular weight contaminants were shown to be degradation products of PpiD and were not seen as significant affecting later applications involving the full length PpiD.

The purified PpiD protein and cell lysate samples were used in binding assays with model peptides. There was no difference in the binding properties between the purified protein and the crude cell lysate. Therefore all the binding assays used the purified protein.

Fragments of PpiD were generated to exclude the parvulin domain. The PpiD2 fragment showed binding to the model peptide Δ -somatostatin, the PpiD3 did not. It therefore can be concluded that the binding region of PpiD is found in the C-terminal region of the protein, C-terminal of the parvulin domain (figure 6.9.1).

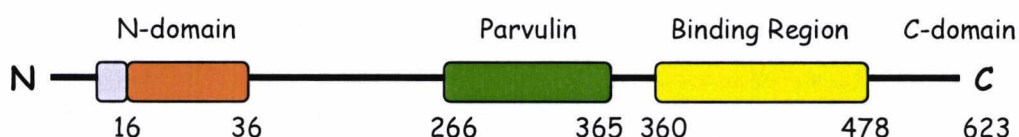


Figure 6.9.1 Diagram showing PpiD. The grey are indicates the signal sequence, followed by the orange region which represents the transmembrane domain. The green area is the parvulin like domain. The yellow region shows the possible binding region.

The purified protein was used in binding studies with the same model peptides as SurA.

The contacts between PpiD and Δ -somatostatin were analysed using STD-NMR. The residues that seemed to be important with the contacts with the PpiD binding site were serine at position 3, phenylalanine at position 6, phenylalanine at position 7, tryptophan at position 8, lysine at position 9, threonine at position 10, phenylalanine

at position 11 and threonine at position 12. But most of the contacts were 41-65%; there were only four instances of 66-100% contacts, which were for residues 4, 6, 8 and 12.

Taken together the results indicate that the interaction between peptides and PpiD is dependant on the size of the peptide and not a specific motif within the peptide.

Chapter 7

General Discussion

Chapter 7: General Discussion

7.1 INTRODUCTION

Over the last fifty years there has been much interest in how proteins fold into their final conformation. As mentioned in the introduction, there were a number of ideas, but with the discovery of chaperones and folding catalysts the general path was much clearer. What was not clear was the mechanism of recognition for the chaperone. So subsequently there have been intense investigations into how chaperones participate in the protein folding process, i.e. how they recognise which protein to bind to.

One of the rate limiting steps in protein folding has been shown to be the *cis/trans* isomerisation of the proline residues, which is catalysed by different peptidyl-prolyl *cis/trans* isomerases.

This study aimed to characterise the interaction between model peptides and the periplasmic PPIase SurA from *E.coli* and to a certain extent PpiD. To investigate the nature of the interaction, cross-linking experiments with radiolabelled model peptides and purified constructs of SurA and PpiD were performed.

The binding site of SurA has been identified using domain constructs of SurA, and by using competition assays, the recognition motif of SurA was explored.

PpiD was selected as it is a periplasmic PPIase but the main difference between PpiD and SurA is that it is believed that PpiD is tethered to the inner membrane in the periplasm. It has also been shown that the double knock out of both SurA and PpiD resulted in the loss of cell viability (Dartigalongue and Raina, 1998).

7.2 C-TERMINUS OF SURA IS REQUIRED FOR STABILITY BUT NOT BINDING

The first 110 amino acids (N-terminal fragment) of SurA excluding the signal sequence are sufficient for the binding of the peptide Δ -somatostatin (Webb et al., 2001). This study investigated the potential of the N-terminal fragment and binding with a wider range of peptides. It has been shown that the N-terminal fragment is capable of binding to the same range of peptides as the full length protein. These

results indicate that the presence of the C-terminal region is not essential for the binding of SurA with model peptides, which has been previously suggested (Behrens et al., 2001). From the fact that the N-terminal domain showed efficient peptide binding, comparable to full length SurA, it can be concluded that it adopts the native structure. There was, however, a difference in the solubility of the protein in comparison to the full length SurA. At low salt concentrations the N-terminal fragment precipitated.

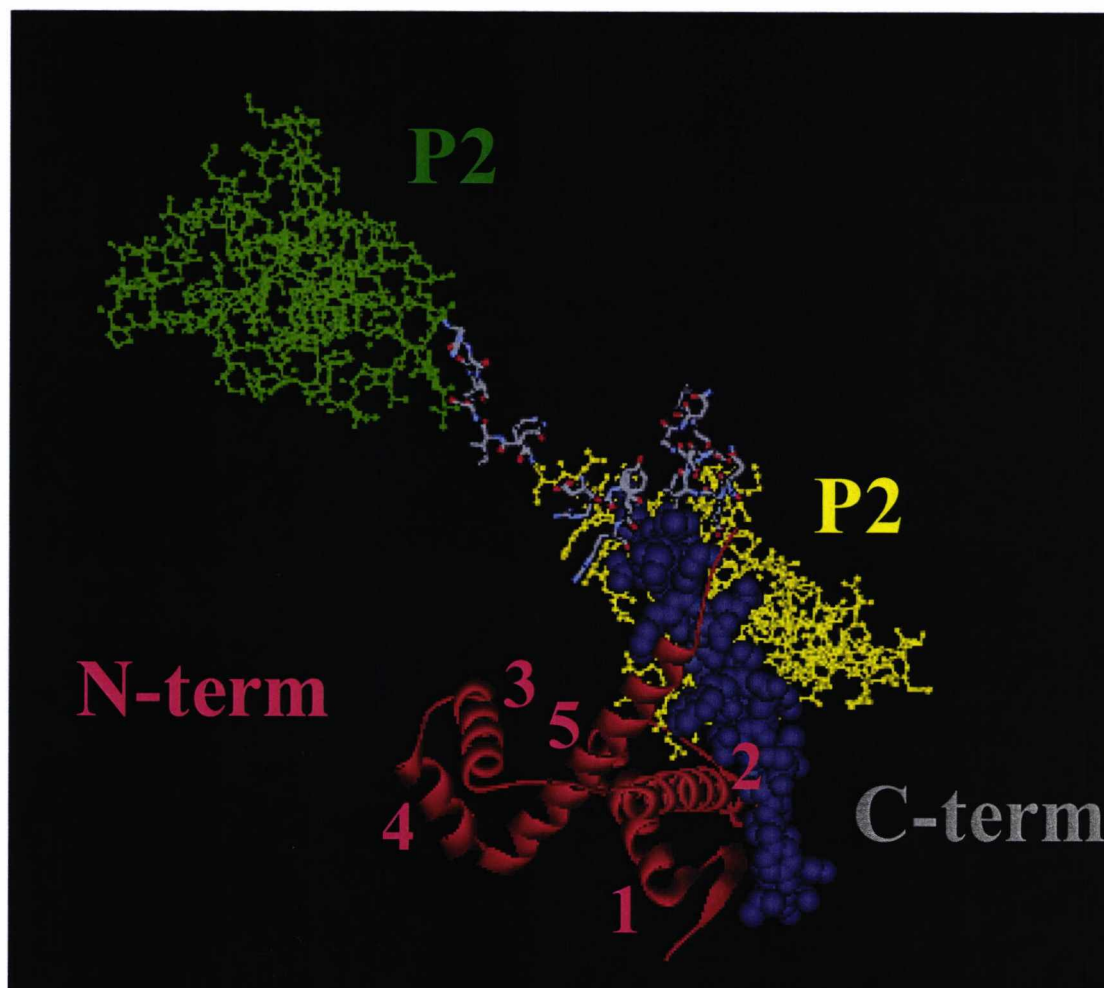


Figure 7.2.1 Crystal structure of SurA with colour-coding of the individual domains. The numbers indicate the helices in the N-terminal binding domain. The image was created with Accelrys DS visualiser version 1.6 (Accelrys Discovery Studio).

The crystallographic structure was solved in 2002; it has enabled an insight into the possible binding region of SurA. Structural studies of SurA offer a clearer picture for the importance of the C-terminal region.

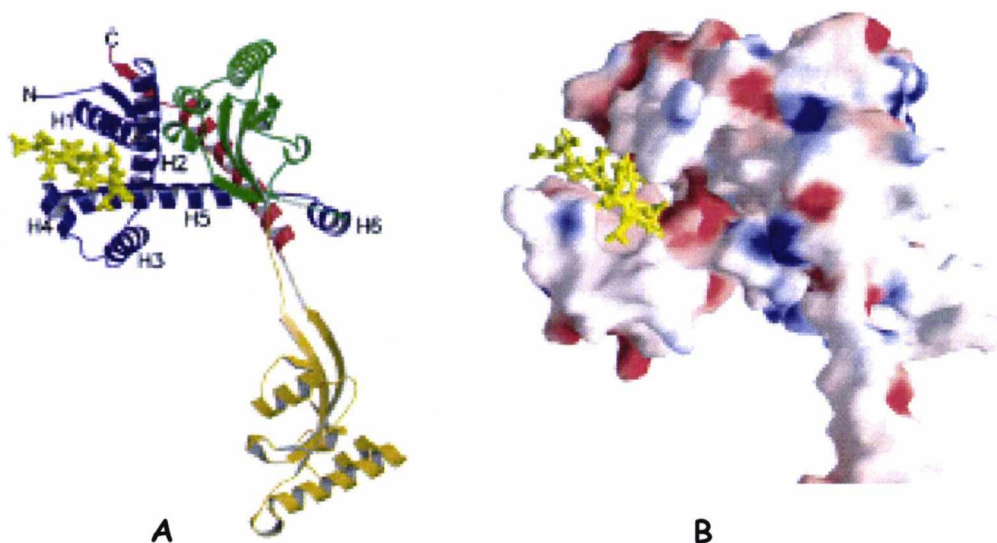


Figure 7.2.2 Peptide binding to SurA. (A) Ribbon drawing showing a small section of the peptide from a neighboring molecule within the final crystallographic structure of SurA binding to the core domain of SurA, red helix is the C-terminal region and the blue the N-terminal region. (B) Surface and electrostatic potential of the core domain of SurA shown in the same orientation as (A) with the same section of peptide in the possible binding cleft of SurA. Images from Bitto *et al* 2002.

The crystal packing for SurA contained four independent protomers, with two predominant sets of crystal packing interactions, those between the core modules and those between the satellite parvulin domains. The images in figure 7.2.2 show the binding of residues 153 – 164 that tether the core module of the SurA protein (shown) to its neighbour in the crystallographic structure. The 11 residues form an α -helix approximately 15Å in length and bind into the crevice formed by the N-domain, the helices of the N-terminal domain bind the peptide (Bitto and McKay, 2002). Helix 1 and helix 2 of the N-terminal domain are possibly structurally supported by the first parvulin domain (P1) and C-terminal domain. Helix 3 and helix 4 are not constrained by any structures and helix 5 runs under the theoretical binding cleft (Bitto and McKay, 2002). These observations support the findings from this study regarding the N-terminal fragment of SurA, confirming that the C-terminal region is not essential for binding.

7.3 BINDING EXPERIMENTS SHOW PREFERENCES OF PPIASES

In native polypeptides about 5 – 7 % of the peptidyl prolyl bonds are in the *cis* configuration and almost half of the 1453 non-redundant protein structures in the protein database contain at least one *cis* peptidyl prolyl bond (Reimer et al., 1998). The conversion of the *trans* peptidyl prolyl bond into the *cis* conformation, which is catalysed by peptidyl prolyl *cis-trans* isomerases, has been reported to be essential for the correct folding of many proteins, e.g. in prokaryotes the folding of outer membrane proteins (Dartigalongue and Raina, 1998; Lazar and Kolter, 1996) and periplasmic proteins as well as certain toxins (Ruddock et al., 1996).

In the periplasmic space of *E.coli* all three major classes of PPIases, ie. a cyclophilin, a FK506 binding protein, and two PPIases with sequence similarity to the catalytic domain of parvulin have been identified. This observation raises the question about the biological significance of the two parvulin-like PPIases SurA and PpiD in the same cellular compartment: Do they interact with different substrates or do they catalyse different reactions? The simultaneous deletion of both *ppiD* and *surA* genes has been reported to confer synthetic lethality and hence it has been suggested that both PPIases have an overlapping substrate specificity (Rizzitello et al., 2001). However, Justice *et al*, who showed that a double deletion of the *ppiD* and *surA* gene did not result in a loss in viability (Justice et al., 2005), questioned this observation. To investigate how both PPIases interact with their substrates and whether they have overlapping substrate specificities, a cross-linking approach was employed, which had been used previously to determine the interaction between peptides and other folding catalysts (Klappa et al., 1997; Klappa et al., 1998).

7.3.1 PPIID INTERACTS WITH MODEL PEPTIDES AND SCRAMBELD RNase A

It has recently been shown that model peptides and ‘scrambled’ RNase A interacted specifically with purified recombinant SurA from *E.coli* (Webb et al., 2001). Using a similar crosslinking approach it was demonstrated here that a recombinant fragment

of PpiD, lacking the leader sequence and the transmembrane segment, also interacted specifically with radiolabelled model peptides and ‘scrambled’ RNase A.

As with SurA it was found that the interaction between PpiD and model peptides was independent of the presence of a proline residue within the peptide. This result is in line with the results for other protein isomerases, like protein disulphide isomerase (PDI) (Klappa et al., 1997) and the PPIases trigger factor (Scholz et al., 1998) (Scholz et al., 1998) and FkpA (Bothmann and Pluckthun, 2000).

7.3.2 INTERACTION OF PPIASES WITH MODEL PEPTIDES

The substrate binding motif of SurA was recently identified and the enzyme was shown to bind to peptides with the motif Ar-X-Ar, where Ar is an aromatic residue (Bitto and McKay, 2003; Bitto and McKay, 2004; Hennecke et al., 2005). The crosslinking results confirmed these observations, however, from STD NMR data it can be concluded that the recognition motif for SurA is more extended and comprises more amino acids. It also appears that the structure of the peptide is also an important factor in the binding process, in addition to the amino acid sequence of the model peptide. For example, peptide S contained the required binding motif Ar-X-Ar, but was not found to interact with SurA. It is unlikely that the lack of the phenylalanine residue in position 11 (F11) is the sole reason for this result, since peptide A, which also lacks F11, shows efficient binding to SurA. Therefore it is proposed that the alanine and serine residues at the C-terminus of peptide S induce a structural change in peptide S, such that the Ar-X-Ar motif is no longer accessible. Interestingly, ‘scrambled’ RNase A does not contain an Ar-X-Ar motif, however the efficient interaction between this misfolded protein and SurA indicates that SurA might recognize hydrophobic patches in a tertiary structure, which put two or more aromatic amino acids in close proximity.

PpiD, like SurA, can interact with aromatic residues in the model peptide Δ -somatostatin. The recognition motif for the interaction with PpiD, however, does not appear to be restricted to aromatic residues, as demonstrated by the binding of peptide M, which does not contain aromatic residues. Therefore it is proposed that the recognition motif of PpiD is less specific than the one for SurA.

Peptide	SurA	PpiD
AGSKNFFWKTFTSS (Δ -som)	+++	+++
AGCKNFFWKTFTSC (SRIF)	+++	+++
AASKNFFWKTFTSS	+++	+++
AGAKNFFWKTFTSS	+++	++
AGSKAFFWKTFTSS	++	++
AGSKNAFWKTFTSS (F6A)	+	+++
AGSKNFAWKTFTSS (F7A)	+	+
AGSKNFFAKTFTSS (W8A)	-	+
AGSKNFFWKAFTSS	+++	+++
AGSKNYFWKTFTSS (F6Y)	+	+++
AGSKNYFAKTFTSS (F7Y)	-	+
AGSKNWFWKTFTSS	+++	+++
AGSKNFFWKTFT	+++	-
AGSKNFFWKT	+++	-
AGSKNYFWKSAS (peptide S)	-	-
AGSKNFFWKS (peptide A)	+++	-
AASKAFFWKS	+++	-
AGSKNFFWAT	+++	-
TKWFFNKSGA	+++	-
--SKNFFWKTFT	+++	-
--SKNFFWKT	-	-
----NFFWKT	-	-
INLKALAALAKKIL (peptide M)	-	+++
WEYIPNV	+	-
WEYIP	-	-
PTIKFFNGDTASPK (peptide P)	-	+++

Table 7.3.2.1 Competition between peptides and radiolabelled Δ -somatostatin for the binding to SurA and PpiD, respectively. *E. coli* cell lysates expressing recombinant SurA and PpiD, respectively, were incubated with 10 μ M radiolabelled Δ -somatostatin in the presence of a tenfold excess of the indicated unlabelled peptides prior to crosslinking. Samples were subsequently incubated with DSG (final concentration 0.5 mM) for 60 min at 0°C. After cross-linking the samples were analyzed on 10 % polyacrylamide gels with subsequent autoradiography. Quantification was performed with a BioRad PhosphoImager. A sample without competing peptides served as a control. Competition was expressed as reduction in the intensity of the respective crosslinking product relative to the control without unlabelled peptides. +++, strong competition (intensity of crosslinking product < 10 % of control); ++, moderate competition (intensity of crosslinking product between 10 % - 30 % of control); +, weak competition (intensity of crosslinking product between 50 % - 80 % of control); -, no competition (intensity of crosslinking product > 80 % of control).

To investigate in more detail the nature of the interactions between model peptides and the PPIases SurA and PpiD competition experiments with unlabelled peptides were used. Replacement of phenylalanine 6 (F6) with alanine in Δ -somatostatin strongly reduced the interaction with SurA, but did not affect the interaction with PpiD. This result is in excellent agreement with the STD NMR data: F6 is an

important residue for the interaction with SurA, but less important for the interaction with PpiD. From the STD NMR experiment it was further concluded that the para-position in F6 is important for the interaction with SurA, figure 4.10.1. Modifications of this position therefore should reduce binding. Indeed, replacing F6 with tyrosine strongly reduced the interaction with SurA. STD NMR results also showed that there are significant interactions between phenylalanine in position 7 and both PPIases, which was confirmed in the competition experiments. Another important residue for the interaction of Δ -somatostatin with SurA and PpiD, respectively, is the tryptophan residue in position 8, as shown by competition and STD NMR analysis, figures 4.10.1 and 6.8.1.

The involvement of aromatic residues in the binding of peptides to SurA/PpiD raises the question about the nature of the interaction. Van-der-Waals forces between the aromatic residues and mainly hydrophobic residues in the binding sites of SurA might play an important role in the binding process. One can also speculate that other forces contribute to the specific binding of peptides and misfolded proteins. For example π - π interactions between aromatic residues in the binding site and the peptide would confer specificity for aromatic residues with a certain degree of flexibility in the binding motif. Indeed, Hunter *et al* reported that such π - π interactions between two phenylalanine residues could contribute significantly to the binding of ligands to proteins (Hunter *et al.*, 1991). A similar effect could result from cation- π interactions in which a positively charged amino acid in the binding site, like a lysine or arginine residue, interacts with an aromatic residue in the binding motif (Gromiha and Suwa, 2005; Petersen *et al.*, 2005).

7.3.3 BIOLOGICAL SIGNIFICANCE

In the experiments the findings by Bitto *et al* that Ar-X-Ar binding motif is essential for the interaction between SurA and model peptides (Bitto and McKay, 2003; Bitto and McKay, 2004; Gromiha and Suwa, 2005; Petersen *et al.*, 2005) were confirmed. It was speculated that this is the signature motif for specific outer membrane proteins, which have been proposed to be the predominant substrates of SurA (Behrens, 2002; Hennecke *et al.*, 2005). The results show that even short peptides (<11 amino acids)

interacted with SurA, as long as they contained this signature motif and probably exhibited some other structural requirements (Behrens, 2002). The interaction with PpiD, however, required a longer peptide chain, with at least 13 amino acids. This difference might reflect the different biological functions of the two PPIases. Therefore it is proposed that the main biological function of SurA is to facilitate the folding of predominantly OMPs, which do contain a simple signature motif for the interaction with SurA. Although the precise mechanisms of the targeting of OMPs to the outer membrane has not yet been established in all its details (for review see (Danese and Silhavy, 1998)), it is likely that translocation of most OMPs from the inner to the outer membrane is *via* the periplasmic space, thus allowing soluble SurA to efficiently interact with incorrectly folded substrates. PpiD, however, is anchored to the inner membrane with the catalytically active site facing the lumen of the periplasmic space. This particular localization makes it likely that PpiD is predominantly involved in the folding of inner membrane-associated proteins rather than soluble proteins. PpiD therefore might interact with a variety of slow-folding proteins, for which a simple and specific recognition motif does not exist. Hence it is not surprising that PpiD appears to have broader substrate specificity than SurA: while PpiD acts as a rather general folding catalyst recognizing various binding motifs, SurA requires only a short and characteristic recognition motif specific for OMPs.

7.4 STD-NMR HIGHLIGHTS ANOTHER SIGNIFICANT RESIDUE FOR SURA BINDING

STD-NMR analysis of full length SurA with Δ -somatostatin confirmed that more residues in the Δ -somatostatin peptide are involved in the binding than just the –FFW– motif. The presence of the aromatic residue at position eleven in the peptides used in this study appears to enable the peptides to bind if part of the Ar – X – Ar motif is not present within the peptide sequence. This is shown with the peptides in table 7.4.1.

Peptide	SurA	PpiD
AGSKNYFAKTFTSS (F7Y)	-	+
AGSKNAFWKTFTSS (F6A)	+	+++

Table 7.4.1 Peptides without the F – X – Ar motif that bind to SurA. The two peptides also contain an aromatic residue at position eleventh.

SurA and PDI are both folding catalysts that have a substrate binding site distinct from the catalytically active site. Neither of them requires the target amino acid to be present for binding (cysteine in the case of PDI, proline for SurA). Interactions are mainly hydrophobic in nature. The chaperone function of SurA might reflect its mechanism: - If SurA (and PDI) catalyse isomerisation in late folding steps one would expect some kind of 'unfolding' of the substrate so that efficient access to the target site is given. This however would expose hydrophobic residues with the danger of aggregation. Both proteins therefore might have an intrinsic chaperone activity to prevent substrate aggregation while unfolded.

The presence of aromatic residues is considered to be of far more importance in the binding of peptides than proline residues as there is a high frequency of aromatic residues in OMPs, LamB, OmpF and OmpA have 12.3% aromatic residues and only 2.86% proline residues in their sequences and integral OMPs can be characterised by their high content of aromatic residues. OMPs have been shown to have a high content of Ar – X – Ar motifs (Bitto and McKay, 2003). And hence the specificity of SurA for aromatic residues is not surprising. It has also been suggested that SurA has a preference for peptides that have a predicted secondary β -strand structure which is often found in OMPs (Hennecke et al., 2005). However analysis in this study has shown that a peptide with a proposed helical structure is also able to bind to SurA and therefore the preference for SurA to bind to proteins with β -strand structure is not the sole reason for binding. It therefore is more likely that SurA recognises the patterns of residues and their orientation.

A recent study has shown that the importance of the PPIases was possibly misunderstood. New evidence suggests that SurA is actually involved in the biogenesis of pili (Justice et al., 2005). Although a quadruple knockout mutant for FkpA, PpiD, PpiA and SurA was viable, the cells were more susceptible to some antibiotics. This observation suggests that the PPIases are involved in the formation

of outer membrane porins, even though the levels of LamB were not reduced. In fact the study showed that SurA alone was important for the maturation of the OMPs LamB and OmpA as well as the pilus biogenesis (Justice et al., 2005).

7.5 MOLECULAR MODELING OF FULL LENGTH SURA HIGHLIGHTS IMPORTANT AMINO ACIDS WITHIN THE SURA STRUCTURE

Following the designation of the binding motif for SurA, further investigation was made into the binding region of SurA. Molecular modeling of the full length SurA predicted changes to the structure when single amino acid mutations were introduced into the four main domains within the protein. The virtual mutations were compared to mutations of SurA by testing the mutant proteins ability to bind to the model peptide Δ -somatostatin. Mutations on the satellite domain (the second parvulin domain) did not have a significant effect to the overall structure of SurA. The most significant effects were seen in the region that has been assigned the binding domain. The higher the RMSD value the less likely it was for SurA to bind to the peptide. This could be due to the distortion to the overall protein structure. Therefore the individual changes could indicate the residues that are significant for the binding of peptides. More than one mutant had a high RMSD value, suggesting that more than one residue is significant. It has been suggested that SurA might interact with multiple peptides at multiple binding sites (Hennecke et al., 2005), but this would appear unlikely as the mutations that had the most significant effect on the protein binding were located in a small region of the binding domain between positions 73 and 99.

7.6 PPiD

The periplasmic PPIase *ppiD* has been reported to be a multicopy suppressor of *surA* (Dartigalongue and Raina, 1998) but a recent study has shown that *ppiD surA* double mutant is viable (Justice et al., 2005).

Up until now the peptide binding/substrate binding has not been described for PpiD. In this study fragments were generated of PpiD. PpiD2 showed binding ability while PpiD3 did not, which suggests that the binding region is between the 360th amino acid and the 478th amino acid. The binding region of PpiD is not found in the single parvulin domain but in the C-terminal domain.

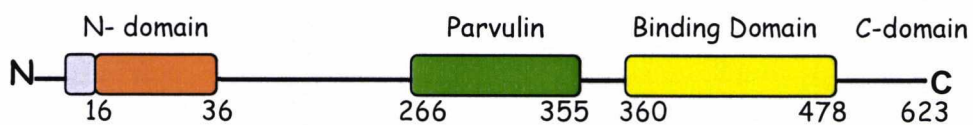


Figure 7.6.1 Domains of PpiD. The grey area indicates the signal sequence, followed by the orange region which represents the transmembrane domain. The green area is the parvulin like domain and the yellow the possible binding region.

Binding studies were used to investigate the possible binding motif for PpiD. SurA has been shown to have a preference for peptides with high aromatic content and the motif Ar – X – Ar. As it has been suggested that PpiD could have overlapping specificity with SurA (Dartigalongue and Raina, 1998), and this study has shown that PpiD does bind to the same motif that SurA recognises. However it appears that PpiD does discriminate according to the size of the peptides as it does not bind to the peptides smaller than 10 amino acids in length.

STD-NMR binding of PpiD and Δ -somatostatin also showed less specific contacts than SurA. The contacts were spread further over the peptide, but with less contact than was seen with SurA. PpiD STD-NMR highlights more residues on the side Δ -somatostatin away from the orientation of the aromatic residues which could suggest that either the peptide binding cleft is physically deeper than the SurA binding cleft, i.e. there are more contacts to the overall peptide or there could be a mechanism that holds the peptide in the binding site, which was originally suggested for the SurA protein and the purpose of the satellite domain (Behrens, 2002).

7.7 THE FUTURE

Although many of the periplasmic *E.coli* PPIases have been identified and studied in some detail there are still fundamental issues to be resolved. These include further analysis into the binding specificities for the different periplasmic PPIases. As it has been shown in this study much emphasis has been placed upon SurA but there has been very little into the other periplasmic PPIases of *E.coli*. By further studying the binding motifs of the different PPIases it may be possible to show over-lapping specificities of the proteins and as there seems to be some disagreement in the data presented on the importance of some of the PPIases. By studying the binding motifs it may be possible to show other interactions of the PPIases, although the quadruple knock-out for PpiA, PpiD, SurA and FkpA was still viable (Justice et al., 2005).

A possible way of extending the future interest of the PPIases is to look more closely at the integral OMPs that they assist with folding.

The data from this study has the potential to be used in the development of inhibitory drugs. For this to be possible the binding of the peptides to SurA needs to be characterised in more detail. This could be achieved by using NMR visualisation of the binding site interacting with a binding peptide. With high through-put screening of many small compounds it could be possible to develop a small molecular weight inhibitor of SurA. SurA is potentially a good target for molecular weight inhibitors because it is located in the periplasm. Being located in the periplasm is an advantage as there is no need to target the drug into the cell where it is more likely to be expelled and resistance formed. As SurA is only found in gram-negative bacteria and not in mammalian cells the inhibition of a fundamental function namely, protein folding, theoretically would be hard to modify and therefore resistance to the inhibitor would be difficult to achieve.

References

REFERENCES

- Andreeva, L., Motterlini, R. and Green, C.J. (1997) Cyclophilins are induced by hypoxia and heat stress in myogenic cells. *Biochem Biophys Res Commun*, **237**, 6-9.
- Anfinsen, C.B., Haber, E., Sela, M. and White, F.H., Jr. (1961) The kinetics of formation of native ribonuclease during oxidation of the reduced polypeptide chain. *Proc Natl Acad Sci U S A*, **47**, 1309-1314.
- Anfinsen, C.B., Redfield, R.R., Choate, W.L., Page, J. and Carroll, W.R. (1954) Studies on the gross structure, cross-linkages, and terminal sequences in ribonuclease. *J Biol Chem*, **207**, 201-210.
- Aono, R., Negishi, T. and Nakajima, H. (1994) Cloning of organic solvent tolerance gene *ostA* that determines n-hexane tolerance level in *Escherichia coli*. *Appl Environ Microbiol*, **60**, 4624-4626.
- Aridor, M. and Balch, W.E. (1999) Integration of endoplasmic reticulum signaling in health and disease. *Nat Med*, **5**, 745-751.
- Arie, J.P., Sassoon, N. and Betton, J.M. (2001) Chaperone function of FkpA, a heat shock prolyl isomerase, in the periplasm of *Escherichia coli*. *Mol Microbiol*, **39**, 199-210.
- Bachinger, H.P. (1987) The influence of peptidyl-prolyl cis-trans isomerase on the in vitro folding of type III collagen. *J Biol Chem*, **262**, 17144-17148.
- Behrens, S. (2002) Periplasmic chaperones--new structural and functional insights. *Structure (Camb)*, **10**, 1469-1471.
- Behrens, S. (2003) Periplasmic chaperones--preservers of subunit folding energy for organelle assembly. *Cell*, **113**, 556-557.
- Behrens, S., Maier, R., de Cock, H., Schmid, F.X. and Gross, C.A. (2001) The SurA periplasmic PPIase lacking its parvulin domains functions in vivo and has chaperone activity. *Embo J*, **20**, 285-294.
- Bernstein, H.D. (2000) The biogenesis and assembly of bacterial membrane proteins. *Curr Opin Microbiol*, **3**, 203-209.
- Bhutani, N. and Udgaonkar, J.B. (2001) GroEL channels the folding of thioredoxin along one kinetic route. *J Mol Biol*, **314**, 1167-1179.
- Bioinformatics, S.I.o. Swiss Prot Protein Knowledge Data Base TrEMBL.
- Bischofberger, P., Han, W., Feifel, B., Schonfeld, H.J. and Christen, P. (2003) D-Peptides as inhibitors of the DnaK/DnaJ/GrpE chaperone system. *J Biol Chem*, **278**, 19044-19047.

- Bitto, E. and McKay, D.B. (2002) Crystallographic structure of SurA, a molecular chaperone that facilitates folding of outer membrane porins. *Structure (Camb)*, **10**, 1489-1498.
- Bitto, E. and McKay, D.B. (2003) The periplasmic molecular chaperone protein SurA binds a peptide motif that is characteristic of integral outer membrane proteins. *J Biol Chem*, **278**, 49316-49322.
- Bitto, E. and McKay, D.B. (2004) Binding of phage-display-selected peptides to the periplasmic chaperone protein SurA mimics binding of unfolded outer membrane proteins. *FEBS Lett*, **568**, 94-98.
- Blaaha, G., Wilson, D.N., Stoller, G., Fischer, G., Willumeit, R. and Nierhaus, K.H. (2003) Localization of the trigger factor binding site on the ribosomal 50S subunit. *J Mol Biol*, **326**, 887-897.
- Bolton, A.E. and Hunter, W.M. (1973) The labelling of proteins to high specific radioactivities by conjugation to a ¹²⁵I-containing acylating agent. *Biochem J*, **133**, 529-539.
- Bothmann, H. and Pluckthun, A. (1998) Selection for a periplasmic factor improving phage display and functional periplasmic expression. *Nat Biotechnol*, **16**, 376-380.
- Bothmann, H. and Pluckthun, A. (2000) The periplasmic Escherichia coli peptidylprolyl cis,trans-isomerase FkpA. I. Increased functional expression of antibody fragments with and without cis-prolines. *J Biol Chem*, **275**, 17100-17105.
- Brandts, J.F., Halvorson, H.R. and Brennan, M. (1975) Consideration of the Possibility that the slow step in protein denaturation reactions is due to cis-trans isomerism of proline residues. *Biochemistry*, **14**, 4953-4963.
- Braun, V. and Sieglin, U. (1970) The covalent murein-lipoprotein structure of the Escherichia coli cell wall. The attachment site of the lipoprotein on the murein. *Eur J Biochem*, **13**, 336-346.
- Brehmer, D., Gassler, C., Rist, W., Mayer, M.P. and Bukau, B. (2004) Influence of GrpE on DnaK-substrate interactions. *J Biol Chem*, **279**, 27957-27964.
- Brodsky, J.L. (1998) Translocation of proteins across the endoplasmic reticulum membrane. *Int Rev Cytol*, **178**, 277-328.
- Brunger, A.T., Adams, P.D., Clore, G.M., DeLano, W.L., Gros, P., Grosse-Kunstleve, R.W., Jiang, J.S., Kuszewski, J., Nilges, M., Pannu, N.S., Read, R.J., Rice, L.M., Simonson, T. and Warren, G.L. (1998) Crystallography & NMR system: A new software suite for macromolecular structure determination. *Acta Crystallogr D Biol Crystallogr*, **54 (Pt 5)**, 905-921.

- Bukrinsky, M.I. (2002) Cyclophilins: unexpected messengers in intercellular communications. *Trends Immunol*, **23**, 323-325.
- Bulieris, P.V., Behrens, S., Holst, O. and Kleinschmidt, J.H. (2003) Folding and insertion of the outer membrane protein OmpA is assisted by the chaperone Skp and by lipopolysaccharide. *J Biol Chem*, **278**, 9092-9099.
- Burchall, J.J. and Hitchings, G.H. (1965) Inhibitor binding analysis of dihydrofolate reductases from various species. *Mol Pharmacol*, **1**, 126-136.
- Callebaut, I. and Mornon, J.P. (1995) Trigger factor, one of the Escherichia coli chaperone proteins, is an original member of the FKBP family. *FEBS Lett*, **374**, 211-215.
- Carlsson, J., Drevin, H. and Axen, R. (1978) Protein thiolation and reversible protein-protein conjugation. N-Succinimidyl 3-(2-pyridyldithio)propionate, a new heterobifunctional reagent. *Biochem J*, **173**, 723-737.
- Carrio, M.M. and Villaverde, A. (2003) Role of molecular chaperones in inclusion body formation. *FEBS Lett*, **537**, 215-221.
- CastilloKeller, M. and Misra, R. (2003) Protease-deficient DegP suppresses lethal effects of a mutant OmpC protein by its capture. *J Bacteriol*, **185**, 148-154.
- Chen, J., Song, J.L., Zhang, S., Wang, Y., Cui, D.F. and Wang, C.C. (1999) Chaperone activity of DsbC. *J Biol Chem*, **274**, 19601-19605.
- Chen, R. and Henning, U. (1996) A periplasmic protein (Skp) of Escherichia coli selectively binds a class of outer membrane proteins. *Mol Microbiol*, **19**, 1287-1294.
- Collet, J.F., Riemer, J., Bader, M.W. and Bardwell, J.C. (2002) Reconstitution of a disulfide isomerization system. *J Biol Chem*, **277**, 26886-26892.
- Collier, D.N., Bankaitis, V.A., Weiss, J.B. and Bassford, P.J., Jr. (1988) The antifolding activity of SecB promotes the export of the E. coli maltose-binding protein. *Cell*, **53**, 273-283.
- Cox, J.S., Chapman, R.E. and Walter, P. (1997) The unfolded protein response coordinates the production of endoplasmic reticulum protein and endoplasmic reticulum membrane. *Mol Biol Cell*, **8**, 1805-1814.
- Cox, J.S., Shamu, C.E. and Walter, P. (1993) Transcriptional induction of genes encoding endoplasmic reticulum resident proteins requires a transmembrane protein kinase. *Cell*, **73**, 1197-1206.
- Crooke, E. and Wickner, W. (1987) Trigger factor: a soluble protein that folds pro-OmpA into a membrane-assembly-competent form. *Proc Natl Acad Sci U S A*, **84**, 5216-5220.

- Danese, P.N. and Silhavy, T.J. (1998) Targeting and assembly of periplasmic and outer-membrane proteins in *Escherichia coli*. *Annu Rev Genet*, **32**, 59-94.
- Danese, P.N., Snyder, W.B., Cosma, C.L., Davis, L.J. and Silhavy, T.J. (1995) The Cpx two-component signal transduction pathway of *Escherichia coli* regulates transcription of the gene specifying the stress-inducible periplasmic protease, DegP. *Genes Dev*, **9**, 387-398.
- Dartigalongue, C., Missiakas, D. and Raina, S. (2001) Characterization of the *Escherichia coli* sigma E regulon. *J Biol Chem*, **276**, 20866-20875.
- Dartigalongue, C., Nikaido, H. and Raina, S. (2000) Protein folding in the periplasm in the absence of primary oxidant DsbA: modulation of redox potential in periplasmic space via OmpL porin. *Embo J*, **19**, 5980-5988.
- Dartigalongue, C., Nikaido, H. and Raina, S. (2004) Protein folding in the periplasm in the absence of primary oxidant DsbA: modulation of redox potential in periplasmic space via OmpL porin. *Embo J*, **23**, 3907.
- Dartigalongue, C. and Raina, S. (1998) A new heat-shock gene, *ppiD*, encodes a peptidyl-prolyl isomerase required for folding of outer membrane proteins in *Escherichia coli*. *Embo J*, **17**, 3968-3980.
- Davies, T.H. and Sanchez, E.R. (2005) Fkbp52. *Int J Biochem Cell Biol*, **37**, 42-47.
- Davis, D.L., Murthy, J.N. and Soldin, S.J. (2000) Biochemical characterization of the minor immunophilins. *Clin Biochem*, **33**, 81-87.
- De Cock, H., Schafer, U., Potgeter, M., Demel, R., Muller, M. and Tommassen, J. (1999) Affinity of the periplasmic chaperone Skp of *Escherichia coli* for phospholipids, lipopolysaccharides and non-native outer membrane proteins. Role of Skp in the biogenesis of outer membrane protein. *Eur J Biochem*, **259**, 96-103.
- Deuerling, E. and Bukau, B. (2004) Chaperone-assisted folding of newly synthesized proteins in the cytosol. *Crit Rev Biochem Mol Biol*, **39**, 261-277.
- Deuerling, E., Patzelt, H., Vorderwulbecke, S., Rauch, T., Kramer, G., Schaffitzel, E., Mogk, A., Schulze-Specking, A., Langen, H. and Bukau, B. (2003) Trigger Factor and DnaK possess overlapping substrate pools and binding specificities. *Mol Microbiol*, **47**, 1317-1328.
- Deuerling, E., Schulze-Specking, A., Tomoyasu, T., Mogk, A. and Bukau, B. (1999) Trigger factor and DnaK cooperate in folding of newly synthesized proteins. *Nature*, **400**, 693-696.
- Dolinski, K., Muir, S., Cardenas, M. and Heitman, J. (1997) All cyclophilins and FK506 binding proteins are, individually and collectively, dispensable for viability in *Saccharomyces cerevisiae*. *Proc Natl Acad Sci U S A*, **94**, 13093-13098.

- Doyle, V., Virji, S. and Crompton, M. (1999) Evidence that cyclophilin-A protects cells against oxidative stress. *Biochem J*, **341** (Pt 1), 127-132.
- Driessen, A.J. (2001) SecB, a molecular chaperone with two faces. *Trends Microbiol*, **9**, 193-196.
- Drouault, S., Anba, J., Bonneau, S., Bolotin, A., Ehrlich, S.D. and Renault, P. (2002) The peptidyl-prolyl isomerase motif is lacking in PmpA, the PrsA-like protein involved in the secretion machinery of *Lactococcus lactis*. *Appl Environ Microbiol*, **68**, 3932-3942.
- Duguay, A.R. and Silhavy, T.J. (2002) Signal sequence mutations as tools for the characterization of LamB folding intermediates. *J Bacteriol*, **184**, 6918-6928.
- Dwivedi, R.S., Breiman, A. and Herman, E.M. (2003) Differential distribution of the cognate and heat-stress-induced isoforms of high Mr cis-trans prolyl peptidyl isomerase (FKBP) in the cytoplasm and nucleoplasm. *J Exp Bot*, **54**, 2679-2689.
- Eisenstark, A., Miller, C., Jones, J. and Leven, S. (1992) *Escherichia coli* genes involved in cell survival during dormancy: role of oxidative stress. *Biochem Biophys Res Commun*, **188**, 1054-1059.
- Ellis, R.J. (2001) Macromolecular crowding: an important but neglected aspect of the intracellular environment. *Curr Opin Struct Biol*, **11**, 114-119.
- Emr, S.D. and Silhavy, T.J. (1982) The signal hypothesis in bacteria. *Prog Clin Biol Res*, **91**, 3-14.
- Evans, P.A., Dobson, C.M., Kautz, R.A., Hatfull, G. and Fox, R.O. (1987) Proline isomerism in staphylococcal nuclease characterized by NMR and site-directed mutagenesis. *Nature*, **329**, 266-268.
- Faou, P. and Tropschug, M. (2003) A novel binding protein for a member of CyP40-type Cyclophilins: *N.crassa* CyPBP37, a growth and thiamine regulated protein homolog to yeast Thi4p. *J Mol Biol*, **333**, 831-844.
- Feifel, B., Schonfeld, H.J. and Christen, P. (1998) D-peptide ligands for the co-chaperone DnaJ. *J Biol Chem*, **273**, 11999-12002.
- Fekkes, P. and Driessen, A.J. (1999) Protein targeting to the bacterial cytoplasmic membrane. *Microbiol Mol Biol Rev*, **63**, 161-173.
- Feldman, D.E. and Frydman, J. (2000) Protein folding in vivo: the importance of molecular chaperones. *Curr Opin Struct Biol*, **10**, 26-33.
- Fink, A.L. (1999) Chaperone-mediated protein folding. *Physiol Rev*, **79**, 425-449.

- Fischer, G., Bang, H. and Mech, C. (1984) [Determination of enzymatic catalysis for the cis-trans-isomerization of peptide binding in proline-containing peptides]. *Biomed Biochim Acta*, **43**, 1101-1111.
- Fischer, G., Tradler, T. and Zarnt, T. (1998) The mode of action of peptidyl prolyl cis/trans isomerases in vivo: binding vs. catalysis. *FEBS Lett*, **426**, 17-20.
- Fischer, G., Wittmann-Liebold, B., Lang, K., Kiefhaber, T. and Schmid, F.X. (1989) Cyclophilin and peptidyl-prolyl cis-trans isomerase are probably identical proteins. *Nature*, **337**, 476-478.
- Frand, A.R., Cuozzo, J.W. and Kaiser, C.A. (2000) Pathways for protein disulphide bond formation. *Trends Cell Biol*, **10**, 203-210.
- Freedman, R.B., Klappa, P. and Ruddock, L.W. (2002a) Model peptide substrates and ligands in analysis of action of mammalian protein disulfide-isomerase. *Methods Enzymol*, **348**, 342-354.
- Freedman, R.B., Klappa, P. and Ruddock, L.W. (2002b) Protein disulfide isomerases exploit synergy between catalytic and specific binding domains. *EMBO Rep*, **3**, 136-140.
- Fujimori, F., Gunji, W., Kikuchi, J., Mogi, T., Ohashi, Y., Makino, T., Oyama, A., Okuhara, K., Uchida, T. and Murakami, Y. (2001) Crosstalk of prolyl isomerases, Pin1/Ess1, and cyclophilin A. *Biochem Biophys Res Commun*, **289**, 181-190.
- G Finch, D.G., S. Ragnar Norrby, Richard J Whitley. (2003) *Anti-Infective Agents and Their Use in Therapy*. Churchill Livingstone.
- Galat, A. (1993) Peptidylproline cis-trans-isomerases: immunophilins. *Eur J Biochem*, **216**, 689-707.
- Galat, A. (2003) Peptidylprolyl cis/trans isomerases (immunophilins): biological diversity--targets--functions. *Curr Top Med Chem*, **3**, 1315-1347.
- Galat, A. and Riviere, S. (1998) *Peptidyl-Prolyl Cis/Trans Isomerases*. Oxford University Press.
- Gannon, P.M., Li, P. and Kumamoto, C.A. (1989) The mature portion of Escherichia coli maltose-binding protein (MBP) determines the dependence of MBP on SecB for export. *J Bacteriol*, **171**, 813-818.
- Gasch, A.P., Spellman, P.T., Kao, C.M., Carmel-Harel, O., Eisen, M.B., Storz, G., Botstein, D. and Brown, P.O. (2000) Genomic expression programs in the response of yeast cells to environmental changes. *Mol Biol Cell*, **11**, 4241-4257.
- Gething, M.J. (1997) *Guidebook to Molecular Chaperones and Protein-Folding Catalysts*. Sambrook and Tooze.

- Gething, M.J. and Sambrook, J. (1992) Protein folding in the cell. *Nature*, **355**, 33-45.
- Geyer, R., Galanos, C., Westphal, O. and Golecki, J.R. (1979) A lipopolysaccharide-binding cell-surface protein from *Salmonella minnesota*. Isolation, partial characterization and occurrence in different Enterobacteriaceae. *Eur J Biochem*, **98**, 27-38.
- Gilbert, H.F. (1997) Protein disulfide isomerase and assisted protein folding. *J Biol Chem*, **272**, 29399-29402.
- Green, N.S., Reisler, E. and Houk, K.N. (2001) Quantitative evaluation of the lengths of homobifunctional protein cross-linking reagents used as molecular rulers. *Protein Sci*, **10**, 1293-1304.
- Gromiha, M.M. and Suwa, M. (2005) Structural analysis of residues involving cation- π interactions in different folding types of membrane proteins. *Int J Biol Macromol*, **35**, 55-62.
- Guignard, L., Ozawa, K., Pursglove, S.E., Otting, G. and Dixon, N.E. (2002) NMR analysis of in vitro-synthesized proteins without purification: a high-throughput approach. *FEBS Lett*, **524**, 159-162.
- Guthrie, B. and Wickner, W. (1990) Trigger factor depletion or overproduction causes defective cell division but does not block protein export. *J Bacteriol*, **172**, 5555-5562.
- Haandrikman, A.J., Kok, J., Laan, H., Soemitro, S., Ledebroer, A.M., Konings, W.N. and Venema, G. (1989) Identification of a gene required for maturation of an extracellular lactococcal serine proteinase. *J Bacteriol*, **171**, 2789-2794.
- Haber, E. and Anfinsen, C.B. (1962) Side-chain interactions governing the pairing of half-cystine residues in ribonuclease. *J Biol Chem*, **237**, 1839-1844.
- Handschumacher, R.E., Harding, M.W., Rice, J., Drugge, R.J. and Speicher, D.W. (1984) Cyclophilin: a specific cytosolic binding protein for cyclosporin A. *Science*, **226**, 544-547.
- Hani, J., Schelbert, B., Bernhardt, A., Domdey, H., Fischer, G., Wiebauer, K. and Rahfeld, J.U. (1999) Mutations in a peptidylprolyl-cis/trans-isomerase gene lead to a defect in 3'-end formation of a pre-mRNA in *Saccharomyces cerevisiae*. *J Biol Chem*, **274**, 108-116.
- Hani, J., Stumpf, G. and Domdey, H. (1995) PTF1 encodes an essential protein in *Saccharomyces cerevisiae*, which shows strong homology with a new putative family of PPIases. *FEBS Lett*, **365**, 198-202.
- Harding, M.W., Galat, A., Uehling, D.E. and Schreiber, S.L. (1989) A receptor for the immunosuppressant FK506 is a cis-trans peptidyl-prolyl isomerase. *Nature*, **341**, 758-760.

- Harding, M.W., Handschumacher, R.E. and Speicher, D.W. (1986) Isolation and amino acid sequence of cyclophilin. *J Biol Chem*, **261**, 8547-8555.
- Harms, N., Koningstein, G., Dontje, W., Muller, M., Oudega, B., Luirink, J. and de Cock, H. (2001) The early interaction of the outer membrane protein phoE with the periplasmic chaperone Skp occurs at the cytoplasmic membrane. *J Biol Chem*, **276**, 18804-18811.
- Hayano, T., Takahashi, N., Kato, S., Maki, N. and Suzuki, M. (1991) Two distinct forms of peptidylprolyl-cis-trans-isomerase are expressed separately in periplasmic and cytoplasmic compartments of Escherichia coli cells. *Biochemistry*, **30**, 3041-3048.
- Hemmingsen, S.M., Woolford, C., van der Vies, S.M., Tilly, K., Dennis, D.T., Georgopoulos, C.P., Hendrix, R.W. and Ellis, R.J. (1988) Homologous plant and bacterial proteins chaperone oligomeric protein assembly. *Nature*, **333**, 330-334.
- Hennecke, G., Nolte, J., Volkmer-Engert, R., Schneider-Mergener, J. and Behrens, S. (2005) The periplasmic chaperone SurA exploits two features characteristic of integral outer membrane proteins for selective substrate recognition. *J Biol Chem*, **280**, 23540-23548.
- Hennig, L., Christner, C., Kipping, M., Schelbert, B., Rucknagel, K.P., Grabley, S., Kullertz, G. and Fischer, G. (1998) Selective inactivation of parvulin-like peptidyl-prolyl cis/trans isomerases by juglone. *Biochemistry*, **37**, 5953-5960.
- Herning, T., Yutani, K., Taniyama, Y. and Kikuchi, M. (1991) Effects of proline mutations on the unfolding and refolding of human lysozyme: the slow refolding kinetic phase does not result from proline cis-trans isomerization. *Biochemistry*, **30**, 9882-9891.
- Hesterkamp, T. and Bukau, B. (1996) The Escherichia coli trigger factor. *FEBS Lett*, **389**, 32-34.
- Hoffman, M. and Chiang, H.L. (1996) Isolation of degradation-deficient mutants defective in the targeting of fructose-1,6-bisphosphatase into the vacuole for degradation in Saccharomyces cerevisiae. *Genetics*, **143**, 1555-1566.
- Holck, A. and Kleppe, K. (1988) Cloning and sequencing of the gene for the DNA-binding 17K protein of Escherichia coli. *Gene*, **67**, 117-124.
- Horibe, T., Yoshio, C., Okada, S., Tsukamoto, M., Nagai, H., Hagiwara, Y., Tujimoto, Y. and Kikuchi, M. (2002) The chaperone activity of protein disulfide isomerase is affected by cyclophilin B and cyclosporin A in vitro. *J Biochem (Tokyo)*, **132**, 401-407.
- Horne, S.M., Kottom, T.J., Nolan, L.K. and Young, K.D. (1997) Decreased intracellular survival of an fkpA mutant of Salmonella typhimurium Copenhagen. *Infect Immun*, **65**, 806-810.

- Horowitz, D.S., Lee, E.J., Mabon, S.A. and Misteli, T. (2002) A cyclophilin functions in pre-mRNA splicing. *Embo J*, **21**, 470-480.
- Huang, G.C., Chen, J.J., Liu, C.P. and Zhou, J.M. (2002) Chaperone and antichaperone activities of trigger factor. *Eur J Biochem*, **269**, 4516-4523
- Humphreys, S., Rowley, G., Stevenson, A., Kenyon, W.J., Spector, M.P. and Roberts, M. (2003) Role of periplasmic peptidylprolyl isomerases in Salmonella enterica serovar Typhimurium virulence. *Infect Immun*, **71**, 5386-5388.
- Humphreys, S., Stevenson, A., Bacon, A., Weinhardt, A.B. and Roberts, M. (1999) The alternative sigma factor, sigmaE, is critically important for the virulence of Salmonella typhimurium. *Infect Immun*, **67**, 1560-1568.
- Hunter, C.A., Singh, J. and Thornton, J.M. (1991) Pi-pi interactions: the geometry and energetics of phenylalanine-phenylalanine interactions in proteins. *J Mol Biol*, **218**, 837-846.
- Ideno, A. and Maruyama, T. (2002) Expression of long- and short-type FK506 binding proteins in hyperthermophilic archaea. *Gene*, **292**, 57-63.
- Jacobs, M., Andersen, J.B., Kontinen, V. and Sarvas, M. (1993) Bacillus subtilis PrsA is required in vivo as an extracytoplasmic chaperone for secretion of active enzymes synthesized either with or without pro-sequences. *Mol Microbiol*, **8**, 957-966.
- Justice, S.S., Hunstad, D.A., Harper, J.R., Duguay, A.R., Pinkner, J.S., Bann, J., Frieden, C., Silhavy, T.J. and Hultgren, S.J. (2005) Periplasmic peptidyl prolyl cis-trans isomerases are not essential for viability, but SurA is required for pilus biogenesis in Escherichia coli. *J Bacteriol*, **187**, 7680-7686.
- Kelley, R.F. and Richards, F.M. (1987) Replacement of proline-76 with alanine eliminates the slowest kinetic phase in thioredoxin folding. *Biochemistry*, **26**, 6765-6774.
- Kiefhaber, T., Quaas, R., Hahn, U. and Schmid, F.X. (1990) Folding of ribonuclease T1. 1. Existence of multiple unfolded states created by proline isomerization. *Biochemistry*, **29**, 3053-3061.
- Klappa, P., Freedman, R.B., Langenbuch, M., Lan, M.S., Robinson, G.K. and Ruddock, L.W. (2001) The pancreas-specific protein disulphide-isomerase PDIp interacts with a hydroxyaryl group in ligands. *Biochem J*, **354**, 553-559.
- Klappa, P., Freedman, R.B. and Zimmermann, R. (1995) Protein disulphide isomerase and a luminal cyclophilin-type peptidyl prolyl cis-trans isomerase are in transient contact with secretory proteins during late stages of translocation. *Eur J Biochem*, **232**, 755-764.

- Klappa, P., Hawkins, H.C. and Freedman, R.B. (1997) Interactions between protein disulphide isomerase and peptides. *Eur J Biochem*, **248**, 37-42.
- Klappa, P., Ruddock, L.W., Darby, N.J. and Freedman, R.B. (1998a) The b' domain provides the principal peptide-binding site of protein disulfide isomerase but all domains contribute to binding of misfolded proteins. *Embo J*, **17**, 927-935.
- Klappa, P., Stromer, T., Zimmermann, R., Ruddock, L.W. and Freedman, R.B. (1998b) A pancreas-specific glycosylated protein disulphide-isomerase binds to misfolded proteins and peptides with an interaction inhibited by oestrogens. *Eur J Biochem*, **254**, 63-69.
- Kleerebezem, M., Heutink, M. and Tommassen, J. (1995) Characterization of an *Escherichia coli* rotA mutant, affected in periplasmic peptidyl-prolyl cis/trans isomerase. *Mol Microbiol*, **18**, 313-320.
- Klein, G., Dartigalongue, C. and Raina, S. (2003) Phosphorylation-mediated regulation of heat shock response in *Escherichia coli*. *Mol Microbiol*, **48**, 269-285.
- Koch, H.G., Hengelage, T., Neumann-Haefelin, C., MacFarlane, J., Hoffschulte, H.K., Schimz, K.L., Mechler, B. and Muller, M. (1999) In vitro studies with purified components reveal signal recognition particle (SRP) and SecA/SecB as constituents of two independent protein-targeting pathways of *Escherichia coli*. *Mol Biol Cell*, **10**, 2163-2173.
- Konno, M., Ito, M., Hayano, T. and Takahashi, N. (1996) The substrate-binding site in *Escherichia coli* cyclophilin A preferably recognizes a cis-proline isomer or a highly distorted form of the trans isomer. *J Mol Biol*, **256**, 897-908.
- Kontinen, V.P. and Sarvas, M. (1993) The PrsA lipoprotein is essential for protein secretion in *Bacillus subtilis* and sets a limit for high-level secretion. *Mol Microbiol*, **8**, 727-737.
- Koradi, R., Billeter, M. and Wuthrich, K. (1996) MOLMOL: a program for display and analysis of macromolecular structures. *J Mol Graph*, **14**, 51-55, 29-32.
- Koski, P., Hirvas, L. and Vaara, M. (1990) Complete sequence of the ompH gene encoding the 16-kDa cationic outer membrane protein of *Salmonella typhimurium*. *Gene*, **88**, 117-120.
- Koski, P., Rhen, M., Kantele, J. and Vaara, M. (1989) Isolation, cloning, and primary structure of a cationic 16-kDa outer membrane protein of *Salmonella typhimurium*. *J Biol Chem*, **264**, 18973-18980.
- Kozutsumi, Y., Segal, M., Normington, K., Gething, M.J. and Sambrook, J. (1988) The presence of malfolded proteins in the endoplasmic reticulum signals the induction of glucose-regulated proteins. *Nature*, **332**, 462-464.

- Kramer, G., Patzelt, H., Rauch, T., Kurz, T.A., Vorderwulbecke, S., Bukau, B. and Deuerling, E. (2004) Trigger factor peptidyl-prolyl cis/trans isomerase activity is not essential for the folding of cytosolic proteins in *Escherichia coli*. *J Biol Chem*, **279**, 14165-14170.
- Kramer, G., Ramachandiran, V., Horowitz, P.M. and Hardesty, B. (2002) The molecular chaperone DnaK is not recruited to translating ribosomes that lack trigger factor. *Arch Biochem Biophys*, **403**, 63-70.
- Laskey, R.A., Honda, B.M., Mills, A.D. and Finch, J.T. (1978) Nucleosomes are assembled by an acidic protein which binds histones and transfers them to DNA. *Nature*, **275**, 416-420.
- Lazar, S.W., Almiron, M., Tormo, A. and Kolter, R. (1998) Role of the *Escherichia coli* SurA protein in stationary-phase survival. *J Bacteriol*, **180**, 5704-5711.
- Lazar, S.W. and Kolter, R. (1996) SurA assists the folding of *Escherichia coli* outer membrane proteins. *J Bacteriol*, **178**, 1770-1773.
- Lee, K.H., Kim, H.S., Jeong, H.S. and Lee, Y.S. (2002) Chaperonin GroESL mediates the protein folding of human liver mitochondrial aldehyde dehydrogenase in *Escherichia coli*. *Biochem Biophys Res Commun*, **298**, 216-224.
- Lee, Y.J., Chen, J.C., Amoscato, A.A., Bennouna, J., Spitz, D.R., Suntharalingam, M. and Rhee, J.G. (2001) Protective role of Bcl2 in metabolic oxidative stress-induced cell death. *J Cell Sci*, **114**, 677-684.
- Levinthal, C. (1968) Are there pathways for protein folding? *Journal de Chimie Physique et de Physico-Chimie Biologique*, **65**, 44.
- Lewin, B. (2000) *Genes VII*. Oxford University Press.
- Li, P., Ding, Y., Wu, B., Shu, C., Shen, B. and Rao, Z. (2003) Structure of the N-terminal domain of human FKBP52. *Acta Crystallogr D Biol Crystallogr*, **59**, 16-22.
- Li, Z.Y., Liu, C.P., Zhu, L.Q., Jing, G.Z. and Zhou, J.M. (2001) The chaperone activity of trigger factor is distinct from its isomerase activity during co-expression with adenylate kinase in *Escherichia coli*. *FEBS Lett*, **506**, 108-112.
- Lin, D.T. and Lechleiter, J.D. (2002) Mitochondrial targeted cyclophilin D protects cells from cell death by peptidyl prolyl isomerization. *J Biol Chem*, **277**, 31134-31141.
- Liu, J. (1993) FK506 and cyclosporin, molecular probes for studying intracellular signal transduction. *Immunol Today*, **14**, 290-295.
- Liu, J. and Walsh, C.T. (1990) Peptidyl-prolyl cis-trans-isomerase from *Escherichia coli*: a periplasmic homolog of cyclophilin that is not inhibited by cyclosporin A. *Proc Natl Acad Sci U S A*, **87**, 4028-4032.

- Lomas, D.A. and Carrell, R.W. (2002) Serpinopathies and the conformational dementias. *Nat Rev Genet*, **3**, 759-768.
- Lu, K.P., Hanes, S.D. and Hunter, T. (1996) A human peptidyl-prolyl isomerase essential for regulation of mitosis. *Nature*, **380**, 544-547.
- Maier, R., Eckert, B., Scholz, C., Lilie, H. and Schmid, F.X. (2003) Interaction of trigger factor with the ribosome. *J Mol Biol*, **326**, 585-592.
- Maier, R., Scholz, C. and Schmid, F.X. (2001) Dynamic association of trigger factor with protein substrates. *J Mol Biol*, **314**, 1181-1190.
- Martin, J. and Hartl, F.U. (1997) The effect of macromolecular crowding on chaperonin-mediated protein folding. *Proc Natl Acad Sci U S A*, **94**, 1107-1112.
- Mayer, M. and Meyer, B. (2001) Group epitope mapping by saturation transfer difference NMR to identify segments of a ligand in direct contact with a protein receptor. *J Am Chem Soc*, **123**, 6108-6117.
- Meusser, B., Hirsch, C., Jarosch, E. and Sommer, T. (2005) ERAD: the long road to destruction. *Nat Cell Biol*, **7**, 766-772.
- Minton, A.P. (2000) Implications of macromolecular crowding for protein assembly. *Curr Opin Struct Biol*, **10**, 34-39.
- Missiakas, D., Betton, J.M. and Raina, S. (1996) New components of protein folding in extracytoplasmic compartments of Escherichia coli SurA, FkpA and Skp/OmpH. *Mol Microbiol*, **21**, 871-884.
- Missiakas, D. and Raina, S. (1997a) Protein folding in the bacterial periplasm. *J Bacteriol*, **179**, 2465-2471.
- Missiakas, D. and Raina, S. (1997b) Protein misfolding in the cell envelope of Escherichia coli: new signaling pathways. *Trends Biochem Sci*, **22**, 59-63.
- Mogensen, J.E. and Otzen, D.E. (2005) Interactions between folding factors and bacterial outer membrane proteins. *Mol Microbiol*, **57**, 326-346.
- Nakamoto, H. and Bardwell, J.C. (2004) Catalysis of disulfide bond formation and isomerization in the Escherichia coli periplasm. *Biochim Biophys Acta*, **1694**, 111-119.
- Newitt, J.A. and Bernstein, H.D. (1998) A mutation in the Escherichia coli secY gene that produces distinct effects on inner membrane protein insertion and protein export. *J Biol Chem*, **273**, 12451-12456.
- Nikaido, H. (1994) Porins and specific diffusion channels in bacterial outer membranes. *J Biol Chem*, **269**, 3905-3908.

- Pathan, N., Aime-Sempe, C., Kitada, S., Haldar, S. and Reed, J.C. (2001) Microtubule-targeting drugs induce Bcl-2 phosphorylation and association with Pin1. *Neoplasia*, **3**, 70-79.
- Petersen, F.N., Jensen, M.O. and Nielsen, C.H. (2005) Interfacial tryptophan residues: a role for the cation-pi effect? *Biophys J*, **89**, 3985-3996.
- Pirneskoski, A., Klappa, P., Lobell, M., Williamson, R.A., Byrne, L., Alanen, H.I., Salo, K.E., Kivirikko, K.I., Freedman, R.B. and Ruddock, L.W. (2004) Molecular characterization of the principal substrate binding site of the ubiquitous folding catalyst protein disulfide isomerase. *J Biol Chem*, **279**, 10374-10381.
- Pogliano, J., Lynch, A.S., Belin, D., Lin, E.C. and Beckwith, J. (1997) Regulation of Escherichia coli cell envelope proteins involved in protein folding and degradation by the Cpx two-component system. *Genes Dev*, **11**, 1169-1182.
- Poole, K. (2005) Efflux-mediated antimicrobial resistance. *J Antimicrob Chemother*, **56**, 20-51.
- Price, E.R., Jin, M., Lim, D., Pati, S., Walsh, C.T. and McKeon, F.D. (1994) Cyclophilin B trafficking through the secretory pathway is altered by binding of cyclosporin A. *Proc Natl Acad Sci U S A*, **91**, 3931-3935.
- Price, E.R., Zydowsky, L.D., Jin, M.J., Baker, C.H., McKeon, F.D. and Walsh, C.T. (1991) Human cyclophilin B: a second cyclophilin gene encodes a peptidyl-prolyl isomerase with a signal sequence. *Proc Natl Acad Sci U S A*, **88**, 1903-1907.
- Rahfeld, J.U., Rucknagel, K.P., Schelbert, B., Ludwig, B., Hacker, J., Mann, K. and Fischer, G. (1994a) Confirmation of the existence of a third family among peptidyl-prolyl cis/trans isomerases. Amino acid sequence and recombinant production of parvulin. *FEBS Lett*, **352**, 180-184.
- Rahfeld, J.U., Schierhorn, A., Mann, K. and Fischer, G. (1994b) A novel peptidyl-prolyl cis/trans isomerase from Escherichia coli. *FEBS Lett*, **343**, 65-69.
- Raina, S., Missiakas, D. and Georgopoulos, C. (1995) The rpoE gene encoding the sigma E (sigma 24) heat shock sigma factor of Escherichia coli. *Embo J*, **14**, 1043-1055.
- Raivio, T.L. and Silhavy, T.J. (2001) Periplasmic stress and ECF sigma factors. *Annu Rev Microbiol*, **55**, 591-624.
- Ramm, K. and Pluckthun, A. (2000) The periplasmic Escherichia coli peptidylprolyl cis,trans-isomerase FkpA. II. Isomerase-independent chaperone activity in vitro. *J Biol Chem*, **275**, 17106-17113.

- Ramm, K. and Pluckthun, A. (2001) High enzymatic activity and chaperone function are mechanistically related features of the dimeric E. coli peptidyl-prolyl isomerase FkpA. *J Mol Biol*, **310**, 485-498.
- Ranganathan, R., Lu, K.P., Hunter, T. and Noel, J.P. (1997) Structural and functional analysis of the mitotic rotamase Pin1 suggests substrate recognition is phosphorylation dependent. *Cell*, **89**, 875-886.
- Reimer, T., Weiwad, M., Schierhorn, A., Ruecknagel, P.K., Rahfeld, J.U., Bayer, P. and Fischer, G. (2003) Phosphorylation of the N-terminal domain regulates subcellular localization and DNA binding properties of the peptidyl-prolyl cis/trans isomerase hPar14. *J Mol Biol*, **330**, 955-966.
- Reimer, U. and Fischer, G. (2002) Local structural changes caused by peptidyl-prolyl cis/trans isomerization in the native state of proteins. *Biophys Chem*, **96**, 203-212.
- Reimer, U., Scherer, G., Drewello, M., Kruber, S., Schutkowski, M. and Fischer, G. (1998) Side-chain effects on peptidyl-prolyl cis/trans isomerisation. *J Mol Biol*, **279**, 449-460.
- Richarme, G. and Caldas, T.D. (1997) Chaperone properties of the bacterial periplasmic substrate-binding proteins. *J Biol Chem*, **272**, 15607-15612.
- Rietsch, A. and Beckwith, J. (1998) The genetics of disulfide bond metabolism. *Annu Rev Genet*, **32**, 163-184.
- Rizzitello, A.E., Harper, J.R. and Silhavy, T.J. (2001) Genetic evidence for parallel pathways of chaperone activity in the periplasm of Escherichia coli. *J Bacteriol*, **183**, 6794-6800.
- Rosen, M.K., Standaert, R.F., Galat, A., Nakatsuka, M. and Schreiber, S.L. (1990) Inhibition of FKBP rotamase activity by immunosuppressant FK506: twisted amide surrogate. *Science*, **248**, 863-866.
- Rouviere, P.E. and Gross, C.A. (1996) SurA, a periplasmic protein with peptidyl-prolyl isomerase activity, participates in the assembly of outer membrane porins. *Genes Dev*, **10**, 3170-3182.
- Rudd, K.E., Sofia, H.J., Koonin, E.V., Plunkett, G., 3rd, Lazar, S. and Rouviere, P.E. (1995) A new family of peptidyl-prolyl isomerases. *Trends Biochem Sci*, **20**, 12-14.
- Ruddock, L.W., Coen, J.J., Cheesman, C., Freedman, R.B. and Hirst, T.R. (1996) Assembly of the B subunit pentamer of Escherichia coli heat-labile enterotoxin. Kinetics and molecular basis of rate-limiting steps in vitro. *J Biol Chem*, **271**, 19118-19123.
- Ruddock, L.W., Freedman, R.B. and Klappa, P. (2000) Specificity in substrate binding by protein folding catalysts: tyrosine and tryptophan residues are the

- recognition motifs for the binding of peptides to the pancreas-specific protein disulfide isomerase PDIp. *Protein Sci*, **9**, 758-764.
- Rulten, S., Thorpe, J. and Kay, J. (1999) Identification of eukaryotic parvulin homologues: a new subfamily of peptidylprolyl cis-trans isomerases. *Biochem Biophys Res Commun*, **259**, 557-562.
- Sardesai, A.A., Genevaux, P., Schwager, F., Ang, D. and Georgopoulos, C. (2003) The OmpL porin does not modulate redox potential in the periplasmic space of *Escherichia coli*. *Embo J*, **22**, 1461-1466.
- Saul, F.A., Arie, J.P., Vulliez-le Normand, B., Kahn, R., Betton, J.M. and Bentley, G.A. (2004) Structural and functional studies of FkpA from *Escherichia coli*, a cis/trans peptidyl-prolyl isomerase with chaperone activity. *J Mol Biol*, **335**, 595-608.
- Schafer, U., Beck, K. and Muller, M. (1999) Skp, a molecular chaperone of gram-negative bacteria, is required for the formation of soluble periplasmic intermediates of outer membrane proteins. *J Biol Chem*, **274**, 24567-24574.
- Schaffitzel, E., Rudiger, S., Bukau, B. and Deuerling, E. (2001) Functional dissection of trigger factor and DnaK: interactions with nascent polypeptides and thermally denatured proteins. *Biol Chem*, **382**, 1235-1243.
- Schiene-Fischer, C., Habazettl, J., Tradler, T. and Fischer, G. (2002) Evaluation of similarities in the cis/trans isomerase function of trigger factor and DnaK. *Biol Chem*, **383**, 1865-1873.
- Schiene-Fischer, C. and Yu, C. (2001) Receptor accessory folding helper enzymes: the functional role of peptidyl prolyl cis/trans isomerases. *FEBS Lett*, **495**, 1-6.
- Schiene, C. and Fischer, G. (2000) Enzymes that catalyse the restructuring of proteins. *Curr Opin Struct Biol*, **10**, 40-45.
- Schmid, F.X. (1993) Prolyl isomerase: enzymatic catalysis of slow protein-folding reactions. *Annu Rev Biophys Biomol Struct*, **22**, 123-142.
- Scholz, C., Mucke, M., Rape, M., Pecht, A., Pahl, A., Bang, H. and Schmid, F.X. (1998) Recognition of protein substrates by the prolyl isomerase trigger factor is independent of proline residues. *J Mol Biol*, **277**, 723-732.
- Scholz, C., Rahfeld, J., Fischer, G. and Schmid, F.X. (1997a) Catalysis of protein folding by parvulin. *J Mol Biol*, **273**, 752-762.
- Scholz, C., Stoller, G., Zarnt, T., Fischer, G. and Schmid, F.X. (1997b) Cooperation of enzymatic and chaperone functions of trigger factor in the catalysis of protein folding. *Embo J*, **16**, 54-58.

- Schonbrunner, E.R. and Schmid, F.X. (1992) Peptidyl-prolyl cis-trans isomerase improves the efficiency of protein disulfide isomerase as a catalyst of protein folding. *Proc Natl Acad Sci U S A*, **89**, 4510-4513.
- Scotti, P.A., Valent, Q.A., Manting, E.H., Urbanus, M.L., Driessen, A.J., Oudega, B. and Luirink, J. (1999) SecA is not required for signal recognition particle-mediated targeting and initial membrane insertion of a nascent inner membrane protein. *J Biol Chem*, **274**, 29883-29888.
- Sekerina, E., Rahfeld, J.U., Muller, J., Fanghanel, J., Rascher, C., Fischer, G. and Bayer, P. (2000) NMR solution structure of hPar14 reveals similarity to the peptidyl prolyl cis/trans isomerase domain of the mitotic regulator hPin1 but indicates a different functionality of the protein. *J Mol Biol*, **301**, 1003-1017.
- Shaw, P.E. (2002) Peptidyl-prolyl isomerases: a new twist to transcription. *EMBO Rep*, **3**, 521-526.
- Shaw, W.V. (1983) Chloramphenicol acetyltransferase: enzymology and molecular biology. *CRC Crit Rev Biochem*, **14**, 1-46.
- Sidhu, S.S., Lowman, H.B., Cunningham, B.C. and Wells, J.A. (2000) Phage display for selection of novel binding peptides. *Methods Enzymol*, **328**, 333-363.
- Siekierka, J.J., Hung, S.H., Poe, M., Lin, C.S. and Sigal, N.H. (1989a) A cytosolic binding protein for the immunosuppressant FK506 has peptidyl-prolyl isomerase activity but is distinct from cyclophilin. *Nature*, **341**, 755-757.
- Siekierka, J.J., Staruch, M.J., Hung, S.H. and Sigal, N.H. (1989b) FK-506, a potent novel immunosuppressive agent, binds to a cytosolic protein which is distinct from the cyclosporin A-binding protein, cyclophilin. *J Immunol*, **143**, 1580-1583.
- Singh, B.B., Patel, H.H., Roepman, R., Schick, D. and Ferreira, P.A. (1999) The zinc finger cluster domain of RanBP2 is a specific docking site for the nuclear export factor, exportin-1. *J Biol Chem*, **274**, 37370-37378.
- Slepenkov, S.V., Patchen, B., Peterson, K.M. and Witt, S.N. (2003) Importance of the D and E helices of the molecular chaperone DnaK for ATP binding and substrate release. *Biochemistry*, **42**, 5867-5876.
- Stenberg, F., Chovanec, P., Maslen, S.L., Robinson, C.V., Ilag, L.L., von Heijne, G. and Daley, D.O. (2005) Protein complexes of the Escherichia coli cell envelope. *J Biol Chem*, **280**, 34409-34419.
- Stoller, G., Rucknagel, K.P., Nierhaus, K.H., Schmid, F.X., Fischer, G. and Rahfeld, J.U. (1995) A ribosome-associated peptidyl-prolyl cis/trans isomerase identified as the trigger factor. *Embo J*, **14**, 4939-4948.
- Stoller, G., Tradler, T., Rucknagel, K.P., Rahfeld, J.U. and Fischer, G. (1996) An 11.8 kDa proteolytic fragment of the E. coli trigger factor represents the domain

- carrying the peptidyl-prolyl cis/trans isomerase activity. *FEBS Lett*, **384**, 117-122.
- Stromer, T., Ehrnsperger, M., Gaestel, M. and Buchner, J. (2003) Analysis of the interaction of small heat shock proteins with unfolding proteins. *J Biol Chem*, **278**, 18015-18021.
- Struyve, M., Moons, M. and Tommassen, J. (1991) Carboxy-terminal phenylalanine is essential for the correct assembly of a bacterial outer membrane protein. *J Mol Biol*, **218**, 141-148.
- Surmacz, T.A., Bayer, E., Rahfeld, J.U., Fischer, G. and Bayer, P. (2002) The N-terminal basic domain of human parvulin hPar14 is responsible for the entry to the nucleus and high-affinity DNA-binding. *J Mol Biol*, **321**, 235-247.
- Suzuki, R., Nagata, K., Yumoto, F., Kawakami, M., Nemoto, N., Furutani, M., Adachi, K., Maruyama, T. and Tanokura, M. (2003) Three-dimensional solution structure of an archaeal FKBP with a dual function of peptidyl prolyl cis-trans isomerase and chaperone-like activities. *J Mol Biol*, **328**, 1149-1160.
- Sydenham, M., Douce, G., Bowe, F., Ahmed, S., Chatfield, S. and Dougan, G. (2000) *Salmonella enterica* serovar typhimurium surA mutants are attenuated and effective live oral vaccines. *Infect Immun*, **68**, 1109-1115.
- Takahashi, N., Hayano, T. and Suzuki, M. (1989) Peptidyl-prolyl cis-trans isomerase is the cyclosporin A-binding protein cyclophilin. *Nature*, **337**, 473-475.
- Teter, S.A., Houry, W.A., Ang, D., Tradler, T., Rockabrand, D., Fischer, G., Blum, P., Georgopoulos, C. and Hartl, F.U. (1999) Polypeptide flux through bacterial Hsp70: DnaK cooperates with trigger factor in chaperoning nascent chains. *Cell*, **97**, 755-765.
- Texter, F.L., Spencer, D.B., Rosenstein, R. and Matthews, C.R. (1992) Intramolecular catalysis of a proline isomerization reaction in the folding of dihydrofolate reductase. *Biochemistry*, **31**, 5687-5691.
- Thome, B.M., Hoffschulte, H.K., Schiltz, E. and Muller, M. (1990) A protein with sequence identity to Skp (FirA) supports protein translocation into plasma membrane vesicles of *Escherichia coli*. *FEBS Lett*, **269**, 113-116.
- Thome, B.M. and Muller, M. (1991) Skp is a periplasmic *Escherichia coli* protein requiring SecA and SecY for export. *Mol Microbiol*, **5**, 2815-2821.
- Thompson, J.A., Lau, A.L. and Cunningham, D.D. (1987) Selective radiolabeling of cell surface proteins to a high specific activity. *Biochemistry*, **26**, 743-750.
- Tormo, A., Almiron, M. and Kolter, R. (1990) surA, an *Escherichia coli* gene essential for survival in stationary phase. *J Bacteriol*, **172**, 4339-4347.

- Uchida, T., Fujimori, F., Tradler, T., Fischer, G. and Rahfeld, J.U. (1999) Identification and characterization of a 14 kDa human protein as a novel parvulin-like peptidyl prolyl cis/trans isomerase. *FEBS Lett*, **446**, 278-282.
- Ulbrandt, N.D., London, E. and Oliver, D.B. (1992) Deep penetration of a portion of Escherichia coli SecA protein into model membranes is promoted by anionic phospholipids and by partial unfolding. *J Biol Chem*, **267**, 15184-15192.
- Ulbrandt, N.D., Newitt, J.A. and Bernstein, H.D. (1997) The E. coli signal recognition particle is required for the insertion of a subset of inner membrane proteins. *Cell*, **88**, 187-196.
- USDA. (2006) Emerging Animal Health Issues. *United States Department of Agriculture*, <http://www.aphis.usda.gov/vs/ceah/cei/taf/emerginganimalhealthissues/files/health.htm>.
- Valent, Q.A., Kendall, D.A., High, S., Kusters, R., Oudega, B. and Luirink, J. (1995) Early events in preprotein recognition in E. coli: interaction of SRP and trigger factor with nascent polypeptides. *Embo J*, **14**, 5494-5505.
- Valent, Q.A., Scotti, P.A., High, S., de Gier, J.W., von Heijne, G., Lentzen, G., Wintermeyer, W., Oudega, B. and Luirink, J. (1998) The Escherichia coli SRP and SecB targeting pathways converge at the translocon. *Embo J*, **17**, 2504-2512.
- van den Berg, B., Ellis, R.J. and Dobson, C.M. (1999) Effects of macromolecular crowding on protein folding and aggregation. *Embo J*, **18**, 6927-6933.
- Velasco, D., del Mar Tomas, M., Cartelle, M., Beceiro, A., Perez, A., Molina, F., Moure, R., Villanueva, R. and Bou, G. (2005) Evaluation of different methods for detecting methicillin (oxacillin) resistance in Staphylococcus aureus. *J Antimicrob Chemother*, **55**, 379-382.
- Vitikainen, M., Lappalainen, I., Seppala, R., Antelmann, H., Boer, H., Taira, S., Savilahti, H., Hecker, M., Vihinen, M., Sarvas, M. and Kontinen, V.P. (2004) Structure-function analysis of PrsA reveals roles for the parvulin-like and flanking N- and C-terminal domains in protein folding and secretion in Bacillus subtilis. *J Biol Chem*, **279**, 19302-19314.
- Vogtherr, M., Jacobs, D.M., Parac, T.N., Maurer, M., Pahl, A., Saxena, K., Ruterjans, H., Griesinger, C. and Fiebig, K.M. (2002) NMR solution structure and dynamics of the peptidyl-prolyl cis-trans isomerase domain of the trigger factor from Mycoplasma genitalium compared to FK506-binding protein. *J Mol Biol*, **318**, 1097-1115.
- von Ahsen, O., Tropschug, M., Pfanner, N. and Rassow, J. (1997) The chaperonin cycle cannot substitute for prolyl isomerase activity, but GroEL alone promotes productive folding of a cyclophilin-sensitive substrate to a cyclophilin-resistant form. *Embo J*, **16**, 4568-4578.

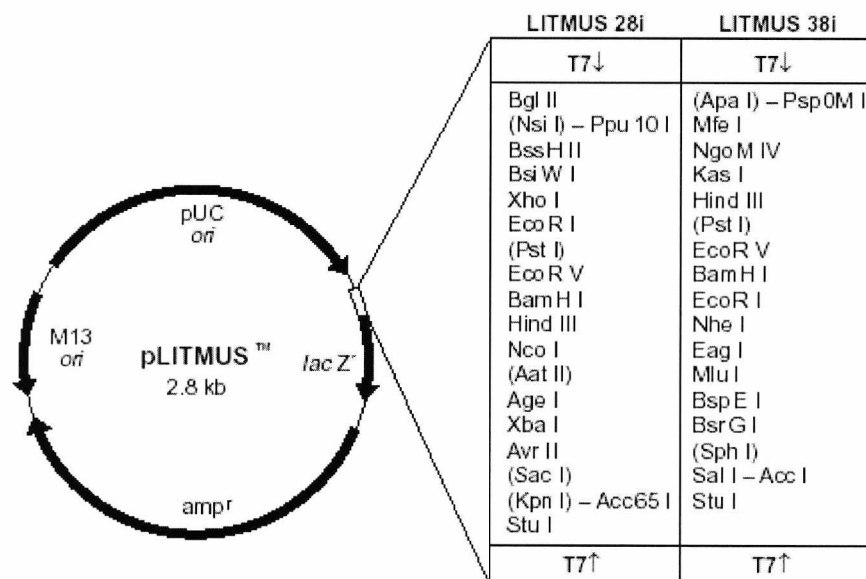
- von Heijne, G. (1989) Control of topology and mode of assembly of a polytopic membrane protein by positively charged residues. *Nature*, **341**, 456-458.
- von Heijne, G. (1990) The signal peptide. *J Membr Biol*, **115**, 195-201.
- Vorderwulbecke, S., Kramer, G., Merz, F., Kurz, T.A., Rauch, T., Zachmann-Brand, B., Bukau, B. and Deuerling, E. (2005) Low temperature of GroEL/ES overproduction permits growth of Escherichia coli cells lacking trigger factor DnaK. *FEBS Lett*, **579**, 181-187.
- Wahlstrom, E., Vitikainen, M., Kontinen, V.P. and Sarvas, M. (2003) The extracytoplasmic folding factor PrsA is required for protein secretion only in the presence of the cell wall in Bacillus subtilis. *Microbiology*, **149**, 569-577.
- Walsh, C.T., Zydowsky, L.D. and McKeon, F.D. (1992) Cyclosporin A, the cyclophilin class of peptidylprolyl isomerases, and blockade of T cell signal transduction. *J Biol Chem*, **267**, 13115-13118.
- Walsh, N.P., Alba, B.M., Bose, B., Gross, C.A. and Sauer, R.T. (2003) OMP peptide signals initiate the envelope-stress response by activating DegS protease via relief of inhibition mediated by its PDZ domain. *Cell*, **113**, 61-71.
- Wang, C.C. and Tsou, C.L. (1998) Enzymes as chaperones and chaperones as enzymes. *FEBS Lett*, **425**, 382-384.
- Wang, J. and Boisvert, D.C. (2003) Structural basis for GroEL-assisted protein folding from the crystal structure of (GroEL-KMgATP)₁₄ at 2.0Å resolution. *J Mol Biol*, **327**, 843-855.
- Wang, J.D., Herman, C., Tipton, K.A., Gross, C.A. and Weissman, J.S. (2002) Directed evolution of substrate-optimized GroEL/S chaperonins. *Cell*, **111**, 1027-1039.
- Webb, H.M., Ruddock, L.W., Marchant, R.J., Jonas, K. and Klappa, P. (2001) Interaction of the periplasmic peptidylprolyl cis-trans isomerase SurA with model peptides. The N-terminal region of SurA is essential and sufficient for peptide binding. *J Biol Chem*, **276**, 45622-45627.
- Wei, J. and Hendershot, L.M. (1996) Protein folding and assembly in the endoplasmic reticulum. *Exs*, **77**, 41-55.
- Weisman, R., Creanor, J. and Fantes, P. (1996) A multicopy suppressor of a cell cycle defect in *S. pombe* encodes a heat shock-inducible 40 kDa cyclophilin-like protein. *Embo J*, **15**, 447-456.
- Werner, J., Augustus, A.M. and Misra, R. (2003) Assembly of TolC, a structurally unique and multifunctional outer membrane protein of Escherichia coli K-12. *J Bacteriol*, **185**, 6540-6547.

- WHO. (2003) Shigella. *World Health Organisation*, http://www.who.int/vaccine_research/diseases/shigella/en/.
- WHO. (2005) Drug Resistant Salmonella. <http://www.who.int/mediacentre/factsheets/fs139/en/>.
- WHO. (2006) Enterotoxigenic *Escherichia coli* (ETEC). *World Health Organisation*, http://www.who.int/vaccine_research/diseases/diarrhoeal/en/index4.html.
- Wickner, W. and Leonard, M.R. (1996) *Escherichia coli* preprotein translocase. *J Biol Chem*, **271**, 29514-29516.
- Wiech, H., Klappa, P. and Zimmerman, R. (1991) Protein export in prokaryotes and eukaryotes. Theme with variations. *FEBS Lett*, **285**, 182-188.
- Wilken, C., Kitzing, K., Kurzbauer, R., Ehrmann, M. and Clausen, T. (2004) Crystal structure of the DegS stress sensor: How a PDZ domain recognizes misfolded protein and activates a protease. *Cell*, **117**, 483-494.
- Willmott, C.J. and Maxwell, A. (1993) A single point mutation in the DNA gyrase A protein greatly reduces binding of fluoroquinolones to the gyrase-DNA complex. *Antimicrob Agents Chemother*, **37**, 126-127.
- Winter, J., Klappa, P., Freedman, R.B., Lilie, H. and Rudolph, R. (2002) Catalytic activity and chaperone function of human protein-disulfide isomerase are required for the efficient refolding of proinsulin. *J Biol Chem*, **277**, 310-317.
- Wood, L.C., White, T.B., Ramdas, L. and Nall, B.T. (1988) Replacement of a conserved proline eliminates the absorbance-detected slow folding phase of iso-2-cytochrome c. *Biochemistry*, **27**, 8562-8568.
- Woodford, N. (2005) Biological counterstrike: antibiotic resistance mechanisms of Gram-positive cocci. *Clin Microbiol Infect*, **11 Suppl 3**, 2-21.
- Wulfing, C., Lombardero, J. and Pluckthun, A. (1994) An *Escherichia coli* protein consisting of a domain homologous to FK506-binding proteins (FKBP) and a new metal binding motif. *J Biol Chem*, **269**, 2895-2901.
- Yaffe, M.B., Schutkowski, M., Shen, M., Zhou, X.Z., Stukenberg, P.T., Rahfeld, J.U., Xu, J., Kuang, J., Kirschner, M.W., Fischer, G., Cantley, L.C. and Lu, K.P. (1997) Sequence-specific and phosphorylation-dependent proline isomerization: a potential mitotic regulatory mechanism. *Science*, **278**, 1957-1960.
- Yang, W.M., Inouye, C.J. and Seto, E. (1995) Cyclophilin A and FKBP12 interact with YY1 and alter its transcriptional activity. *J Biol Chem*, **270**, 15187-15193.

- Yokoi, H., Kondo, H., Furuya, A., Hanai, N., Ikeda, J.E. and Anazawa, H. (1996a) Characterization of cyclophilin 40: highly conserved protein that directly associates with Hsp90. *Biol Pharm Bull*, **19**, 506-511.
- Yokoi, H., Shimizu, Y., Anazawa, H., Lefebvre, C.A., Korneluk, R.G. and Ikeda, J.E. (1996b) The structure and complete nucleotide sequence of the human cyclophilin 40 (PPID) gene. *Genomics*, **35**, 448-455.
- Young, J.C. and Hartl, F.U. (2003) A stress sensor for the bacterial periplasm. *Cell*, **113**, 1-2.
- Yura, T., Mori, H., Nagai, H., Nagata, T., Ishihama, A., Fujita, N., Isono, K., Mizobuchi, K. and Nakata, A. (1992) Systematic sequencing of the *Escherichia coli* genome: analysis of the 0-2.4 min region. *Nucleic Acids Res*, **20**, 3305-3308.
- Zarnt, T., Tradler, T., Stoller, G., Scholz, C., Schmid, F.X. and Fischer, G. (1997) Modular structure of the trigger factor required for high activity in protein folding. *J Mol Biol*, **271**, 827-837.
- Zhang, J. and Herscovitz, H. (2003) Nascent lipidated apolipoprotein B is transported to the Golgi as an incompletely folded intermediate as probed by its association with network of endoplasmic reticulum molecular chaperones, GRP94, ERp72, BiP, calreticulin, and cyclophilin B. *J Biol Chem*, **278**, 7459-7468.
- Zhang, Z., Li, Z.H., Wang, F., Fang, M., Yin, C.C., Zhou, Z.Y., Lin, Q. and Huang, H.L. (2002) Overexpression of DsbC and DsbG markedly improves soluble and functional expression of single-chain Fv antibodies in *Escherichia coli*. *Protein Expr Purif*, **26**, 218-228.

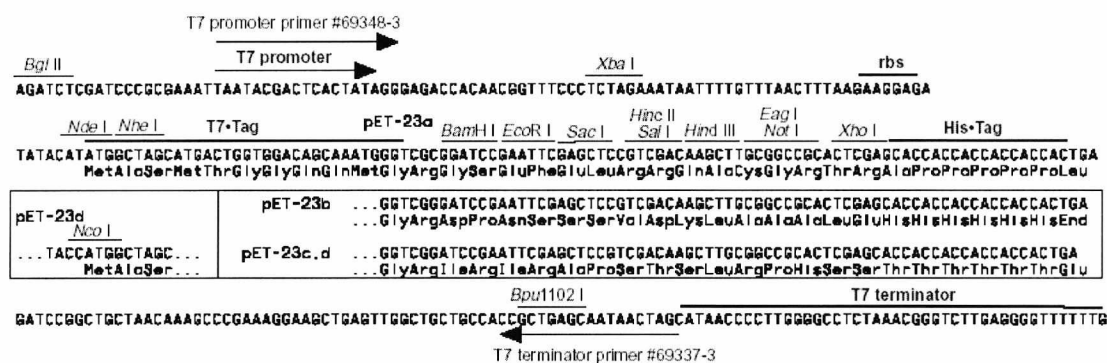
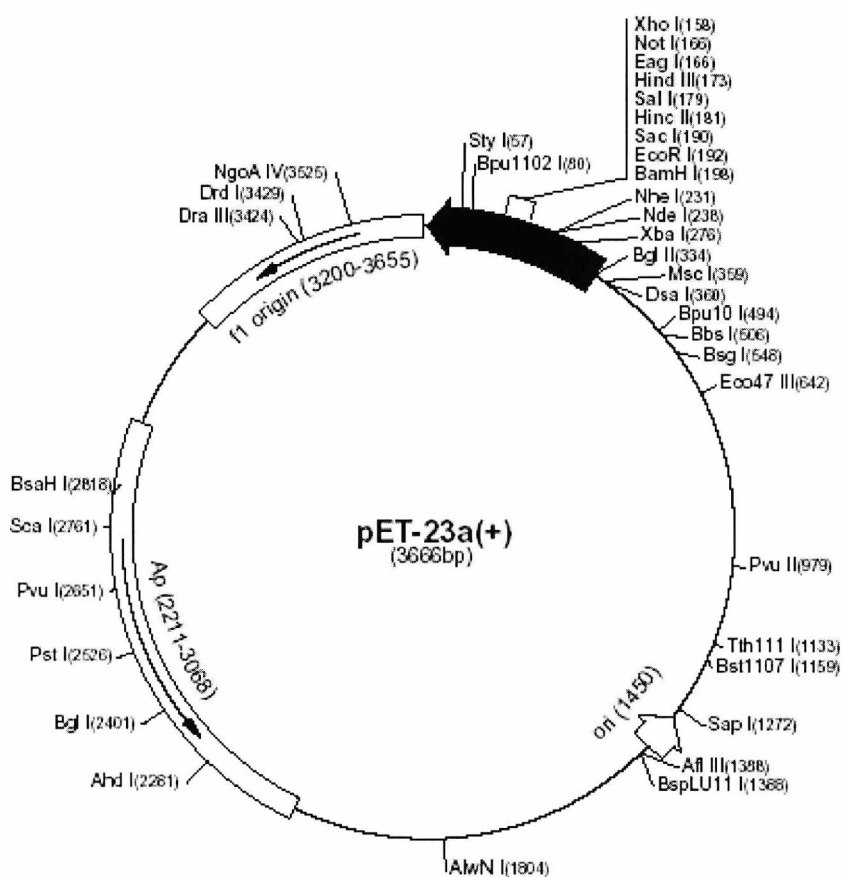
Appendices

APPENDIX I



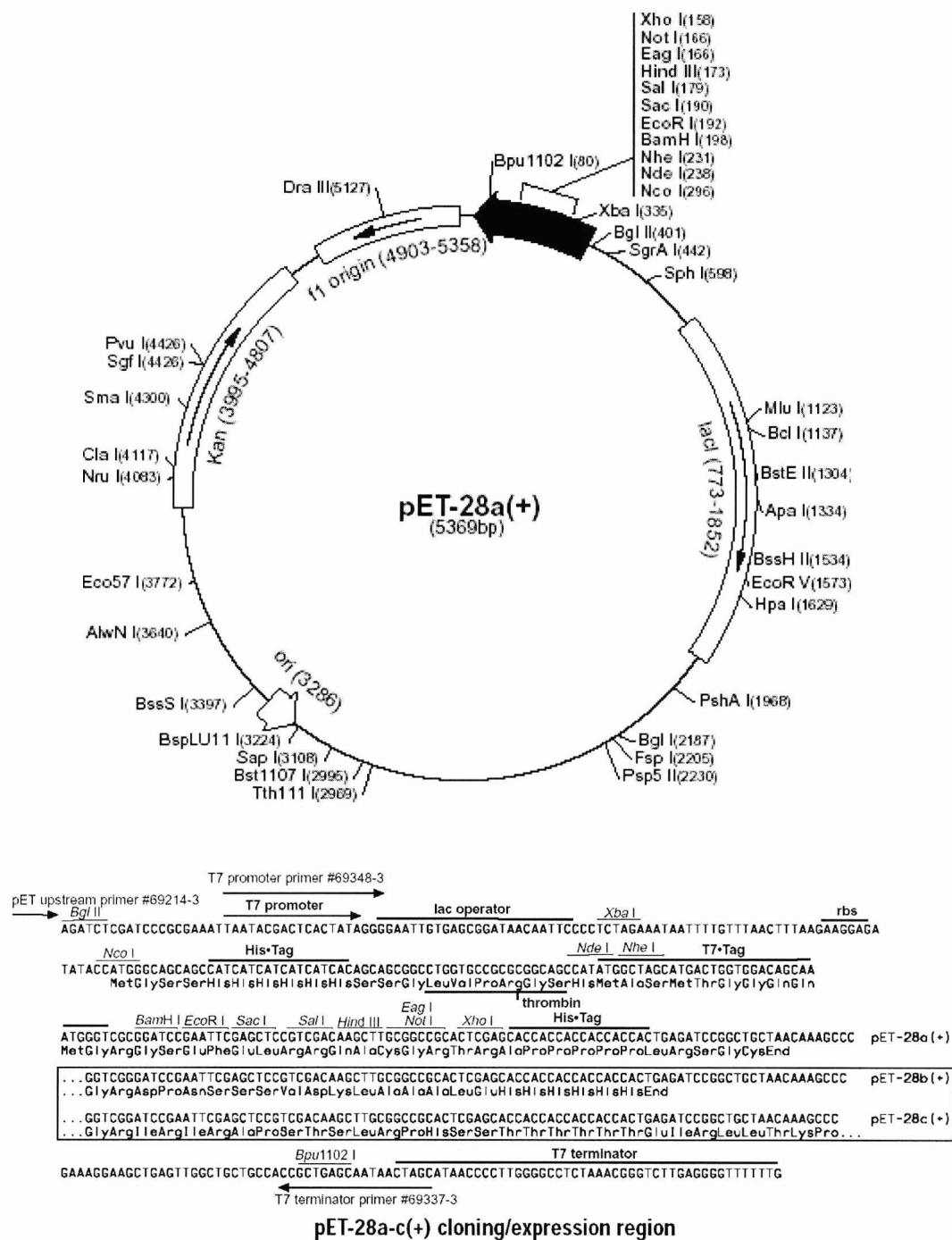
Appendix 1 pLitmus 28i Vector from New England Biolabs. Image from the New England Biolabs webpage, www.neb.com

pLITMUS 28i is a multi-purpose cloning/*in vitro* transcription phagemid vector. The molecule is a small, double-stranded circle 2,823 base pairs in length (molecular weight = 1.8×10^6 daltons).

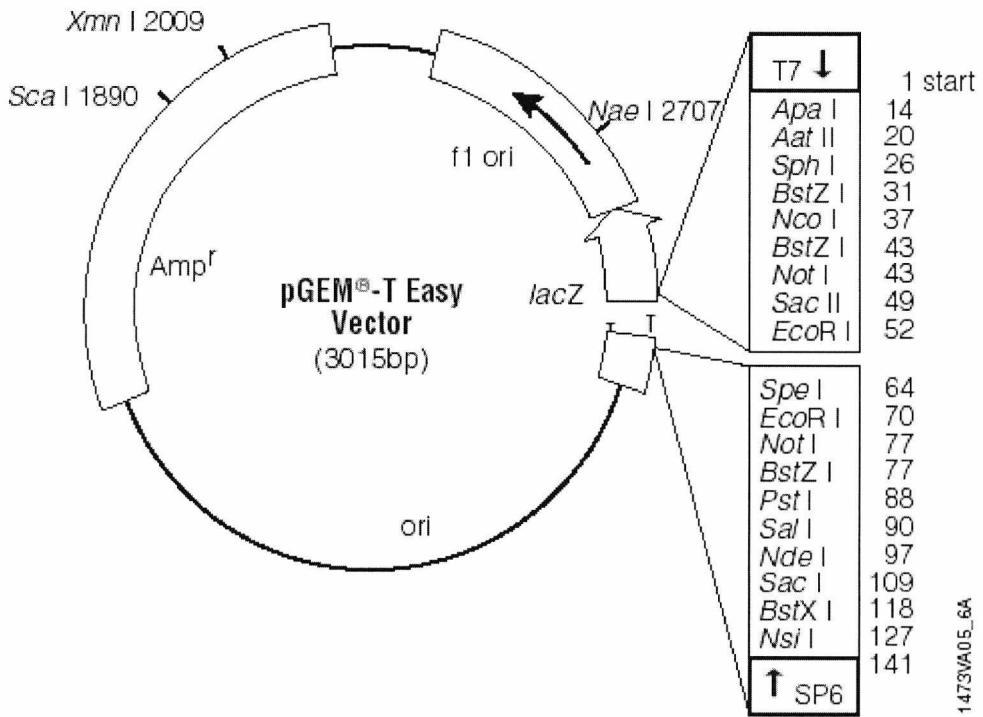


pET-23a-d(+) cloning/expression region

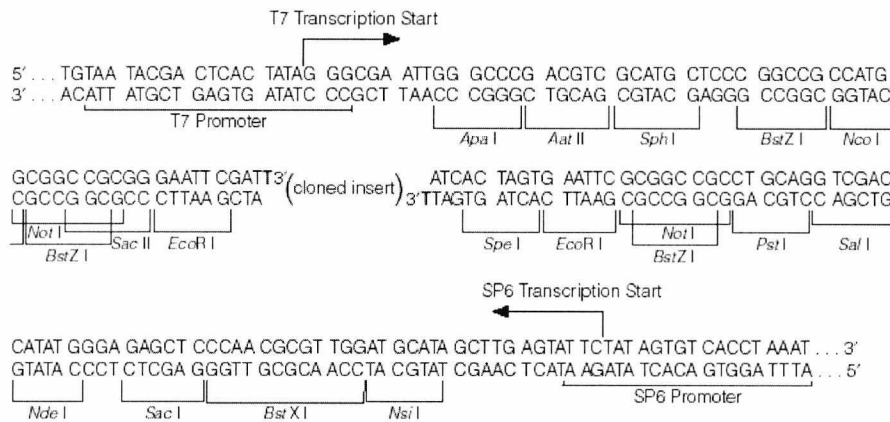
Appendix 2 pET-23a (+) Vector from Novagen/Merck. Image taken from the Novagen/Merck webpage, www.merckbiosciences.co.uk



Appendix 3 pET-28a (+) Vector from Novagen/Merck. Image taken from the Novagen/Merck webpage, www.merckbiosciences.co.uk



1473VA05_6A



Appendix 4 pGEM-T Easy Vector from Promega. Image taken from www.promega.com.

APPENDIX II

SurA from *E.coli*. Swiss-prot entry POABZ6

Length: **428 AA** [This is the length of the unprocessed precursor]

Molecular weight: **47284 Da** [This is the MW of the unprocessed precursor]

```

      10      20      30      40      50      60
MKNWKTLLLG IAMIAN TSFA APQVV DKVAA VVNGGVVLES DVDGLMQSVK LNAAQARQQL

      70      80      90     100     110     120
PDDATLRHQI MERLIMDQII LQMGMKMGVK ISDEQLDQAI ANIAKQNNMT LDQMRSRLAY

     130     140     150     160     170     180
DGLNYNTYRN QIRKEMIISE VRNNEVRRRI TILPQEVESL AQQVGNQNDÄ STELNLSHIL

     190     200     210     220     230     240
IPLPENPTSD QVNEAESQAR AIVDQARNGA DFGKLAI AHS ADQQALNGGQ MGWGRIQELP

     250     260     270     280     290     300
GIFAQALSTA KKGDIVGPIR SGVGFHILKV NDLRGESKNI SVTEVHARHI LLKPSPIMTD

     310     320     330     340     350     360
EQARVKLEQI AADIKSGKTT FAAAAKEFSQ DPGSANQGGD LGWATPDIFD PAFRDALTRL

     370     380     390     400     410     420
NKGQMSAPVH SSFGWHLIEL LDTRNVDKTD AAQKDRAYRM LMNRKFSEEA ASWMQEQRAS

AYVKILSN

```

PpiD from E.coli. Swiss-prot entry POADY1Length: **623 AA** [This is the length of the unprocessed precursor]Molecular weight: **68150 Da** [This is the MW of the unprocessed precursor]

10 20 30 40 50 60
 MMDSLRTAAN SLVLKIIIFGI IIVSFILTVG SGYLIGGGNN YAAKVNDQEI SRGQFENAFN

70 80 90 100 110 120
 SERNRMQQQL GDQYSELAAN EGYMKTLRQQ VLNRLIDEAL LDQYARELKL GISDEQVKQA

130 140 150 160 170 180
 IFATPAFQVD GKFDNSRYNG ILNQMGMTAD QYAQALRNQL TTQQLINGVA GTDFMLKGET

190 200 210 220 230 240
 DELAALVAQQ RVVREATIDV NALAAKQPVT EQEIASYYEQ NKNNFMTPEQ FRVSYIKLDA

250 260 270 280 290 300
 ATMQQPVSDA DIQSYDQHQ DQFTQPQRTR YSIIQTKTED EAKAVLDELN KGGDFAALAK

310 320 330 340 350 360
 EKSADIISAR NGGDMGWLED ATIPDELKNA GLKEKGQLSG VIKSSVGFLI VRLDDIQPAK

370 380 390 400 410 420
 VKSLDEV RDD IAAKVKEKA LDAYYALQQK VSDAASNDTE SLAGAEQAAG VKATQTGWFS

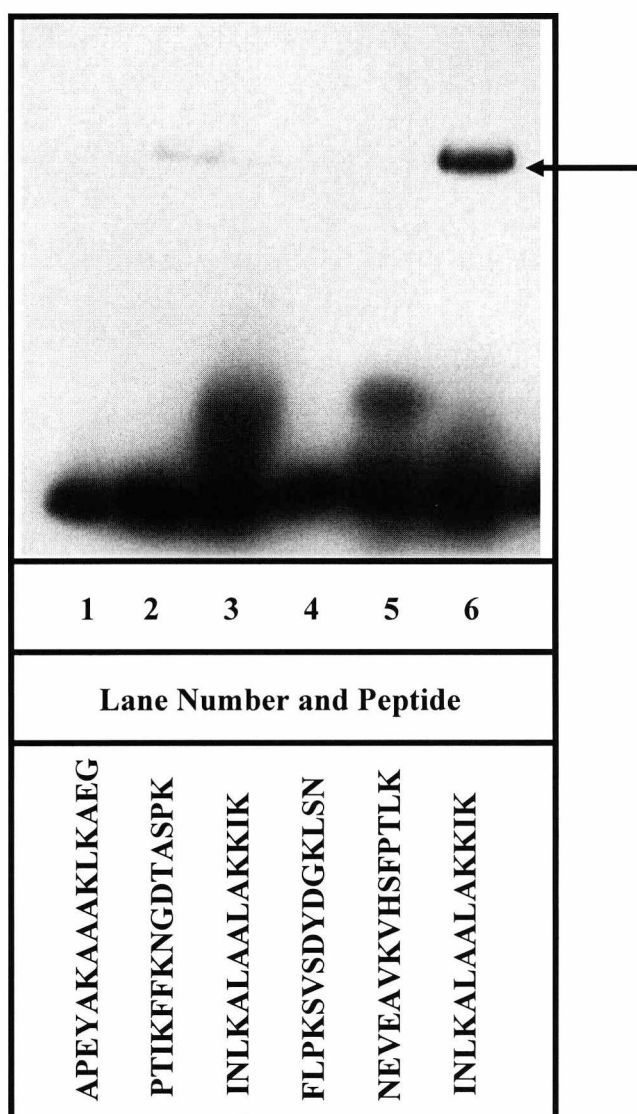
430 440 450 460 470 480
 KDNLPEELNF KPVADAI FNG GLVGENGAPG INSDIITVDG DRAFVLRISE HKPEAVKPLA

490 500 510 520 530 540
 DVQEQVKALV QHNKAEQQA K VDAEKLLVDL KAGKGAEAMQ AAGLKFGEPK TLSRSGRDP I

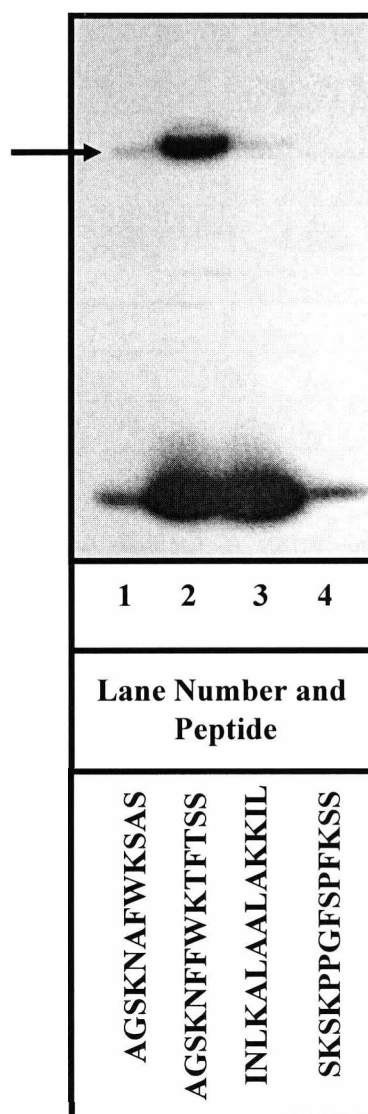
550 560 570 580 590 600
 SQAALPLP AKDKPSYGMA TDMQGNVLL ALDEVKQ GSM PEDQKKAMVQ GITQNNAQIV

610 620
 FEALMSNLRK EAKIKIGDAL EQQ

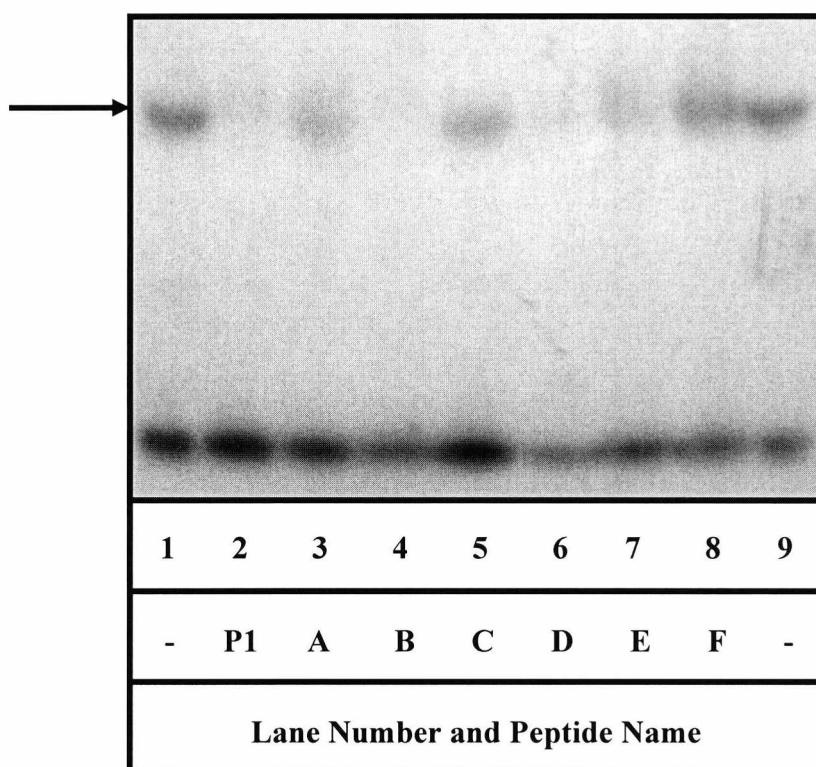
APPENDIX III



Binding of Radiolabelled peptides to SurA. 33 μ M of [125 I] Bolton-Hunter labelled peptides were incubated with 3.3 μ M SurA for 10 minutes at 0°C in a total volume of 10 μ l. Samples were subsequently incubated with DSG (final concentration of 0.5mM) for 60 minutes at 0°C. After cross-linking the samples were run on 10% polyacrylamide gels with subsequent autoradiography. The peptide sequences are shown in the figure.

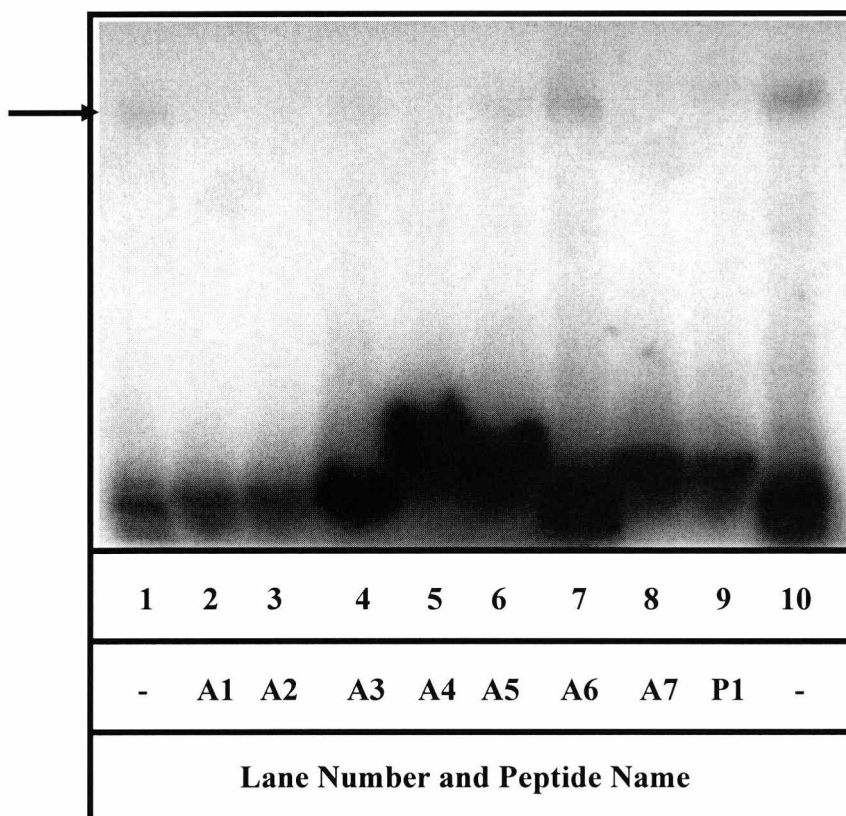


Binding of further radiolabelled peptides to SurA. 33 μ M of [125 I] Bolton-Hunter labelled peptides were incubated with 3.3 μ M SurA for 10 minutes at 0°C in a total volume of 10 μ l. Samples were subsequently incubated with DSG (final concentration of 0.5mM) for 60 minutes at 0°C. After cross-linking the samples were run on 10% polyacrylamide gels with subsequent autoradiography. The peptide sequences are shown in the figure, lane 1 is peptide P2, lane 2 is peptide P1 also known as Δ -somatostatin, lane 3 is peptide P3 and lane 4 is peptide P4. The band indicating the binding is shown by the arrow.



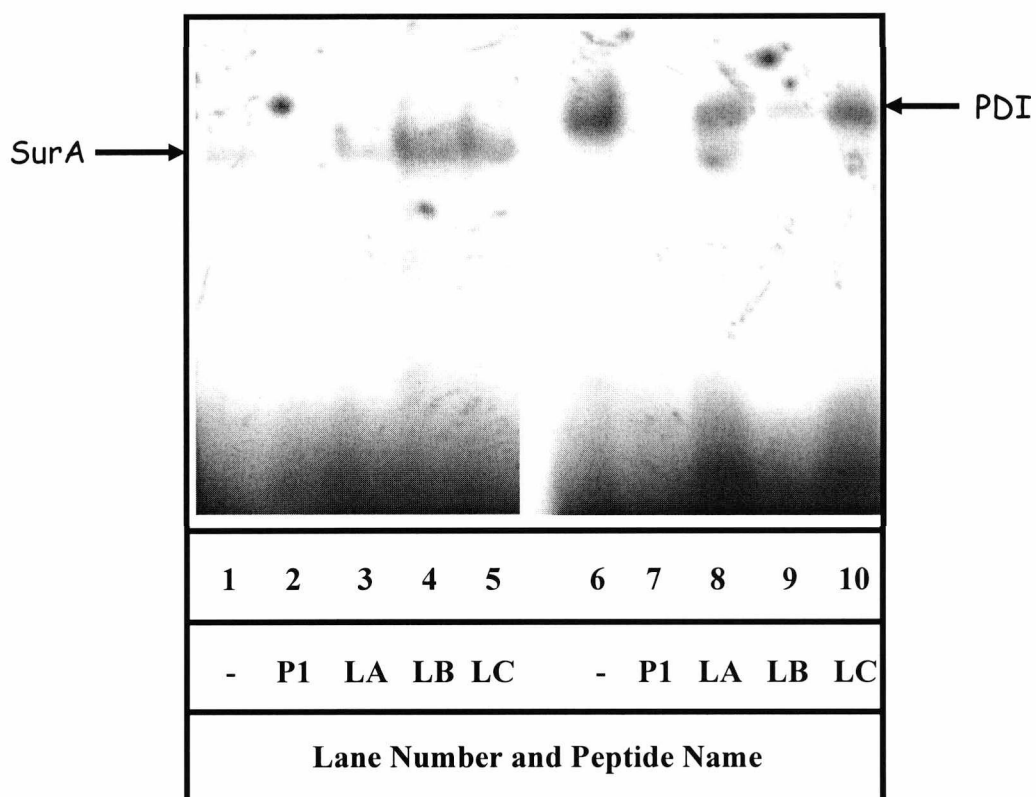
Competition Assay for peptides A-F. Peptides A-F compete with radiolabelled Δ -somatostatin. $33\mu\text{M}$ of [^{125}I] Bolton-Hunter labelled Δ -somatostatin was incubated with $3.3\mu\text{M}$ SurA and $33\mu\text{M}$ peptide A-F for 10 minutes at 0°C in a total volume of $10\mu\text{l}$. Samples were subsequently incubated with DSG (final concentration of 0.5mM) for 60 minutes at 0°C . After cross-linking the samples were run on 10% polyacrylamide gels with subsequent autoradiography. The SurA bands are indicated by the arrow. The – is no peptide and P1 is Δ -somatostatin.

Name	Peptide
A1	AASKNFFWKTFSTSS
A2	AGAKNFFWKTFSTSS
A3	AGSKAFFWKTFSTSS
A4	AGSKNAFWKTFSTSS (F6A)
A5	AGSKNFAWKTFSTSS (F7A)
A6	AGSKNFFAKTFSTSS (W8A)
A7	AGSKNFFWKAFTSS



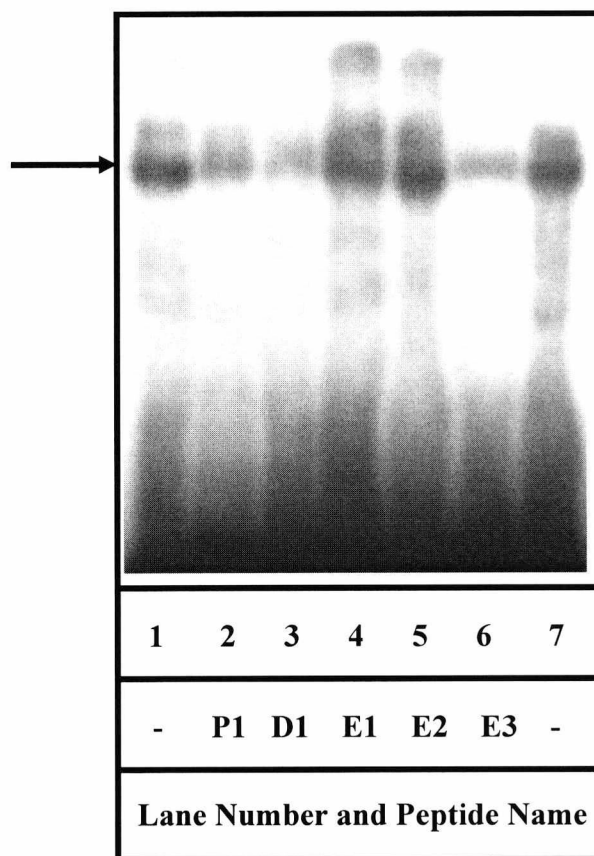
Competition Assay for peptides A1-A7. Peptides A1-A7 compete with radiolabelled Δ -somatostatin. $33\mu\text{M}$ of [^{125}I] Bolton-Hunter labelled Δ -somatostatin was incubated with $3.3\mu\text{M}$ SurA and $33\mu\text{M}$ peptide A-F for 10 minutes at 0°C in a total volume of $10\mu\text{l}$. Samples were subsequently incubated with DSG (final concentration of 0.5mM) for 60 minutes at 0°C . After cross-linking the samples were run on 10% polyacrylamide gels with subsequent autoradiography. The SurA bands are indicated by the arrow. The - is no peptide and P1 is Δ -somatostatin.

Name	Peptide
A1	AASKNFFWKTFTSS
A2	AGAKNFFWKTFTSS
A3	AGSKAFFWKTFTSS
A4	AGSKNAFWKTFTSS (F6A)
A5	AGSKNFAWKTFTSS (F7A)
A6	AGSKNFFAKTFTSS (W8A)
A7	AGSKNFFWKAFTSS



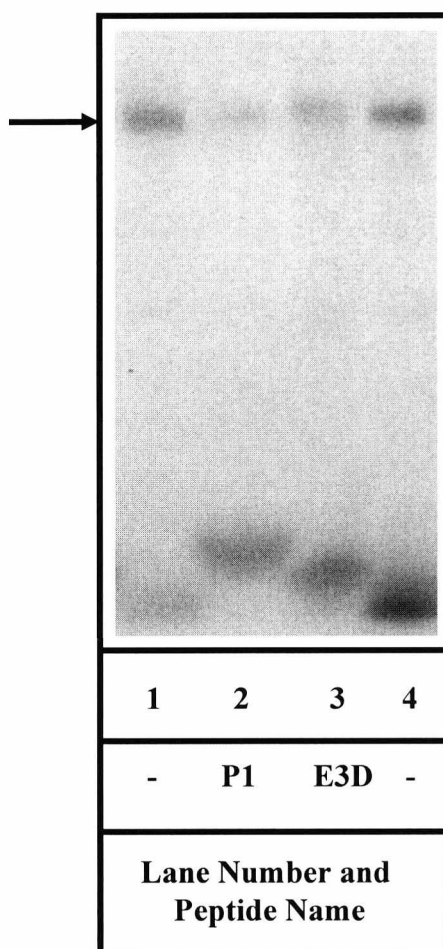
Competition Assay for peptides LA, LB and LC. Peptides LA, LB and LC compete with radiolabelled Δ -somatostatin for binding with SurA and PDI. $33\mu\text{M}$ of [^{125}I] Bolton-Hunter labelled Δ -somatostatin was incubated with $3.3\mu\text{M}$ SurA and $33\mu\text{M}$ peptide A-F for 10 minutes at 0°C in a total volume of $10\mu\text{l}$. Samples were subsequently incubated with DSG (final concentration of 0.5mM) for 60 minutes at 0°C . After cross-linking the samples were run on 10% polyacrylamide gels with subsequent autoradiography. SurA is on the right and PDI is on the left, bands are indicated by the arrow.

Name	Peptide
LA	KNFFWS
LB	RNFFWS
LC	KNFFWSN
LE	RNFFWSN



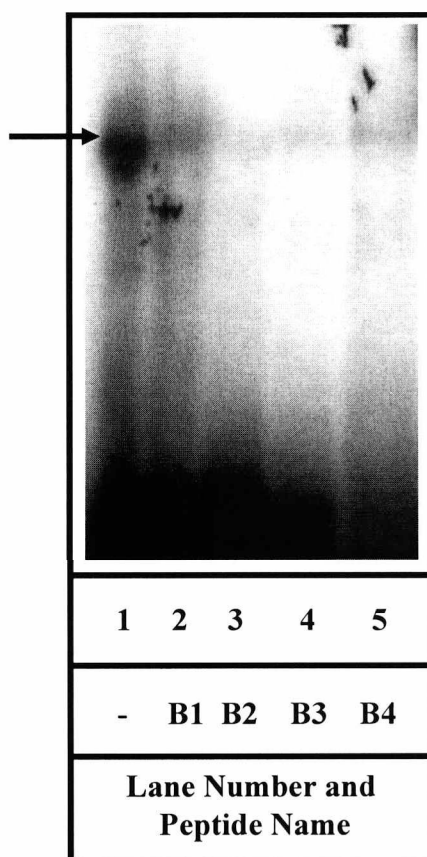
Competition assay for peptides D1, E1, E2 and E3. Peptides D1, E1, E2 and E3 compete with radiolabelled Δ -somatostatin for binding with SurA. $33\mu\text{M}$ of $[^{125}\text{I}]$ Bolton-Hunter labelled Δ -somatostatin was incubated with $3.3\mu\text{M}$ SurA and $33\mu\text{M}$ peptide A-F for 10 minutes at 0°C in a total volume of $10\mu\text{l}$. Samples were subsequently incubated with DSG (final concentration of 0.5mM) for 60 minutes at 0°C . After cross-linking the samples were run on 10% polyacrylamide gels with subsequent autoradiography. PDI is on the left of the figure and SurA is on the right. Lanes 3-6 are D1-E3 respectively. Lanes 1 and 7 are control lanes with PBS and lane 2 is unlabelled Δ -somatostatin.

Name	Peptide
D1	--SKNFFWKTF
E1	--SKNFFWKT
E2	----NFFWKT
E3	AGSKNFFWKS (peptide A)
E3D	AGSKNFFWKS (peptide A)



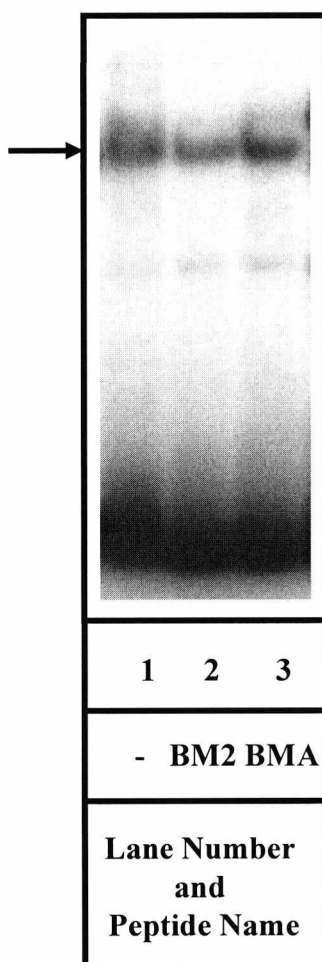
Competition assay for peptide E3D. Peptide E3D competes with radiolabelled Δ -somatostatin for binding with SurA. $33\mu\text{M}$ of [^{125}I] Bolton-Hunter labelled Δ -somatostatin was incubated with $3.3\mu\text{M}$ SurA and $33\mu\text{M}$ peptide A-F for 10 minutes at 0°C in a total volume of $10\mu\text{l}$. Samples were subsequently incubated with DSG (final concentration of 0.5mM) for 60 minutes at 0°C . After cross-linking the samples were run on 10% polyacrylamide gels with subsequent autoradiography. PDI is on the left of the figure and SurA is on the right. Lane 3 is E3D. Lanes 1 and 4 are control lanes with PBS and lane 2 is unlabelled Δ -somatostatin, shown as P1. The bands are indicated by the arrow.

Name	Peptide
E3D	AGSKNFFWKS (peptide A)



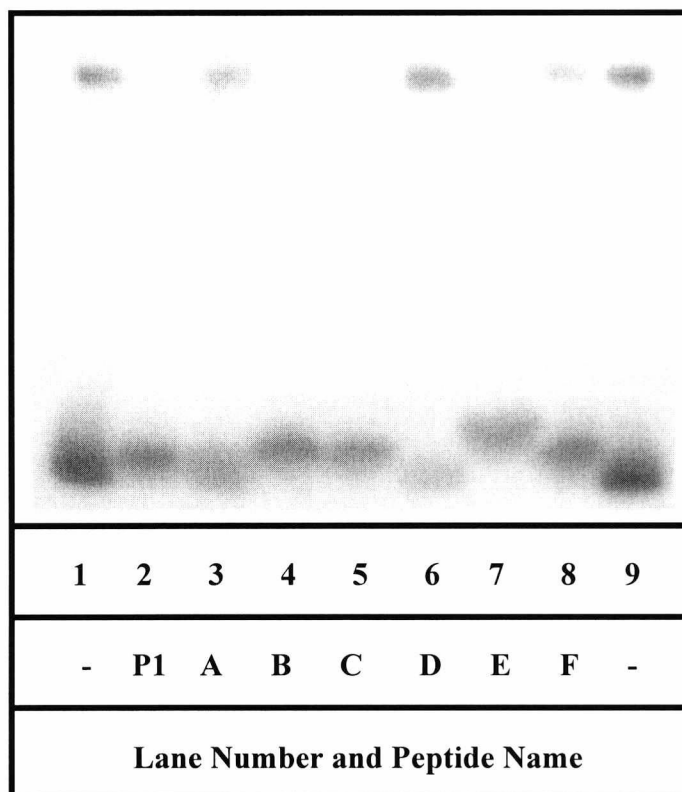
Competition assay for peptides B1 – B4. Peptides B1 – B4 competes with radiolabelled Δ -somatostatin for binding with SurA. $33\mu\text{M}$ of [^{125}I] Bolton-Hunter labelled Δ -somatostatin was incubated with $3.3\mu\text{M}$ SurA and $33\mu\text{M}$ peptide A-F for 10 minutes at 0°C in a total volume of $10\mu\text{l}$. Samples were subsequently incubated with DSG (final concentration of 0.5mM) for 60 minutes at 0°C . After cross-linking the samples were run on 10% polyacrylamide gels with subsequent autoradiography. Lane 1 has no peptide, and is therefore the control. Lanes 2 – 5 are peptides B1 – B4 respectively.

Name	Peptide
B1	AASKAFFWKS
B2	AGSKNFFWKT
B3	AGSKNFFWAT
B4	TKWFFNKSGA



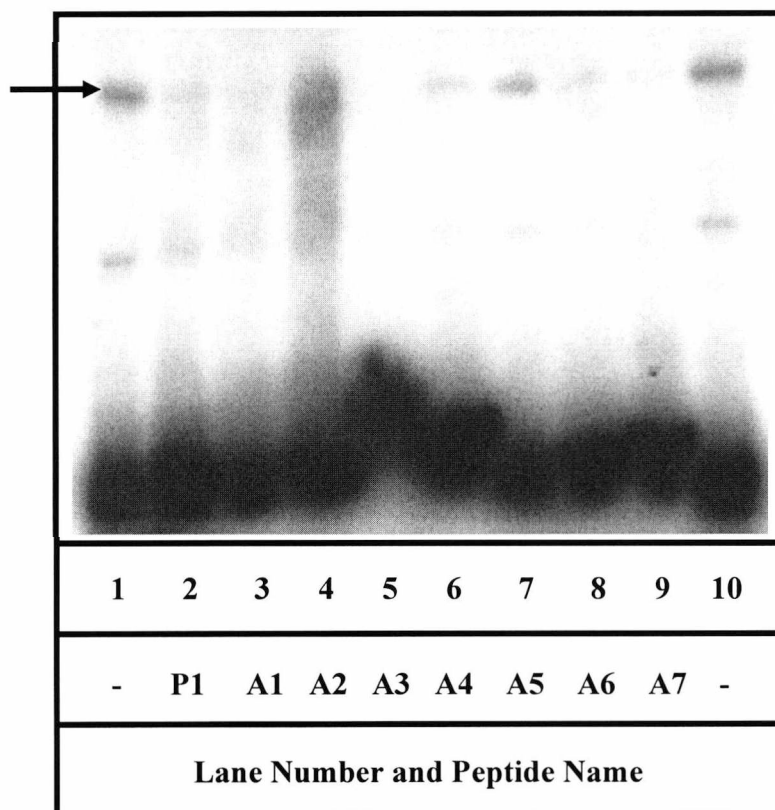
Competition assay for BMA and BM2 peptides. BM2 and BMA compete with radiolabelled Δ -somatostatin for binding to SurA. $33\mu\text{M}$ of [^{125}I] Bolton-Hunter labelled Δ -somatostatin was incubated with $3.3\mu\text{M}$ SurA and $33\mu\text{M}$ peptide A-F for 10 minutes at 0°C in a total volume of $10\mu\text{l}$. Samples were subsequently incubated with DSG (final concentration of 0.5mM) for 60 minutes at 0°C . After cross-linking the samples were run on 10% polyacrylamide gels with subsequent autoradiography.

Name	Peptide
BM2	WEYIPNV
BMA	WEYIP



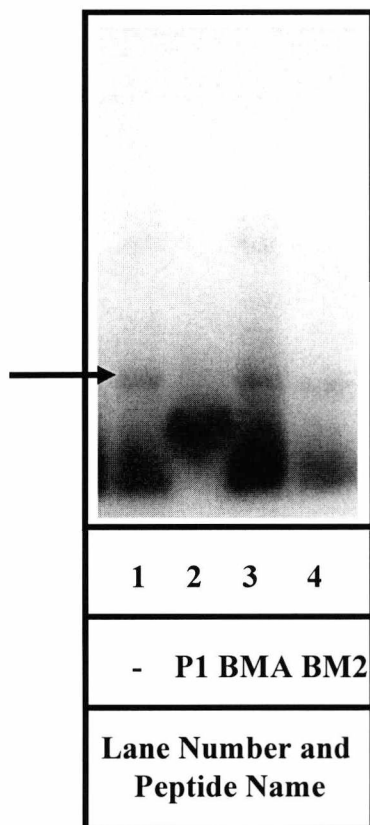
Competition Assay for peptides A-F. Peptides compete with radiolabelled Δ -somatostatin for binding with PDI. $33\mu\text{M}$ of [^{125}I] Bolton-Hunter labelled Δ -somatostatin was incubated with $3.3\mu\text{M}$ SurA and $33\mu\text{M}$ peptide A-F for 10 minutes at 0°C in a total volume of $10\mu\text{l}$. Samples were subsequently incubated with DSG (final concentration of 0.5mM) for 60 minutes at 0°C . After cross-linking the samples were run on 10% polyacrylamide gels with subsequent autoradiography.

Name	Peptide
A	AGSKNYFWKTFTSS (F6Y)
B	AGSKNYFAKTFTSS (F7Y)
C	AGSKNAFWKTFTSS (F6A)
D	AGSKNFFWKFTT
E	AGSKNFFWKT
F	AGSKNYFWKSAS (peptide S)

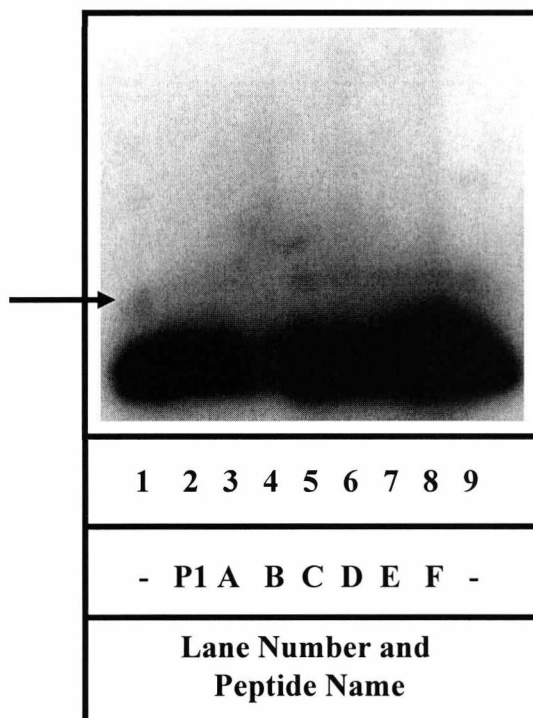


Competition Assay for peptides A1-A7. Peptides compete with radiolabelled Δ -somatostatin for binding with PDI. $33\mu\text{M}$ of [^{125}I] Bolton-Hunter labelled Δ -somatostatin was incubated with $3.3\mu\text{M}$ SurA and $33\mu\text{M}$ peptide A-F for 10 minutes at 0°C in a total volume of $10\mu\text{l}$. Samples were subsequently incubated with DSG (final concentration of 0.5mM) for 60 minutes at 0°C . After cross-linking the samples were run on 10% polyacrylamide gels with subsequent autoradiography.

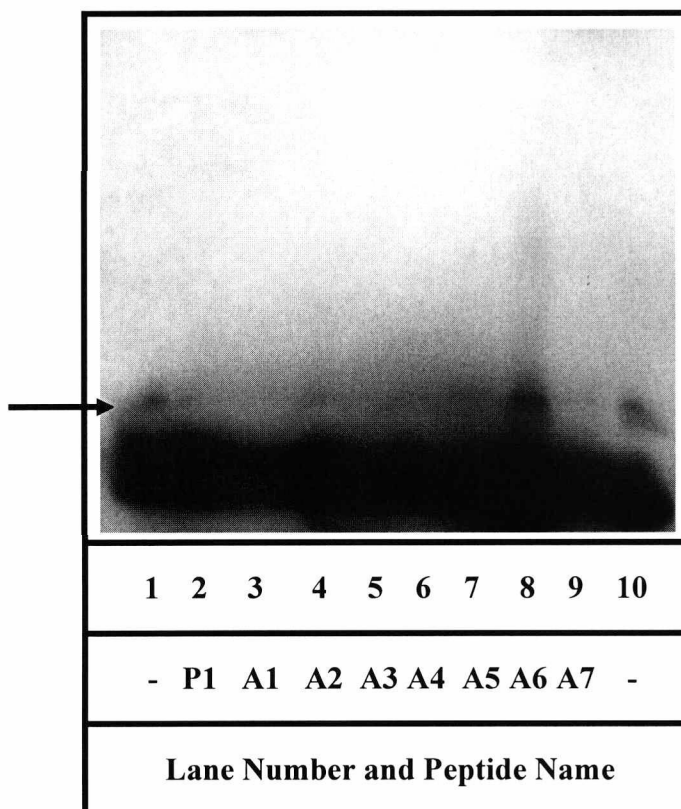
Name	Peptide
A1	AASKNFFWKTFTSS
A2	AGAKNFFWKTFTSS
A3	AGSKAFFWKTFTSS
A4	AGSKNAFWKTFTSS (F6A)
A5	AGSKNFAWKTFTSS (F7A)
A6	AGSKNFFAKTFTSS (W8A)
A7	AGSKNFFWKAFTSS



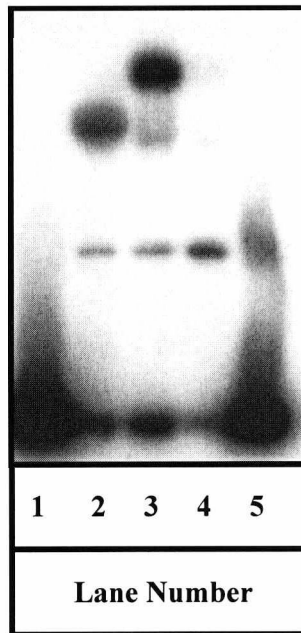
Competition Assay for peptides BMA and BM2. Peptides compete with radiolabelled Δ -somatostatin for binding with PDI. $33\mu\text{M}$ of [^{125}I] Bolton-Hunter labelled Δ -somatostatin was incubated with $1\mu\text{M}$ N-terminal fragment of SurA and $33\mu\text{M}$ peptide A-F for 10 minutes at 0°C in a total volume of $10\mu\text{l}$. Samples were subsequently incubated with DSG (final concentration of 0.5mM) for 60 minutes at 0°C . After cross-linking the samples were run on 10% polyacrylamide gels with subsequent autoradiography. Lane 1 is the N-terminal fragment of SurA with PBS, lane 2 is competition with unlabelled Δ -somatostatin, and lanes 3 and 4 are BMA and BM2 respectively. The arrow indicates the bands.



Competition Assay for peptides A-F. Peptides compete with radiolabelled Δ -somatostatin for binding with PDI. $33\mu\text{M}$ of [^{125}I] Bolton-Hunter labelled Δ -somatostatin was incubated with $1\mu\text{M}$ N-terminal fragment of SurA and $33\mu\text{M}$ peptide A-F for 10 minutes at 0°C in a total volume of $10\mu\text{l}$. Samples were subsequently incubated with DSG (final concentration of 0.5mM) for 60 minutes at 0°C . After cross-linking the samples were run on 10% polyacrylamide gels with subsequent autoradiography. Lane 1 is the N-terminal fragment of SurA with PBS, lane 2 is competition with unlabelled Δ -somatostatin, and lanes 3 and 8 are A-F respectively. The arrow indicates the bands.



Competition Assay for peptides A1-A7. Peptides compete with radiolabelled Δ -somatostatin for binding with PDI. $33\mu\text{M}$ of [^{125}I] Bolton-Hunter labelled Δ -somatostatin was incubated with $1\mu\text{M}$ N-terminal fragment of SurA and $33\mu\text{M}$ peptide A-F for 10 minutes at 0°C in a total volume of $10\mu\text{l}$. Samples were subsequently incubated with DSG (final concentration of 0.5mM) for 60 minutes at 0°C . After cross-linking the samples were run on 10% polyacrylamide gels with subsequent autoradiography. Lane 1 is the N-terminal fragment of SurA with PBS, lane 2 is competition with unlabelled Δ -somatostatin, and lanes 3 and 9 are A1-A7 respectively. The arrow indicates the bands.



PpiD binding with radiolabelled peptide E. Lanes 1 and 5 are PpiD with PBS, lane 2 is SurA, lane 3 is PDI and lane 4 is PpiD all were incubated with radiolabelled peptide E.

